Techno-economic Evaluation of Integrated Process Flowsheets for Vinasse Management with Value Addition for Decision Making

By

Rony Mung'asia Azegele

A thesis submitted in partial fulfilment of the requirements for the degree of Master of Science in Engineering

Faculty of Engineering and Built Environment

University of Cape Town

February 2018

Plagiarism Declaration

I know the meaning of plagiarism and declare that all the work in the document, save for that which is properly acknowledged, is my own. The thesis/dissertation has been submitted to the Turnitin module (or equivalent similarity and originality checking software) and I confirm that my supervisor has seen my report and any concerns revealed by such have been resolved with my supervisor.

Rony Mung'asia Azegele

16 February 2018

Signed by candidate

Acknowledgements

I would like to thank the Lord Almighty for the gift of life, knowledge, quick understanding, peace and a sound mind that enabled me to accomplish the task of undertaking this research.

I would also like to thank my supervisors for the great support throughout this research. To Prof Harrison – thank you for the philosophical guidance, encouragement and technical feedback you provided that challenged me to do better in my research. Dr Thanos – thank you for technical advice, criticism and feedback that have honed my research capabilities.

I also extend my gratitude to members of my research group whose feedback was invaluable in the past two years

I would also like to thank my friends in UCT Chem Eng. who supported me throughout my postgraduate journey. The great conversations, travel and support made this journey worthwhile. To my friends outside university, I thank you for the support system you all provided.

My sincere gratitude goes out to my nuclear family who sacrificed immensely and supported me unconditionally as I embarked on my studies. May the Lord bless and keep you. To my extended family, I thank you for the unwavering support throughout the past 7 years.

Last, but not least, I would like to thank the Sugar Milling Research Institute and CSIR for the continued involvement in this research as well as the financial support.

Executive Summary

Bioethanol production through fermentation of sugarcane juice and its derivatives such as molasses is gaining popularity worldwide as focus shifts towards renewable energy production. However, ethanol fermentation results in the production of large volumes of a dark brown and low pH liquid waste termed vinasse. At a vinasse production rate of 12-15 liters per liter of ethanol, sustainability of this bioprocess is impacted as effluent handling costs are high. If disposed onto the land, breakdown of the organic matter within may lead to the release of greenhouse gases into the atmosphere. Additionally, disposal into water bodies results in eutrophication due to the overload of plant nutrients (N, P and K). Further, owing to the high potassium content, the use of dewatered vinasse as animal feed supplements has been shown to cause digestive tract problems in ruminants depending on the supplementation rates (>10%). To increase sustainability of bioethanol fermentation processes through combined treatment and resource recovery from vinasse, biological and physico-chemical processes have been developed and implemented in industry.

Conventionally, raw vinasse is dewatered through evaporation processes (MEE) as a means of volume reduction. Membrane processes such as reverse osmosis (RO) have in the recent past become popularized as water recovery options from vinasse due to process simplicity and lower costs of equipment. Resulting concentrates from RO and MEE can be used as fertilizer. Due to the high organic content, vinasse is a suitable candidate for anaerobic digestion (AD) where the organic matter is broken down to biogas and an effluent that can be safely used as fertilizer. Additionally, the biogas from AD may be harnessed for electricity generation through combined heat and power processes or upgraded to biomethane to be used as a substitute for natural gas. For high moisture content substrates such as vinasse, upflow anaerobic sludge blanket reactors are best suited as sludge residence time is prolonged thereby increasing contact time with substrate which leading to higher methane yields. AD is often sensitive to changes in temperature, substrate composition, loading rate and pH. The presence of inhibitory components such as potassium salt ions (>11.6 g/L) in the vinasse feed result in a reduction of methanogenic activity manifested through reduced biogas and methane yields. Salt recovery processes including electrodialysis and ion-exchange have been investigated in literature on a pilot scale for the removal of K^+ ions from raw vinasse. To improve resource productivity, integration of vinasse treatment processes has been implemented in industry. Integration combines biological and physico-chemical processes which results in performance optimization and energy efficiency thereby improving economic feasibility of the projects. During the project conceptualization phase, process modelling is a vital tool that can be used to predict outcomes such as substrate utilization rates, product yields and optimal operating conditions of integrated processes in a timely and cost effective manner. In addition, techno-economic analyses can be used to determine cost sensitive areas and overall feasibility of the integrated processes.

Having reviewed the current industrial practices, this project sought to develop integrated flowsheets consisting of biological and physical processes for the combined vinasse treatment and value creation. Value creation was demonstrated through the recovery of valuable products including energy, salts and water from the raw vinasse. Due to its simplicity and cost effectiveness, AD was selected as the primary technology for vinasse treatment and biogas production. This was coupled with a combined heat and power system for electricity generation to form the base case flowsheet. It was hypothesized that incorporation of pre- and

post-treatment as well as alternative biogas utilization processes to the base case flowsheet for recovery of salts and water would generate additional revenue and cost savings. Profitability of the base case process was expected to increase with the additional pre- and post-treatments. To fulfil the objective set out and prove the hypothesis, a three step research approach was taken. The first step involved simulation and benchmarking of the base case flowsheet (AD and CHP). Using techno-economic analyses, the effect of individual addition of pre- and post-treatment options to the base case flowsheet on profitability was investigated. A framework was then developed to investigate the incorporation of combined pre- and post-treatment options to the base case flowsheet. Thereafter, a decision support tool that in comparing various combinations of vinasse treatment routes in terms of process performance and profitability was developed to aid in the synthesis of vinasse treatment processes in industry.

As bioprocess modelling is complex, it was important to select an appropriate simulation platform. Given the availability of a dedicated bioprocess compound database, sensitivity and optimization features and flexible customization options within Aspen Plus, it was preferred as the primary simulation platform over SuperPro Designer and high performance programming languages (C++, Java). In developing the base case AD flowsheet, several frameworks in the literature were considered. These included ADM1 (Batstone et al., 2002), ADM-3P (Ikumi et al., 2011) and a comprehensive model by Angelidaki et al. (1993). The presence of a well defined stoichiometric framework motivated the decision to adopt the comprehensive model by Angelidaki et al. (1993). Using a combination of in-built unit operations as well as customized user models (calculator blocks), the AD model by Angelidaki et al. (1993) was implemented on Aspen Plus. As ADM1 was considered an extension of the comprehensive model (Angelidaki et al., 1993) with several similarities, kinetic constants describing substrate uptake and microbial growth were adapted from ADM1. To ascertain the predictive quality of the built AD model, four case studies in the literature concerning the AD of manure (cow and swine) and municipal solid waste were simulated and the predicted simulation results compared to the experimental results. The developed AD model accurately predicted the methane yields of the four case studies as evidenced by the average difference of 10% between simulation and experimental results. A regression analysis between experimental and predicted data yielded a value of 0.74. Given the assumptions made in simplifying the developed model, the R^2 value was deemed acceptable and further affirmed the agreement between the model and experimental results.

To investigate the robustness of the developed AD model, sensitivity analyses on the feed composition as well as organic loading were conducted. Increasing inhibitory compound concentrations above certain thresholds was shown to negatively impact methanogenic activity as evidenced by the decreasing methane yields. Although ammonia is inhibitory at concentrations above 0.22 g/L, it is an important nitrogen source for biomass growth. Similarly, while acetic acid is inhibitory to acetogenic microbes, it is a crucial substrate for the growth of methanogenic archaea and methane production. Inorganic salt inhibition on the other hand may be reduced through extraction of K_2SO_4 through pre-treatment processes. The compositional sensitivity analyses as well as the benchmarking study showed that the built AD model had a solid core framework which accurately predicted experimental data for a range of substrates. Combined with a simplified CHP model of a Jenbacher spark ignition engine (General Electric, 2008) to form the base case flowsheet, the built AD model was used for all further simulations in this work. To determine the financial standing of the base case, simulation and subsequent techno-economic analyses were conducted. At an industrial

reactor capacity of 2000 m^3 and a loading rate of 25 $kgCOD/m^3.day$, simulation of the base case process resulted in a methane yield of 45 $L\text{-}CH_4/kgVS_{added}$ and an electrical production capacity of 410 kW. Discounted cash flow analyses (USD, 2016) showed that the base case was not profitable within a 20-year project lifetime as evidenced by the low return on investment and internal rate of return. However, a further sensitivity on profitability of the base case showed that decreasing potassium ion concentrations in the feed would result in higher profitability higher methane yields because of decreased K^+ inhibition. Despite the positive effect of on AD performance, further analyses were required to validate feasibility of K_2SO_4 recovery processes as well as water recovery processes aimed at further value creation from vinasse.

To investigate the effect of pre-treatment on base case flowsheet economics, an ion exchange process adapted from Zhang et al. (2012) was incorporated based on the comparatively higher degree of selectivity to K^+ ions exhibited by the ion exchange process than ozonation and electrodialysis. As expected, improved CH_4 yields (14%), electrical production and consequently, increases (>100%) in profitability indicators were observed. However, the pretreated base case (IEX-AD-CHP) remained unprofitable which was an indication that the marginal revenue from increased electrical production and K_2SO_4 sales did not match the additional capital costs. To increase profitability of the base case, biogas upgrading using a HPWS system was used in place of the CHP. Due to the comparatively low cost of HPWS equipment coupled with the increased revenue from biomethane sales, the AD-HPWS process exhibited higher profitability (ROI: 19.6%) than the base case (ROI: 0%). As evidenced by the IRR (16.3%) that was greater than the cost of capital (15%), the AD-HPWS option was profitable over a 20 year lifetime. Resource recovery from the AD effluent was sought through incorporation of RO and MEE to form the AD-CHP-RO and AD-CHP-MEE routes. Most notably, there was a significant (170%) increase in cost savings with the use of RO and MEE concentrates as fertilizer compared to the raw AD effluent from the base case. Additional cost savings of up to $27 700 were achieved with upstream reintegration of RO permeate or MEE condensate water. This savings was based on the municipal water tariff of R5/kL. The combined cost savings led to increased profitability of the base case as evidenced by the increase in ROI from 0% to 3%.

Potential knock-on effects of pre-treatments on efficiency of post-treatment or biogas utilization processes were noted. These were investigated through the simultaneous addition of pre- and post-treatment combinations to the base case AD process to form a decision making framework. Through techno-economic comparisons drawn between the 12 distinct vinasse treatment routes resulting from various combinations of pre- and post-treatment options in the decision making framework, three major decision criteria were established. Despite the improved performance and methane yields observed with pre-treatment addition, there was a decline in profitability of the AD-HPWS-RO/MEE processes owing to increased capital costs that remain unrecovered by marginal revenue obtained from biomethane sales. The contrary is observed with the AD-CHP-RO/MEE processes as evidenced by the 20 to 30% increase in profitability indicators upon addition of pre-treatment. This is attributed to the marginal revenues from increased electrical output as well as the cost savings from water reuse and RO/MEE concentrates. Due to the contrasting effect of pre-treatment on CHP and HPWS affiliated processes and profitability, the presence of inhibitory potassium ions was considered a decision criterion.

Due to the low cost of HPWS equipment, it was observed that choosing to upgrade biogas to biomethane as opposed to using CHP exhibited higher performance (energy output) and profitability in all process combinations. This was evidenced by the higher ROI and IRR of the AD-HPWS, AD-HPWS-RO/MEE and IEX-AD-HPWS-RO/MEE process options compared to the CHP counterparts. As a result, the choice of biogas utilization was considered an important decision criterion affecting profitability.

Because of increased cost savings with upstream reintegration of water and the use of concentrates as fertilizer, the implementation of RO and MEE was observed to increase profitability of all process options including AD-CHP/HPWS and IEX-AD-CHP/HPWS. This was majorly through cost savings from use of RO and MEE concentrates as fertilizer ($250 000/yr) and upstream reintegration of water. This led to the conclusion that the recovery of concentrates from vinasse is an important decision criterion when looking to increase profitability and process sustainability.

Overall, based on the techno-economic analyses, the most profitable vinasse treatment process included an anaerobic digester coupled with a high-pressure water scrubbing system for biomethane production and reverse osmosis process for water recovery (ROI: 22.9%, NPV: $540 000). This facilitated both increased energy output from biomethane and cost savings from water reuse. Further research is recommended around the AD modelling aspect to extend functionality to ionic speciation and pH prediction. it is recommended that equipment quotes from suppliers within South Africa be sourced as opposed to costing heuristics in the literature to increase the accuracy of capital and operating expenditure.

Table of Contents

Table of Figures

List of Tables

Acronyms

AD	Anaerobic Digestion
BOD	Biological Oxygen Demand
CAPEX	Capital Expenditure
CHP	Combined Heat and Power
CEPCI	Chemical Engineering Plant Cost Index
CMS	Condensed Molasses Solids
COD	Chemical Oxygen Demand
EPASA	Ethanol Producers Association of South Africa
HPPL	High Performance Programming Languages
HPWS	High Pressure Water Scrubbing
HRT	Hydraulic Retention Time
IRR	Internal Rate of Return
IEX	Ion Exchange
LCFA	Long Chain Fatty Acids
LCOE	Levelized Cost of Energy
MEE	Multi-effect Evaporation
MSW	Municipal Solid Waste
MF, NF	Micro-filtration, Nano-filtration
NPV	Net Present Value
NRTL	Non-random Two Liquid
NREL	National Renewable Energy Laboratory
NERSA	National Energy Regulator (South Africa)
NPK	Nitrogen, Phosphorus, Potassium
OPEX/OC	Operating Expenditure/Operating Costs
OOM	Order of Magnitude
OLR	Organic Loading Rate
ODE	Ordinary Differential Equation
PBP	Payback period
PCE	Purchase Cost of Equipment
RO	Reverse Osmosis
REFIT	Renewable Energy Feed in Tariff
SRT	Sludge Retention Time
VFA	Volatile Fatty Acids
UASB	Upflow Anaerobic Sludge Blanket
VS	Volatile Solids
WACC	Weighted Average Cost of Capital

Glossary

COD	Measure of organic content within a substrate or waste water.
Ancillary equipment	Minor pieces of equipment used to support the function of major equipment.
Capital Expenditure	Fixed cost of purchase (equipment).
FORTRAN	Programming language used for numerical computing
Fertirrigation	Irrigation of agricultural land using high moisture content fertilizer
Internal Rate of Return	A measure of profitability when comparing different projects
Java	Object oriented programming language.
Net Present Value	The current value of money compared to its value in the future after it has been compounded.
Operating Expenditure	Day to day running expenses.
REFIT	Sale tariff for electricity from renewable energy set by the government
Vinasse	Dark brown liquid waste generated from the bioethanol fermentation process.
WACC	The cost of borrowing capital for the start-up of a project.

1. Introduction

1.1 Background and Context

Production of biofuels enables diversification of the energy supply, reduction of greenhouse gas emissions and decreased dependence on fossil fuels for transportation (Moraes et al., 2015). In Southern Africa, bioethanol production through fermentation of sugarcane molasses is well established (Illovo Sugar, 2013; Tongaat Hulett, 2015). In this process, sugarcane molasses derived from sugar processing plants as a by-product is diluted and then fermented using various strains of yeast to produce bioethanol. Though relatively sustainable, the bioethanol production process, comprising fermentation and distillation as its primary unit operations, results in the excessive production of a dark brown liquid termed vinasse that is drawn off the distillery bottoms section during the bioethanol recovery.

The volume of vinasse produced per liter of ethanol varies depending on upstream process conditions and dilution rates. Volumes of between 15 and 20 litres of vinasse formed per litre of ethanol have been reported in the literature (Djalma Nunes Ferraz Júnior et al., 2016; Rodrigues Reis and Hu, 2017; Saha et al., 2005). Its composition differs globally depending its geographical location and the climate under which the sugarcane is grown. However, characteristics such as its high organic content, low pH, and relatively high salinity are common (Christofoletti et al., 2013; P. Zhang et al., 2012).

Raw vinasse has several applications owing to its high organic and macronutrient content (potassium). It can be re-applied to the sugarcane fields as a fertilizer to enrich the soils and increase crop productivity (Ryan et al., 2009; Tongaat Hulett, 2015). However, recent studies show that its repeated use may salinize soils and release greenhouse gases (GHG) over extended periods (Moraes et al., 2015) depending on application rates. Dewatered vinasse is commonly used as an animal feed supplement for ruminants (Christofoletti et al., 2013) although digestive complications in ruminants have been reported at supplementation rates above 10%. Free disposal of into water bodies is unsustainable as it disrupts the aquatic ecosystems through macronutrient overload. As a result, eutrophication occurs which reduces the dissolved oxygen concentrations and the exposure of underwater plants to sunlight (Siles et al., 2011), further aggravating oxygenation through reducing photosynthesis.

To reduce the strength of this wastewater and potentially create value that benefits both industry and environment, existing biotechnologies have been adapted for vinasse treatment. One such process is anaerobic digestion (AD) that results in the reduction of organic matter, produces biogas and an effluent that can be used as an organic fertilizer (Djalma Nunes Ferraz Júnior et al., 2016). The biogas generated from this process can be used to generate electricity and heat through combined heat and power systems (CHP). Alternatively, raw biogas can be upgraded to biomethane (97%) and used as a substitute for natural gas in domestic or industrial applications (Leme and Seabra, 2017). Efficiency and biogas yield in the anaerobic digestion of vinasse is frequently impeded by the presence of inhibitory compounds such as inorganic salt cations, and phenolic compounds. These often disrupt microbial activity thereby causing a decrease in the methane yields.

In light of this, physico-chemical processes such as chemical precipitation, ozonation, ion exchange and electrodialysis have been implemented for removal and recovery of inhibitory compounds prior to the anaerobic digestion treatment step (Kim, 2011; Liu et al., 2015; P. Zhang et al., 2012). Recovery of inhibitory compounds such as inorganic salts may be

beneficial from an economic standpoint as they are valuable products used in the manufacture of synthetic fertilizers. Further value creation from the digestate may be explored through implementation of water recovery processes. Thermal processes (Carvalho, 2011) and membrane technologies such as multi effect evaporation and reverse osmosis have been used to recover fit for purpose water from the digestate which can be used locally in the plant or purified further to generate potable water (Nataraj et al., 2006). In addition, the resulting concentrate can be used as a soil amendment and animal feed supplement as it is rich in macronutrients.

1.2 Project Objectives

The specific objectives of this study are to:

- Conduct an extensive literature review on the characteristics, uses, disposal, treatment and valorization of vinasse globally.
- Identify and compare potential biological and physico-chemical vinasse treatment processes.
- Develop a base case flow diagram consisting of a vinasse AD plant to form the basis upon which addition of other processes can be explored.
- Investigate and compare the merits and shortcomings of AD models in the literature. Key principles and aspects of these frameworks will be adopted in the development of an AD model for the base case flowsheet. Selection of the most appropriate bioprocess simulation software will follow.
- Simulate the base case flowsheet consisting of AD on the selected simulation software package. Investigate its sensitivity to variations in the feed compositions and disturbances. An initial techno-economic analysis on the base case is to be developed.
- Investigate the impact of the addition of pre- and post-treatments on the energy consumption, resource recovery and profitability. This will lead to the development of an economically preferred process route.
- Develop a tool that can assist and direct decision making when developing vinasse treatment processes.

Successful completion of the above objectives will be the first step towards the development of processes for the remediation of vinasse with concomitant value creation. Methods of clean energy production such as biogas will be studied. Through this, the project addresses the 7th Sustainable Development Goal that seeks to promote the production of affordable and clean energy (Griggs et al., 2013). The biogas produced through the biodigestion of vinasse will provide a clean and renewable energy source for either upstream or downstream processes

1.3 Hypothesis

Anaerobic digestion of vinasse results in the production of biogas with high methane concentrations between 55 and 65% (Albanez et al., 2016). Owing to its high calorific values, biogas can be harnessed for heat and electricity production for internal or commercial purposes (Fuess and Zaiat, 2017; Leme and Seabra, 2017). Previous techno-economic studies have shown that integration of sugarcane vinasse AD systems with biogas utilization

processes is profitable and promotes sustainable energy production (Fuess and Zaiat, 2017; Moraes et al., 2014). Another study on integration of vinasse treatment processes showed that the energy generated using biogas from vinasse AD can be purposed both internally to meet utility requirements for a digestate water recovery system (reverse osmosis), and commercially to increase profitability of the overall process (Ryan et al., 2009).

It is therefore hypothesized that, in the flowsheets developed, incorporation of pre- and post-treatments to the primary vinasse AD step will generate additional revenues, result in cost savings and have an overall positive impact on the profitability of the final flowsheets presented.

Key questions arising from this are:

- What are the characteristics of vinasse produced in South Africa?
- What are the most common vinasse handling, disposal and treatment techniques applied in the industry?
- To what degree of detail should the AD of vinasse be simulated to provide accurate results concerning methane productivities, reactor sizes and energy requirements?
- Which water and salt recovery process are most ideal for implementation considering their effectiveness, energy requirements, costs and availability?
- What are the economic implications of process additions in relation to yield improvements?

1.4 Scope and Limitations

To ensure continued growth of the biofuels industry in Southern Africa, it is important to develop feasible processes that integrate the wastewater treatment technologies to maximize resource productivity and value creation. This study therefore seeks to develop integrated process flowsheets at a conceptual design level for the treatment and concomitant remediation of sugar cane vinasse using Aspen Plus as the engineering simulation platform. This commences with the review and development of a base case simulation consisting of an anaerobic digestion process with the aim of reducing the organic matter content in vinasse and recovering biogas for energy production. Inclusion of pre-treatment processes is investigated to recover inorganic salts which can be commercialized for economic gain and overall, result in a more efficient AD process with higher methane yields due to reduced inhibitor concentrations in the AD feed. Incorporation of dewatering processes to recover usable process water and concentrates from the digestate is explored. Notably, throughout this process it is necessary to ensure that the process configurations remain economically viable within the South African context. To ensure feasibility, the selection of pre- and post-treatments is done through a techno-economic approach by analysing the marginal benefits and revenues against the costs of process additions. This leads progressively to the development of a framework to be used in decision making when developing vinasse waste treatment processes that consider a variety of compositional, technical and environmental factors.

This project is limited to process flowsheeting and, as such, the models developed will be benchmarked against existing models and experimental data from the literature. The integrity of the results from the simulation package will be dependent on the accuracy of the physical property methods within. Assumptions and information used to perform the techno-economic analyses will be justified appropriately.

1.5 Dissertation Structure

Having presented a background into vinasse production, potential treatment methods and the overall research objectives in the introduction section, a comprehensive review of relevant literature is conducted in Chapter 2. This goes deeper into vinasse characterization, treatments and flowsheeting as a means of process integration for additional value recovery. Chapter 3 outlines the research approach that involves the base case model development and the techno-economic approach taken in the analyses of vinasse treatment routes. Following the research approach, benchmarking and sensitivity studies aimed at testing the robustness of the simulation developed for anaerobic digestion of vinasse on Aspen Plus are presented in Chapter 4. Results concerning the performance and techno-economic analyses of the base case vinasse treatment flowsheet are also presented in Chapter 4. Having identified process optimization avenues in AD of vinasse, investigations into the effect of individual addition of pre- and post-treatments to the base case on process performance and profitability are presented in Chapter 5. Having investigated viable pre- and post-treatment processes in Chapter 5, a decision-making framework is developed in Chapter 6. The decision framework explores the knock-on effects of pre-treatment on the choice of post-treatment options and culminates in the determination of key decision criteria to be considered when developing vinasse treatment processes in industry. The conclusion is presented in Chapter 7. This summarizes key findings within the results chapters (4 to 6) while alluding to the specific objectives presented in Chapter 3. Recommendations for the optimal vinasse treatment process as well as future work are presented as well.

2. Literature Review

2.1 Vinasse Production

Bioethanol production through fermentation processes has led to the production of large volumes of residual waste water termed as vinasse. In industry, this waste is often termed as molasses spent wash, dunder, or stillage and is typically dark brown in colour with an average water content of 90%. Depending on the raw material used for bioethanol production, the concentration of dissolved solids varies. Vinasse originating from sugarcane, sugarcane derivatives such as molasses, sugar beet and grapes generally has a high concentration of dissolved solids.

In Southern Africa, sugarcane molasses, a concentrated liquid by-product of the sugar refining process, is widely used as a substrate for bioethanol production (EPASA, 2013). It predominantly contains sugars that can be converted into ethanol through yeast fermentation. In the fermentation process, cane molasses is pre-treated by dilution to a specific gravity of 1.1, then fed to a series of fermenters inoculated with 10% volume of yeast (Saha et al., 2005) in which the residual sugar is converted to ethanol.

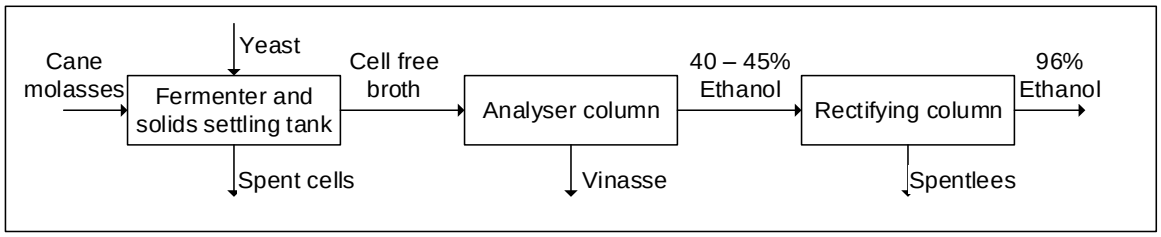

Figure 2.1: Simplified block flow diagram of the bioethanol fermentation process

The spent cells are separated from the spent broth in a settling tank. The cell free spent broth is preheated and sent to the distillation columns. The broth is fractionated to produce 40 – 45% alcohol vapours in the analyser column overheads. The alcohol vapours are sent to the rectifying columns which result in 96% liquid ethanol in the overheads (Satyawali and Balakrishnan, 2008). Vinasse is recovered from the analyser column bottoms at approximately 90°C.

For every litre of ethanol produced, approximately 12 to 15 litres of the vinasse waste water is discharged from the bottoms of the rectifying columns (España-Gamboa et al., 2011). This production rate may be higher and largely depends on the industry location and the extent of molasses dilution in the fermentation process (Ahmed et al., 2013). Vinasse has been a significant environmental issue for the bioethanol industry owing to its high organic content and salinity (Christofoletti et al., 2013). Traditional disposal practices include fertirrigation in major ethanol producing countries including Brazil and India. Vinasse can also be dried to form condensed molasses solids that are used as animal feed supplements. Because of its high organic content, these practices may have adverse health and environmental impacts depending on application rates (>300 m^3/ha) (Christofoletti et al., 2013).

2.2 Vinasse Management and Disposal

The choice of vinasse disposal methods is often dependent on the additional cost implications. Free disposal of raw vinasse into waterbodies was in the past common in major ethanol producing countries (Brazil) but its feasibility is dependent on proximity owing to the high cost

of transporting large liquid volumes (Carvalho, 2011). Although free disposal presents a quick solution, the environmental implications are severe and could cause imbalances in the natural aquatic ecosystems (Siles et al., 2011). Increased concentrations of macronutrients (NPK) in the water may lead to eutrophication. In addition, reduced sunlight penetration and oxygen, owing to high COD and BOD levels in the vinasse, could cause the death of aquatic life (Christofoletti et al., 2013).

Vinasse has a relatively high concentration of macronutrients such as potassium, nitrogen and calcium (Table 2.1). Hence, it can be used as an organic fertilizer to increase crop productivity and enhance soil properties. Application of raw vinasse to the soil through fertirrigation can be used to replace or supplement commercial fertilizer and may result in a cost saving subject to its proximity to the sugarcane plantations. This is done using low cost pumps, irrigation channels and truck decanters (Rein et al., 2011). Through concentration by evaporation to produce CMS, a significant reduction in volume may be achieved (~90% to ~40%), which may decrease transport costs (Turner et al., 2002). This is, however, is strongly dependent on the energy requirements of the evaporation processes. These may drive operation costs up and render the project infeasible. The value of CMS is two-fold in that it can be applied to the soil as fertilizer or used as an animal feed supplements for ruminants and pigs.

Continuous use of raw vinasse and CMS increases moisture retention and porosity of the soil; these are beneficial to crops (España-Gamboa et al., 2012). However, some studies have shown that the repeated use of vinasse as a fertiliser could salinize soils with high concentrations of Mg, Ca, K, and SO_4 ions, negatively impacting crop yields. Increases in soil porosity may further promote seepage of vinasse into groundwater reservoirs, thereby contaminating this resource (Christofoletti et al., 2013). The extent of these adverse impacts is dependent on the application rates. Raw vinasse and CMS application rates below 300 m^3/ha and 3 tonnes/ha, respectively, showed an increase in sugarcane yields (Turner et al., 2002). Rates above these resulted in negative effects such as decreased sucrose yields and increased soil salinity in the medium to long term.

The vinasse management and disposal techniques discussed above have several merits and shortcomings. Application of vinasse and CMS may lead to cost savings depending on the cost of transportation or additional operating expenditure of the drying processes. However, investigations in the literature show that free disposal into water bodies has detrimental effects on the wellbeing of aquatic ecosystems. In addition, application onto the soil could lead to contamination of ground water resources and an increase in soil salinity. This analysis shows that the negative health and environmental effects of vinasse disposal are because of high salinity, organic content (COD and BOD) and elevated macronutrient concentrations. Alternative methods of managing vinasse through treatment processes have been developed in industry that reduce its organic content whilst promoting the recovery of valuable products such as water, biogas and salts. Before examining these treatment processes, one must understand the composition of sugarcane vinasse and its derivatives.

2.3 Vinasse Characterization

The composition of vinasse is dependent on the type of feedstock used in the fermentation process (España-Gamboa et al., 2012). However, similarities lie in their high COD content and acidic nature. Table 2.1 shows the different types of vinasse and the compositions sourced from major biofuels producers in Brazil and India. Irrespective of the vinasse source, these by-products exhibit a dark brown pigment with pH ranges between 3.5 and 5. The

characteristic pigment is caused by the presence of heavy polymers termed as melanoidins, which are formed as a result of the reaction between reducing sugars and amino acids in the molasses fermentation process (Chandra et al., 2008).

Table 2.1: A comparison of vinasse compositions from different feedstocks (Wilkie et al., 2000, Salomon and Silva Lora, 2009)

Feedstocks (mg/L)	Cane juice	Cane molasses	Beet Molasses	Sorghum
BOD	16700	39500	27500 - 44900	46000
COD	30400	84900 - 95000	55500 - 91100	79900
Nitrogen (N)	102 - 628	153 - 1230	1800 - 4750	800
Phosphorus (P)	71 - 130	190	163 - 163	1990
Potassium (K)	1733 - 1952	4893 - 11000	10000	-
Magnesium (Mg)	200 - 490	420 - 520	1.23	-
Calcium (Ca)	130 - 1540	450 - 5180	0.71	-
Sulfates (SO_4)	1356	1500 - 3480	3500 - 3720	-
pH	4.04 -4.6	4.46 - 4.8	4.2 - 5.35	4.5

There is a consistently high concentration of potassium ions across all vinasse types. These could be extracted in their salt form and be used as an ingredient in the manufacture of synthetic fertilizer. Elevated sulfate concentrations in sugarcane and its molasses are mostly due to the accumulation of sulfate compounds during the clarification step that makes use of sulphite additives in the sugar refining process. The presence of sulphur compounds can influence its biological treatment through anaerobic digestion (Wilkie et al., 2000) through the unwanted degradation of the organic content by sulfate reducing bacteria (SRB) to produce H_2S as opposed to methane.

The chemical oxygen demand (COD) and biological oxygen demand (BOD) are a measure of the organic content in a substrate or waste stream. All vinasse streams exhibit high COD concentrations above 10 g/L. The relative amounts of volatile fatty acids (VFA) and other organic compounds present in vinasse vary depending on the feedstock and upstream processing. The major organic compounds in vinasse are acetic acid, ethanol and glycerol (Wilkie et al., 2000). Additionally, sugar decomposition products such as phenols, tannins and anthocyanins are present in vinasse. These are recalcitrant and toxic to bacteria involved in wastewater treatment processes. Because of its high organic content (COD>1000 mg/L) and presence of recalcitrant compounds, vinasse has been termed as a high strength wastewater (Hamza et al., 2016).

Crude protein, amino acids and other nitrogen based organic compounds are also present in vinasse (Wilkie et al., 2000). The protein content in cane vinasse ranges between 6% and 8% on a mass basis and varies depending on the upstream fermentation process. The amino acid profiles in sugarcane vinasse obtained from South America (Scull et al., 2012) and South Africa (Rein et al., 2011) are detailed in Table 2.2.

Table 2.2: A comparison of amino acid profiles in sugarcane vinasse from South America and South Africa

Amino acids	Scull et al. (2012)	Turner et al. (2002)
Aspartic acid	0.83	2
Glutamic acid	**1.31**	**2.2**
Serine	0.47	0.9
Glycine	0.38	2
Histidine	0.49	0.1
Arginine	0.90	0.1
Phenyl Alanine	0.49	0.2
Lysine	0.96	0.2
Methionine	0.23	0.13
Threonine	0.65	0.7
Alenine	0.31	2.4
Proline	0.55	1.3
Tyrosine	0.56	1.5
Valine	0.64	1.3
Isoleucine	0.63	0.7
Leucine	0.38	0.9

Irrespective of the source of sugarcane vinasse, the essential amino acids such as aspartic and glutamic acid, isoleucine and lysine predominate (Table 2.2). However, notable differences include the low concentration of lysine, arginine, histidine and phenyl alanine in South African vinasse compared to the South American by-product. Presence of these essential amino acids increase the biological value of vinasse to be used as a good animal feed supplement or organic fertilizer (Scull et al., 2012).

In South Africa, the reported ethanol production capacity from sugar is 125000 kLaa/annum (anhydrous alcohol) with a vinasse to ethanol ratio between 7 and 16. This translates to an annual vinasse production between 1 and 2 billion litres (EPASA, 2013) depending on capacity utilization. Arguably, vinasse from SA may be compositionally different to vinasse sourced from South America and India owing to the difference in region as well as industry practices. The limited published literature on characterization of South African vinasse is summarised in Table 2.3.

Table 2.3: South African sugarcane vinasse composition on a mass basis sourced from Turner et al. (2002)

Compounds	% Concentration
Organic material	***69%***
• **Volatile Fatty Acids**	21
• **Total reducing sugars**	12
• **Glycerol**	6.35
• **Protein**	1.15
• **Amino acids**	1.66
Minerals – Total Ash	***31%***
• **Potassium**	10
• **Calcium**	1.8
• **Magnesium**	1.45
• **Phosphorus**	0.29

When examining vinasse characteristics, a dry mass basis is used to measure the composition of condensed molasses solids (CMS) that includes both its organic material and the total ash content (Table 2.3). These CMS are mostly used as a fertilizer to recycle increasingly expensive minerals back to the ground (Rein et al., 2011). Prior to drying, the raw vinasse has a high water content between 90 and 92%. The drying process to produce CMS reduces this value to 45%, with the remainder being unfermented sugars, proteins, amino acids and glycerol. The dominant mineral cations include potassium, calcium and magnesium.

It is important to understand the characteristics of vinasse because this information gives insight into disposal limitations and potential processes that could be used for its treatment. For instance, the high organic content makes vinasse a suitable substrate for biotransformation processes such as anaerobic digestion which will result in the production of biogas as an energy source. In addition, physico-chemical processes such as multi-effect evaporation and ion-exchange can be used to reduce the high water and salt content in vinasse. This will reduce effluent transport costs (Carvalho, 2011) as well as result in the recovery of a water stream for either domestic or commercial applications.

2.4 Vinasse Treatment Processes

Distillery effluents have a high-water content which results in high volumes and increased handling and transportation costs. Water recovery from vinasse can be achieved through conventional evaporative processes or membrane technologies. Evaporative processes result in a volume reduction which results in a savings with regards to handling, storage and transportation costs (Carvalho, 2011). Membrane technologies such as micro- and ultrafiltration as well as reverse osmosis may lead to relatively high salts and contaminant rejection rates. This results in a permeate stream that is essentially water with a low concentration of contaminants, and a concentrated reject stream (retentate) that is rich in salts, volatile acids and organic matter (Nataraj et al., 2006). While water recovery processes are beneficial, they are more often constrained by fouling due to the high organic content and total dissolved solids (TDS) concentrations in vinasse. Biological treatments such as aerobic and anaerobic digestion have been used successfully to reduce the organic content and TDS concentrations (Bick et al., 2012).

The production of energy from vinasse in the form of biogas through biological treatments has been popularised over the past three decades (Moraes et al., 2014). This is mainly achieved through anaerobic approaches. Anaerobic systems are preferred as they are able to handle high-strength wastewaters with elevated COD and BOD concentrations. An added advantage is biogas production. In addition to biogas, anaerobic systems have 50% lower sludge production compared to aerobic processes which result in excessive sludge production (Lier et al., 2008). Higher operating costs due to aeration, sludge handling, and temperature control associated with aerobic digestion are also incurred. Anaerobic systems, on the other hand, are economically attractive due to their low energy demands, higher biogas yields and the production of sludge that can be commercialized (Hamza et al., 2016; Lier et al., 2008).

Vinasse has a high concentration of inorganic salts, especially potassium (see Table 2.1). The high potassium content has its benefits and demerits depending on the vinasse disposal or treatment method. When used as fertilizer, the potassium is beneficial as it is an important plant macronutrient. However, when used as an animal feed supplement, the high salinity may result in digestive tract problems in ruminants (Christofoletti et al., 2013). High potassium concentrations may also disrupt microbial activity during the biological treatment of vinasse by

causing osmotic imbalances (Chen et al., 2008). Extraction and purification of these salts from vinasse prior to treatment or disposal is therefore beneficial. Locally, they can be used as a raw material for fertilizer production and consequently reduce the bulk importation of synthetic potassium fertilizers (DAFF, 2015). In addition, desalted vinasse can be used as an animal feed supplement without the risk of causing digestive tract problems in ruminants (Christofoletti et al., 2013). Desalting processes such as ion-exchange and electrodialysis are gaining popularity due to their effectiveness and relatively low costs (Decloux et al., 2002; Zhang et al., 2012).

2.4.1 Biological Treatments for Vinasse

The treatment of vinasse using bioprocess technologies is gaining popularity due to economic and environmental benefits, including (1) energy recovery (2) reduced wastewater strength and (3) increased resource productivity. Biological treatments can be classified into aerobic and anaerobic processes which are distinguished by the environmental requirements of the microorganisms for growth (Moraes et al., 2014).

Aerobic treatments include fungal (Pant and Adholeya, 2007a), bacterial (Jain et al., 2002) and algal treatments (Francisca Kalavathi et al., 2001) which are commonly used as secondary treatments to AD effluents. They are useful in degrading recalcitrant polymers, and decolorization of the vinasse effluent. However, they are susceptible to contamination which could result in huge financial losses (Shayegan et al., 2005).

2.4.2 Anaerobic Digestion for Vinasse Treatment and Value Creation

Anaerobic digestion is the most common biotransformation route for distillery wastewaters (Moraes et al., 2014). It is a complex process where multiple subset communities within the microbial community interact synergistically to catalyse the reactions to transform the complex substrate to methane, carbon dioxide and hydrogen (Mohana et al., 2008). AD typically involves four key steps: (1) hydrolysis, (2) acidogenesis, (3) acetogenesis and (4) methanogenesis (Seadi et al., 2008). Hydrolysis involves the breakdown of complex components in the substrate such as polysaccharides, proteins and lipids to monosaccharides (glucose, dextrose), amino acids and fatty acids as well as glycerol. This process is often catalysed by enzymes secreted by hydrolytic microbes (Yu et al., 2013). Hydrolysis products are then anaerobically fermented by acidogenic bacteria. This results in the production of volatile fatty acids (butyric, propionic, acetic and valeric acid) as well as carbon dioxide and hydrogen. The VFA are then converted to acetic acid by acetogenic bacteria in acetogenesis. Acetic acid is then degraded by aceticlastic methanogens to methane and carbon dioxide. This occurs in methanogenesis where hydrogen is also converted to methane and water by hydrogenotrophic methanogens (Seadi et al., 2008). Advantages of this process include low sludge volume production, low energy requirements and the production of biogas (dos Reis et al., 2015). Anaerobic digestion is sensitive to disturbances in the organic loading rate and substrate composition. These may lead to the accumulation of VFAs and pH imbalances that decrease methane yields and may causedigester failure (Barros et al., 2016). AD is considered as a consolidated technology suitable for the treatment of waste streams containing a variety of substrates. It involves a multitude of simultaneous biochemical reactions driven by a consortium of micro-organisms (Donoso-Bravo et al., 2011). These microorganisms, in the absence of oxygen, are responsible for the bioconversion of carbohydrates, proteins and other complex recalcitrant material found in the biomass to a mixture of gases termed biogas (CH_4, CO_2, H_2, NH_3 and H_2S). Inorganic carbon, nitrogen and

phosphorus compounds are further mineralized to species ready for uptake by plants thereby making the digestate a more effective fertilizer (Moraes et al., 2014).

2.4.2.1 Reactor Considerations for AD of High Strength Liquid Effluents

Anaerobic reactor configurations and process conditions depend on the type of substrate and its composition. Vinasse is a suitable candidate for AD with its high organic content in terms of COD and BOD (dos Reis et al., 2015; Moraes et al., 2015). However, it has a relatively low total solids content, between 4 and 7%, which would result in a very large stirred tank reactor to maintain reasonable retention times to allow for sufficient digestion (Barros et al., 2016; Janke et al., 2015). Stirred tanks are therefore unsuitable for the bioconversion of vinasse. For high water content substrates, biomass retention is important. Biomass retention allows for the decoupling of solids retention times (SRT) and hydraulic retention times (HRT) (Janke et al., 2015). This could be done using upflow anaerobic sludge blanket (UASB) reactors that retain the biomass to facilitate elongated SRTs. A further advantage of these reactors is that they are run continuously. This results in significantly lower HRTs and reactor size.

Various AD reactor configurations and process conditions have been investigated. These include studies into feed loading rates, decoupling of microbial interactions and effluent recycling on overall performance. More recently, the separation of the acidogenic and methanogenic stages in the AD of vinasse under thermophilic conditions was studied (Djalma Nunes Ferraz Júnior et al., 2016). This configuration consisted of two UASB reactors (acidogenic and methanogenic) which resulted in a total COD reduction of 96% at a maximum OLR of 25 kg $CODm^{-3}d^{-1}$. This configuration allowed for maximization of the methane yield to 0.32 $L\text{-}CH_4.g^{-1}COD_{removed}$, which is 91.4% of the maximum theoretical methane yield (0.35 $L\text{-}CH_4.g^{-1}COD_{removed}$). Another study conducted showed that increasing OLR and effluent recirculation in the mesophilic AD of vinasse resulted in downward trends on the methane yield and COD reduction (Barros et al., 2016). Recirculation of the effluent reduced the COD conversion to methane by 39% and this was attributed to the accumulation of recalcitrant organic material in the reactor feed. A low methane yield of 0.185 $L\text{-}CH_4.g^{-1}COD_{removed}$ at an OLR of 7.5 kg $CODm^{-3}d^{-1}$ was recorded. This was only 53% of the maximum theoretical methane yield. These results show that the accumulation of recalcitrant and inhibitory compounds may lead to decreased AD efficiency and digester failure.

2.4.2.2 Process Considerations for Vinasse AD

The presence of inhibitory compounds and changing operating conditions such as pH and temperature affect the performance of AD systems. The major inhibitory compounds include volatile fatty acids, ammonia, inorganic salts (K, Ca, Mg, Na) and phenols (Chen et al., 2008). The compounds, depending on their concentrations, disrupt microbial activity in several ways such as dehydration, upset of osmotic balances (salts) and cell membrane destruction (phenols) (Hierholtzer and Akunna, 2014). Varying digester pH is often caused by the accumulation of free ammonia which is inhibitory to methanogens and results in over 50% reduction in activity at concentrations above 5 g/L. This is often accompanied by a reduction in NH_4^+ ions in solution and an accumulation of VFA which causes a decline in the pH. These counteracting effects of VFA and NH_3 bring about an inhibited steady state where methane yields are low (Angelidaki et al., 1993). Understanding the composition of the substrate before biological treatment is therefore important to establish the necessity of pre-treatment processes to remove inhibitors to optimise process conditions for maximum efficiency.

2.4.2.3 Economic Considerations for AD

Despite the disadvantages and sensitive nature of anaerobic digestion, it remains a relatively affordable process for the degradation of organic matter, with the added benefit of value recovery through biogas. The initial start-up investments arise from the equipment purchases as well as the working capital (Barros, Duda and Oliveira, 2016). Operating expenses are low. They include labour costs as well as the cost of alkaline dosing for pH control. In the case of vinasse, AD is reported as the most cost effective biomass to energy option compared to have high energy combustion or gasification alternatives (Rein et al., 2011). The revenue generating biogas produced from AD may either be converted into electricity and heat using combined heat and power cycles or alternatively upgraded through physical, chemical or membrane technologies to biomethane to be injected into the gas grid for commercial use.

2.4.3 Biogas utilization

The biogas produced from the AD process is a potential renewable energy source with a calorific value that lies between 19 and 23 kJ/L (Ryan *et al.*, 2009). Owing to this, it has several uses ranging from electricity production to transportation fuel. In South Africa, the most common applications are electricity production using CHP systems (Section 2.4.3.2) and generation of heat through combustion in boilers (Section 2.4.3.1). Alternative direct use and upgrading options for biogas utilization in industry are further presented in Sections 2.4.3.3. The latter includes discussion on amine scrubbing and membrane processes.

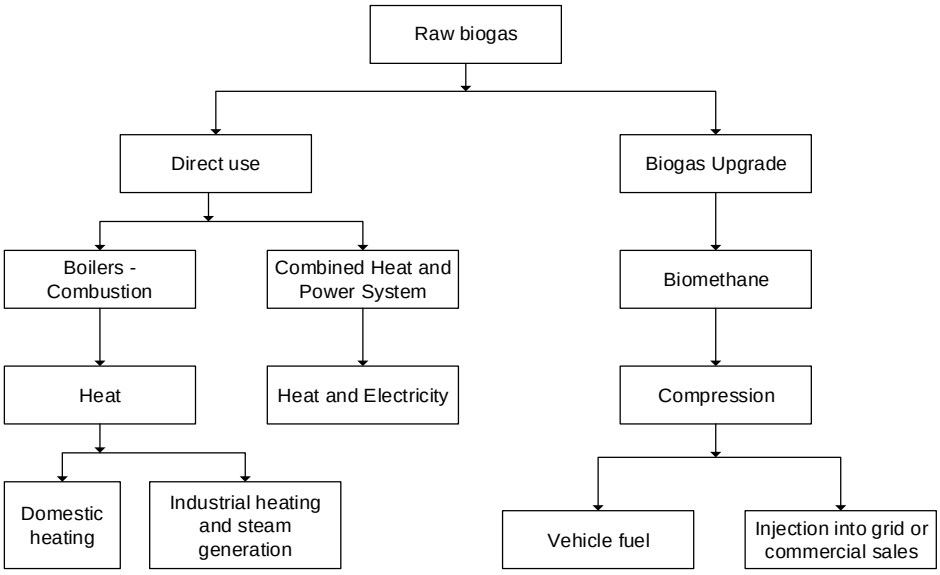

Figure 2.2: A summary of biogas utilization options (Seadi et al., 2008)

2.4.3.1 Direct Combustion and Heat Production

Biogas can be directly combusted in boilers to produce heat. These boilers do not require high quality gas; however, it is important to maintain a low concentration of H_2S to prevent severe environmental pollution through release of SO_2 (Nguyen, 2014). In large scale commercial plants, the heat produced can be used for steam generation or digester temperature control. Small scale biogas utilization on farms may include cooking gas and space heating (Nguyen, 2014).

2.4.3.2 Combined Heat and Power Systems

Combined heat and power generation is a popular and typically highly efficient method of biogas utilization. CHP engines are used for this purpose and typically consist of a compression system, fuel injection and combustion chamber, and a turbine for electricity generation. Heat is then often recovered from the off gas and used to generate steam (Magnusson, 2011). Prior to its utilization, it is important that the gas be dried and conditioned as engines have varying thresholds for water and H_2S. The total efficiency (thermal and electrical) ranges between 85 and 90% with the remainder accounted for in energy losses to the environment through noise and heat (Seadi et al., 2008). Despite the high reported efficiencies, operating a CHP requires a steady biogas flowrate. Erratic flowrates may lead to unstable voltages which present a safety hazard. This can be solved through gas storage as a buffer to facilitate constant gas flow into the CHP system.

2.4.3.3 Biogas Upgrading

Biogas is largely composed of CH_4 and CO_2 which account for 65 – 70% and 25 – 30% by volume, respectively. The remaining 5 to 10% may consist of H_2S, H_2O, NH_3, siloxanes and other inert gases. Of these gases in the mixture, only CH_4 contributes to the amount of energy the biogas possesses (Wheeler et al., 1999b). To increase the calorific value of the gas and make it suitable for commercial use as a vehicle fuel or as a substitute for natural gas, it is necessary to remove CO_2 as well as contaminants such as H_2S, NH_3 and siloxanes (Axelsson et al., 2012).

Biogas upgrading is the process by which CO_2 is removed from the biogas mixture to form biomethane with a purity of 95 – 97%. Removal of carbon dioxide is done to increase the calorific value of the biogas (22 kJ/L) to natural gas standards (38 – 40 kJ/L) (Ryckebosch et al., 2011). However, a loss of methane is common with CO_2 removal (Nguyen, 2014). Removing gaseous contaminants prevents corrosion of equipment and gas pipelines as well as the release of harmful oxides upon combustion. Dehydration of the gas is also key in controlling the dew point, and preventing condensation.

Several technologies have been developed for biogas upgrading. These include physical and chemical absorption techniques, pressure swing adsorption, cryogenic separations and membrane technologies. Of these, cryogenic separations are least common due to the high energy requirements for refrigeration.

i. Water Scrubbing

This separation technology harnesses the differences in solubility between the methane and carbon dioxide in water. Carbon dioxide is 25 times more soluble than methane at ambient conditions. In addition, its solubility in water is a strong function of pressure and temperature. Lower temperature and higher pressures increase the solubility of CO_2 (Cozma et al., 2013b). In this process, raw biogas is compressed to ca. 10 bar and is fed to the bottom stage of an absorption column packed with plastic or metal pall rings. Water at 10 bar is fed at the top stage. Through mass transfer, the CO_2 moves into the liquid phase which is recovered at the bottom stage. Biomethane is recovered at the top stage with purity of 95% (Axelsson et al., 2012). Further compression of the gas may be done for storage or sale purposes. To reduce methane losses, the CO_2 rich water stream leaving the absorber is depressurized in a flash column from 10 to 3 bar. This causes a release of gases, mostly CH_4, CO_2 and water vapour which may be recycled to the water absorber.

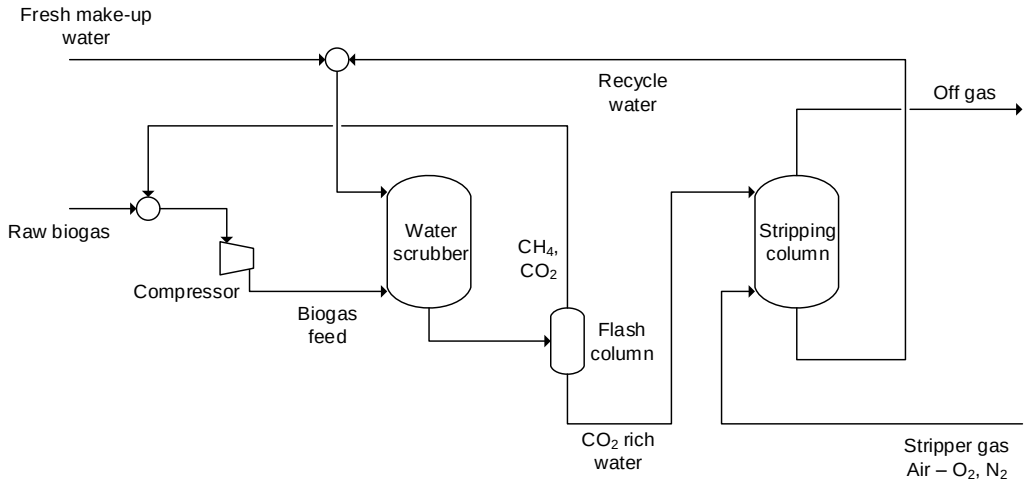

Figure 2.3: A simplified block flow diagram of the water scrubbing process (Axelsson et al., 2012)

The CO_2 rich water stream leaving the flash column may be regenerated in an air stripping column depending on the availability of water. Air is fed at ambient pressure at the bottom stage and counter-currently strips the CO_2 and other contaminant gases from the water. The off gas leaving the top of the stripper column is often released to the atmosphere. Regeneration of the water leads to a more sustainable process. However, it is necessary to include a fresh water make up stream to cater for lost water and a purge to prevent a build-up of inert gases in the system. It is estimated that 1000 m^3 of biogas requires a water recirculation loop of 200 m^3 (Axelsson et al., 2012).

Physical absorption using water is the simplest biogas upgrading technology as it does not involve any hazardous chemicals or extreme operating conditions (Leme and Seabra, 2017). In addition, regeneration and recycling of water makes the process sustainable and economical. However, one notable disadvantage is that absorption of CO_2 decreases solution pH and may lead to corrosion especially in systems with elevated H_2S concentrations (Nguyen, 2014).

ii. Amine Scrubbing

In this process, aqueous chemical solutions of amines are used in the absorption process. The amine solution chemically binds with CO_2 in a reversible reaction. The most common amines used are monoethylamine (MEA), diethylamine (DEA) and monodiethylamine (MDEA) (Kasikamphaiboon et al., 2013). Raw biogas is fed to the bottom stage of the absorption column at ambient temperature and pressure. The gas is contacted counter currently with the amine solution coming in from the top stage. The reaction is exothermic and increases the solution temperature from 30^{o}C to approximately 55^{o}C (Axelsson et al., 2012). This increase in temperature is, however, not thermodynamically advantageous as CO_2 solubility decreases.

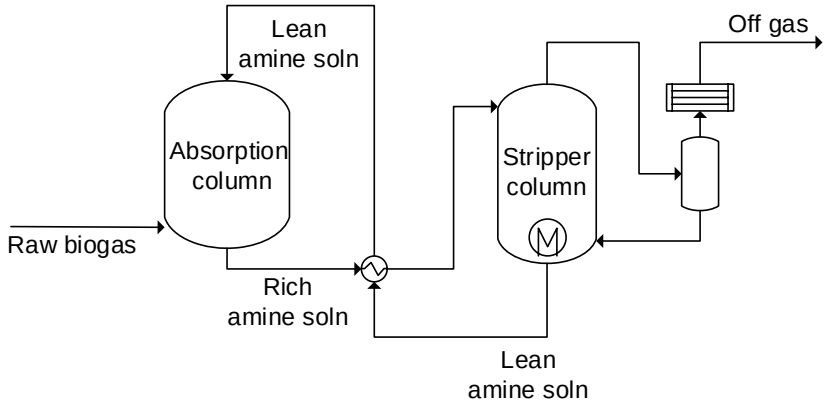

Figure 2.4: A simplified block flow diagram of the amine absorption process (Axelsson et al., 2012)

The upgraded gas exits the top of the absorber column and may be compressed for further applications. The CO_2 rich amine solution is regenerated in a stripper column where it is contacted with steam. CO_2 is released throughout the column and leaves through the top stage. The stripper is fit with a partial reboiler to generate steam at 130^{o}C and to boil part of the amine solution.

The use of chemical absorption is generally applied to large scale plants. The operating costs are higher compared to water scrubbing due to the additional chemicals needed and energy demands during regeneration (Axelsson et al., 2012). Some advantages, however, include the ability to simultaneously absorb H_2S and operate at a lower pressure of 2 bar compared to water scrubbers.

iii. Membrane Processes

This technology takes advantage of the differences in molecular sizes of the components in the raw biogas. In this process, pressurized biogas is passed through a series of semi-permeable membranes which permeates CO_2 and some other gaseous components. The retentate stream contains mostly CH_4. To avoid major methane losses, permeate from the second membrane in the series is recycled (Nguyen, 2014). Conditioning of the gas to remove suspended particles, H_2S and other impurities is necessary as the membranes are prone to fouling and corrosion (Axelsson et al., 2012).

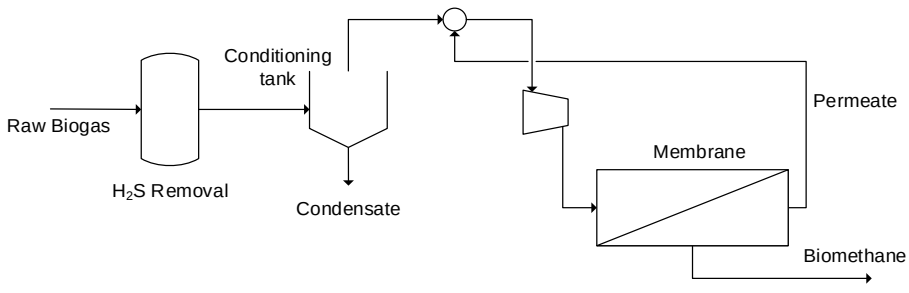

Figure 2.5: A simplified block flow diagram of the gas permeation process (Axelsson et al., 2012)

Membrane separation processes are increasingly gaining popularity due to their simplistic nature and ease of operation. It does not require any water or harsh chemicals to facilitate separation. However, the high capital and operation costs of gas compression and membrane replacement can be disadvantageous (Leme and Seabra, 2017). This technology is highly recommended for low volumetric flowrates and high methane concentrations.

2.4.3.4 Energy Consumption and Cost Comparisons

The level of energy consumption for biogas upgrading is greatly dependent on the heating and compression requirements. It is therefore important to consider the relative energy requirements and normalized costs to adopt the appropriate technology. Water scrubbing and membrane separations occur at high pressures between 10 and 20 bar which increases the electrical energy demand (Leme and Seabra, 2017). On the other hand, amine scrubbing demands a great deal of heat for solvent regeneration. Figure 2.6 shows the energy requirements for chemical and physical absorption, as well as membrane separation technologies amongst others (Axelsson et al., 2012). Although amine scrubbing has the lowest electrical energy demand, it requires a significant amount of heat energy (Figure 2.6). Water scrubbing and membrane processes have similar electrical energy demands as they operate at similar pressures.

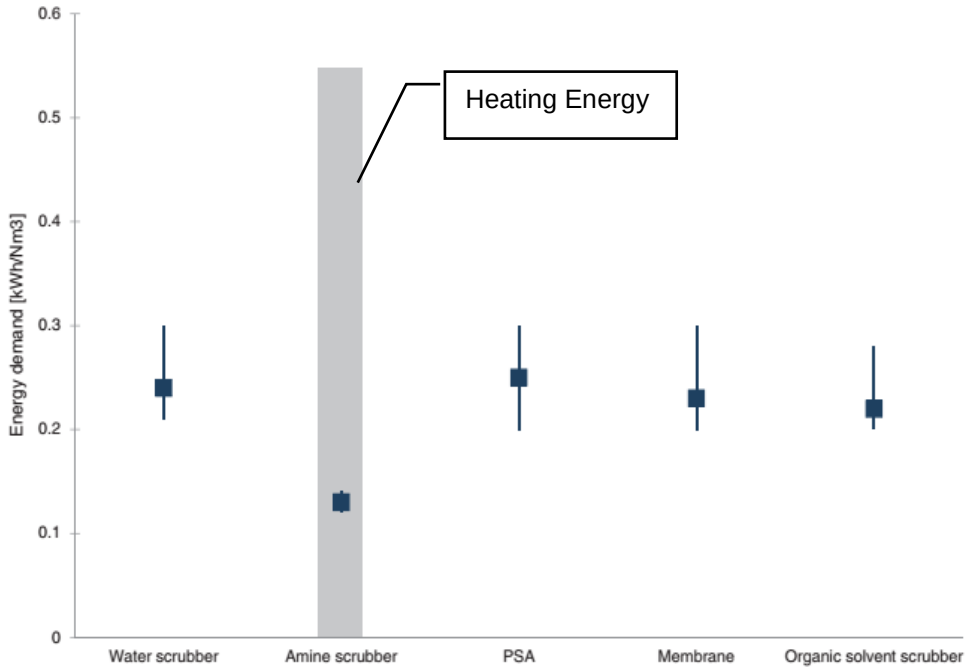

Figure 2.6: The specific energy demand for biogas upgrading technologies adapted from (Axelsson et al., 2012)

The specific unit costs ($/GJ$_{biomethane}$) of biomethane vary for each of these technologies and are largely governed by differing capital investments, labour, chemical requirements and energy costs incurred (Figure 2.7). For the technologies presented in Figure 2.7, there is a 14% cost variation. This variation stems from the differences in total energy and raw material costs. An example is the case of amine scrubbing where the cost is driven up by the heating requirement; however, the total costs remain within range due to lower electrical energy costs. Water scrubbing on the other hand has higher electrical energy costs compared to membranes and amine scrubbing due to solvent (water) cooling requirements in addition to the energy required for raw biogas compression. Another notable factor is the cost of membrane replacement (CO_2 media). This significantly impacts the specific unit cost of membrane technologies which would have otherwise been the lowest (<30 R$/GJ$_{biomethane}$) (Leme and Seabra, 2017). Aside from costs, factors that need to be considered when selecting biogas upgrading processes include safety, availability of equipment, and scale of processes.

This will facilitate the generation of an optimized process design that delivers the required result.

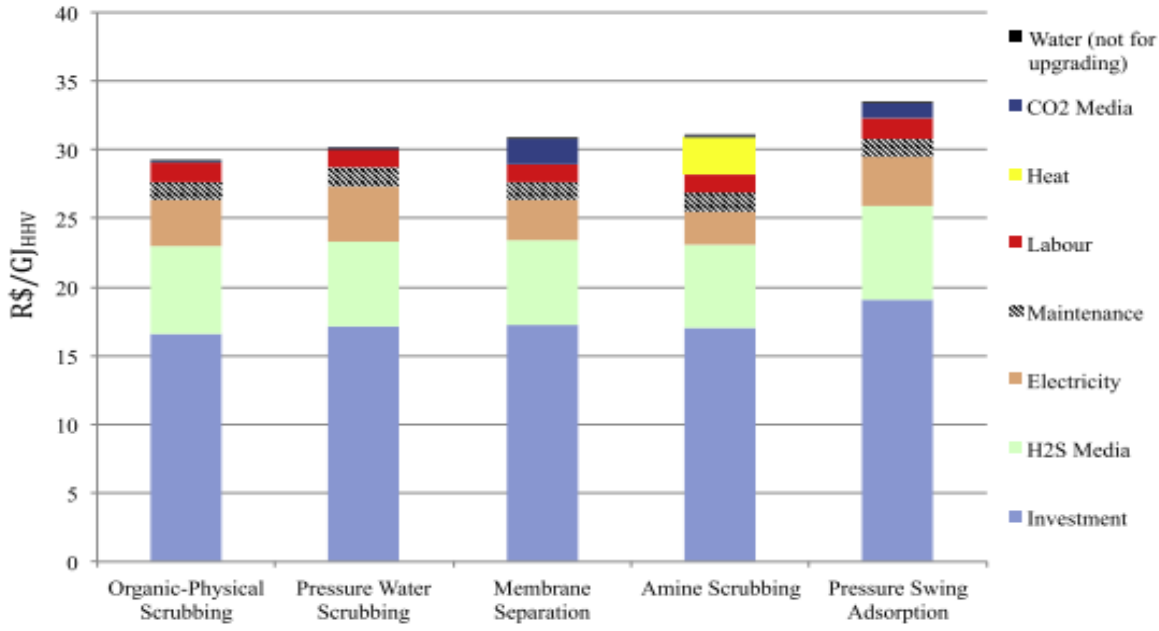

Figure 2.7: A breakdown of the specific unit costs for biogas upgrading processes adapted from Leme and Seabra (2017)

2.4.4 Desalting Processes

Vinasse has a relatively high concentration of potassium salts (11 g/L) in the form of phosphates, potash and sulfates (Wilkie et al., 2000). The concentration of these salts above certain thresholds is suggested to negatively affect biological treatment processes such as AD through inhibition of microbial activity (Kugelman and Mccarty, 1965). In addition, elevated salt concentrations may cause digestive complications if the raw vinasse is used as an animal feed supplement. The use of vinasse as a fertilizer may also be compromised owing to the risk of nutrient overloading in the soil due to high potassium concentrations (Christofoletti et al., 2013). Extraction of potassium salts from vinasse may mitigate these problems and potentially provide an additional revenue stream.

Several laboratory and pilot scale studies on vinasse desalting techniques have been conducted (Decloux et al., 2002; Y. Zhang et al., 2012). One promising technology is strong acid ion exchange where potassium ions are adsorbed onto a resin packed inside a column. In this technology, a styrene series ion exchange gel resin, ZGC108, can be used (Zhang et al., 2012). This general sodium-based resin contains a sulphonic group (SO^3H^-) and has an overall ion exchange capacity of 2 mmol/ml. Potassium ions in the vinasse are adsorbed onto the resin, after which a strong acid eluent is used to regenerate the resin. Potassium ions in the eluent are then recovered through heat crystallization in a stirred tank reactor. K_2SO_4 crystals are then recovered through membrane filtration (0.45 μm). The choice of acid eluent used to regenerate the resin is dependent on the specific desorption capacity. With increasing acid strength, higher capacities are achieved as strong acids dissociate more readily compared to weak and intermediate acids. At H_2SO_4 concentrations of ca. 0.4 mol/l, 99.6% of the potassium can be desorbed from the resin with 93.2% of the potassium sulfate crystallizing.

Another promising technology is electrodialysis. This involves the transport of salt from the diluate (wastewater) to the concentrate through a semi permeable membrane by applying a potential difference (Strathmann, 2010). In a study by Decloux et al. (2002), pre-treatment of vinasse through filtration was necessary to reduce the turbidity. A 75% reduction in potassium ion concentration was achieved with a further favourable 50% reduction in the initial calcium and sodium ion concentrations, which migrated across the membrane into the concentrate.

As a pre-treatment process for the desalting of raw vinasse, electrodialysis may not be preferable. The raw vinasse may cause severe fouling of the membranes (Kim, 2011). Although ion exchange resins are less susceptible to fouling, it is postulated that the energy demands arising from pumping and heating crystallization (Zhang et al., 2012) may make this process unfeasible. As such, it may be necessary to define or establish the threshold salt concentrations at which the salts become inhibitors in AD, toxic to animals or unfit for land disposal. This will dictate the necessity and scale of the pre-treatment processes.

2.4.5 Water Recovery Processes

The water present in the raw or digested vinasse can be recovered and repurposed for applications such as feed dilution, biogas upgrading and boiler feed water (Tewari et al., 2007). It can also be used as a nutrient supplement for fungal and algal bioprocesses depending on the residual nitrogen and phosphorus concentrations (Pant and Adholeya, 2007b). Dewatering the vinasse not only reduces its volume, but results in a concentrate that can be transported easily and used as a fertilizer. Two common dewatering processes are multi-effect evaporation and reverse osmosis.

Although multi-effect evaporation on an industrial scale is commonly used in sugar refining (Rein, 2007), it has also been implemented in Brazil for the reduction (75%) of vinasse water content (Carvalho, 2011). In this set up, vapour recovered from one evaporator was used as an energy source for the next evaporator. With a feed of 100 m^3/h of vinasse, 80 m^3/h of condensate (water) and 20 m^3/h of concentrated vinasse was recovered with a solids concentration between 20% and 25% (m/v). The savings accrued in the Brazilian distillery from the concentration of vinasse were quantified through an economic distance evaluation. Increasing the effluent solids concentration caused a decrease in the transportation costs due to significant volume reductions. However, concentration of the vinasse above 25% did not lead to higher savings due to increased capital and operational energy costs of the evaporation plant.

The common alternative to evaporation is the use of membrane processes. One such process is reverse osmosis (RO) which could theoretically recover 99% of the water (Nataraj et al., 2006). It is a pressure driven membrane process used to separate solute and solvent by order of molecular size. RO requires elevated pressures to overcome the osmotic pressure of the fluid which may lead to high capital and operating costs (Ryan et al., 2009). The membranes are also prone to fouling which is mitigated by coupling RO with a pre-treatment using micro-filtration (MF) or nano-filtration (NF). These techniques ensure the removal of suspended solids and heavy molecules prior to the RO process.

2.4.6 Physico–Chemical Treatment Processes

Biological treatment of vinasse and other substrates results in the concentration of recalcitrant organics and polymers such as phenols and melanoidins in the effluent which are responsible for the dark brown pigment (Barros et al., 2016). The dark brown pigment reduces sunlight

penetration into water bodies when vinasse is freely disposed into water bodies. In addition, the polymers and recalcitrant substances may lead to severe fouling of membranes and resins.

One process to decrease the dark brown colour in vinasse is coagulation and flocculation. During coagulation, iron or aluminium salts are used to decrease the negative charges on the colloids and reduce their repulsion forces. This promotes collision between the colloids to form flocs which then join to form larger flocs. Coagulants such as ferric hydroxysulfate have been used to successfully decolorize bio-digested vinasse. Coagulation and flocculation has several drawbacks. The reagents required are expensive, corrosive and difficult to store and handle (Ryan et al., 2009).

Electro-coagulation is an alternative process to chemical coagulation. It is advantageous as it results in less sludge formed compared to conventional coagulation (Satyawali and Balakrishnan, 2008) In addition, it does not require expensive and corrosive reagents. Instead, an electrochemical reactor is used with electrodes that provide the sacrificial ions. A potential difference is used to promote removal of ions from solution and consequently precipitation of the colloids to result in a decolorization of up to 96%.

2.5 Integration of Vinasse treatment processes

Integration of the vinasse treatment technologies using a biorefinery approach is beneficial from both economic and ecological perspectives. The volume of disposed waste is reduced which, in turn, promotes sustainable biofuel (Ryan et al., 2009). High energy biogas from vinasse AD can be used for electricity generation via combined heat and power plants or biomethane production through upgrading processes. Implementation of either of these strategies has been reported to increase the profitability of vinasse AD plants through cost savings on electricity and vehicular transport fuels (Fuess and Zaiat, 2017; Moraes et al., 2014). However, this is dependent on the external factors such as the availability of biomethane powered trucks and the presence of an electrical grid feedback system.

Products of value such as potassium extracted through pre-treatment processes can be commercialized to further increase the performance of the AD process and profitability of the integrated process (Lameloise et al., 2015). Several post-treatment processes may be implemented for the recovery of decolorized water and nutrient rich concentrates to be used as fertilizer. Physico-chemical treatments such as coagulation and flocculation can be used to decolorize (Guerreiro et al., 2016) the digested vinasse prior to membrane treatment via reverse osmosis for water recovery. Alternatively, the digestate can be further treated aerobically to reduce the organic content and then freely disposed after sufficient dilution with fresh water (Ryan et al., 2009) (Figure 2.8). Thermal treatments such as spray-drying and evaporation may also be used to treat raw or digested vinasse. However, these processes are often energy intensive and expensive thereby invalidating their economic feasibility (Ryan et al., 2009). The various pre- and post-treatment options are summarized in Figure 2.8 that is adapted from Ryan et al. (2009),

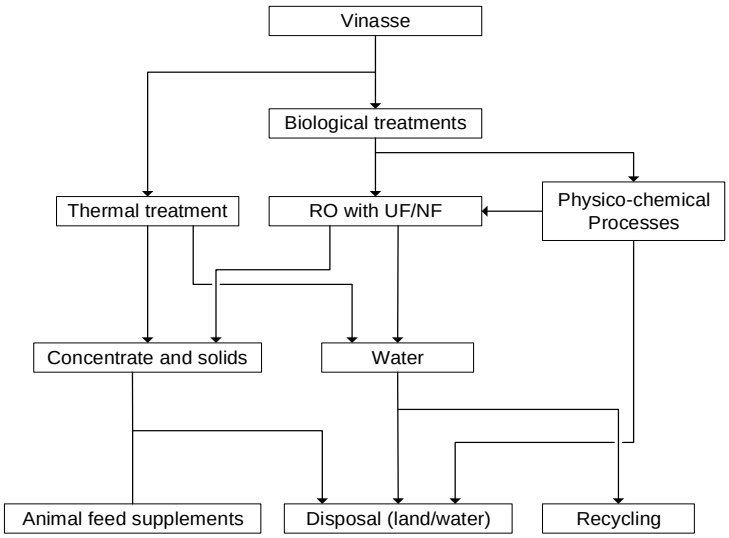

Figure 2.8: A schematic showing vinasse treatment process routes (Ryan et al., 2009)

The choice of an appropriate treatment route depends on the feed composition, economic feasibility and the desired products of value. Modelling these processes on simulation platforms can provide estimates on the scale, energy requirements, productivities and potential bottlenecks (Donoso-Bravo et al., 2011). From review of the literature, it is clearly seen to be important to develop models that closely mimic reality to obtain credible estimates and results. However, this can be a challenge especially with biological processes which involve simultaneous reactions typically influenced by many internal and external factors (Yu et al., 2013). Of the treatment technologies discussed in Section 2.4, simulation of anaerobic digestion is known to be fairly complex owing to the mix of simultaneous reactions and wide range of influencing variables such as pH, temperature, substrate and inhibiting ion concentrations. Additionally, it is a 3-phase (solid, liquid and gas) process which requires mass transfer and activity coefficient modelling to accurately represent the interaction between the gas and liquid phases.

Several scholars have developed models for the anaerobic digestion of waste substrates with varying degrees of complexity (Angelidaki et al., 1993; Batstone et al., 2002; Symons and Buswell, 1933). The models typically consist of material flow algorithms either through stoichiometric reactions or COD balances coupled with kinetic equations to predict microbial growth. While implementation of the models on software platforms may be difficult owing to the resulting differential equations, they have shown to predict process parameters and results such as biogas yields, effluent concentrations and pH quite accurately (Barrera et al., 2015; Koch et al., 2010; Rajendran et al., 2014).

2.6 Anaerobic Digestion Modelling

Approximately 2,200 large scale AD plants are in operation worldwide, highlighting the increasing need for developing accurate, representative, mathematical models to simulate these mechanisms (Lauwers et al., 2013). These models should allow for prediction of product yields, substrate consumption and operating conditions. From these, process parameters and costs can be determined to provide an improved understanding of the system with greatly reduced economic risk. This is because the modelling process can be completed internally and in good time at minimal cost as opposed to development of pilot scale plants for the same purpose.

Mathematical modelling of anaerobic digestion has been progressively developed over the past two decades (Angelidaki et al., 1993; Batstone et al., 2002; Ikumi, 2011). Modelling of this process typically involves the translation of the biochemical mechanisms into linear and nonlinear equations which are then solved to obtain outputs in terms of concentration profiles and energy balances (Yu et al., 2013). However, this is complicated by the reactions in AD occurring concurrently, mediated by multiple microbial populations that are modelled in a multistage approach. Owing to this, determining kinetic constants, growth or death rates and other related parameters is challenging, hence their scarcity (Donoso-Bravo et al., 2011). The degree of complexity of any AD model is determined by its purpose i.e. the outputs to be predicted (Yu et al., 2013). In this review, AD models that were assessed for the treatment of vinasse were ADM-1 (Batstone et al., 2002), ADM-3P (Ikumi, 2011), comprehensive AD model (Angelidaki et al., 1993) and a theoretical stoichiometric model (Symons and Buswell, 1933).

2.6.1 Theoretical stoichiometric model

This is a simple 'black box' stoichiometric AD model which predicts the degradation of a well-defined substrate to its products. The products include CH_4, CO_2, NH_3 and H_2S. It was initially developed by Symons and Buswell (1933) to predict the degradation of substrates containing carbohydrates under anaerobic conditions. In this model, the substrate must be accurately defined by its constituent elements (C, H, N, O, and S). Model calibration can be done using experimental data which provides the biogas composition and methane yields composition. The model assumes the stoichiometric equation as presented in Equation 2.1.

$$C_cH_hO_oN_nS_s + y\,H_2O \rightarrow x\,CH_4 + (c-x)\,H_2O + n\,NH_3 + s\,H_2S \qquad \textit{Equation 2.1}$$

where: $x=\frac{1}{8}(4c+h-2o-3n-2s)$ and $y=\frac{1}{4}(4c+h-2o+3n+3s)$

The stoichiometric model proposed by Symons and Buswell (1933) is limited in that it does not explicitly predict intermediate AD products such as VFAs or biomass. The model is most appropriately used when the main concern is predicting the biogas and methane yields as well as composition (Nguyen, 2014).

2.6.2 Comprehensive model for bioconversion of substrates

The model proposed by Angelidaki et al. (1993) presents a framework for the anaerobic digestion of complex wastes (Figure 2.9). It decouples the feed into its constituent carbohydrates, lipid and protein contents. This enables the prediction of process parameters and compounds such as pH (ionic speciation), VFA and ammonia (mass balance) whose monitoring and control is critical for the success of AD. Additional algorithms focused on predicting the effect of free ammonia concentrations on the pH and methanogenic activity, gauged using the biogas yield, are implemented in this model.

Intermediate reactions and products as well as the interactions involved within the 4 stages of AD are included in the model. In each stage, different types of bacteria and archaea are responsible for the organic matter degradation. Inorganic components that influence microbial activity through inhibition feature in this model as well. Further, the characterization of the substrate into the three measurable components allows the model to be used for a wide range of organic wastes. The interaction between the different processes incorporated in the AD model (Angelidaki et al., 1993) is shown in Figure 2.9.

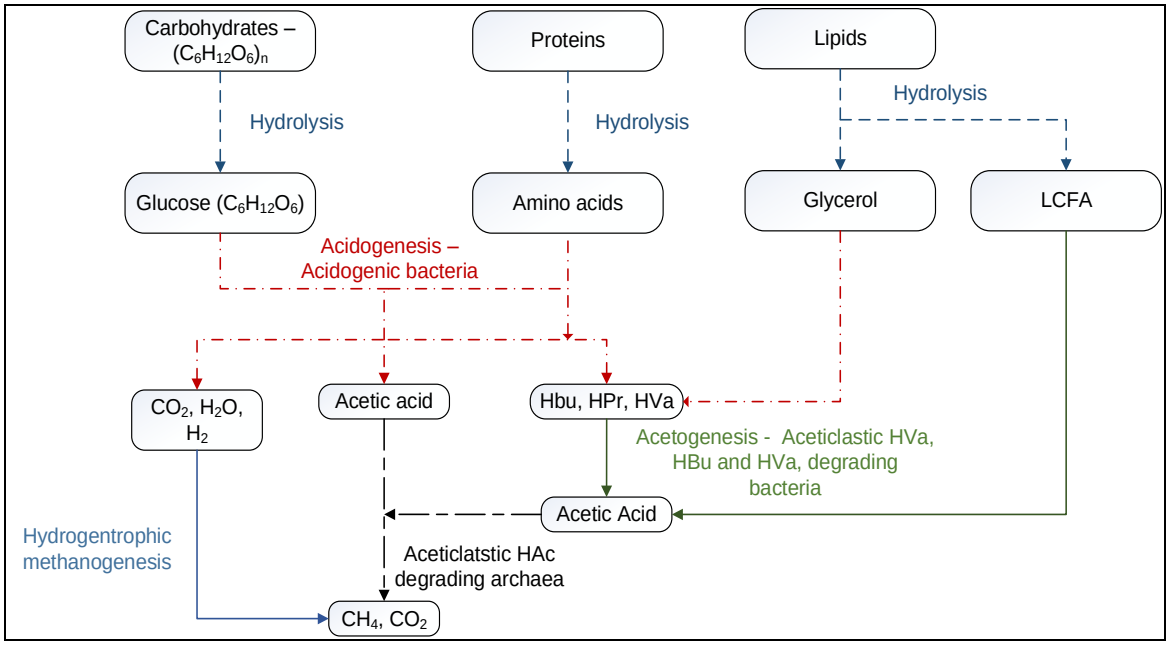

Figure 2.9: A flowchart detailing the flow of materials and overall AD framework used in the model by Angelidaki et al. (1993).

The breakdown of proteins, carbohydrates and lipids to simple sugars, amino acids and oleate occurs via hydrolysis, which is often rate limiting (Vavilin et al., 2008). Hydrolysis was modelled using first order kinetics based on the substrate concentration. Inhibition by VFA in this model during hydrolysis was implemented using inhibition terms based on the total volatile fatty acid concentrations. The simple sugars, amino acids, glycerol and oleate are then broken down into volatile fatty acids, CO_2 and H_2S by acidogens. The VFAs are broken down to by VFA degraders to acetic acid, H_2 and CO_2. Acetic acid and hydrogen are further broken down to methane by methanogens.

The model adopts experimentally determined yield coefficients from Hill (1982) to derive the reaction stoichiometry. The AD mechanism by Angelidaki et al. (1993) is presented below (Sections 2.6.3 to 2.6.6) and has been grouped into three categories which correspond to the substrate constituents. The conversion of material from carbohydrates, lipids and proteins to methane, carbon dioxide and the liquid digestate components is shown progressively for each constituent. It must be noted that these reactions occur in parallel as intermediate production such as VFA are present in the substrate.

2.6.3 Carbohydrates

Complex carbohydrates are broken down into soluble and insoluble carbohydrates through hydrolysis via Equation 2.2. The rate limiting nature of this step owing to the presence of insoluble and inert fractions was incorporated into the model using first order kinetics.

$$(C_6H_{12}O_6)_{total} \rightarrow Y_c\,(C_6H_{12}O_6)_{soluble} + (1\text{-}Y_c)\,(C_6H_{12}O_6)_{insoluble} \qquad \textit{Equation 2.2}$$

Where Y_c represents the biodegradability of the carbohydrate.

The insoluble fraction consisted of organic material such as lignin and structural cellulose that were assumed to be inert. Soluble carbohydrates represented by glucose, are further broken down by acidogenic bacteria into extracellular VFAs such as propionic, acetic and butyric acid, as well as, CO_2 and H_2O.

Although all microbes in this model were assumed to have an empirical formula of $C_5H_7NO_2$, appropriate specifications were added to differentiate their characteristics in terms of growth rates and product yields. Carbohydrate acidogenesis is shown by Equation 2.3 that results the growth of the acidogenic bacteria and formation of volatile fatty acids.

$$C_6H_{12}O_6 + 0.1115\,NH_3 \rightarrow 0.1115\,C_5H_7NO_2 + 0.744\,C_2H_4O_2 + 0.5\,C_3H_6O_2 + 0.4409\,C_4H_8O_2 + 0.6909\,CO_2 + 1.0254\,H_2O \quad \textit{Equation 2.3}$$

VFAs formed from acidogenesis are then converted to acetic acid by propionate (Equation 2.4), butyrate (Equation 2.5) and valerate (Equation 2.6) degrading acetogens.

$$C_3H_6O_2 + 0.0458\,NH_3 + 1.764\,H_2O \rightarrow 0.0458\,C_5H_7NO_2 + 0.9345\,C_2H_4O_2 + 2.804\,H_2 + 0.902\,CO_2 \quad \textit{Equation 2.4}$$

$$C_4H_8O_2 + 0.0544\,NH_3 + 1.7818\,H_2 + 0.0544\,CO_2 \rightarrow 0.0544\,C_5H_7NO_2 + 1.8909\,C_2H_4O_2 + 1.8909\,H_2 \quad \textit{Equation 2.5}$$

$$C_5H_{10}O_2 + 0.0653\,NH_3 + 0.8045\,H_2O + 0.5543\,CO_2 \rightarrow 0.0653\,C_5H_7NO_2 + 0.8912\,C_2H_4O_2 + 0.02904\,C_3H_6O_2 + 0.4454\,CH_4 \quad \textit{Equation 2.6}$$

There are two possible pathways through which methanogenesis occurs (Angelidaki et al., 1993). The first is utilization of hydrogen and CO_2 formed from the acetogenic steps (Equation 2.7 and Equation 2.8) and the second is conversion of acetic acid to methane by acetate degraders (Equation 2.9).

$$2.804\,H_2 + 0.01618\,NH_3 + 0.7143\,CO_2 \rightarrow 0.001618\,C_5H_7NO_2 + 0.6604\,CH_4 + 1.45\,H_2O \quad \textit{Equation 2.7}$$

$$1.8909\,H_2 + 0.0109\,NH_3 + 0.4999\,CO_2 \rightarrow 0.0109\,C_5H_7NO_2 + 0.4452\,CH_4 + 0.978\,H_2O \quad \textit{Equation 2.8}$$

$$C_2H_4O_2 + 0.022\,NH_3 \rightarrow 0.022\,C_7H_5NO_2 + 0.945\,CH_4 + 0.066\,H_2O + 0.945\,CO_2 \quad \textit{Equation 2.9}$$

Hydrogen utilizing reactions were combined with the butyrate degrading reaction (Equation 2.5) in a bid to simplify the mechanism. Although this led to a reduction in model dynamism, the overall effect was assumed to be insignificant as the hydrogenotrophic methanogenic reactions were relatively fast compared to the acetogenic ones (Angelidaki et al., 1993).

2.6.4 Lipids

Lipid, represented by glycerol trioleate (GTO), were broken down to glycerol and oleate (as a representative fatty acid) (Equation 2.10) by glycerol fermenting bacteria (Angelidaki et al., 1993).

$$C_{57}H_{104}O_6 + 3H_2O \rightarrow C_3H_8O_3 + 3C_{18}H_{34}O_2 \quad \textit{Equation 2.10}$$

The glycerol formed is instantly converted to propionate and biomass by the fermentative bacteria.

$$C_3H_8O_3 + 0.04071NH_3 + 0.0291CO_2 \rightarrow 0.04071C_5H_7NO_2 + 0.9418C_3H_6O_2 + 1.09305\ H_2O$$ *Equation 2.11*

The presence of oleate inhibits bacterial processes in AD (Hanaki et al., 1981) and therefore maintaining low concentrations allows for uninhibited lipid degradation (Angelidaki et al., 1993). The overall GTO degradation was obtained by combining GTO and glycerol degradation shown above to obtain Equation 2.12.

$$C_{57}H_{104}O_6 + 1.9065H_2O + 0.04071NH_3 + 0.0291\ CO_2 \rightarrow 0.04071C_5H_7NO_2 + 0.9418C_3H_6O_2 + 3C_{18}H_{34}O_2$$ *Equation 2.12*

The degradation of oleate by the long chain fatty acid (LCFA) degraders results in the formation of acetic acid and hydrogen. Hydrogen utilizing methanogens convert the hydrogen to methane. In this model, these two steps are combined to form the following overall LCFA degrading step.

$$C_{18}H_{34}O_2 + 7.7401\ H_2O + 4.0834\ CO_2 + 0.2537\ NH_3 \rightarrow 0.2573\ C_5H_7NO_2 + 8.6988\ C_2H_4O_2 + 3.4139\ CH_4$$ *Equation 2.13*

The propionic and butyric acid formed in the lipid degradation are converted to acetic acid and carbon dioxide and thereafter to methane via Equation 2.4, Equation 2.5 and Equation 2.9. While the degradation of lipids is well defined in this model, it applicability is constrained to glycerol trioleate as the starting lipid as this model has only been validated when using GTO. There may be deviations in the results with changing lipid compositions in different substrates.

2.6.5 Proteins

The model developed by Angelidaki et al. (1993) used manure as a substrate with the protein composition represented by gelatin as a model protein. It has a molecular formula of $CH_{2.03}O_{0.6}N_{0.3}S_{0.001}$. Proteins are first hydrolysed to amino acids and residual insoluble proteins (Equation 2.14).

$$\text{Proteins} \rightarrow (Y_p)\ \text{Amino acids} + (1\text{-}Y_p)\ \text{Proteins}_{\text{insoluble}}$$ *Equation 2.14*

where Y_p represents the fraction of the protein that was degradable.

Amino acids were then degraded further by acidogenic bacteria to form VFAs. The stoichiometric coefficients used to predicted VFA yields were determined experimentally (Angelidaki et al., 1993) as presented in Equation 2.15. The VFAs are converted to acetic acid and methane via Equation 2.4, Equation 2.5 and Equation 2.9.

$$CH_{2.03}O_{0.6}N_{0.3}S_{0.01} + 0.3006\ H_2O \rightarrow 0.017013\ C_5H_7NO_2 + 0.29742\ C_2H_4O_2 + 0.02904\ C_3H_6O_2 + 0.02286\ C_4H_8O_2 + 0.0013202\ C_5H_{10}O_2 + 0.07527\ CO_2 + 0.28298\ NH_3 + 0.001\ H_2S$$ *Equation 2.15*

As with the lipid degradation mechanism, protein degradation as described by Angelidaki et al. (1993) may be limited to the use of gelatin as the representative. The model takes a black box approach to amino acid degradation and does not describe their individual breakdown of amino acids to VFA through stickland reactions (Ramsay and Pullammanappallil, 2001). An extension of this model (Angelidaki et al., 1993) by Peris (2011) saw the inclusion of stickland

reactions that enabled application of the model to wastes from bioethanol fermentation that had varying concentrations of individual amino acids.

2.6.6 Reaction rates and kinetic data

Growth kinetics in the model by Angelidaki et al. (1993) were defined using a rate limiting approach. This assumes that the slowest steps within AD could be used to define the AD process. For this model, these were hydrolysis, acetogenesis and methanogenesis. The hydrolysis steps (Equation 2.16) were modelled as first order reactions and were inhibited by the total VFA concentrations in the reactor.

$$R_{hyd} = k_0.\left(\frac{k_i}{k_i+\sum VFA}\right).S \qquad \textit{Equation 2.16}$$

In Equation 2.16, k_i represents the inhibition constant associated with VFA accumulation and the substrate is denoted by S (g/L). To simulate anaerobic processes, several algorithms including the Monod (Monod, 1949), Contois (Contois, 1959), Haldane (Lokshina et al., 2001) and Hashimoto (Chen and Hashimoto, 1980) kinetic models have been developed. The abovementioned bio-chemical kinetics are based on the microbial growth and nutrient consumption rates. Owing to the close agreement of experimental data and simulation results (95% confidence interval), the Monod model has been commonly utilized for AD simulations (Yu et al., 2013). In the model by Angelidaki et al. (1993), the acidogenic, acetogenic and methanogenic steps are assumed to adhere to Monod type kinetics with respect to their primary substrates. The growth rates take the form seen in Equation 2.17 as initially described by Monod (1949) and later modified by Angelidaki et al. (1993) to contain additional substrate utilization and inhibition terms.

$$\mu = \mu_{\max}(T).\left(\frac{1}{1+\frac{K_S}{S}}\right).\left(\frac{1}{1+\frac{K_{S2}}{S_2}}\right).\left(\frac{1}{1+\frac{S}{K_{inhibition}}}\right).F(pH) \qquad \textit{Equation 2.17}$$

The ammonia co-substrate was included because all microbial steps require a nitrogen source for growth. This is denoted by the K_{s2} term. Depending on its concentration, ammonia also non-competitively inhibited the methanogenic reactions. The effect of pH was included in the form of a normalized Michaelis pH function that increased or decreased the growth rate of the methanogens depending on the pH.

The hydrolytic constants and maximum growth rates for carbohydrates and proteins as well as VFA degraders are considerably lower (see Table 2.4) compared to the maximum growth rates for the acidogenic microorganisms. This further affirms the rate limiting approach taken by the model where acidogenic reactions were assumed to proceed much faster compared to methanogenic and hydrolytic reactions.

While this model was successful in AD simulations of animal waste, it has some drawbacks that may limit its application to complex wastes such as vinasse, municipal solid wastes and industrial effluents. One major drawback is that it uses compounds including glycerol trioleate and gelatin that may not be present in the above mentioned complex wastes. These wastes may contain other lipids and proteins that degrade differently thereby reducing the applicability of the mechanisms proposed by Angelidaki et al. (1993). Later models including ADM1 (Batstone et al., 2002) have alleviated this problem through characterization of feed constituents by their COD concentrations.

Table 2.4: Kinetic constants and rate data used in the model (Angelidaki et al., 1993)

Kinetic constant	μ_{max} (day^{-1})	K_s (g/L)	K_s (NH_3) (g/L)	K_i (g/L)	K_i (g/L)
Hydrolysis					
Carbohydrates	1	-	-	0.33	-
Protein	1	-	-	0.33	-
Acidogenesis					
Glucose	5.1	0.05	0.05	-	5
GTO	0.53	0.01	0.05	-	5
LCFA	0.55	0.02	0.05	-	5
Amino Acids	6.38	-	-	-	-
Acetogenesis					
Propionic acid	0.49	0.259	0.05	0.96 (HAc)	5
Butyric acid	0.67	0.176	0.05	0.72 (HAc)	5
Valeric acid	0.69	0.175	0.05	0.4 (HAc)	5
Methanogenesis					
Acetic acid	0.6	0.12	0.05	0.26 (NH_3)	5

The introduction of the ammonia inhibition kinetics in this model greatly improved the simulation of AD reactors at high VFA concentrations. While previous models predicted digester failure at high VFA concentrations, this model predicted an inhibited steady state where methane yields remained low through exploring NH_3 and VFA interactions.

2.7 Anaerobic Digestion Model 1

Anaerobic digestion model 1 (ADM1) was developed through the collaboration of expert scholars under the International Water Association (IWA). The aim was to introduce a standardised convention and framework that could be used to model the biodigestion of substrates to produce effluents, methane and other byproducts (Batstone et al., 2002). The approach is similar to the convention proposed by Angelidaki et al. (1993) where complex substrates are broken down into carbohydrates, proteins, fats and inert components. These then undergo the four AD steps of hydrolysis, acidogenesis, acetogenesis and methanogenesis (Figure 2.10). In addition, this model takes into account the breakdown of particulate matter and the presence of active biomass in the substrate. Enzymatic hydrolysis reactions are modelled as first order. Monod-type kinetics are used to model the intracellular microbial reactions which include acidogenic fermentation, acetogenesis and methanogenesis.

A COD balance is used to track substrate degradation in the biochemical reactions, whereas in previous models, such as Angelidaki et al. (1993), conventional reaction stoichiometry and mass balances were used. This makes the ADM1 versatile as most substrates can be characterized in terms of their soluble and insoluble COD. The yield, Monod half saturation coefficients and biomass growth terms are used to compute reaction rates and generate the material balances, thereby eliminating the need for stoichiometric reactions. ADM1 is similar to the model of Angelidaki et al. (1993) in the reaction steps as well as growth rate and inhibition expressions. However, ADM1 is extended to introduce detailed physico-chemical reactions that govern ion speciation for the prediction of pH and gas phase composition. These are relatively fast compared to the biological reactions. Inhibition of acidogenesis by H_2 is also introduced, as is the selective production of VFA depending on H_2 concentration. In addition to cell growth, lysis is also taken into account through the COD balance.

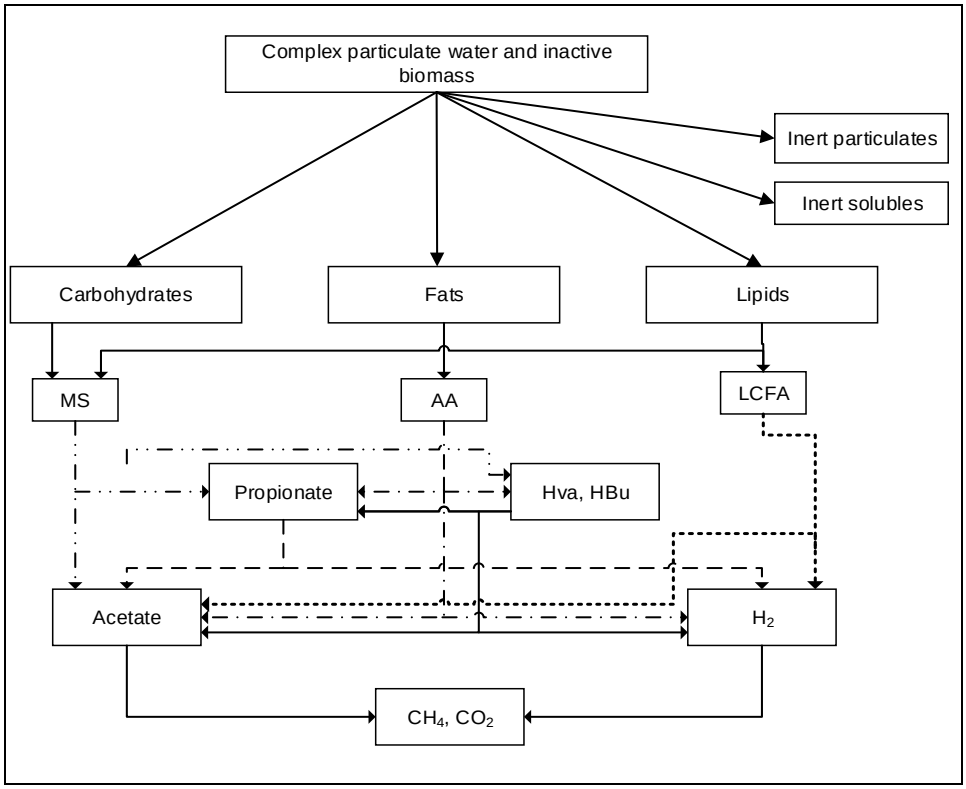

Figure 2.10: A flowchart showing the main pathways followed by material in ADM1 - adapted from (Batstone et al., 2002)

Through modification, ADM1 has been applied to different substrates such as food waste and grass (Nguyen, 2014; Thamsiriroj and Murphy, 2011). The original experimentally determined kinetic constants such as growth rates, saturation and yield coefficients have also been calibrated accordingly to simulate AD of vinasse (Barrera et al., 2015). Although ADM1 has been validated widely, it requires many input parameters, some of which are not easily measured in an industrial context. This makes it suitable for simulation purposes but inappropriate for plant wide process control and optimization (Yu et al., 2013).

2.8 Anaerobic digestion model - 3 Phase

This anaerobic digestion model, developed by Ikumi et al. (2011) on the WEST modelling platform for treatment of municipal wastewater, expanded on the UCTADM1 (University of Cape Town – ADM1) model, a two phase (aqueous-gas) AD model that was developed by Sötemann et al. (2005) as an extension of the ADM1 model. The UCTADM1 model includes hydrolysis, growth and lysis catalyzed by the four microbial populations involved in AD. In this model, sewage sludge is characterized into its elemental C, H, O and N content. The elementally defined substrate ($C_XH_YO_ZN_A$) is then hydrolysed to a model 'glucose' component. The subsequent acidogenic, acetogenic and methanogenic reactions are handled stoichiometrically and are assumed to occur faster than the rate limiting hydrolysis step. The model additionally includes effects of pH on the conversion of glucose to VFAs, thereby predicting digester behaviour under failure conditions.

ADM-3P builds on UCTADM1 through the addition of (1) a detailed characterization of soluble and particulate biodegradable material, (2) an ionic speciation routine for pH prediction and weak acid base chemistry, (3) mineral precipitation processes such as struvite formation and (4) the digestion of waste activated sludge rich in phosphorus (Ikumi et al., 2011). The ionic

speciation sub-routines and mineral precipitation modules were coded separately to reduce stiffness which could lead to dynamic model failure. In this manner, the routine computes ionic concentrations and thereby digester pH at each time step. A schematic of the AD process model implemented in ADM-3P is presented in Figure 2.11 (Ikumi et al., 2011)

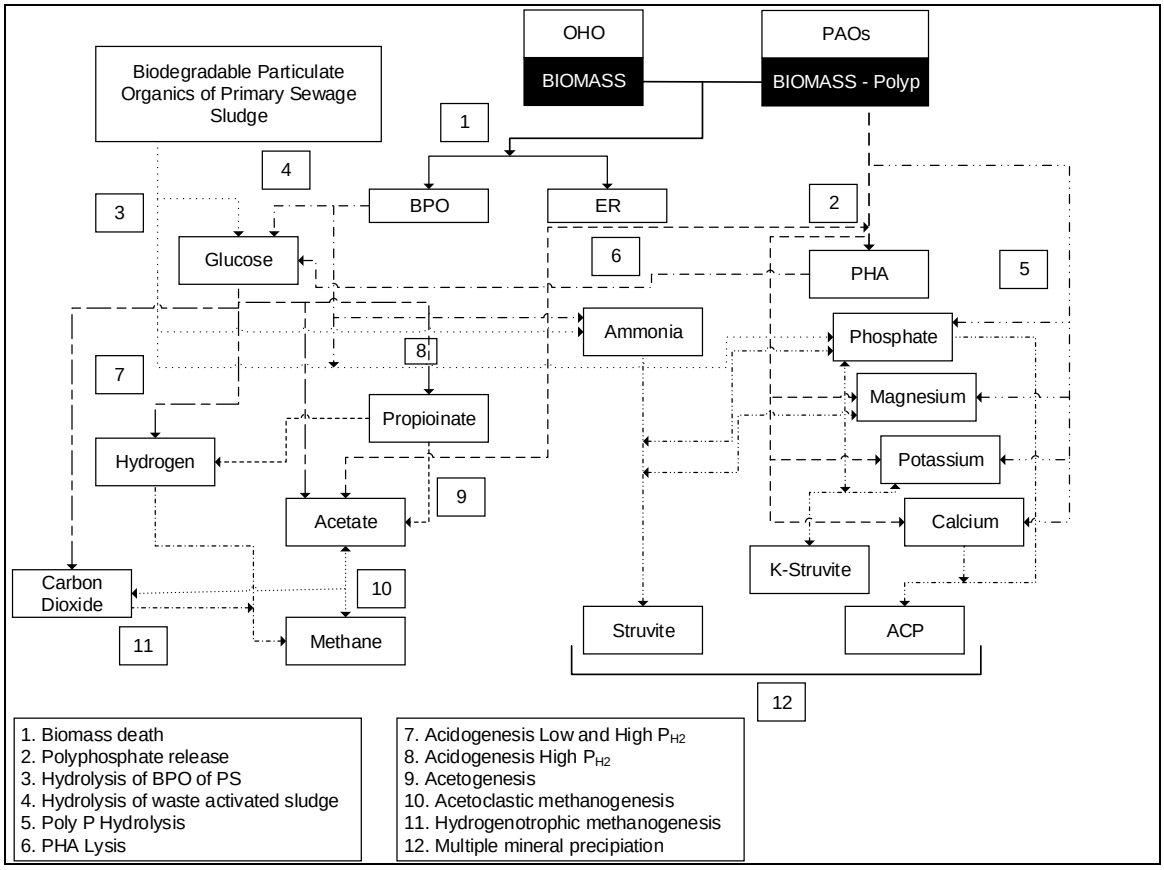

Figure 2.11: Process schematic used in the development of ADM 3P adapted from Ikumi et al. (2011)

The AD process steps in ADM3P can be classified into hydrolysis, polyphosphate release, polyhydroxyalkanoates uptake, acidogenesis, acetogenesis, methanogenesis and cell death (cell lysis) of the respective microbial communities involved. In addition, mineral precipitation and dissolution reactions were implemented so as to simulate digestion of phosphorous rich water accurately. Kinetic parameters were initially sourced from previously published literature values and calibrated by fitting the simulated results to replicated experimental data (Ikumi et al., 2011)

ADM-3P has been used to develop a plant-wide wastewater treatment model which incorporates pre-treatments such as settling and aerobic digestion. The results can be used to influence unit operation design and plant layouts. Although ADM-3P predicts the outcomes from lab scale experiments accurately, it has not yet been used to model industrial plant-wide setups where factors such as fluid dynamics and mixing are pronounced (Ikumi et al., 2011). Further, ADM-3P has yet to be rigorously applied to feed substrates other than municipal wastewater and sewage.

2.9 Comparison of AD Models

The stoichiometric model developed by Symons and Buswell (1933) simplifies the AD process to the conversion of a formulaic substrate ($C_xH_yO_zN_aS_b$) to biogas. It does not model the formation of intermediates (VFAs) and the AD effluents, nor does it account for the molecular components present in the feedstock in terms of specific reactions. This model is applicable when the main focus is the substrate conversion factor and biogas composition. The comprehensive AD model developed by Angelidaki et al. (1993) extended the functionality of the stoichiometric model. It rigorously models the four AD processes to incorporate hydrolysis, acidogenesis, acetogenesis and methanogenesis using reaction stoichiometry that includes a distinction between microorganisms involved in each of the reaction steps. Substrate characterization into carbohydrates, lipids and proteins enables the application of this model to a variety of waste streams. Further to this, empirically determined Monod model parameters including half saturation constants, growth rates and yields can be calibrated depending on the substrate.

ADM1 tracks the degradation of components and formation of products through a chemical oxygen demand (COD) balance and not reaction stoichiometry (Yu et al., 2013). The absence of elaborate stoichiometry may restrict its use to coding platforms as common platforms such as SuperPro Designer and Aspen Plus require well defined stoichiometry. The feedstock characterization in ADM1 requires the definition of quantities such as soluble VFA concentrations that are not easily measured in an industrial context (Ikumi et al., 2011). Assumptions regarding these parameters may introduce error in the AD simulations based on ADM1.

ADM-3P, on the other hand, is a flexible model that incorporates an independent ionic speciation routine and mineral precipitation processes in addition to the typical AD mechanistic steps. It is solely developed in C++ on WEST, a wastewater modelling platform which can be extended to include other biotransformation processes such as activated sludge models. To date, its application has been limited to municipal wastewater.

Through repeated studies and modifications, kinetic parameters and equations for anaerobic digestion models can be well calibrated to make them suitable for most waste substrates. Parameter estimation techniques have been used to calibrate ADM1 kinetics to suit different substrates including vinasse (Barrera et al., 2015) and food waste (Nguyen, 2014). Direct and cross validation with experimental data will further ensure that the intermediate and final AD simulation results obtained are credible and representative of the systems on the ground.

2.10 Review of Simulation Software Packages

Using computer aided software to simulate processes has become an indispensable tool in industrial applications. Simulations provide material and energy balances which aid in the design of equipment for processes (Georgiadis, 2012). Further, design optimizations can be performed through objective functions using these simulation packages by using key operating variables that significantly impact plant operation. In the simulation of dynamic bioprocesses, several software packages have been successfully implemented for this purpose. These include Aspen Plus, SuperPro Designer, gPROMS, Matlab/Simulink and CHEMCAD (Nguyen, 2014).

Although there are various flowsheeting platforms available, simulating bioprocesses remains a challenge. They involve unit operations that are not well defined or established in many

simulation packages (Shanklin et al., 2001). These include bioreactors, fermenters and batch reactors for example. Further, biological systems typically include complex components such as carbohydrates, proteins and long chain polymers whose structures are not well defined and are difficult to simulate in these environments. Unlike chemical process, bioprocesses do not typically rely on chemical and phase equilibria. They contain micro-organisms which rely on biological and physical phenomena which change throughout the operation. The availability of batch and fed-batch operating modes in the flowsheeting platforms must be considered as most bioprocesses operate in these modes. The development of bioprocess simulations therefore require careful consideration of the applied assumptions and their verified representation of the process (Shanklin et al., 2001).

Identifying the intended purpose of the flowsheets before commencing on a selected platform is essential (Georgiadis, 2012). This governs the level of detail required in the model development. Using complementary software to diversify and supplement functions that are not available within the primary software may also be of value when simulating these processes (Nguyen, 2014).

This review investigates the suitability of flowsheeting software in simulating the bioconversion of sugarcane vinasse to energy and fertilizer, considering their merits and shortcomings. Of the five software packages mentioned earlier, SuperPro Designer, Matlab/Simulink and Aspen Plus were selected for review based on their current availability, customizability and successful application in bioprocess modelling in previous studies (Nguyen, 2014; Woinaroschy, 2009a).

2.10.1 SuperPro Designer

This flowsheeting software package was developed for the modelling and simulation of a wide range of bioprocesses. These include, but are not limited to, wastewater treatment, environmental assessments, fermentation and water purification (INTELLIGEN, 2005). Routines for waste minimization and pollution prevention as well as various unit operations such as stirred tanks, plug flow reactors and absorber/stripper columns are present in this simulation package (Malakahmad et al., 2012). Water purification and solids separation modules are also included, further highlighting the appropriateness of the software to bioprocess modeling. Examples of these are its application in ethanol and biodiesel production (Haas et al., 2006) as well as in anaerobic digestion simulations (Malakahmad et al., 2012).

SuperPro is greatly favored by bioprocess engineers as it allows for input of microbial kinetics such as Monod and Michaelis-Menten kinetic models (INTELLIGEN, 2005). The simulation package further contains an economic analysis tool that is used to generate reports on total and operating costs as well as to provide profitability indicators such as the return on investments, payback period and net present values. However, the software has limited thermodynamic information, thereby introducing a certain degree of uncertainty in simulation outputs (Meireles, 2008). A further limitation is the lack of sensitivity analyses features, making evaluation cumbersome when the input datasets are large (Woinaroschy, 2009b). To perform these analyses, an alternate application such as Microsoft Excel is often recommended.

2.10.2 High Performance Programming Languages (HPPL) – Matlab/Simulink, Scilab

Biological process simulations involving reactions, variances in operating conditions, kinetics, stresses due to physical properties and changes in material streams can be formulated as a mixture of partial differential and differential algebraic equations (Georgiadis, 2012). These can then be simulated in programming languages such as Matlab/Simulink and Scilab. These contain ordinary differential equation (ODE) solvers that are used to evaluate material and energy balances to produce concentration profiles as a function of time (Sevella and Bertalan, 2000). Sensitivity and optimization on these platforms are readily done through the adjustment of relevant syntax and objective functions (Sevella and Bertalan, 2000). Modeling anaerobic digestion using ADM1 has been demonstrated successfully in Matlab/Simulink and this is often the preferred platform due to its flexibility. This is because a multitude of parameters can be incorporated with limited constraint (Barrera et al., 2015; Nguyen, 2014).

One disadvantage is that the programming platforms are not equipped with physical and chemical properties of components involved in bioprocesses. However, this can be overcome by linking to open source property databases, thereby increasing the platforms' capabilities or manually inputted into the code of the programme. (Georgiadis, 2012). These platforms have varying capabilities and are flexible. Simulation of specialized unit operations, absent in generic simulation software packages, can be done through unique user defined algorithms. However, this is severely limited by end-user capabilities as high-level programming skills are required.

2.10.3 Aspen Plus Engineering Simulation Package

Aspen Plus is an industrial process modelling and simulation tool developed by Aspen Technologies (Aspen Technology, 2000). It enables the assembly of material, work or energy streams to unit operations resulting in flowsheets which can be run at steady state or dynamic conditions (Nguyen, 2014). The unit operations are models developed to mimic the extensive range of processing units found in industry. Aspen Plus contains relevant processing units such as stirred tank reactors, filters, heat exchangers, pressure regulators, centrifuges and columns which are found in typical bioprocessing plants. These unit operations in Aspen Plus can be customized by the end-user with models that interface with external spreadsheets. Further customization within select processing blocks can be achieved through integration with FORTRAN. Aspen Custom Modeller (ACM) expands the software's capabilities allowing the user to develop customized unit operations that are otherwise unavailable, using the developer coding language (Aspen Technology, 2000).

Aspen Plus contains extensive component databases for chemicals, polymers, electrolytes and solids which are updated by the United States National Institutes of Standards and Technology (NIST). Appropriate physical property methods (equations of state), and Henry's components, which have a major impact on the accuracy of the results, are also specified (Aspen Technology, 2000). One drawback is that complex components and solids involved in biological reactions are absent. However, organizations such as the National Renewable Energy Laboratory (NREL) have created databases for several biological components that can be manually registered in Aspen Plus (Wooley and Putsche, 1996). The software is equipped with an economic analysis feature which generates reports on the capital and operating costs of the flowsheet that are customizable to suit the user's needs (Shanklin et al., 2001). One of the major advantages is that it is user friendly. It permits the gradual build-

up of flowsheets, providing constant feedback with relevant error messages indicating system failure or incorrect input data specification (Shanklin et al., 2001).

Although Aspen Plus contains extensive databases and a wide range of unit operations, it lacks specific modules that allow the input of bioreaction kinetics. However, anaerobic digester modules have been developed on Aspen Plus through integration with FORTRAN (Peris, 2011). Rajendran *et al.* (2014) further developed a Process Simulation Model on Aspen Plus which was validated against existing anaerobic digesters. Biogas processing models have also been developed through gas turbines (Nguyen, 2014).

The suitability of the three simulation platforms for bioprocess modelling purposes varies depending on the pros and cons of each. SuperPro Designer is most preferred for bioprocesses owing to the availability of input specifications for Monod and Michaelis-Menten reaction kinetics as well as batch mode operation. However, it is lacking in sensitivity analyses features. While Aspen Plus contains sensitivity and economic analyses features, it lacks crucial complex components and solids that participate in bioprocesses. High performance programming languages on the other hand are a powerful platform owing to their customizability. Nonetheless, they require a high level of coding knowledge.

2.11 Summary – Literature Review

Bioethanol production via fermentation processes results in the formation of vinasse that is high in organic content and inorganic salt concentration. Vinasse can be used as an animal feed supplement or applied to cane fields as a soil amendment. However, depending on application rates, these practices may be unsustainable due to their potential negative impacts on the environment with repeated exposure to this waste stream.

Biological and physical processes have been used in industry to reduce the organic content and salt concentrations in vinasse. In the context of vinasse, anaerobic digestion is the most preferred bio-transformation reported to date. It reduces the organic content and results in the production of biogas, a potential energy source. Aerobic bio-transformation processes make use of fungal, algal and bacterial systems to degrade recalcitrant polymers and reduce the dark brown pigmentation in vinasse; however, they are mostly suggested as secondary treatments. From the literature, suggested recovery processes for valuable products including water and inorganic salts is sought through physico-chemical processes. Inorganic salts may inhibit microbial activity in AD and can be recovered through pre-treatments using ion exchange and electrodialysis. Dewatering processes such as reverse osmosis and evaporation are often used to reduce the water content in vinasse. The biogas produced can be harnessed for heat and electricity generation via CHP plants. Another alternative is to upgrade the biogas to saleable biomethane to compete with natural gas for utilization as energy sources in the transport sector.

There is a need for integration of these processes to promote resource productivity with concomitant environmental protection. Integration allows the combination of unit operations to form process routes whose performance, resource productivity, energy utilization and feasibility can be determined during the project development phase. Modelling of these integrated process routes facilitates accurate predictions of performance, costs and feasibility. In addition, individual elements and combined configurations can be compared in an efficient, timely and cost-effective manner. Among the biological and physical processes suggested for vinasse treatment, anaerobic digestion is the most complex to simulate. This is mainly due to the presence of multiple microbial groups involved in many simultaneous reactions that are

sensitive to operating conditions such as temperature, pressure, inhibitor concentrations and pH. In addition, the presence of complex compounds in the substrate may further introduce uncertainty as kinetics are mostly validated for degradation of model compounds.

Several AD models exist in the literature which vary in complexity. Early AD simulations saw the development of simple stoichiometric models that predicted biogas production upon substrate degradation. This was limiting owing to the inability of the model to predict effluent compositions. A comprehensive model for AD was developed by Angelidaki et al. (1993). It simulated the four AD steps in conjunction with the micro-organisms responsible through well-defined reaction and kinetic equations. Later, ADM1 was developed as a baseline for anaerobic digestion modelling. It tracks the degradation of components and formation of products through a chemical oxygen demand (COD) balance that results in the accurate prediction of biogas yields and overall substrate degradation. However, one downfall is the exhaustive substrate characterization in terms of individual species concentrations in COD required to adequately define substrates in ADM1 model.

Bioprocess modelling has historically proven to be a challenge due to the lack of unit operations in many simulation packages. In addition, organic components involved in bio-reactions are not well defined in the simulation environments (Shanklin et al., 2001). When choosing a simulation software, it is important to consider the availability of model components, thermodynamic packages and supporting literature. The user friendliness and transferability of the package needs to be considered to ensure continuity of the research or operation. SuperPro designer and Aspen Plus have been used for bioprocess simulations in the past. Although both contain economic reporting tools and friendly interfaces, SuperPro designer has been criticized for its limited thermodynamic packages and the absence of sensitivity analyses feature (Meireles, 2008; Woinaroschy, 2009b). High Performance programming using software such as Matlab/Simulink and Scilab have been successfully used to model bio-processes. Addition of external thermodynamic packages can extend their functionality (Sevella and Bertalan, 2000). Flexibility of these platforms in a key asset in bioprocess modelling, however, a high level of programming proficiency is required which limits the transferability of the model.

Successful simulation of the AD process will generate mass and energy inventories that can be used to evaluate performance. To improve resource productivity, it is necessary to explore the inclusion of pre- and post-treatments to the AD process and their effect on productivity and process economics. Discounted cash flow analyses are instrumental in determining process feasibility through progressive calculation of total capital investments, operating costs, revenues and cumulative cash flows. Total capital investments consist of the purchase, installation and delivery of major equipment whose costs can be evaluated using manufacturer quotes, order of magnitude estimations as well as costing equations found in the literature (Balaban, 2000; Turton et al., 2008). Thereafter, Lang factors are commonly used to evaluate the cost of equipment installation, delivery and site preparation. Operating expenditures arise from the costs incurred during the day to day operation of the plant. Profitability indicators such as return on investment, internal rate of return and the payback period can then be extracted from the discounted cash flow analysis (Sinnott, 2005). Using these indicators, cost-benefit analyses can be drawn and used to justify or reject the need for additional treatments to the vinasse AD process. Using these tools, the practicality of vinasse processing routes can be evaluated in a South African context.

3. Research Approach and Model Development

The overall aim of this research was to create a tool that can assist in decision making regarding the inclusion of energy, salt and water recovery technologies when developing vinasse treatment processes. This was supported by the development of simulations for alternative vinasse treatment process designs together with the associated techno-economic analyses that were used to evaluate profitability. Using the profitability results, a framework was developed to provide information concerning the marginal costs and benefits of adding various pre- and post-treatment technologies for water and salt recovery to the primary vinasse treatment process. This culminated in the creation of a decision support tool that compared various combinations of vinasse treatment routes in terms of process performance and profitability.

This section presents the systematic approach followed, and associated assumptions made towards the realization of this objective, overviewed in Figure 3.1.

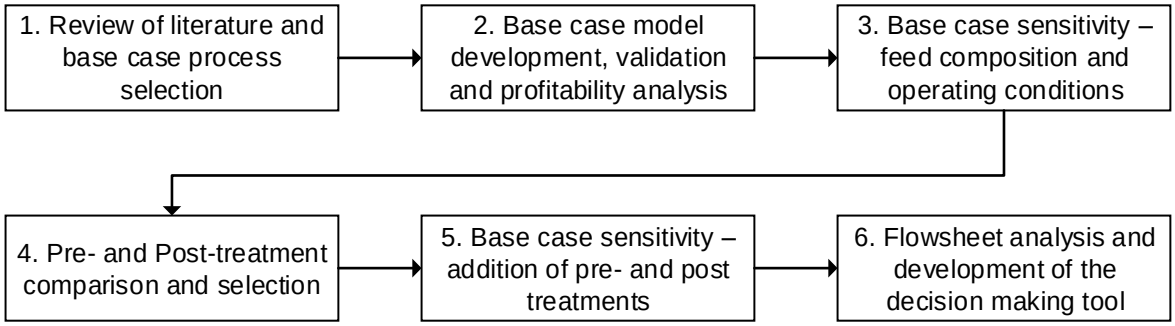

Figure 3.1: A schematic of the overview of the research approach

The base case flowsheet consists of a primary biological treatment step as vinasse has been continually proven as a viable bio-based feedstock owing to its high organic content and nutrient concentrations (Djalma Nunes Ferraz Junior et al., 2016; Moraes et al., 2015). Biogas produced from the biological treatment is utilized for electricity production through a combined heat and power system which can be used to meet internal energy demands or sold externally (Darrow et al., 2015). Expansion of the base case led to the integration of pre- and post-treatment processes that were aimed at improving AD performance (decreased inhibition) and value creation from the vinasse waste through water and inorganic salt recovery (Ryan et al., 2009) and potentially increasing the profitability of the base case flowsheet. Order of magnitude (OOM) estimations and literature based costing heuristics were used to evaluate capital and operating expenditures. Thereafter, profitability of the base case process and the impact of incorporating secondary treatments was evaluated using discounted cash flow analyses. While the assumptions in developing techno-economics are justifiable, the cost and revenue estimations remain ca. 30% accurate owing to diverse economic climates and regional differences. Conclusions are therefore largely drawn from relative cost-benefit analyses, deduced from comparisons of techno-economics and profitability indicators, which would be similar despite changes in the underlying assumptions.

3.1 Selection of Base Processes, Unit Operations and Simulation Packages

3.1.1 Anaerobic Digestion

A comprehensive literature review on the biological and physico-chemical processes was conducted (see Section 2.4). Although vinasse is largely composed of water (ca. 90%) it has a high organic matter content with CODs ranging between 150 to 200 g/L. Anaerobic digestion was selected as the primary treatment option for the simultaneous reduction of COD and biogas production. This technology has been successfully implemented for ethanol distillery wastewater treatment for biogas production and the generation of a nutrient rich effluent that can be used for the fertirrigation of agricultural land (España-Gamboa et al., 2011; Fuess et al., 2017). Alternative bio-transformations such as aerobic digestion require significant energy input of 1 kWh/kgCOD for aeration and heating purposes. In addition, 50% of the COD is converted to sludge. Comparatively, anaerobic digestion does not require aeration which reduces its energy requirement (Lier et al., 2008). Further, it results in a 90% reduction of excess sludge. The use of UASB reactors for substrates with low solids content (less than 10%) such as vinasse facilitates biomass retention and lowers the hydraulic retention time. Biomass retention leads to increased exposure of the microbes to the substrate and reaction environment which results in higher conversions.

3.1.2 Biogas Utilization – Combined Heat and Power

Given its high calorific value (19 to 28 kJ/L), biogas produced from the AD process is a potential energy source (Ryan et al., 2009; Wheeler et al., 1999a). This energy can be exploited in the form of heat produced through combustion or electricity generated using CHP systems. Alternatively, the biogas may be upgraded to biomethane (95%) by removing CO_2 through absorption or membrane processes.

In South Africa, several established biogas-to-electricity projects use spark-ignition engines to generate power (Strachan and Pass, 2012). This type of CHP system is based on the Otto cycle which consists of four reversible processes: (1) isentropic compression of air (2) constant volume heat addition through ignition (3) isentropic expansion and (4) constant volume heat rejection (Cengel and Boles, 2002).

Jenbacher spark ignition engines, manufactured by General Electric Ltd. (Strachan and Pass, 2012), are designed for small to medium scale processes with capacities between 0.2 and 1 MW. These internal combustion engines have electrical efficiencies that range between 40 and 50% depending on the size and the nature of the feed gas stream (General Electric, 2008). The exhaust gas can be released to the atmosphere at a temperature of approximately 180^{o}C. Alternatively, the gas may be used to generate low pressure steam in a heat recovery system.

When developing the base case simulation, the biogas generated from AD was utilized for electricity production through a CHP system. This approach was selected as it is a common practice in industrial biogas plants which results in the production of a viable utility that can be readily used internally or sold off commercially. Due to their simple design, moderate efficiency and availability in the South African market, the Jenbacher engines were chosen as the biogas utilization process. Following the industry standard, a simple process flow diagram of the base case AD of vinasse along with the CHP process is presented in Figure 3.2.

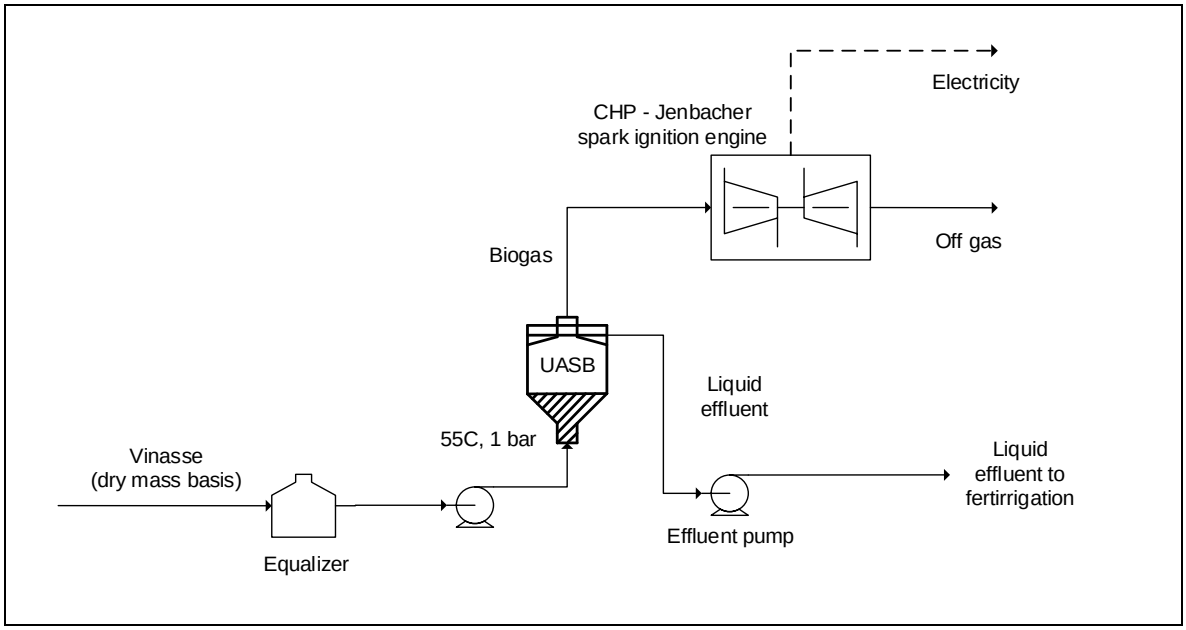

Figure 3.2: A process flow diagram showing the base case flowsheet consisting of an AD and CHP system

The process flow diagram for the base case consisted of three major items of equipment which were (1) the equalizer, (2) UASB reactor and (3) CHP system. This formed a basis which was transferred into the process modelling stage in an appropriate simulation package whose selection is presented in Section 3.1.3.

3.1.3 Selection of Engineering Simulation Software Packages

To model the base case flowsheet (Figure 3.2) as well as the secondary processes sufficiently, a readily customizable simulation package was required so as to accommodate additional algorithms that aid in mimicking the behaviour of participating microbes in AD. Additional characteristics of the ideal simulation package included transferability and the availability of sensitivity and economic analyses features which would aid in process optimization and profitability evaluation.

Aspen plus, SuperPro designer and high-performance programming platforms (e.g. Matlab and Scilab) were reviewed and compared to gauge the applicability of their features to bio-process modelling (see Section 2.10). A summary of the findings based on the review is shown in Table 3.1. High performance programming languages (HPPL) exhibit a high degree of flexibility with an extensive array of built-in solver functions. However, these platforms lack direct access to component databases and property methods without interfacing the software to external property databases. Techno-economic analyses features are also lacking and need to be coded into the simulations or evaluated on third party software such as MS Excel. In addition, simulations developed in the HPPL platforms are not easily transferrable as they are limited to users with advanced programming skills. Unlike HPPL, SuperPro has inbuilt unit operations that can be dragged and dropped onto the user interface. It has extensive bio-specific unit operations complete with bio-kinetics (Monod and Michaelis Menten), extensive component databases, and economic evaluation features. Although SuperPro is ideal for bioprocesses (Shanklin et al., 2001; Woinaroschy, 2009a), the lack of direct sensitivity analyses features is a drawback which constrains the optimization process.

Table 3.1: A comparison of the features within the software simulation packages reviewed

Functionality	C, Scilab, Matlab	SuperPro	Aspen Plus
Graphical User Interface or ease of use	Requires a high level of coding knowledge	User friendly but lacks extensive component databases	User friendly
Economic analysis features	× - Can be coded in or developed externally in MS Excel	✓	✓
Customisability or flexibility	✓	×	✓
Sensitivity analyses and optimization	✓	× - these functions can be added through interfacing with third party software	✓
Extensive and customizable component databases	User has to specify the components and properties but can link to open source property databases	CAS numbers for additional components required	Additional databases can be created

Contrary to HPPL and SuperPro, sensitivity, design specification and optimization features are built directly into Aspen Plus and are readily accessible. It is flexible, customizable and has demonstrated sufficient performance in AD and biogas utilization (Peris, 2011; Rajendran et al., 2014). For these reasons, it was chosen as the simulation platform for the development of the vinasse treatment flowsheets in this study.

3.1.4 AD Model/Framework Selection and Development

Modelling anaerobic digestion in Aspen Plus requires clearly defined stoichiometric reaction pathways, operating conditions and reaction kinetics to simulate the process accurately. AD models proposed by Angelidaki et al., (1993), Batstone et al. (2002), and Symons and Buswell, (1933) were reviewed for the model development of the base case AD digester. The model was then incorporated into Aspen Plus using a combination of the built-in unit operations and FORTRAN subroutines.

The availability of information describing the reaction pathways, stoichiometry and kinetic data within each of the reviewed AD models is critical in the selection process. Although ADM1 was developed as a baseline for AD modelling, it does not use a conventional stoichiometric approach but rather tracks the degradation of components and formation of products through a COD balance (Yu et al., 2013). Similarly developed, ADM-3P has a wide range of capabilities but is currently developed for domestic wastewater applications with no customization for vinasse in the literature. Both ADM1 and ADM-3P require an extensive knowledge of high performance programming languages such as C++ and Java which decreases the ease of transferability between users. The comprehensive AD model developed by Angelidaki et al. (1993) was therefore selected as the preferred model as it rigorously describes the reaction stoichiometry of the AD mechanism. The model (Angelidaki et al., 1993) could be readily implemented on Aspen Plus which makes it easily transferrable due to the presence of inbuilt unit operations and minimal use of programming languages.

Given that ADM1 is an extension of the model by Angelidaki et al. (1993) and their similarities, calibrated kinetic parameters from ADM1 were deemed appropriate for use as initial inputs into the Aspen Plus AD simulation that was based on the framework by Angelidaki et al. (1993). Moreover, ADM1 has been used to model the AD of vinasse in UASB reactors with relevant changes to the constants through calibration (Barrera et al., 2015). This further motivated the use of this kinetic data going forward in the flowsheet development stages. Any unknown kinetic parameters such as growth rates and half saturation constants specific to vinasse were assumed from well documented literature (Angelidaki et al., 1999; Barrera et al., 2015).

3.2 Anaerobic Digestion Model Developed for the Base Case Flowsheet

The AD model for this work was developed using kinetic and mechanistic aspects proposed by Angelidaki et al. (1993) as mentioned in Section 3.1.4. Mechanistic aspects included the reaction stoichiometry as well as substrate uptake and product yields. Kinetic parameters such as growth rates, inhibition and half saturation constants were sourced from ADM1 (Batstone et al., 2002). The aim was to develop a simplified anaerobic digestion model, with sufficient complexity to accurately predict AD performance comparable to existing comprehensive models. While vinasse is a complex substrate, the definition was limited to the carbohydrate, lipid and protein contents. Organics in vinasse can be split into these three main components. Moreover, this corresponds with the characterization of substrates in existing models which streamlined the simulation process (Donoso-Bravo et al., 2011; Yu et al., 2013). From the models studied (Angelidaki et al., 1993; Batstone et al., 2002), 11 key reactions were selected to represent the AD mechanism which included four sub-processes. Carbohydrates, lipids and proteins were first hydrolysed to glucose, fats and amino acids. Through acidogenesis by fermentative bacteria, the hydrolysis products were converted to VFA. Volatile fatty acids were then converted to acetic acid, CO_2 and H_2 through acetogenesis by acetogenic bacteria. Methanogens thereafter utilized acetic acid and H_2 to form methane and CO_2. Selection of the 11 reactions was based on the abundance of the primary reactant in the raw vinasse stream. VFA, ammonia and light metal cations were also included in the initial substrate definition to determine the inhibitory contribution of these compounds on the overall digester performance.

3.2.1 Model development: Mass balance, Reaction Stoichiometry, and Kinetics

3.2.1.1 Mass Balance and Kinetic Equations

To adequately describe the flow and transformation of material through the AD system, it was necessary to develop a reactor mass balance equation. A continuous reactor operation mode was adopted as it facilitated relatively high substrate throughput and conversion compared to batch systems for low solids substrates such as vinasse. Using the principle of conservation of mass and further assuming a constant reactor volume, Equation 3.1 was formulated (Sinnott, 2005) with the accumulation term reduced to zero owing to steady state operation. A total of three mass balance equations are formed by replacing X_{in} and X_{out} with the substrate (S), biomass (X) and product (P) concentrations.

$$\frac{dX}{dt} = X_{in} - X_{out} + \frac{1}{Y}\mu X \qquad \textit{Equation 3.1}$$

The volumetric growth rate (μX) in Equation 3.1 is a product of the specific growth rate and biomass concentration. This can be positive or negative depending on the nature of the mass balance. For products and substrates, the generation terms are likely to be always positive and negative respectively. Due to omission of the cell lysis process, the biomass mass balance always exhibited a positive generation term. Substrate and product yields represented by *1/Y* in Equation 3.1, where Y is the yield coefficient ($g_{biomass}/g_{substrate}$), were used to develop the reaction stoichiometry using linear programming techniques. In this technique, element balances for each reaction are used to formulate a set of linearly independent equations with the substrate and product yields being the unknowns. The abovementioned equations and unknowns are then solved to obtain stoichiometric coefficients for the balanced reactions. To ensure better representation of the biomass in terms of its physical properties in the model, the biomass molecular formula ($C_5H_7NO_2$) was replaced by $CH_{1.8}O_{0.5}N_{0.2}$ (Roels, 1980). The equations were then re-balanced accordingly.

The microbial growth, substrate utilization and product formation mechanisms were modelled using Monod-type kinetics where specific growth rates (μ) are directly proportional to the substrate concentrations *S* (Equation 3.2) at very low concentrations. At high substrate concentrations, Equation 3.2 becomes zero order. While this choice of biokinetics was directly influenced by Angelidaki et al. (1993), the Monod model has proven to simulate anaerobic digestion adequately and reproduce experimental data with relatively small errors at a 95% confidence interval (Yu et al., 2013). The nitrogen source is provided by ammonia which therefore acts as a secondary substrate (S_2) in the acidogenic, acetogenic and methanogenic steps.

$$\mu = \mu_{max}(T).\left(\frac{1}{1+\frac{K_{S1}}{S}}\right).\left(\frac{1}{1+\frac{K_{S2}}{S_2}}\right).\left(\frac{1}{1+\frac{S_i}{K_{inhibition}}}\right).F(pH) \qquad \textit{Equation 3.2}$$

The primary and secondary half saturation coefficients for the substrates are represented by K_{S1} and K_{S2} in Equation 3.2 .Non-competitive inhibition by ammonia and volatile fatty acids was implemented in methanogenic and acetogenic phases respectively (Angelidaki et al., 1993), with $K_{inhibition}$ denoting the inhibition constants. Inhibitor concentrations are represented by Si in Equation 3.2. To model the influence of pH on the growth rates, a normalized Michaelis pH function was implemented (Equation 3.3). This was developed by fitting an equation to the Michaelis pH curve that describes pH inhibition factors as a function of digester pH. Upper and lower pH limits are incorporated in this function as pK_h and pK_l, respectively (Equation 3.3). Additionally, a centre value of 1 is obtained at an optimal digester pH of 7.1 (Angelidaki et al., 1993).

$$F(pH) = \frac{1+2*10^{0.5(pK_l-pK_h)}}{1+10^{pH-pK_h}+10^{pK_l-pH}} \qquad \textit{Equation 3.3}$$

The maximum growth rates, half saturation, and inhibition constants are summarized in Table 3.2. These were used in conjunction with Equation 3.1, Equation 3.2 and Equation 3.3 to complete the mass balance equations for biomass growth, substrate uptake and product formation. To predict the effect of operating temperatures on growth rates, the Arrhenius equation was used.

Table 3.2: A summary of growth rates, half saturation and inhibition constants implemented in the developed model (Angelidaki et al., 1993; Batstone et al., 2002)

Kinetic constant	μ_{max} (day^{-1})	K_s (g/L)	K_s (NH_3) (g/L)	K_i (g/L)
Hydrolysis (constants)				
Carbohydrates	10	-	-	0.33 (total VFA)
Fats (GTO)	10			
Protein	10	-	-	0.33 (total VFA)
Acidogenesis				
Glucose	30	0.26	0.05	-
Glycerol	6	0.01	0.05	-
Amino Acids	50	0.21	-	-
Acetogenesis				
Propionic acid	13	0.066	0.05	0.96 (HAc)
Butyric acid	20	0.11	0.05	0.72 (HAc)
LCFA	6	0.02	0.05	-
Valeric acid	30	0.175	0.05	0.4 (HAc)
Methanogenesis				
Acetic acid	8	0.14	0.05	0.26 (NH_3), 5.86 (K^+)

In Aspen Plus, yields are embedded into the reaction stoichiometry. The reactions can be grouped into four categories to adequately describe the AD mechanism (see Section 3.2.1.2 – 3.2.1.5).

3.2.1.2 Hydrolysis

Hydrolysis is the process by which complex organic compounds are degraded into solutes that can be metabolized by microbes in AD. While several viable hydrolysis mechanisms have been implemented in the literature, enzymatic hydrolysis was selected owing to its proven success in previous models (Angelidaki et al., 1993; Rajendran et al., 2014) and relative simplicity. It involves the secretion of enzymes by microbes to degrade the complex organic substrates and is often slow and rate limiting (Yu et al., 2013). The organics in vinasse requiring hydrolysis were characterised into carbohydrates, proteins and lipids. These are denoted by *S* in Equation 3.6 and are hydrolysed to simple sugars, amino acids, and fatty acids and glycerol respectively. These can be utilized by acidogenic bacteria. Complex carbohydrates, represented by sucrose in Equation 3.4, or by polymers such as starch and glycogen, are broken down into glucose in the presence of water (Angelidaki et al., 1993).

$$C_{12}H_{22}O_{11} + H_2O \rightarrow 2C_6H_{12}O_6$$ *Equation 3.4*

As Aspen Plus is primarily developed for the chemical industry, biological compounds such as crude protein are not present in the native database. Introduction of these as pseudo components in the database lead to inaccurate results due to the absence of many of the physical properties. As such, when modelling the mechanistic aspects of hydrolysis in vinasse the dominant amino acids, glutamic acid, lysine and aspartic acid, from protein hydrolysis were used to overcome this obstacle. Consequently, the protein hydrolysis reaction was omitted while reserving the carbohydrate and lipid hydrolysing steps.

Lipids were represented by glycerol tri-oleate in this mechanism. Glycerol tri-oleate is most abundant in vegetable oils (Angelidaki et al., 1999) and was also assumed to be present in vinasse which originates from a plant species. It is hydrolysed to glycerol and oleic acid (Equation 3.5).

$$C_{57}H_{104}O_6 + 3H_2O \rightarrow C_3H_8O_3 + 3C_{18}H_{34}O_2$$ *Equation 3.5*

Glycerol is an intermediate product that is instantly converted to propionate in acidogenesis (Angelidaki et al., 1999). Oleate is further broken down by acetogenic bacteria to form acetic acid.

In accordance with Angelidaki et al. (1993), 1st order rate laws, inhibited by the total VFA concentration (propionic, butyric and acetic acid), were used to simulate hydrolysis kinetics (Equation 3.6). The rate (R_{hyd}) is influenced by both substrate and total VFA concentrations.

$$R_{hyd} = k_0.\left(\frac{k_i}{k_i+\sum VFA}\right).S$$ *Equation 3.6*

The initial rate of reaction (k_0) represents the hydrolysis constant (day^{-1}) which varies depending on the substrate (Batstone et al., 2002; Koch et al., 2010).

3.2.1.3 Acidogenesis

Acidogenesis is the breakdown of the hydrolysis products such as simple sugars, glycerol and amino acids by acidogenic fermentative bacteria to volatile fatty acids (propionic, butyric, acetic and valeric acid), carbon dioxide and water. Amino acid degradation was modelled using Stickland reactions (Ramsay and Pullammanappallil, 2001). This mechanism of degradation involves pairs of amino acids which act as either electron donors or acceptors. It is a rapid mechanism compared to uncoupled amino acid degradation and has been used successfully by previous researchers to simulate the acidogenic fermentation of amino acids (Rajendran et al., 2014). Although Stickland mechanisms typically involve 10 pairs of amino acids, the three most abundant amino acids in molasses and vinasse were selected to participate in the acidogenic step in this model (Scull et al., 2012). Selecting the most abundant amino acids eliminated additional reactions relating to amino acids present in trace amounts thereby reducing complexity of the model. Glucose and glycerol were similarly degraded through anaerobic fermentation to form biomass and a mixture of VFA, water, and carbon dioxide (Equation 3.10 and Equation 3.11).

It was assumed that acidogenesis followed Monod-type growth kinetics similar to Equation 3.2 with respect to the primary substrate concentrations. Primary substrates resulting from the hydrolysis of vinasse were accounted for in the model. These included amino acids, glycerol and glucose. Additionally, in accordance with Angelidaki et al. (1993), ammonia was chosen as a co-substrate (K_{s2} in Equation 3.2) in all reactions except amino acid degradation as it a nitrogen source required for microbial growth. Despite this requirement of ammonia for growth, its contribution as an inhibitor (K_i in Equation 3.2) was also implemented in the acetogenic (Section 3.2.1.4) and methanogenic steps (Section 3.2.1.5) at concentrations above 0.22 g/L. This was done to take into account the inhibitory effects of ammonia on the pH, methane yields and VFA concentrations (Angelidaki et al., 1999). The balanced equations shown in Table 3.3 are the acidogenic reactions implemented in this model.

Table 3.3: Acidogenic reactions implemented in the developed base case AD model

Amino Acids		
Glutamic acid	$C_5H_9O_4N + 2\ H_2O \rightarrow C_2H_4O_2 + 0.5\ C_4H_8O_2 + NH_3 + CO_2$	*Equation 3.7*
Aspartic acid	$C_4H_7O_4N + 2\ H_2O \rightarrow C_2H_4O_2 + NH_3 + 2\ CO_2 + H_2$	*Equation 3.8*
Lysine	$C_6H_{14}O_2N_2 + 2\ H_2O \rightarrow C_2H_4O_2 + 0.5\ C_4H_8O_2 + 2\ NH_3$	*Equation 3.9*
Simple sugars		
Glucose	$C_6H_{12}O_6 + 0.0223NH_3 \rightarrow 0.1115\ CH_{1.8}O_{0.5}N_{0.2} + 0.964\ C_2H_4O_2 + 0.5\ C_3H_6O_2 + 0.4409\ C_4H_8O_2 + 0.6964\ CO_2 + 0.741\ H_2O$	*Equation 3.10*
Fat components		
Glycerol	$C_3H_8O_3 + 0.00814\ NH_3 + 0.00429\ CO_2 + 0.00005\ H_2 \rightarrow 0.04071\ CH_{1.8}O_{0.5}N_{0.2} + 0.98786\ C_3H_6O_2 + 1.0125\ H_2O$	*Equation 3.11*

3.2.1.4 Acetogenesis

The acetogenic reactions involve the breakdown of propionic acid (Equation 3.12), valeric acid (Equation 3.15) butyric acid (Equation 3.13) and oleic acid (Equation 3.14) by acetogenic bacteria to form acetic acid, water and carbon dioxide. The methane produced in this step is as a result of hydrogen utilizing methanogens which convert the hydrogen formed in acetogenesis to methane and carbon dioxide via Equation 2.7 and Equation 2.8. Integration of these two equations to Equation 3.12, and Equation 3.13 reduced the model complexity with a negligible loss in dynamism (Angelidaki et al., 1993)

Table 3.4: Acetogenic reactions implemented in the developed base case AD model

VFAs		
Propionic acid	$C_3H_6O_2 + 0.01239\ NH_3 + 0.7172\ H_2O \rightarrow 0.06198\ CH_{1.8}O_{0.5}N_{0.2} + 0.9345\ C_2H_4O_2 + 0.660412\ CH_4 + 0.408608\ CO_2 + 0.490194\ H_2$	*Equation 3.12*
Butyric acid	$C_4H_8O_2 + 0.01306\ NH_3 + 1.22825\ H_2O + 0.51527\ H_2 + 0.2931\ CO_2 \rightarrow 0.0653\ CH_{1.8}O_{0.5}N_{0.2} + 1.8909\ C_2H_4O_2 + 0.446\ CH_4$	*Equation 3.13*
Oleic acid	$C_{18}H_{34}O_2 + 0.05074\ NH_3 + 8.38584\ H_2O + 4.0834\ CO_2 \rightarrow 0.22537\ CH_{1.8}O_{0.5}N_{0.2} + 9.21289\ C_2H_4O_2 + 3.40392\ CH_4$	*Equation 3.14*
Valeric acid	$C_5H_{10}O_2 + 0.0653\ NH_3 + 0.8045\ H_2O + 0.5543\ CO_2 \rightarrow 0.0653\ CH_{1.8}O_{0.5}N_{0.2} + 0.8912\ C_2H_4O_2 + 0.02904\ C_3H_6O_2 + 0.4454\ CH_4$	*Equation 3.15*

3.2.1.5 Methanogenesis

The main products from acetogenesis (acetic acid and hydrogen) are finally converted to methane and carbon dioxide via methanogenesis by aceticlastic and hydrogen utilizing methanogens to CH_4 and CO_2. Acetic acid is broken down, with associated biomass formation, as shown in Equation 3.16:

$$C_2H_4O_2 + 0.0044\,NH_3 \rightarrow 0.022\,CH_{1.8}O_{0.5}N_{0.2} + 1.6\,CH_4 + 0.0099H_2O \qquad \textit{Equation 3.16}$$

The hydrogen produced in the acetogenic steps was immediately consumed by the hydrogen utilizing methanogens, together with CO_2. As described in Section 3.2.1.4, these reactions were combined with the acetogenic reactions to form combined equations shown in Equation 3.12, Equation 3.13, and Equation 3.14.

Although several features present in ADM1 such as ionic speciation, microbial death, sulphur reducing bacteria (SRB) kinetics and pH estimation have been excluded to maintain model simplicity, the model predicted biogas productivity relatively well compared to existing literature models (Section 4.2). Inclusion of these features increases the degree of complexity and may require a more in-depth definition of the feed, and consequently, reaction kinetics using customized calculator blocks with FORTRAN code. The model as presented does not require extensive programming knowledge and can be adopted for multiple applications with limited training.

3.3 Base Case Model Development and Implementation in Aspen Plus

3.3.1 Overview of Model Development

The AD model described in Section 3.2 was simulated on Aspen Plus V9. Segments of the AD model were progressively implemented into the system to allow for continuous troubleshooting during the modelling process. In preparation for this phase, component and reaction lists as well as appropriate kinetic data were collated and stored on a spreadsheet for easy access. The flow chart in Figure 3.3 shows the steps followed in executing the model.

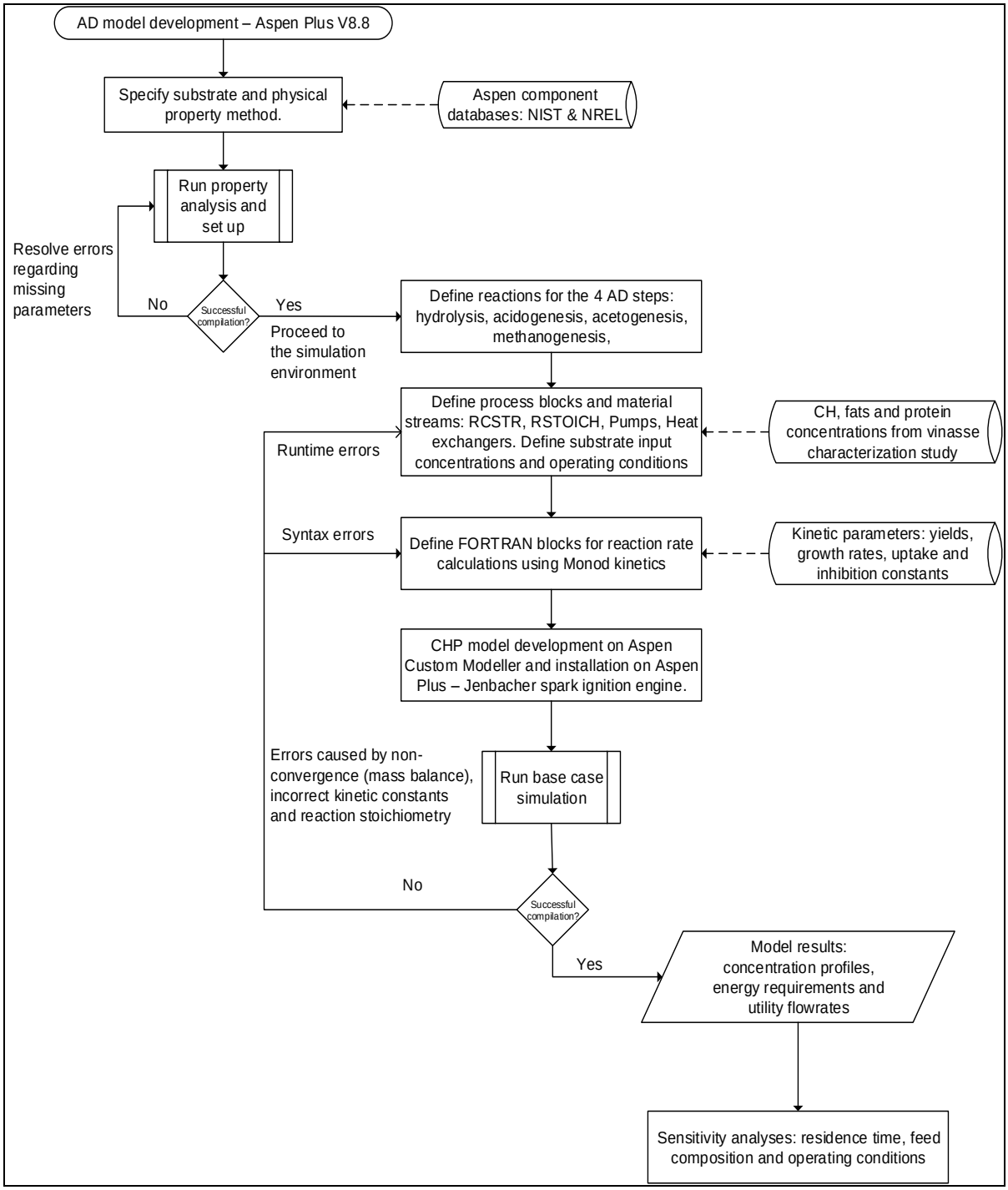

Figure 3.3: A flowchart showing the detailed AD model development stages on Aspen Plus v9 (NIST: National Institute of Standards and Technology, NREL: National Renewable Energy Laboratory, CH: Carbohydrates)

3.3.2 Components and physical property methods

Simulation on the Aspen Plus environment was divided into two phases: (1) property analysis and (2) simulation development. In the property analysis phase, chemical components participating in the process were selected from various databases available in the Aspen Plus databank. Components were classified as conventional (liquid), solid or pseudo-components (Aspen Technology, 2000). Physical property methods such as equations of state were also accordingly specified in this phase. It is important to select an appropriate equation of state

as it governs chemical interactions and vapor-liquid equilibria which inform the simulation results (Aspen Technology, 2000).

The vinasse substrate was not available in the component databases. As such, it was defined by its constituents which are carbohydrates, proteins and lipids (Barrera et al., 2015). Proteins and lipids, due to their complex nature, were further simplified to amino acids and glycerol tri-oleate (Angelidaki et al., 1999). Glutamic acid, lysine and aspartic acid were chosen as they are most abundant in vinasse (Scull et al., 2012). Additional components participating in the process such as volatile fatty acids and water and gases were defined. An additional biofuels database developed by the National Renewables Energy Laboratory (NREL) was added to Aspen Plus through the database manager (Wooley and Putsche, 1996). This contained the biomass ($CH_{1.8}O_{0.5}N_{0.2}$) component which was defined in the simulation as a solid. The NRTL (non-random two liquid) activity coefficient model was selected. It correlates activity coefficients to mole fractions in the liquid and gas phases and is widely used for low pressure aqueous systems such as AD (Aspen Technology, 2000; Rajendran et al., 2014).

The property analysis phase was compiled successfully. Compilation errors arose mainly from incomplete or missing physical properties for individual components. These include the theoretical biomass heat of formation, and amino acid standard molecular volumes. The properties were added manually (Peris, 2011).

3.3.3 Simulation environment

3.3.3.1 *Anaerobic Digestion Modelling*

The simulation environment on Aspen Plus provides a graphical user interface with a wide selection of predefined and customizable unit operations which can be added to the flowsheet (Aspen Technology, 2000; Nguyen, 2014). Additionally, different types of reactions, and process utilities can be defined. The simulation environment also provides functionalities such as sensitivity, design specification, optimization and user defined calculator blocks. Simulation results can be viewed and exported (Aspen Technology, 2000).

In this model, the biochemical mechanisms in AD were defined as kinetic reactions governed by the power law. However, underlying FORTRAN code would be used to compute the reaction rates using the Monod model. Material streams, and a well-mixed kinetic reactor were added to the flowsheet (Figure 3.4). The continuous stirred tank reactor (RCSTR) simulated an upflow anaerobic sludge blanket (UASB) reactor which is common in industrial applications of AD of vinasse (Fuess et al., 2017). A CSTR was used to represent the UASB reactor as both are well mixed. Biogas produced in UASB reactors bubbles up through the sludge blanket which promotes sufficient mixing. Although biomass retention could not be simulated effectively on Aspen Plus, there was a constant biomass inventory in the reactor with no accumulation. Biomass formed through reaction exited through the effluent. Hydrolysis reactions were modelled using first order kinetics with respect to the primary substrate (Equation 3.6). Monod kinetics, not present in Aspen Plus, were implemented using user defined calculator blocks with underlying FORTRAN code to compute reaction rates for acidogenic, acetogenic and methanogenic reactions (Equation 3.2).

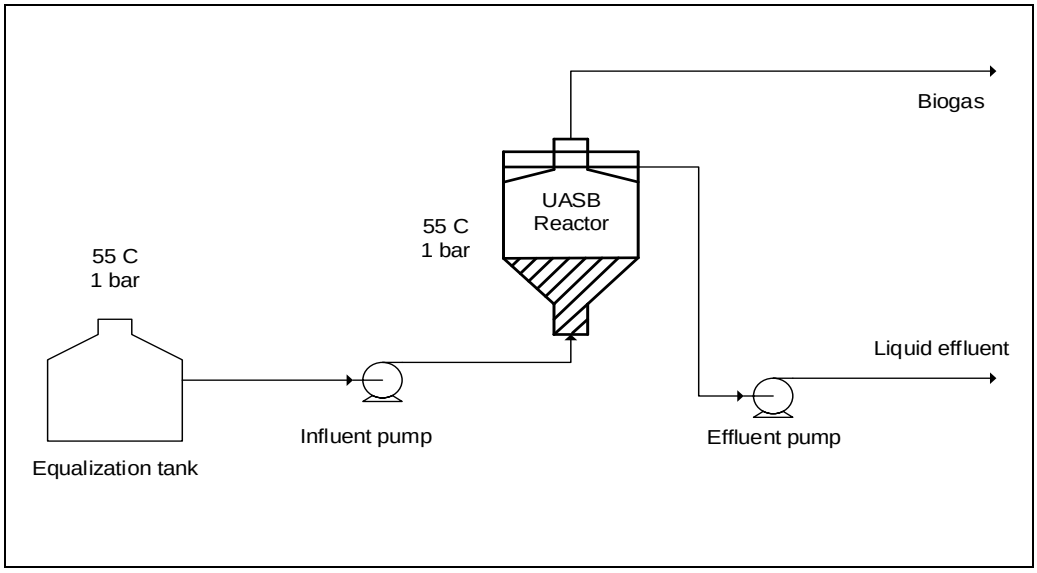

Figure 3.4: Process flow diagram of the AD process as developed on Aspen Plus

Initially, a reactor volume of 250 m^3 was set for preliminary simulations prior to scale up. Operating conditions such as temperature and pressure were adapted from the literature (Barrera et al., 2015) with thermophilic conditions being preferred due to increased microbial activities at these elevated temperatures. Raw vinasse was fed at an organic loading rate of 25 kgCOD/(m^3.day) which is typical of industrial scale processes. The raw vinasse flowrate was then computed from this value using the feed stream density and reactor volume. The result was manually input to the reactor specifications tab. Residence time was then calculated by the simulation. The feed composition on a dry mass basis is shown in Table 3.5. An additional water stream was mixed with the dry vinasse feed separately prior to reactor entry to facilitate easier control of the moisture content and overall stream composition.

Table 3.5: The vinasse feed stream composition on a dry mass basis (Scull et al., 2012; Turner et al., 2002)

Component	**Mass fraction**
Sucrose	0.235
Acetic Acid	0.205
Valeric Acid	0.205
Glutamic acid	0.017
Lysine	0.009
Aspartic Acid	0.0086
Biomass	0
Glycerol	0.125
K_2SO_4	0.194
Chemical Oxygen Demand (g/L)	227
VS (approximation) (g/L)	103
Density (kg/m^3)	1040

The vinasse composition used in this study was based on published data from an ethanol distillery in KwaZulu Natal (Turner et al., 2002). Amino acid concentrations were obtained from Scull *et al.* (2012) who quantifies the amino acid profiles in molasses and vinasse. This characterization formed a composition basis which was assumed to be representative of vinasse produced in South African ethanol distilleries.

3.3.3.2 CHP modelling on Aspen Plus

Operation of the Jenbacher engine (General Electric, 2008) was simulated using a combination of a combustion reactor, and custom model to convert the heat generated to heat and work. The air flow was set to 1.7 times the biogas flowrate to facilitate complete combustion of the methane (Francois et al., 2013). The two streams ("air" and "raw biogas" in Figure 3.5) were mixed at constant pressure and sent to the reactor ("combustion chamber") where complete combustion of the biogas occurred at 1 bar. The exhaust gases were used to generate low pressure steam at 124 kPa in a shell and tube heat exchanger. The heat energy (kW) generated by the combustion reactions is routed through a heat stream to the custom model developed on Aspen Custom Modeller (ACM). The custom model uses the efficiency specified (44%) for the Jenbacher engine to calculate the electrical work generated and the waste heat.

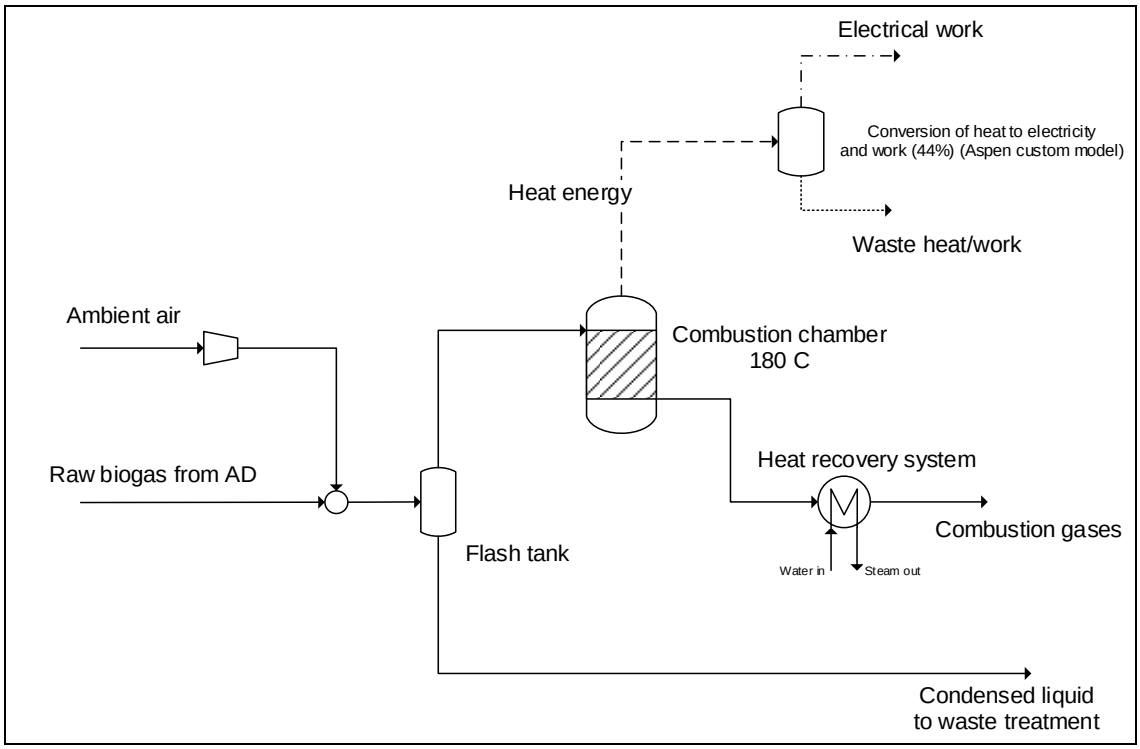

Figure 3.5: The combined heat and power system (Jenbacher spark engine) as developed on Aspen Plus

The simulation results from Aspen Plus were presented in their SI units. These were transferred to MS excel for further analysis. Methane yield ($L\text{-}CH_4/kgVS_{added}$) was calculated by dividing the total biogas volume by the mass (kg) of volatile organic matter in the vinasse feed. Although much of the organic matter in vinasse is dissolved (solutes), part of the volatile matter remains suspended. Owing to challenges in differentiating between volatile suspended and dissolved solids on Aspen Plus, all organic matter was termed as volatile solids (VS). This greatly simplified the substrate definition and avoided creation of pseudocomponents to represent suspended matter. The component concentrations throughout the process were obtained in g/L. COD concentrations in the feed, effluent and biogas was computed by multiplying the stream COD fraction (from the Aspen Plus results sheet) by the density in kg/m^3. The energy produced or dissipated by a unit operation calculated using enthalpy balances within Aspen Plus was obtained from the results sheet. Electricity production from the CHP plant was measured in kW which was then converted to kWh.

After successful execution, benchmarking and validation of the base case flowsheet was conducted. Benchmarking tested the applicability of the model to different substrates (manure and municipal waste) as well as its performance relative to published AD simulations. Validation tested the ability of the model to replicate experimental results. Methane yield (L-CH_4/kgVS_{added}) was used as the comparative parameter because it is commonly reported by experimental AD studies. In addition, it provided an adequate measure of performance as it compared the volume of the AD product of interest (CH_4) relative to the mass of organics fed into the reactor.

Once benchmarked and validated against experimental data, the sensitivity of the AD model to compositional disturbances was tested. This was to further ascertain model credibility in terms of trends observed relative to what is published in the literature and aid in identifying potential optimization opportunities.

3.4 Sensitivity Analysis

Sensitivity analyses were used to investigate the robustness of the model and identify potential opportunities of process optimizations in terms of energy recovery. A multistage approach was taken in the sensitivity analyses. First, the key elements that directly affected biogas yields (L-CH_4/kgVS_{added}) and effluent concentrations were identified along with the appropriate justifications. Their sensitivity was then investigated by running multiple simulations using appropriate ranges of variation for each of the elements and analysing the results to identify trends and opportunities for process optimization. After the first stage in which the base case flowsheet was analysed, the impact of adding pre- and post-treatment processes on the resource productivity, energy utilization and profitability was compared to the base case configuration (AD-CHP) in the second stage of the sensitivity analysis.

3.4.1 Sensitivity analysis – Organic Loading Rate and Feed Composition

The first stage of the sensitivity analyses was used to test the credibility of the AD model built through monitoring of biogas productivity and effluent concentrations with varying feed loading rates and composition. Inhibitory compounds present in raw vinasse such as acetic acid, ammonia and potassium ions were targeted for this purpose due to their significant effect on productivity and overall AD stability. Inhibitory compound concentrations above certain thresholds may lead to 50% inhibition of methanogenic activity and downward trends in methane productivity (Chen et al., 2008). Vinasse AD systems are also sensitive to the organic loading rate. High loading rates are often accompanied by high flowrates and result in biomass washout and low methane productivity owing to decreased methanogen population. On the other hand, low loading rates call for larger reactor sizes or longer residence times to obtain reasonable methane yields (Uellendahl and Ahring, 2010). The abovementioned trends in the literature were compared to the base case (AD-CHP) simulation behaviour with changing OLR and inhibitor concentrations. This way, the correctness and integrity of the model's core framework could be ascertained. In addition, analysing the predicted behaviour with changing inhibitor concentrations may reveal process thresholds required to run an efficient AD process. The results from the first stage of sensitivity could be used to determine the scale of secondary treatment processes to improve performance. Thereafter, evaluation of techno-economic analyses can be used to assess the economic benefits relative to the costs of adding pre- and post-treatment processes to the base case flowsheet.

3.5 Techno-Economic Analyses

The techno-economic feasibility was developed to determine the profitability of the project as well as highlight the cost sensitive areas and potential revenue generation opportunities. A schematic depicting the approach followed is shown in Figure 3.6. Aspen Plus has within it a process economic analysis tool which can be used to evaluate the economic feasibility of a model. It makes use of a sizing and costing routine that leverages proprietary equipment costing algorithms coupled with current economic data. However, there is uncertainty in the results obtained as they cannot be justified due to the proprietary nature of the algorithms used. As such, a manual approach to sizing and costing was followed.

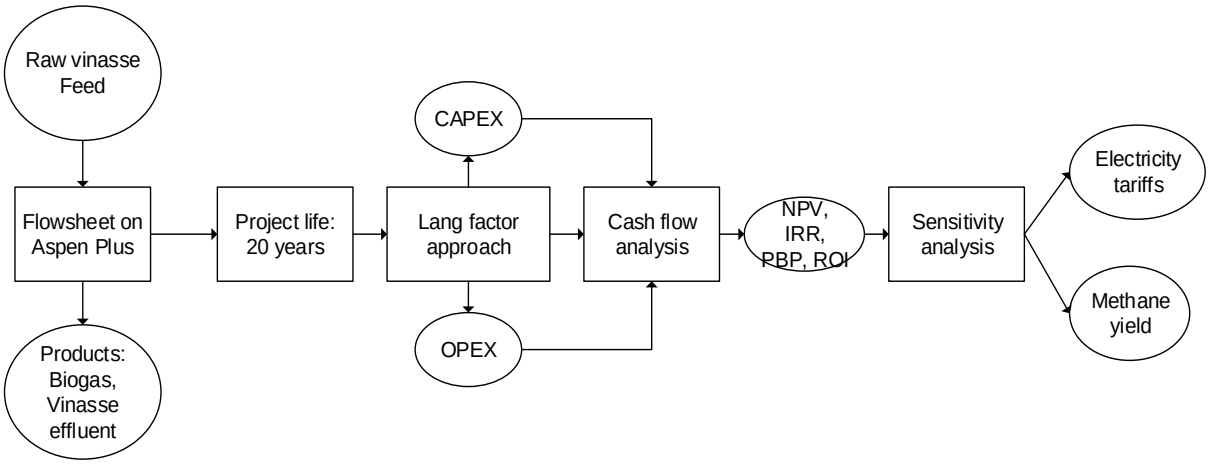

Figure 3.6: The approach taken in the development of techno-economic analyses for the vinasse processing routes

Several revenue streams were considered depending on the flowsheet configuration. The base case configuration consisted of an anaerobic digester coupled with a combined heat and power plant for electricity generation from the biogas. The electricity was sold by feedback into the national grid at the recommended renewable energy feed-in-tariff of $0.1/kWh (NERSA, 2011). The treated vinasse effluent from the base case process will be applied to the sugar cane fields through fertirrigation. As such, it was considered as an indirect revenue stream in the form of a cost saving on the synthetic fertilizer required for the sugar cane plantations. In further configurations, pre- and post-treatment processes resulted in additional revenue streams such as potassium sulfate and biomethane.

The equipment costs were computed using costing curves, manufacturer quotes (Davis et al., 2013) and heuristics along with OOM estimations (Turton et al., 2008). The fixed capital investment was then computed using a Lang factor approach which considered the installation, design and contingency fees involved in setting up the plant. Working capital was assumed to be 15% of the fixed capital investment. A closer look on large scale biogas projects in Africa showed that the Lang factors associated with installation, piping, contingencies and fees varied greatly from conventional published values (Amigun and Blottnitz, 2007).

The Lang factors evaluated for African biogas installations are 60% lower than the conventional ones. This was mainly attributed to the differences in economic standing and development in the regions where the factors were first estimated (Amigun and Blottnitz, 2007). Development of Lang factors specific to southern Africa has proven useful in the accurate evaluation of the project's feasibility.

Table 3.6: A comparison between the conventional Lang factors and modified Lang factors for biogas installations in South Africa.

	Conventional	Biogas installations (Africa)
PCE	1	1
Installation, development (f_x)	3.15	1.6
Design, fees, contingency (f_y)	1.4	0.19
Total	4.45	1.79
Fixed capital investment	$FCI = PCE * (f_x + f_y)$ (Turton et al., 2008)	$FCI = PCE * (f_x + f_y)$ (Amigun and Blottnitz, 2007)

The plant running costs were subdivided into fixed and variable costs. Fixed costs largely arose from equipment maintenance, wages and other miscellaneous costs such as insurance and contingencies. Variable costs were dependent on the production capacity which included the cost of utilities and raw materials. For each configuration, the total cost of utilities was calculated and summed. Operation and maintenance costs varied for each unit operation and as such were calculated separately. With regards to labour, it was assumed that there would be three shifts per day with an operator working to monitor the operation of each processing unit. Additionally, one chemical engineer would be present at the plant along with two laboratory staff. The annual wage bill was calculated using recent data from Payscale SA, (2017)

The profitability indicators were then determined through a cash flow analysis done over a project life cycle of 20 years. Plant construction took place over the first two years with production commencing on the third. Revenues and expenses were escalated accordingly using the current inflation rate in South Africa. Depreciation was accounted for using the straight-line method where equipment values were decreased evenly throughout the project life time to their scrap value. Net profit before tax was computed by taking the difference between the gross profit and depreciation in each year. The sum of net profit after tax and depreciation formed the cash flow which was then discounted using the minimum acceptable return (15%). This was done to reflect its present value. Cumulative cash flows (discounted and normal) plots were used to obtain the profitability indicators such as payback period (PBP), net present value (NPV), return on investment (ROI), and internal rate of return (IRR). These indicators provided a normalized profitability comparison of the different process configurations. However, it must be noted that the estimations concerning costs, and revenues at this feasibility stage are approximately 25 to 40% accurate.

Initial results from the techno-economic feasibility of the base case process provided information about the status of the project in terms of its profitability in a South African context. From this, potential revenue generating opportunities could be identified and exploited through incorporation of additional processing units to recover products of value for commercial purposes.

3.6 Potential for Process Improvement through Addition of Pre- and Post-Treatments.

Expansion of the base case flowsheet functionality was sought through inclusion of dewatering, desalting and biogas utilization processes. Notably, addition of recovery processes may influence biogas productivity, energy utilization, and profitability. As such, it was necessary to evaluate the cost-benefit of these inclusions. Figure 3.7 summarizes the methodology used in this sensitivity investigation.

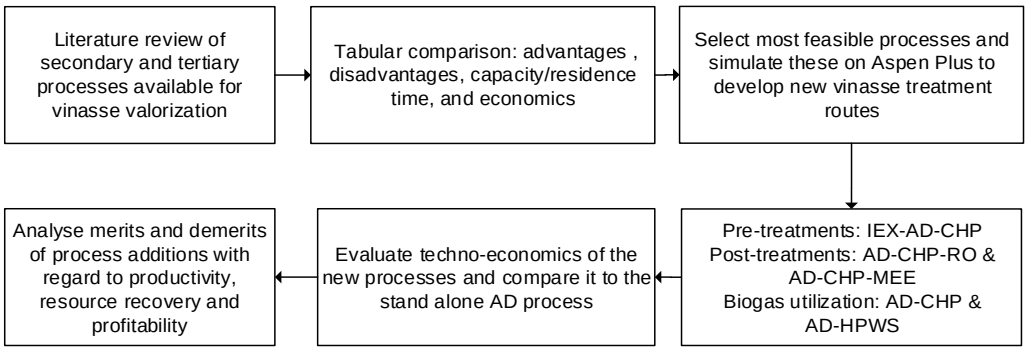

Figure 3.7: The approach to sensitivity analysis in terms of pre- and post-treatment unit operations

Due to time constraints, developing rigorous and elaborate models for all suggested unit operations as in Figure 3.7 was not feasible. Instead, an in-depth literature comparison of pre-treatment, post-treatment and biogas utilization processes was compiled to aid in selection. The most feasible processes were then modelled on Aspen Plus using the in-built unit operations. Five process configurations containing the base case and a pre-treatment or post-treatment process were simulated on Aspen Plus. Results from these simulations were used to evaluate profitability through discounted cash flow analyses. The new process configurations were compared to the base case (AD) to evaluate the marginal benefits of process inclusions in terms of productivity, and profitability relative to the additional costs incurred.

3.7 Flowsheet analysis and the Decision-Making Tool

Section 3.6 investigated the potential of process improvement (performance and economics) through individual addition pre- and post-treatments to the base case process. Although these results shed light on the marginal costs and benefits of process inclusions, they do not highlight the interacting effects of pre- and post-treatment options on the overall flowsheet feasibility. One potential interaction is the effect of pre-treatment on the choice of biogas utilization processes and water recovery processes. Another interaction is the impact of biogas utilization processes on the choice of water recovery process.

In Section 3.7, a decision-making framework was developed to analyse the abovementioned interactions and compare the profitability of the treatment routes arising from the combinations of pre- and post-treatments that were added to the base case (AD-CHP). The framework was divided into three block-flow diagrams that highlighted the additional costs of the pre- and post-treatments as well as graphical comparisons of the profitability indicators of each process. This tool was expected to aid in decision making when developing vinasse treatment processes by highlighting the additional costs incurred and the marginal benefits of adding pre- and post-treatments to the base case.

4. The Base Case Vinasse AD Model

Given the benefits of AD when treating organic wastes and the need for value addition through energy production, a base case flowsheet was developed in Chapter 3. The base case vinasse treatment flowsheet consisted of an AD for biogas production as well as a CHP system for energy generation. As a first step in flowsheet development, AD and CHP models were developed through adoption of existing frameworks (Angelidaki et al., 1993; Batstone et al., 2002) and then implemented in Aspen Plus v9 (see Section 3.2). Following model development, this chapter seeks to investigate the base case flowsheet and model in terms of its credibility through sensitivity analyses. In addition, preliminary techno-economics are conducted to determine the cost-sensitive areas.

4.1 Description of the Base Case Flowsheet

The anaerobic digestion simulation for vinasse treatment developed on Aspen Plus v9 consisted of an equalizer, influent pump and an upflow anaerobic sludge blanket reactor and a combined heat and power plant (Figure 4.1). Inclusion of equalizers in industrial AD processes is common. It facilitates reactant mixing and provides a buffer in the event of an irregular feed supply. Given the high organic content of vinasse, the loading rate was controlled by varying the reactor feed flowrate (m^3/hr) to avoid organic overloads.

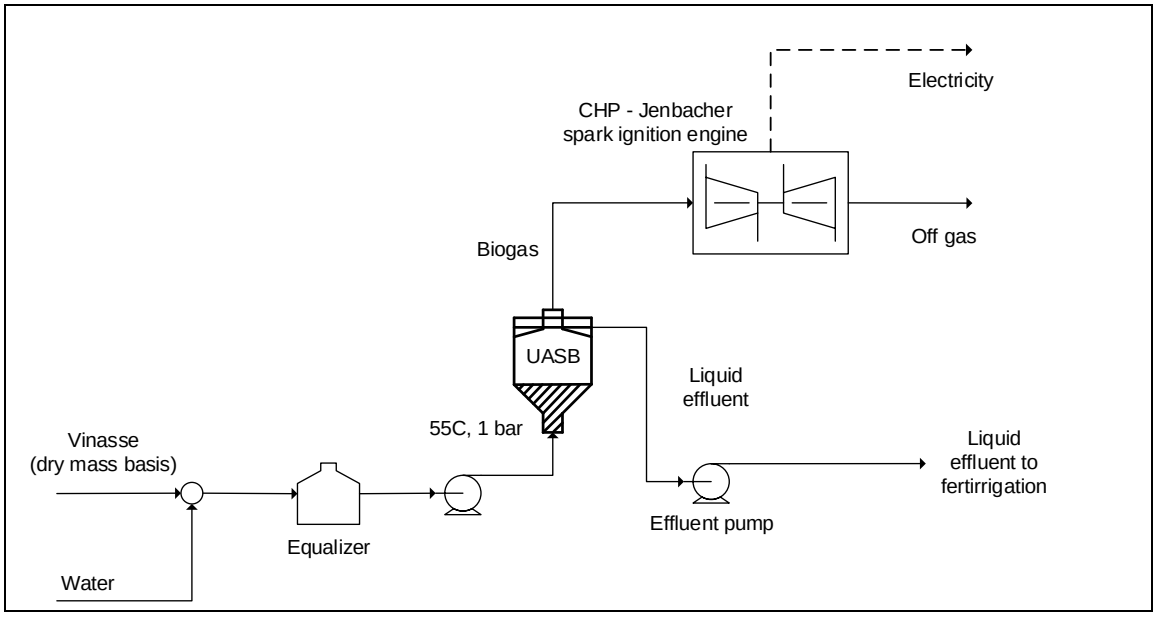

Figure 4.1: Vinasse AD flowsheet for the simulation in Aspen Plus v9

Theoretical separation of the feed stream into the 'Vinasse' and 'Water' streams allowed for easier manipulation of the composition and flowrate in the simulation. As seen in Figure 4.1, the vinasse composition (Table 3.5) was input to the feed stream ('Vinasse') in the simulation on a dry mass basis and water was added separately via the 'Water' stream. Design specifications were used to control the water content and overall flowrate of the vinasse feed stream. Based on the mass flowrate of the 'Vinasse' stream, one design specification calculated the flowrate of water needed to form a vinasse AD feed with a 90% moisture content. Using the flowrate of both the 'vinasse' and 'water' streams, a nested design specification was used to manipulate the AD reactor feed flowrate. To better simulate pilot and small scale industrial AD processes, an initial reactor capacity of 250 m^3 was selected and

was maintained at thermophilic conditions (55°C) and atmospheric pressure to facilitate increased methanogenic activity (Djalma Nunes Ferraz Junior et al., 2016). Due to limitations in Aspen Plus, organic loading rate calculations were performed externally in Microsoft Excel. The volumetric flowrate per day (m^3/day) was calculated using the organic loading rate of 25 kgCOD/(m^3.day) recommended by Souza et al. (1992) and the reactor size. This flowrate was then input using the flowrate design specification which together with reactor volume facilitated mean residence time calculations by the simulation. The biogas produced is fed to the spark ignition engine located in the CHP plant where electricity is generated at an overall efficiency of 44% (General Electric, 2008). Any off gas leaving this system at 180°C is reintegrated into the AD plant for low pressure steam generation.

4.2 Benchmarking of the Anaerobic Digestion Model

The AD simulation developed in Section 3.2.1 adopts the model framework by Angelidaki et al. (1993) and utilizes kinetic data from ADM1 (Batstone et al., 2002). As such, it was necessary to benchmark its performance against existing AD simulations to establish whether the model is fulfilling its intended purpose. This process also serves to ascertain the predictive quality of the anaerobic digestion model (Donoso-Bravo et al., 2011) and its applicability to varying substrates

The base case AD flowsheet developed in Aspen is intended to operate in a steady state manner. Results obtained from this model could be validated using AD steady state data for processes similar to Figure 4.1 with the exception of the CHP plant (Rajendran et al., 2014). Experimental data was sourced from four independent case studies to provide a diverse data set using different substrates. Municipal solid waste (MSW) as well as cow and pig manure were chosen for the benchmarking studies (Budiyono et al., 2011; Eliyan, 2007; Forgács et al., 2012; Fujita et al., 1980). The predicted results obtained from the published AD simulations using these feedstocks were used to benchmark and validate the developed AD framework. The variables extracted from the experimental data that were used as model inputs included: (1) feed composition (% carbohydrates, lipids, proteins as in Section 3.2), (2) loading rates, (3) temperature, (4) reactor size (L), (5) residence times (days) and (6) the methane yields (Table 4.1). The results from the base case AD flowsheet were compared against the literature simulation predictions. In addition, raw experimental data from the studies were compared to the base case results. To determine model accuracy, a regression (R^2) analysis was conducted to supplement and affirm the visual observations made based on Figure 4.2. The regression analysis takes into account the difference between the experimental data and the predicted (simulation) values to give a “goodness-of-fit” measure presented as a number between 0 and 1 (Donoso-Bravo et al., 2011). While an excellent fit would ideally produce an R^2 of 1, AD simulations typically exhibit R^2 values between 0.7 and 0.9 due to the significant uncertainty involved in mimicking microbial behaviour (Donoso-Bravo et al., 2011).

For each case in Table 4.1, the reactor size, temperatures and feed stream compositions were input into the AD Aspen model developed. Experiments on the case studies in Table 4.1 were all conducted at atmospheric pressure. The simulation results were compared against the experimental data and associated literature simulation results and plotted on Figure 4.2. In this steady state validation, the main result considered was the volumetric methane yield (m^3-CH_4/kgVS_{added}).

Table 4.1: Case studies used for validation (C – carbohydrates, L – lipids and P – proteins with remainder as ash. CH_4 yields in m^3/(KgVS.day))

#	Substrate	Feed composition	Reactor size (L)	T (°C)	RT (days)	Loading Rate	CH_4 Yields	Source
1	Cow manure	C: 70%, L: 2%, P: 2%	5	35°C	15	0.33 L/day	0.354	Budiyono et al. (2011)
2	MSW (Lab)	C: 61.5%, L: 10%, P: 16%	5	55°C	21	3 g VS/(L.day)	0.54	Forgács et al. (2012)
3	MSW (Pilot)	Not available	600	55°C	25	2 g VS/(L.day)	0.4	Eliyan and Penh (2007)
4	Pig manure	C: 44.06%, L: 4.9%, P: 23%	30	55°C	8	7.68 g VS/(L.day)	0.27m^3	Fujita et al. (1980)

As seen in Figure 4.2, the base case AD model ("Aspen Simulation") predicted the methane yield within a 10% margin of accuracy on average for both cow and pig manure substrates. Experimental results for the laboratory scale municipal solid waste system were also matched accurately. However, a significant difference between the literature results for the pilot scale MSW system was noted. This disparity may be due to different feed stream compositions in the literature simulation and AD base case model.

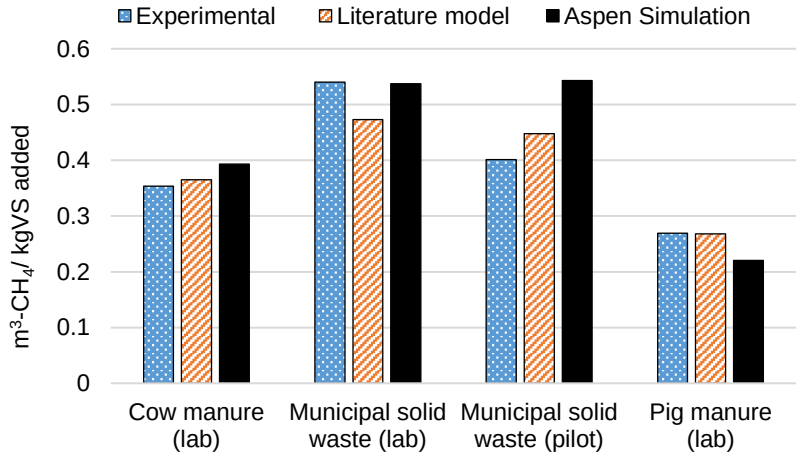

Figure 4.2: A comparison between the base case AD model results, experimental data and literature simulation results concerning the volumetric methane yield of the four case studies considered.

The MSW feed composition at pilot scale was not published, and as such, a generic composition was used (Rajendran et al., 2014). This result shows that the feed composition has a significant impact on simulation results. In addition, it was anticipated that issues associated with scale-up such as the development of unsteady state conditions as well as unpredicted changes in reactor hydrodynamics were experienced in the pilot scale experiment (Case 3 in Table 4.1). These dynamic changes could not be replicated in the model thereby leading to a larger margin of error. A regression analysis conducted to determine the extent of agreement between the experimental and model results yielded an R^2 value of 0.74. Considering the assumptions and simplifications made in developing the AD model as well as the scale up issues noted, the goodness of fit (R^2) was above average and acceptable.

The base case model exhibited the expected behaviour i.e. conversion of organic matter to biogas with achieved methane yield predictions within 10-15% for varying waste streams.

Benchmarking of the model developed serves to show that the adopted AD model structure from literature is robust and can be used for further simulation work.

4.3 Base Case Vinasse AD Simulation

Benchmarking and validation of the model showed accurate prediction of the performance of the anaerobic digestion of diverse waste streams with a reasonable margin of error i.e. within 10% of experimental results (Figure 4.2). Having demonstrated satisfactory benchmarking in Section 4.2, the AD of raw vinasse was simulated to assess the efficiency of the model in terms of its stability and biogas yield predictions. In the simulation, raw vinasse with a composition as shown in Table 3.5 was fed to the AD reactor after preliminary mixing in the equalizer. To have a better representation of an industrial AD, an organic loading rate of 25 kgCOD/(m^3.day) was used as recommended by Souza et al. (1992) and Fuess et al. (2017). Kinetic parameters used in this initial simulation were adopted from ADM1 (Batstone et al., 2002) (Table 3.2). To facilitate better simulation of vinasse AD, two key modifications to the maximum growth rates were made (Table 4.2), based on Barrera et al. (2016).

Table 4.2: Calibrated kinetic parameters (maximum growth rates) for vinasse AD simulation sourced from Barrera et al. (2015) compared to the parameters used in ADM1

Maximum growth rate (μ_{max})	**units**	**Default ADM1**	**Calibrated for vinasse**
Propionate degraders	day^{-1}	13	16
Acetate degraders	day^{-1}	8	12
		(Batstone et al., 2002)	(Barrera et al., 2015)

Calibration of kinetic parameters concerning the maximum microbial growth rates in vinasse AD simulations was initially conducted by Romli et al. (1995) using experimental data. They showed that the activity and growth of propionate, acetate and hydrogen degraders is favoured by the composition of sugarcane molasses and vinasse. This led to an adjustment of the maximum growth rates of the abovementioned microbes using parameter estimation techniques. A similar approach was used by Barrera et al. (2015) for the calibration of ADM1 kinetic parameters which involved adjusting maximum growth rates for propionate, acetate and hydrogen degraders to be used in vinasse AD simulations. Altering these parameters improved the predictive quality of the COD reductions and methane yields by approximately 10% in the AD model (Barrera et al., 2015). These improvements motivated the adoption of the adjusted parameters for all the AD simulations going forward in this work. Hydrogen degradation parameters were not adopted as this step was incorporated into the acetogenic reactions (Section 3.2.1.4).

Using the selected composition discussed in Section 3.2 and the adjusted parameters for vinasse (Table 4.2), the simulation was successfully executed at 55°C and 1 bar to yield material flows as presented in Table 4.3. Thermophilic conditions (55°C) were preferred and used as they have shown to result in higher methane yields owing to increased microbial activity as predicted by the Arrhenius equation (Angelidaki et al., 1999). There is a 0.1% difference between the mass flows in and out of the AD system. During the simulation, non-linear programming techniques are used in Aspen Plus to solve differential equations representing the mass and energy balances. The Newton's methed closure of the mass balance as evidenced by the -0.5% discrepancy.

Following the mechanism of anaerobic digestion, the carbohydrates, fats and proteins in vinasse are degraded via the four AD steps (see Section 3.2.1) to form a liquid digestate and biogas. Ammonia, although not shown in Table 4.3, is formed during the acidogenic fermentation of amino acids and actively taken up by microorganisms as a nitrogen source for growth. Given its proven negative influence on methane yields at concentrations above 0.22 g/L (Angelidaki et al., 1993), ammonia was implemented as an inhibitor to methanogenesis. Similar to ammonia, potassium salts are required for microbial growth. but only in trace amounts (Chen et al., 2008). Aside from the inhibitory influence on methanogenesis (concentrations >5 g/L), potassium salts remain largely inert and pass through unreacted (Kugelman and Mccarty, 1965). The effects of ammonia and potassium on methane yields are investigated in Section 4.4.1.2 and 4.4.1.3.

Table 4.3: Initial Base Case Vinasse AD simulation results as obtained from Aspen Plus at a reactor size of 250 m^3 and OLR of 25 kgCOD/m^3.day (MB – Mass Balance, CB – Carbon Balance)

	Vinasse (kg)	C-in (kg/h)	Digestate (kg)	C-out (kg/h) (digestate)	Biogas (kg/h)	C-out (kg/h) (Biogas)	Biogas (m^3/hr)
Carbohydrates	54.4	22.9	0.7	0.3			
Glycerol tri-oleate	28.8	11.3	0.3	0.1			
Glutamic acid	3.99	1.63	0.69	0.28			
Aspartic acid	1.98	0.72	0.34	0.12			
Lysine	1.98	0.98	0.34	0.17			
Water	1307	-	1296	-	3		4
Acetic acid	47.4	18.9	106.5	42.6			
Propionic acid	0	0	31.6	15.4			
Valeric acid	47.3	27.85	11.2	6.6			
Butyric acid	-	-	5.67	3.09			
Glucose	-	-	14.1	5.64			
Potassium salts	44.8	-	44.8	-			
Methane	-	-	-	-	8.52	6.39	11.9
CO_2	-	-	-	-	11.3	3.07	5.74
Mass totals (kg/hr)	**1537**	**84**	**1516**	**74**	**24**	**9**	
Difference (%) – MB	**0.1**						
Difference (%) – CB	**-0.5**						
Yield (L-CH_4.kgVS_{added}^{-1})	**51**						
Biogas calorific value (kJ/l)	**22**						
Electricity produced (kW)	**53**						

In agreement with typical industrial scale vinasse AD operation, a 65:35 ratio of methane to CO_2 in the biogas was achieved on a volumetric basis in the base case simulation. However, a low biogas methane purity of 53% (v/v) was noted. The observed impurity is associated with high H_2O and NH_3 concentrations in addition to CO_2 in the gas phase (see Table 4.3). Concentrations of ammonia and water are governed by the vapour-liquid equilibrium in the system. Further, high CO_2 production rates and slow uptake by hydrogenotrophic methanogens of this gas results in CO_2 accumulation to reduce CH_4 purity. Despite the impurities, the biogas has a relatively high calorific content of 22 kJ/L that is comparable to values reported in the literature (Ryan et al., 2009). In the CHP process, this energy was converted to electricity to produce 53 kW of electrical work with an efficiency of 44% (General Electric, 2008).

Given the good predictions concerning biogas composition, VFA concentrations and electricity production, the base case simulation showed that the model can be applied to vinasse anaerobic digestion systems. However, the reactor performance is characterized by low purity methane and excessive amounts of VFA in the system. One reason for this could be the presence of inhibitory compounds that disrupt methanogenic activity, thereby slowing the conversion of VFAs to methane. Further, with the current high loading rate, low conversions of VFAs are attributed to the washout of biomass that potentially lead to low methane productivities (Uellendahl and Ahring, 2010). Consequently, investigating the sensitivity of the base case vinasse AD system to compositional changes in the feed and other process conditions is necessary to better understand the influence of these parameters on AD performance. Identifying potential inhibitors and process perturbations that may disrupt AD efficiency will inform decisions regarding additional treatment requirements or alterations in operating conditions to stabilize the AD process and result in higher process.

4.4 Sensitivity analyses – Anaerobic Digestion

The AD of vinasse is affected by several factors that may either result in the improvement or the decline of process efficiency (Yu et al., 2013). The effect of these factors on the process is explored through sensitivity analyses to identify the most influential parameters on the methane yield and biogas productivity.

Temperature and pressure, based on previous studies (Djalma Nunes Ferraz Junior et al., 2016; Fuess et al., 2017), were maintained at 55°C and 1 bar as in the base case simulation (Section 4.3). The variables considered in the sensitivity analyses were the organic loading rate (OLR) and the feed concentrations of amino acids, acetic acid and potassium sulfate. The organic loading rate is a measure of the strength of the wastewater feed as defined in Section 2.3. As such, it is important to control the OLR to prevent overload of organic material and washout of the active biomass (Uellendahl and Ahring, 2010). The presence of inhibitory compounds such as ammonia, inorganic salts and acetic acid negatively affect methane yields by creating pH and osmotic imbalances that may destroy cell membranes thereby disrupting methanogenic activity (Chen et al., 2008). Analysing the sensitivity results with changing inhibitor concentrations will help in identifying of process thresholds so as to ensure efficient AD process operation. Consequently, the need and scale of pre- and post-treatment processes for product recovery may be determined that may ultimately have a positive impact on the overall feasibility of the project.

4.4.1 Feed Stream Composition and Inhibitor Concentrations

Phenols, inorganic salts, ammonia and volatile fatty acids have the potential to reduce microbial activity through inhibition thereby leading to a decline in methane yields (Chen et al., 2008). The extent of inhibition is dependent on the concentrations of the inhibitory compounds. In practice, inhibitory concentrations are experimentally determined and are incorporated into the AD model via inhibition constants (K_i) in Michaelis-Menten type kinetics (see Section 3.2.1). In the developed base case anaerobic digestion model, ammonia, VFAs (as acetic acid) and potassium sulfate are the inhibitors considered to have the greatest influence on the overall AD performance. To evaluate the effect of these inhibitors, compositions of the inhibitors in the vinasse feed stream were varied whilst keeping the remaining components constant. As per the base case simulation, the reactor volume and the organic loading rate for these simulations were maintained at 250 m^3 and 25 kgCOD/(m^3.day), respectively, while the selected inhibitor concentration was varied.

4.4.1.1 *Volatile Fatty Acids*

The VFAs present in vinasse AD systems are acetic, propionic, valeric and butyric acids. These are weak acids which dissociate into their ionic species that include hydrogen ions that ultimately influence the system pH (Wilkie et al., 2000). The degree of inhibition of these compounds is determined by the extent of dissociation of these VFAs into their conjugate bases and hydrogen ions. However, due to a conflict in the physical property methods required for ionic speciation and AD simulation as well as missing physical ionic properties, the base case scenario does not predict pH. Ionic speciation was therefore not implemented and the base case simulations were limited to systems where pH is controlled externally.

The inhibiting effect of VFA concentrations in the feed stream on the methane yield was studied by varying the acetic acid concentration in the feed stream (Figure 4.3). While other VFA such as propionic, valeric, and butyric acid also affect pH and cause inhibition, focus was placed on acetic acid due to its abundance and also in accordance with Angelidaki et al. (1993). In this model, the acetogenic reactions which convert propionic, valeric and butyric acid to acetic acid are inhibited by the concentration of acetic acid in the reactor (Equation 4.1)

$$\mu = \mu_{max}(T).\left(\frac{1}{1+\frac{K_{S_{VFA}}}{S_{VFA}}}\right).\left(\frac{1}{1+\frac{K_{S_{NH_3}}}{S_{NH_3}}}\right).\left(\frac{1}{1+\frac{S_{HAc}}{K_{i,HAc}}}\right)$$

Equation 4.1

With increasing conversion of VFAs to acetic acid, there is a decrease in the inhibition term in Equation 3.2 which, in turn, causes a decline in the calculated growth rate (μ) of the acetogens. Over time, VFAs accumulate in the reactor due to slow uptake by acetogens. Following this, a consequent reduction in the methane yield due to the accumulation of unconverted VFA is expected. The results of the process response to changing acetic acid concentrations in the feed stream is shown in Figure 4.3 with the base case concentration presented at 0%.

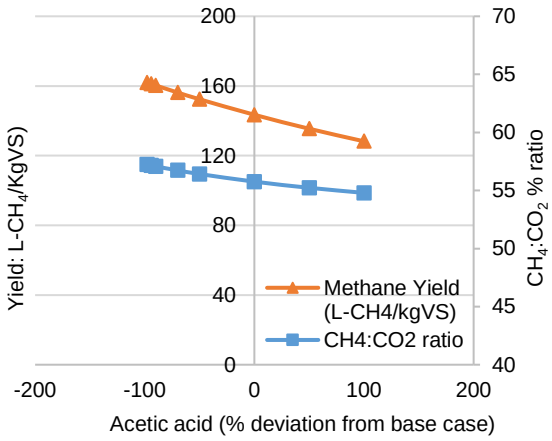

Figure 4.3: Effect of varying acetic acid on the methane yields and CH_4:CO_2 ratio in the base case simulation

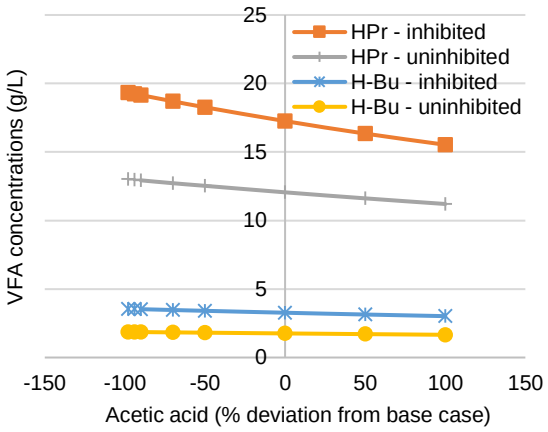

Figure 4.4: Effect of acetic acid inhibition on VFA concentrations (butyric and propionic acid) in the base case simulation

When doubling the acetic acid concentration, an 11% decrease in the methane yield from 143 L-CH_4/(kgVS) (0% deviation in Figure 4.3) to 128 L-CH_4/(kgVS) (100% deviation in *Figure 4.3*) was noted. Consequently, halving the concentration resulted in a 10% increase the yield (-50% deviation in Figure 4.3). The CH_4 to CO_2 ratio in the biogas remained fairly constant between 55 and 58%. In the absence of acetic acid inhibition on acetogenesis, the VFA concentrations were approximately 20% lower at steady state confirming the accumulation of VFAs in the reactor was due to acetogenic inhibition by acetic acid (Figure 4.4). These results are consistent with literature studies which show that acetic acid may inhibit the functioning of the methanogenic archaea causing significant declines in methane productivity and COD reductions (Angelidaki, Ellegaard & Ahring, 1999; Uellendahl & Ahring, 2010).

4.4.1.2 Amino acids and Ammonia

Crude protein is a constituent of vinasse that often results from the breakdown of yeast cells in the molasses fermentation process (Scull et al., 2012). These complex proteins are further broken down to amino acids in AD through hydrolysis. Ammonia is then formed through the acidogenic fermentation of amino acids (Yu et al., 2013). In this model, the crude proteins were simplified to three amino acids namely glutamic acid, lysine and aspartic acid. These are known to be the most abundant amino acids present in vinasse and would have the greatest contribution to the methanogenic response at elevated concentrations of these compounds (Turner et al., 2002). Ammonia acts as a nitrogen source for the microbial communities and is modelled as a co-substrate in all the AD reactions except for the acidogenesis of amino acids (Angelidaki et al., 1999). However, studies have shown that free ammonia may cause a 50% reduction of methanogenic activity through cell membrane penetration and disintegration when its threshold concentration of 0.56 g/L is exceeded (Sung and Liu, 2003). This effect was investigated by altering the amino acid concentration in the feed stream (Figure 4.5 and Figure 4.6). As expected, a decrease in the methane yield is observed with increasing amino concentration.

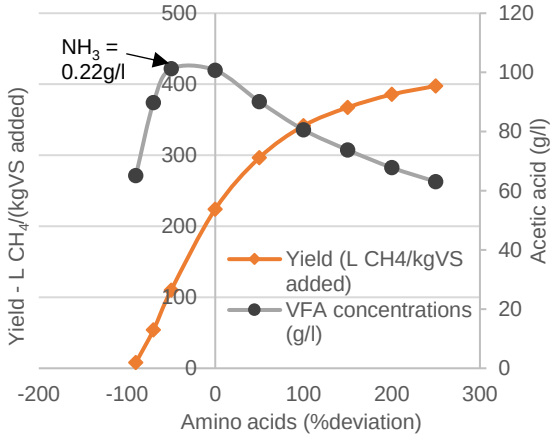

Figure 4.5: Effect of varying amino acid concentrations on the methane yield and acetic acid concentrations in the base case simulation

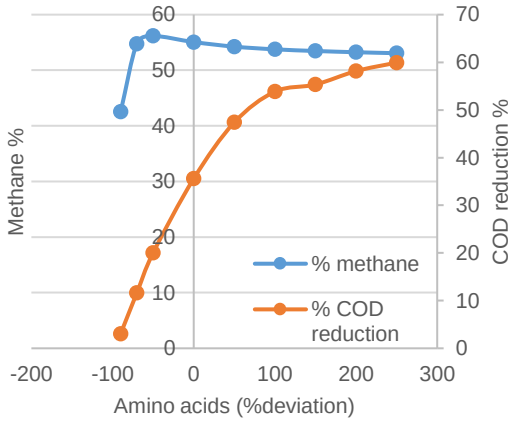

Figure 4.6: Effect of varying amino acids on the COD reduction and biogas composition in the base case simulation

Figure 4.5 and Figure 4.6 show the influence of increasing amino acids on the methane yield, biogas composition and COD reduction. As seen in Figure 4.5, a maximum in the acetic acid concentration is noted in the reactor at an ammonia concentration of 0.22 g/L, which corresponds to the point of inflection in the methane yield curve (Chen et al., 2008). Although

this ammonia concentration is lower compared to the threshold (0.56 g/L) suggested by Sung and Liu (2003), the observation was deemed credible as it corresponded to the inhibition constant (K_{iNH3}) adopted from Angelidaki et al. (1993) and initially coded in the developed model. The maximum concentration after which ammonia starts becoming inhibitory is also seen in Figure 4.6 where the methane composition reaches a maximum of 57%. Inhibition is only noted once the amino acid concentration in the feed stream exceeds 60% of the base case feed concentration and goes above the 0.22 g/L threshold (-60% in Figure 4.5 and Figure 4.6). The methane composition thereafter decreases and levels off as seen in Figure 4.6. Acetic acid concentrations also begin to decrease (VFA curve in Figure 4.5), which could be a result of secondary inhibition by acetic acid on acetogenic reactions.

These results are consistent with trends observed in literature where elevated crude protein concentrations resulted in consequent decreases in methane production as well as VFA accumulation at ammonia concentrations above 0.5 – 0.3 g/L in the reactor (Angelidaki et al., 1999).

4.4.1.3 Inorganic Salts – K_2SO_4

Salt cations play an important role in microbial growth and development in anaerobic digestion. However, above certain threshold concentrations, cations such as sodium, magnesium, calcium and potassium may inhibit growth. Previous studies have shown that methanogens are often affected by elevated salinity in AD reactors (Hierholtzer and Akunna, 2014; Kugelman and Mccarty, 1965). Potassium salts are the most abundant cations in vinasse, it is therefore important to determine the effect of these salt concentrations on the methane yield (Wilkie et al., 2000). To establish the effect of K^+ concentration, the concentration was varied between a half and two-fold the base line vinasse concentration and resultant CH_4 yield explored (Figure 4.7).

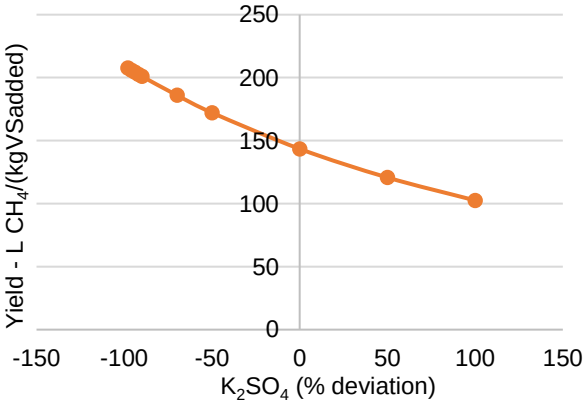

Figure 4.7: Effect of K_2SO_4 concentrations on the methane yields

Increasing the inorganic salt concentration two-fold (0 to 100% in Figure 4.7) resulted in a 30% decrease in the methane yield. Although the effects of high salinity are varied in the literature, it is postulated that high salt concentrations result in an increase of the osmotic pressure regulating water flow across cell membranes (Chen et al., 2008). This, in turn, causes cell dehydration and death. On the other end, at trace K^+ concentrations -100%, there is a 45% increase in methane yield. Concentrations of K^+ ions in the medium above 11.6 g/L may result in 50% decrease in methanogenic activity as suggested by Kugelman and Mccarty (1965). Although decreasing methanogenic activity could not be directly quantified in the simulation, it is evidenced by the decline in methane yields with increasing K^+ ion

concentrations above the threshold concentrations (11.6 g/L) . This threshold corresponds to 60% of the base case concentration (-60% on Figure 4.7).

4.4.1.4 Organic Loading Rate

The organic loading rate (kg COD/m^3/day) is a function of the overall COD concentration of the feed stream (kg COD/m^3), stream flowrate (m^3/day) and reactor volume (m^3). This was varied by altering the COD concentration in the feed whilst maintaining a constant reactor mean residence time of 1 day. This was to ensure that in each simulation the substrate spent an equal amount of time in the reactor thus eliminating the compounding effects of flow on the resultant performance. The vinasse composition used was based on published data from an ethanol distillery in KwaZulu Natal (see Section 3.3.2, Table 3.5).

The OLR, typical of pilot and industrial scale vinasse AD operations (Fuess et al., 2017; Souza et al., 1992), was varied from 0 to 30 kgCOD/(m^3.day) (Figure 4.8). Having set the residence time to 1 day in this sensitivity, the OLR was equivalent to 0 – 30 kgCOD/m^3. Loading rates below 5 kgCOD/(m^3.day) typically used in laboratory settings were also included in the investigation (Barros et al., 2016). In these simulations, the volumetric methane yield (L-CH_4/kgVS_{added}) was used as an indicator of system performance as it provides a measure of the biogas produced relative to the volatile solids added.

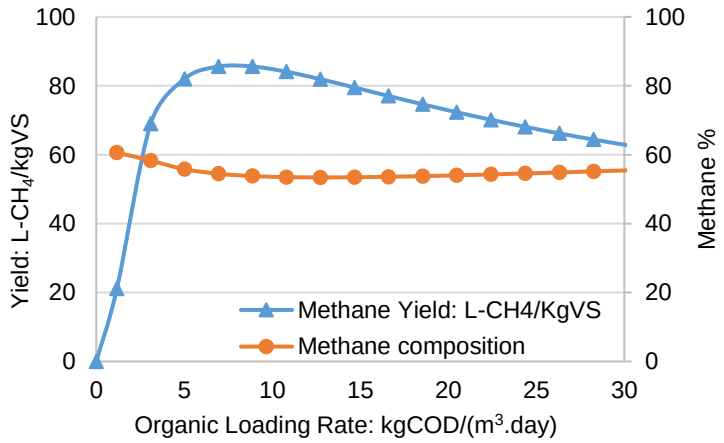

Figure 4.8: The effect of increasing OLR on the volumetric methane yield and COD reduction

Increasing the loading rate leads to an initial increase in the methane yields (Figure 4.8). A maximum of 85 L-CH_4/kgVS_{added} is observed when the organic loading rate is increased to ca. 7 kgCOD/(m^3.day). Further increase in the OLR results in a gradual decrease in the methane yield with the average methane composition remaining fairly constant throughout between 55 and 60% (v/v).

Initially, increasing the organic loading rate availed more substrate for uptake by the microorganisms which led to increased activity and consequently, higher methane yields up to the maximum. The decline in the methane yield after the maximum was due to a build-up of VFAs, which contribute to the organic loading, and other inhibitory compounds such as K^+, NH_3 and acetic acid in the reactor that inhibit methanogenic activity (Barros et al., 2016).

The sensitivity analyses conducted show that the inhibitory compounds have a negative impact on the methane yield and biogas production. Of these compounds, acetic acid and ammonia also act as co-substrates for biomass growth. Inorganic salts (K_2SO_4), on the other hand, are not crucial for microbial growth and can be extracted from vinasse to potentially

increase the methane yields (P. Zhang et al., 2012). However, it is important to first determine the economic standing of the base case and establish cost sensitive areas before considering any process additions. Techno-economic analyses were used to determine flowsheet feasibility through the calculation of profitability indicators such as the return on investment, internal rate of return and payback period. Incorporation of pre- and post-treatment processes can be considered depending on the additional capital investment required versus the marginal benefits accrued in terms of revenues or cost savings.

4.5 Techno-economic Analysis for the Base Case Flowsheet (Vinasse AD & CHP)

A techno-economic analysis is aimed at evaluating the economic feasibility of a project. It is an important tool for decision making that quantifies the profitability of a venture. As described in Section 3.5, this is done through the determination of capital and operating expenditures which are then used in conjunction with the revenues to develop a discounted cash flow analysis (Balaban, 2000). From this, profitability indicators such as the net present value (NPV), return on investment (ROI) and internal rate of return (IRR) are determined. As the costs in this investigation are calculated using detailed factorials (Balaban, 2000; Seider et al., 2003), the accuracy of these estimates are between 15 to 25% and are therefore suited for a pre-design budgeting and profitability analysis. To improve the level of confidence and accuracy of these investments, a definitive cost analysis is recommended at the later engineering design level where all equipment quotes can be obtained from the manufacturers. Presently, the former approach is used throughout the subsequent analyses.

An initial techno-economic analysis was conducted on the base case AD flowsheet to evaluate its economic feasibility in a South African context (see Figure 4.1). The reactor capacity was increased to 2000 m^3 in a bid to simulate an industrial vinasse treatment plant (Fuess et al., 2017). Notably, scale up is expected to cause changes in the yields, mean residence time and effluent concentrations. To ensure comparable results, the raw vinasse mass flowrate was adjusted accordingly to maintain a constant organic loading rate of 25 kgCOD/m^3.day and a mean residence time of 132 hours in the rest of the simulations going forward. Following the adjustments, it was assumed that the trends discussed in Section 4.4 applied proportionally to the scaled up base case flowsheet. A simplified schematic of the base case flowsheet is shown on Figure 4.1.

4.5.1 Mass and Energy Balances

Following the change in reactor capacity to 2000 m^3 and adjustments to the feed flowrates to maintain an OLR of 25 kgCOD/m^3.day (Section 4.3), mass and energy balances were regenerated. These were used to account for the flow of material, compute performance indicators (methane yields) and provide data to be used in equipment sizing. In addition, the mass and energy balance (Table 4.4) provided information on the magnitude of product streams and utility requirements necessary for the computation of the revenues and operating expenditures.

Table 4.4: Summarized mass and energy balance of the scaled-up (2000 m^3) base case simulation

Key components	Raw vinasse (kg/hr)	Digestate (kg/hr)	Biogas (kg/hr)	Biogas (m^3/hr)
Carbohydrates	450	6.4	-	-
Glycerol tri-oleate (fats)	240	2.4	-	-
Amino acids (Protein)	66	12	-	-
Glutamic acid	33	5.9	-	-
Aspartic acid	17	2.9	-	-
Lysine	16	3	-	-
Water	10770	10700	24	30
VFA	780	1270	-	-
Potassium salts	370	370	-	-
Methane (m^3/hr)			65	92
CO_2 (m^3/hr)			85	44
Mass totals (kg/hr)	12670	12504	182	
Difference (%)	**0.1%**			
Yield (L-CH_4.kgVS_{added}^{-1})	**48.5**			
Biogas calorific value (kJ/L)	**21.9**			
Electricity produced (kW)	**410**			

Although scale up challenges such as unsteady states affecting CH_4 yields were expected to arise, the general trends of the small (250 m^3) and large (2000 m^3) scale systems remained fairly similar. For instance, the large scale methane yield achieved (48.5 L-CH_4.kgVS_{added}^{-1}) (Table 4.4) differed by only 4% with the small scale yield (51 L-CH_4.kgVS_{added}^{-1}) (Table 4.3). This further affirmed the assumption that, proportionally, the scaled up system would exhibit similar trends as the small scale system.

The biogas produced from AD in this simulation was routed to the Jenbacher spark engine to generate 410 kW of electricity which translates to 3.6 million kWh electricity per annum. The exhaust gas was routed to a heat recovery system where it was used to generate low pressure steam at 124 kPa at a flowrate of 90 kg/hr. This additional steam was regarded in the techno-economic evaluation as a savings on utility costs in the plant. The liquid effluent was transported to the sugar cane fields and used as fertilizer that resulted in a cost saving on synthetic potassium based fertilizer purchase that was included in the operating expenditures.

4.5.2 Capital Expenditure – CAPEX

The total capital investment consists of the fixed and working capital costs. Fixed capital takes into account the equipment purchase, site preparation and delivery costs, as well as any other miscellaneous expenses incurred up to the start of production. The working capital refers to the money required to operate the plant during its start-up phase. It is estimated to be 15% of the fixed capital investments (Turton et al., 2008).

The equipment purchase costs (Table 4.5) were calculated using published cost curves (Balaban, 2000) and standard order of magnitude (OOM) estimates (6-tenths rule) (Seider et al., 2003). A detailed approach was documented in Section 3.5. These costs were then adjusted for inflation using the Chemical Engineering Plant Cost Indices (CEPCI) for 2016 (Mignard, 2014).

Table 4.5: Purchase cost of equipment (PCE) for the base case flowsheet obtained using OOM estimations and equipment manufacturer quotes published in the literature (to the nearest $1 000)

Equipment	Capacity	MOC	Costs (USD, 2016)	Source
UASB reactor	2000 m^3	Reinforced concrete	651 000	(Fuess and Zaiat, 2017)
Influent and effluent pumps	0.21 m^3/min	Carbon steel	7 350	(Fuess and Zaiat, 2017)
Ancillary equipment	-	-	11 180	(Fuess and Zaiat, 2017)
Equalization tank	1820 m^3	Reinforced concrete	385 000	(Seider et al., 2003)
Jenbacher™ 620	-	-	$1 770 000	(Darrow et al., 2015)
Total cost			**$2 821 000**	

The UASB and ancillary equipment costs were obtained from a literature study that evaluated the capital and operating expenditures incurred in a vinasse treatment facility in South America (Fuess et al., 2017). These were adjusted accordingly using the 6th tenths rule and updated using the CEPCI for 2016. Manufacturer quotes from General Electric documented in Darrow et al. (2015) were used to compute the equipment cost of the CHP system. The detailed Lang factorials documented in Table 3.6 (Amigun and Von Blottnitz, 2010) for 3 phase systems that account installation and site development costs were used to estimate the physical plant costs (PPC) from the PCE.

The fixed capital cost was calculated using three additional factorials (Table 3.6) that represented the engineering and contingency fees (Turton et al., 2008). As expected, the Jenbacher engine made up a significant portion (64%) of the total equipment costs (Table 4.5). This proportional estimate corresponds to Fuess and Zaiat (2017) who found that CHP equipment costs made up 40-56% of the total purchase cost in industrial vinasse AD power plants. Although spark ignition engines are historically known to be expensive, they are preferred due to their compact nature and ability to withstand impure biogas feeds. Ancillary equipment included in the techno-economics included biogas flow meters, seals as well as pH and gas analyzers. Although the costs vary depending on the ancillary equipment models, it remains the lowest (3%) relative to the other equipment needed for the AD power plant (Table 4.6). The higher cost per volume (m^3) for the equalizing tank compared to the reactor is attributed to economies of scale. A manual costing approach, using published equipment cost curves (Seider et al., 2003), resulted in a 0.3% difference (Table 4.6) in the PCE compared to the OOM approach used above.

Table 4.6: A summary of AD plant costs computed using the OOM and heuristic approaches

Cost summary of AD Equipment	Heuristic approach	OOM approach
UASB	651 000	650 900
Pumps	7 400	4 500
Auxilliary equipment	11 180	11 180
Equalizer	384 700	384 700
Totals	**$1 054 200**	**$1 051 300**
Percentage difference	**0.27%**	

The proximity in the calculated costs using different techniques reinforced confidence in the calculated expenditures using the current approach and the calculated fixed capital cost using these estimates (Table 4.7).

Table 4.7: Fixed capital investment calculations using a detailed factorial method (to the nearest $1 000)

Detailed factorial cost estimation	Lang Factors	Costs (USD, 2016)
Purchase cost of equipment (PCE)		**2 820 400**
Installation, electrical, site, instrumentation factors	1.6	
Physical Plant Cost (PPC) = PCE* (above factors)		**4 513 000**
Design, Engineering and Contingency factors	1.19	
Location factor	1	
Fixed Capital Investment (FCI) = PCE* SUM(Factors)	**1.6 + 1.19**	**5 370 000**
Working Capital (15%)		805 500
Total Capital Investment (TCI)		**$6 176 000**

In these estimates, the PPC amounts to 1.6 times the PCE as the plant processes all material phases including gases, liquids and solids, contributing to these elevated costs. The working capital was estimated at 15% of the FCI (Turton et al., 2008).

4.5.3 Operating Costs – OPEX

The day to day running of the plant, the operating expenditure, is divided into two categories namely, the fixed and variable costs. In the base case AD flowsheet, the fixed operating costs included labour, supervision, maintenance and plant overheads. Variable costs on the other hand consist of utility and raw material costs. The total operating costs in Table 4.8 were calculated using a heuristic approach and industry benchmarks reported in the literature (Amigun and Von Blottnitz, 2010; Mohammed et al., 2016)

Table 4.8: A breakdown of the operating costs to the nearest $1 000 for the base case AD flowsheet

Operating Expenditures	Costs/yr (USD,2016)	Source
Raw Materials		
NaOH (dosing)	38 690	(Alibaba, 2017)
Labour and utility		
Labour Costs	172 000	(Payscale SA, 2017)
Utility and transport costs (liquid digestate)	16 000	
Operation and Maintenance		
AD system – O&M costs (1.5% of PPC)	28 000	(Amigun and Von Blottnitz, 2010)
CHP system – O&M costs ($0.02/kWh)	81 000	(Darrow et al., 2015)
Potential cost savings for synthetic fertilizer	-92 000	(Alibaba, 2017)

Total Operating Costs per annum	**$244 000**

In estimating the annual total operating costs, the cost of labour was calculated for personnel with salaries approximated from a reputable online payment database (Payscale SA, 2017). The required personnel in this estimation included three operators (one per shift), an engineer and 2 laboratory technicians. The labour costs were found to be significantly higher than the utility or raw material costs (Table 4.8).

Anaerobic digestion is known to be a low maintenance process that requires minimal additional inputs other than the substrate and initial inoculum. As a predominantly passive process, the raw material costs are limited to NaOH requirements for pH buffering and control in the reactor. In this evaluation, the amount of NaOH was estimated from AD studies on vinasse that recommended an optimal dosing rate of 0.004 kg NaOH/kgCOD (Souza et al., 1992).

The operation and maintenance costs were estimated from industry benchmarks obtained from published literature (Amigun and Von Blottnitz, 2010; Masebinu et al., 2014). As AD plants are relatively cheap to operate and maintain, the operation and maintenance costs were estimated between 1 and 2% of the physical plant costs (Mohammed et al., 2016). On the other hand, CHP plants require specialized maintenance and service after every operating year (8000 hours). According to Darrow et al. (2015), this cost is dependent on the amount of electricity units produced in kWh. For the Jenbacher^{TM} 620 spark engine with a total capacity of 1000 kW, maintenance costs amounted to $0.02 per kWh generated. It was assumed that the effluent would be used for fertirrigation of agricultural land at an application rate of 350 m^3/ha. This resulted in a cost savings from the purchase of synthetic K based fertilizer valued at $400/ton (Alibaba, 2017).

4.5.4 Cash Flow and Financial Analysis

In evaluating the profitability of the base case vinasse treatment project, the discounted cash flow was estimated over the project life. The lifetime of this project was taken to be 20 years. During the project start-up phase, the cumulative cash flow is negative owing to the fixed and working capital costs incurred. It was projected that the plant construction would take a period of two years during which 70% of the fixed capital would be used in the first year and the remainder in the second. Half of the working capital was incurred in each construction year (Balaban, 2000).

The revenue streams considered in the economic evaluation included electricity. The electricity price was set at the recommended renewable energy feed in tariff of at $0.1 per unit of electricity (KWh) from biogas as set by the National Energy Regulator (NERSA, 2011). It is noteworthy that this tariff is higher compared to the coal power tariff ($0.07/kWh) (Bischof-Niemz and Fourie, 2016). This is largely due the 40% higher levelized cost of energy (LCOE) when producing electricity from coal relative to biogas. The liquid vinasse effluent was assumed to be an indirect revenue used in place of commercial synthetic fertilizers thereby reducing the sugarcane plantation running costs (Turner et al., 2002).

Factors relating to the South African economy such as depreciation, scrap value, inflation rate and the average cost of capital were taken into consideration when developing the cash flow analysis. The weighted average cost of capital (WACC) was assumed to be 15%. This was largely based on sale limitations of electricity back into the electrical grid that are not well established and are often barred by heavy regulations and policies that increased the project

risk rating. However, the biogas production technology together with the CHP engine are widely practiced making this a medium risk venture. The economic influencers as well as a summary of costs and revenues are reported in Table 4.9.

Table 4.9: A summary of revenues, costs and economic factors (to the nearest $1 000) used to develop the discounted cash flow analysis for the base case vinasse treatment process.

Revenues and Costs	**Amount (USD, 2016)**
Production rate (KWh/yr)	3 600 000
Renewable Energy Feed in Tariff ($/KWh)	0.1
Annual Revenue	**360 000**
Annual Operating costs (OC)	**336 000**
Cost savings (steam and liquid effluent)	99 000
Total Annual Operating costs = OC – CS	**$244 000**
Fixed capital	5 370 000
Working capital	805 500
Total Capital Investment = FCI + WC	**$6 176 000**
Economic factors	
Taxation (%)	28
Escalation (%)	6.2
Years of depreciation	10
Scrap value (%)	5
WACC (discount rate, %)	15

In this financial analysis, depreciation of physical plant assets was accounted for using the straight line method where their value decreased equally over a period of 10 years. It was assumed that the physical assets will eventually assume the scrap value of 5%. The revenues and costs were escalated accordingly by the inflation rate. Using this information, the cumulative normal and discounted cash flows were calculated. The normal cash flow is the difference between revenues and cost, taking into account the inflation and depreciation. On the other hand, the discounted cash flow takes the WACC into account and represents the present value of money. The discounted cash flow (Figure 4.9) was used to determine profitability indicators such as the ROI, IRR and NPV.

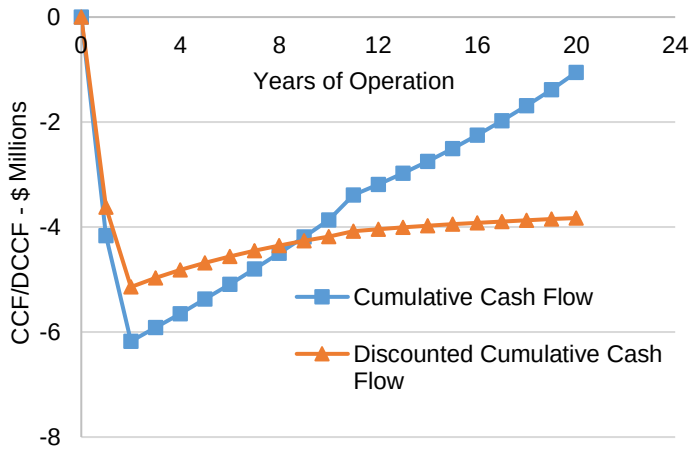

Figure 4.9: Cumulative cash flow analysis (USD, 2016) for the base case vinasse treatment flowsheet for a 20 year project lifetime.

In Figure 4.9, the intersection of the two curves after year 9 represents a crossover from negative to positive net profits. The payback period for this project was calculated to be 18.9 years at which point the fixed capital costs would be recovered. The ROI was calculated as 0% indicating that this venture will not yield positive returns throughout its lifetime. Further analysis showed that there would be a 0% rate of return which translates to negligible growth. At this IRR, the cost incurred whilst financing the venture will not be recovered within the 20 year project lifetime. A low NPV of - $4 million was obtained after 20 years, which shows that the projected earnings will not cover the anticipated costs signalling a net loss. Although the base case proved unprofitable, choosing to dispose the raw vinasse (305 kL/day) into the municipality wastewater treatment facility bears an annual cost of approximately $80 700 – considering the average industrial effluent disposal tariffs (R9/kL) in SA (Ethekwini Water and Sanitation, 2018). This shows that there is a cost of 'doing nothing' which prompts further investigation into ways of increasing profitability of the base case through addition of combined pre- and post-treatment options.

As the calculations rely on assumptions regarding the cost of capital, inflation, projected earnings and costs, the prevailing economic climate may lead to changes in costs and revenues within the project's lifetime. This may result in changes in the profitability indicators. As such, it is necessary to investigate the profitability of the vinasse treatment process to key factors such as the methane yield and feed in tariffs.

4.5.5 Sensitivity Analysis on Profitability of the Base Case

Sensitivity analyses were used to gauge how sensitive the profitability indicators are to various input variations. The concentration of inhibitory compounds was identified as the key variable affecting the methane productivity and consequently, the revenue. It is therefore expected that removing inhibitory compounds such as potassium cations may lead to an increase in the biogas production rate and consequently increased returns. In addition, the recovered potassium salts presents a potential revenue stream.

Another key factor affecting the profitability of the vinasse treatment project is the renewable energy feed in tariff (REFIT) for biogas that is set by the National Energy Regulator, South Africa (NERSA, 2011). Based on the levelized cost of energy production, the REFIT is set slightly higher to facilitate increased investing in the electricity supply industry. However, due

to the economic climate in South Africa, the levelized cost of energy is volatile and may lead to an increase or decrease in the REFIT. This will have a direct impact on the profitability.

4.5.5.1 Inhibitor Concentrations – Potassium cations

Potassium cation concentrations in the form of K_2SO_4 was varied as presented in Figure 4.7 in a bid to understand the effect of inhibitory compounds on the profitability. At this stage, the sale of electricity was the sole revenue stream. To indirectly supplement the revenues, two cost savings strategies were implemented: (1) application of digested vinasse effluent onto the sugar cane fields, and (2) steam utility generation using the CHP exhaust gas.

The base case K_2SO_4 concentration is represented by the 0% mark. Changes in NPV, ROI and IRR are shown in Figure 4.10 and Figure 4.11.

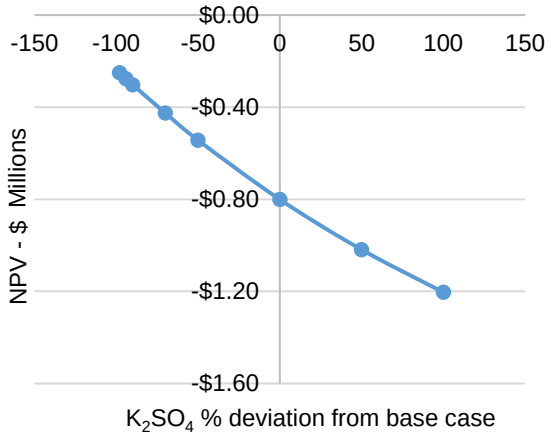

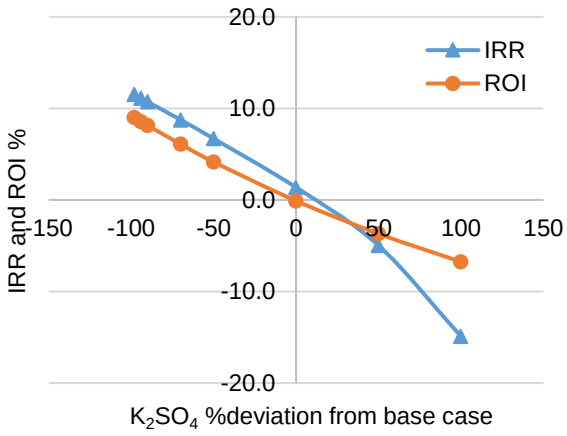

Figure 4.10: Effect of varying K_2SO_4 concentrations on the NPV (USD, 2016) of the base case flowsheet

Figure 4.11: Effect of varying K_2SO_4 concentration on the IRR and ROI of the base case flowsheet

Figure 4.10 shows the response of the NPV to changing salinity in the vinasse feed. Decreasing the salinity of the feed stream effected an increase in methane yields as a result of decreased cationic inhibition by K^+ ions represented by K_2SO_4 in the developed model (Figure 4.7). This increase in CH_4 yields consequently resulted in a profitability increase and general upward trend in the NPV with decreasing salinity. Halving the potassium sulfate concentration to 50% of the base case led to a 60% increase in the NPV. The best case scenario of a 99% reduction in K_2SO_4 concentrations results in an NPV of -$276 100 after a 15 years within the project life time. Figure 4.11 shows a 9% increase in the IRR and ROI with a 99% reduction in the K_2SO_4 concentrations. Similarly, there is an upward trend in the IRR and ROI as salinity in the feed decreases which shows that the project is gradually becoming favourable in relation to the initial capital invested.

The base case AD flowsheet with CHP is not feasible. However, the removal of AD inhibitors through a pre-treatment approach is promising and may lead to increased methane yields, biogas production rates and revenues. There is potential to breakeven with the inclusion of revenues from recovered potassium sulfate. However, this comes at an increased cost as an additional processing unit is required for pre-treatment.

4.5.5.2 *Renewable Energy Feed in Tariff*

Unprecedented changes in the renewable energy feed in tariff are bound to significantly influence profitability. A sensitivity analysis on the REFIT was conducted to determine the effect of its variability on the economics of the base case vinasse treatment project. The REFIT was varied on both positive and negative extremes relative to its base value of $0.1/kWh as seen in Figure 4.12.

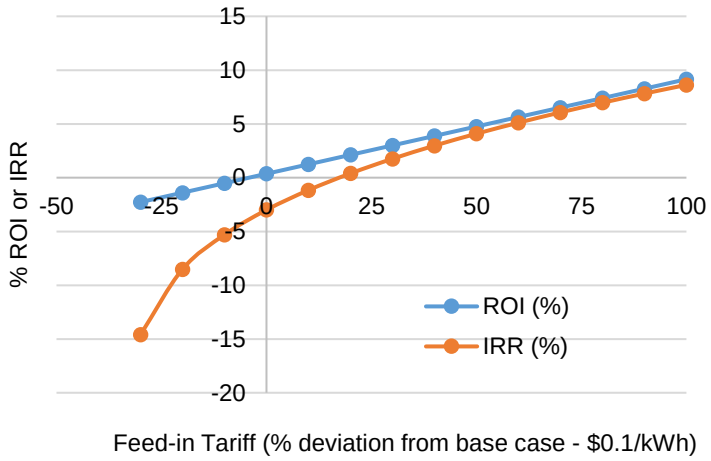

Figure 4.12: Effect of varying the REFIT on profitability (USD, 2016) of the base case vinasse treatment flowsheet.

As expected, increasing the REFIT resulted in a subsequent increase in the revenues and profits. Similarly, decreasing the REFIT resulted in a corresponding decrease in revenues. The return on investment is directly dependent on the profit after tax. As such, it responded proportionally to changes in the tariffs.

Moving from the extreme negative deviation ($0.07/kWh) towards the base value, there is a sharp increase in the internal rate of return. Positive growth is realized at tariffs greater than $0.12/kWh as evidenced by the positive IRR. Thereafter, the IRR increases linearly with each tariff increase. Doubling the tariff (100%) results in an 8.7% increase in the IRR and ROI as seen in Figure 4.12. However, even in this best case scenario, the IRR remains lower than the weighted average cost of capital that is set at 15%.

4.5.5.3 *Summary of the Sensitivity Analyses on Profitability of the Base Case Vinasse AD Flowsheet*

As seen in Figure 4.7 the concentration of potassium cations in vinasse have a significant impact on the AD performance and methane yields. Doubling the potassium ion concentration leads to a 30% decline in the methane yield. There is a knock-on effect of the decline in methane yields on the profitability of the flowsheet as seen in Figure 4.11. This is due to inorganic salts such as potassium ions being inhibitory to AD and result in an overall decrease in the biogas yield and electrical energy produced by the CHP plant.

To maintain and possibly increase the methane yields, it is important to investigate pre-treatment technologies aimed at the recovery of potassium ions from the raw vinasse. This will increase the CH_4 yields and total power generated by the CHP plant. Additionally, the recovered potassium salt is a revenue stream worth approximately $400/ton (Alibaba, 2017). This initiative is expected to increase the profitability of the vinasse treatment process. Further value creation can be sought through the incorporation of post-treatment and biogas utilization

processes to recover water and produce electricity or biomethane. However, a deeper investigation of the additional cost implications is necessary to evaluate the economic feasibility of these modifications and the resulting vinasse treatment routes.

5. Pre-treatment and Post-Treatment Considerations for Value Creation

Sensitivity analyses conducted on base case vinasse process showed that a reduction in inorganic salt (K^+) concentrations prior to AD is beneficial to both performance and profitability of the process. This was attributed to improved methane yields which led to increased electricity production from CHP. Following this result, it would be beneficial to evaluate the economic impact of the inclusion of a pre-treatment process to the base case flowsheet aimed at reducing the concentration of potassium cations.

Further opportunities for value creation from the biogas and liquid digestate produced are present (see Section 2.4). The base case process currently contains a CHP engine to convert biogas to electricity. Alternatively, the biogas can be upgraded to produce biomethane with a significantly higher energy content that can be used as a substitute for natural gas (Masebinu et al., 2015). Both strategies aim to produce energy that can be reused internally to power energy intensive processes or sold commercially. The liquid digestate has a relatively high moisture content ranging between 85 and 90% (Wilkie et al., 2000). In the base case flowsheet, this is directly applied to the sugarcane field and results in cost savings on synthetic fertilizer purchase. Although fertirrigation results in a cost savings, there is a need to explore water recovery strategies from the digestate to increase resource productivity and sustainability by reducing the amount of fresh water required for upstream processes.

The possibility of process additions to the base case with the aim of determining optimal vinasse treatment process configurations is explored in this chapter. Selected pre-treatment, biogas utilization and water recovery process were incorporated into the base case flowsheet. The effect of these additions on the methane yield, energy production and profitability were analysed to form the second phase of sensitivity analyses that was focused on unit operations.

5.1 Selection and Implementation of Pre-treatment Processes

The performance of an anaerobic digestion process is sometimes hampered or reduced by inhibitory compounds present in the substrate (Chen et al., 2008). In the case of vinasse, potassium cations are dominant and may cause a 50% reduction in methanogenic activity at concentrations above 11g/L (Section 4.4.1.3). Through pre-treatment, it is possible to recover the potassium from the raw vinasse prior to AD (P. Zhang et al., 2012).

The most common vinasse pre-treatment processes reported in the literature include ozonation, strong acid cation exchange, electrodialysis and reverse osmosis. In an attempt to fully understand the benefits of these processes, an in-depth comparative review was conducted and is presented in Table 5.1. The selection process was guided by four criteria – availability, costs, capacity and selectivity to potassium ions.

Table 5.1: A comparison of vinasse pre-treatment processes documented in the literature

Attributes	**Advanced oxidative process - Ozonation (O_3)**	**Electrodialysis (ED)**	**Strong Acid Cation Exchange (H_2SO_4)**	**Reverse Osmosis**
Brief methodology	Ozone generated by an ozone generator breaks down phenols, melanoidins and other recalcitrant organics in vinasse to biodegradable molecules (Aquino and Pires, 2016)	This set up contains cells within cation and anion membranes arranged between an anode and cathode. Application of an electric charge promotes movement of ions into the membranes. (Zhang *et al.*, 2012)	This involves the selective adsorption of ions onto a resin packed in a column. A strong acid eluent is used to desorb the ions from the resin. The salt can then be recovered through an evaporative crystallization process. Acid eluent can be recycled. (P. Zhang et al., 2012)	Reverse osmosis is a pressure driven membrane process which separates solutes from a solution by way of molecular size (Dave et al., 2012; Garud et al., 2011)
Advantages	Increased biodegradability (BOD/COD), 40% decrease in phenol (inhibitor), 30% increase in methane yield (mL-CH_4/gCOD) (Aquino and Pires, 2016; Siles et al., 2011)	High salt recovery: 75%, simple to install, and manage. (Zhang *et al.*, 2012)	High acid elution rate: 99% desorption of K^+ from the resin. 76.2% potassium recovery through crystallization Increased to 89.3% with recycling. (P. Zhang et al., 2012)	Very popular method – used by 51.6% of desalination plants worldwide. High dissolved solids (TDS) separations above 90%. COD reduction > 90% (Chaudhari and Murthy, 2009)
Disadvantages	Minimal to no COD reduction, Ozone generators have a low efficiency (6%) (Aquino and Pires, 2016)	Fouling and scaling of electrodes and membranes by salt precipitation and solids (Decloux *et al.*, 2002; Kim, 2011; Zhang *et al.*, 2012)	Crystal formation on the resin. This can be avoided by increasing elution time and quantity of acid. Resin is expensive to replace. Sulphuric acid is corrosive and dangerous. (P. Zhang et al., 2012)	High pressures (50 to 70 bar) required to overcome osmotic pressure. It is not ionic species selective. Membrane fouling can occur. Requires ultrafiltration pre-treatment (Garud et al., 2011; Ryan et al., 2009)

Capacity and residence times	15 to 30 minutes depending on the ozone concentrations (Siles et al., 2011)	Pilot plant, vinasse flowrate: 12 L/hr. (Zhang *et al.*, 2012) (Ryan et al., 2009)	Lab scale: 0.36 L/hr vinasse. Elution: 1.08 L/hr. Residence time: 6 to 7 hours (P. Zhang et al., 2012)	Pilot plant: Feed pressure 20 bar, flowrate 15 L/min. Residence time: 30 mins (Chaudhari and Murthy, 2009)
Energy utilization	Energy required to pre-treat vinasse: 33.6 kWh/m^3 when using air, 19.2 kWh/m^3 when using pure O_2 (Siles et al., 2011)	Pumping power: 0.037 kWh/m^3. ED power consumption: 0.08 kWh/m^3 (Zhang *et al.*, 2012)	These involve heating and cooling energy requirements for crystallization (between 20 and 70 C). Pumping power should be factored in. (P. Zhang et al., 2012)	3 - 9.4 kWh/m^3 of product - this is largely comprised on pumping requirements (Garud et al., 2011) (Loutatidou and Arafat, 2015)
Economics and feasibility	14 kWh/m^3 vinasse is used for pre-treatment. Additional energy produced from methane after pre-treatment is low (30% of the energy used for pre-treatment). Increasing efficiency of the ozonator could make it feasible. (Siles et al., 2011)	Pilot plant with feed flowrate of 12 L/hr, and 30 A/m^2: OPEX - R 7.25/m^3, CAPEX: R 700,000. Membrane replacement costs: R 145,000 (Zhang et al., 2012)	Resin price is variable: R 100/Litre. Energy costs and sulfuric acid must be factored in.	**Costs** - Brackish water: R 0.176/m^3 effluent for a plant running at 190 m^3/day (Yeo, 2010) Vinasse: R 9.8/m^3 at 45 m^3/d (Tewari et al., 2007)

Although ozonation shows significant phenol concentration reductions and increased methane yields, it is considered infeasible due to the high cost of O_3 generation. This is brought about by the low efficiency (6%) of the ozone generation technology which leads to a low marginal accrued benefit (6 kWh/m^3) in terms of energy produced from the additional methane compared to the energy input required for the pre-treatment (14 kWh/m^3) (Siles et al., 2011). In addition, ozonation is non-selective to potassium ions (Aquino and Pires, 2016) which reduces its efficacy as a pre-treatment process. Ozonation was therefore discounted as a pre-treatment in this study due to the high cost and non-selectivity to potassium ions.

Electrodialysis is selective to potassium ions and has the potential to reduce its concentrations by up to 75% (Y. Zhang et al., 2012). However, the presence of fine suspended solids and heavy polymers increase the chances of membrane fouling. This would require a regular membrane replacement which negatively impacts the process economics (Kim, 2011). In addition, it requires a constant supply of electricity to facilitate movement and detachment of ions through and from the membrane surfaces. Membrane processes such as reverse osmosis allow for over 90% reduction in the total dissolved solids (TDS) and COD (Chaudhari and Murthy, 2009). Reverse osmosis has been used mostly as a vinasse post-treatment process for the recovery of water in the permeate stream (Tewari et al., 2007). Using this pre-treatment approach for raw vinasse could lead to heavy fouling and clogging of the membranes due to the high TDS and suspended solids concentrations. Additional pre-treatments such as nano-filtration and chemical pre-treatment of the raw vinasse would be required to mitigate the abovementioned risks. (Garud et al., 2011).

The use of a strong acid cation exchange resin as an adsorption technique has shown potassium ion reductions over 70%. Subsequent extraction of the potassium salt from the eluent through heating crystallization is an established technology which results in recoveries of 76% on average (P. Zhang et al., 2012). Recycling of the strong acid eluent may yield a further 13% increase in potassium ion elution from the resin. In addition, the extraction of salts from potassium using this process requires a lower energy input compared to ozonation and electrodialysis. Given the superior benefits of ion exchange relative to potassium ion selectivity and energy efficiency, this technology was selected as the preferred pre-treatment method for vinasse AD. Consequently, the base case flowsheet in Figure 4.1 was adjusted accordingly to reflect this addition (Figure 5.1).

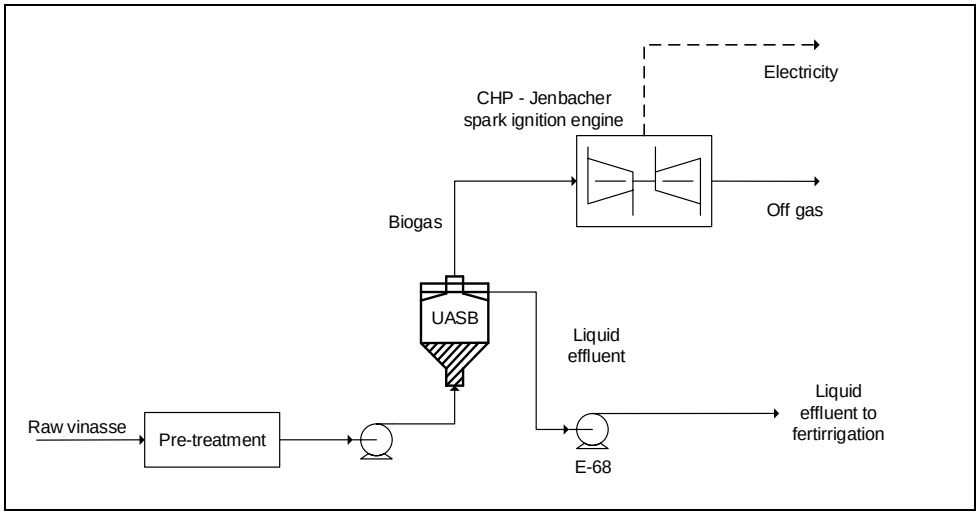

Figure 5.1: A schematic representation of the updated base case flowsheet to include a vinasse pre-treatment process as developed on Aspen Plus.

5.1.1 Ion-Exchange Simulation on Aspen Plus

During the ion exchange process, potassium ions in the vinasse are first adsorbed by the amberlite resin packed into the ion exchange column. The sulfuric acid eluent is then routed to the column where it desorbs ions from the resin to form a potassium rich solution. This solution is routed to a crystallizer where solid K_2SO_4 crystals are then recovered. Implementation of this ion exchange model to the base case flowsheet on Aspen Plus was limited by the lack of unit operations to adequately represent the process. Ion exchange is an adsorption process that is dynamic in nature whereas the base case flowsheet was a steady state simulation. Although ion exchange models can be developed externally on Aspen Adsorption modeller, integration of these into the base case flowsheet was a major challenge due to the difference in operating modes.

For simplicity, a separation unit was used to model the complex ion exchange process. This unit operation provided flowrates and separation factors which were sufficient for sizing and costing purposes through the use of published heuristics (Balaban, 2000) and quotes from manufacturers in the literature (Davis et al., 2013). Potassium ions were represented as aqueous K_2SO_4 to avoid the inclusion of ionic species in the framework with physical properties that are not fully defined in Aspen Plus. This was to circumvent any potential uncertainties in the material and energy balances. A design specification was used to reduce K_2SO_4 concentration by 70% to a concentration of 10g/L that is below the inhibition threshold (11.6 g/L) (see Section 4.4.1.3). The operation of an ion exchange plant involves additional supporting processes such as acid elution and crystallization to recover solid K_2SO_4 crystals and the acid eluent for recycling purposes. Although these aspects were not simulated, their impact on the techno-economics of the process was taken into account using sizing and costing routines based on the feed flowrate and order of magnitude estimations obtained from the literature (Davis et al., 2013).

5.1.2 Effect of the Ion Exchange on Process Performance

Performance of the vinasse treatment flowsheet was gauged using the methane yield and electrical output from the CHP. Upon successful integration of the ion exchange model into the base case flowsheet (Figure 4.1), the simulation was executed and the outputs compared to the initial base case results (Figure 5.2). Details of the initial base case results can be found in Section 4.3.

During the ion exchange process, potassium ions in the raw vinasse are adsorbed by the amberlite resin packed into the ion exchange column. The sulfuric acid eluent is then used to desorb the ions and form a potassium rich solution that is sent to a crystallizer where solid K_2SO_4 crystals are recovered. The separation efficiency was assumed to be 70% and this resulted in a residual potassium concentration of 7 g/L in the lean vinasse outlet stream (P. Zhang et al., 2012) which was lower than the inhibition threshold (11.6 g/L) At the current plant capacity, an annual potassium sulfate production of 1500 tons was achieved.

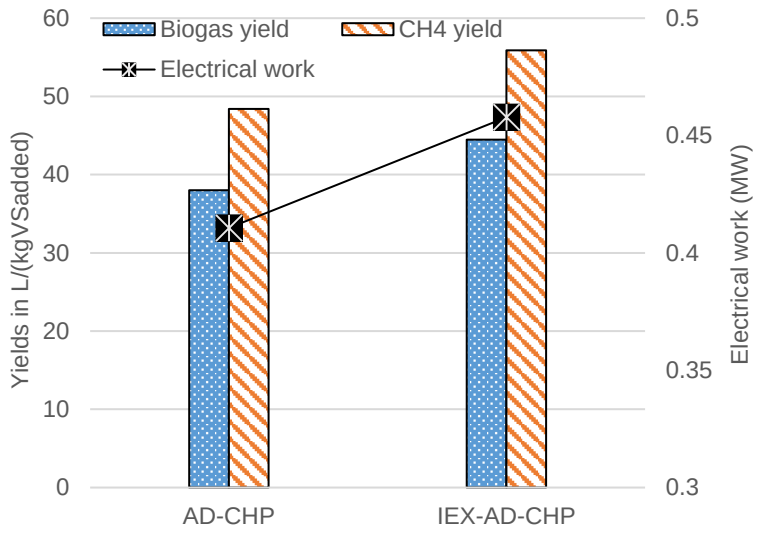

Figure 5.2: Effect of inclusion of a pre-treatment process on the performance of the flowsheet. Biogas yield is reported in $L_{biogas}/(kgVS_{added})$ and methane yields in $L\text{-}CH_4/kgVS_{added}$.

At a separation factor of 70%, the inclusion of an ion-exchange process into the base case flowsheet results in a 12% increase in the methane yields from 48 to 55 $L\text{-}CH_4/kgVS_{added}$ (Figure 5.2). Consequently, there is a 16% increase in the electrical output from the CHP plant. In the developed AD model (Section 3.3), the inhibitory effect of potassium on methanogenesis is implemented using a non-competitive Michaelis Menten equation that takes into account the inhibitor (potassium ions) concentration in the reactor as well as its threshold concentration (Equation 5.1)

$$\mu = \mu_{max}(T).\left(\frac{1}{1+\frac{K_{S_{HAc}}}{S_{HAc}}}\right).\left(\frac{1}{1+\frac{K_{NH_3}}{S_{NH_3}}}\right).\left(\frac{1}{1+\frac{S_{NH_3}}{K_{i,NH_3}}}\right).\left(\frac{1}{1+\frac{S_{K+}}{K_{i,K+}}}\right) \qquad \textit{Equation 5.1}$$

With the inclusion of (pre-treatment) ion exchange to the base case flowsheet, there is a decline in potassium ions concentration which effects an increase in the denominator term of the K^+ inhibition expression (Equation 5.1). The K^+ inhibition term tends to a value of 1 thereby effectively reducing the degree of inhibition and effectively increasing methanogenic growth rates. As a consequence, more acetic acid is converted to methane and CO_2. The expected increase in performance can be therefore attributed to the reduction in potassium ions that are inhibitory to methanogens in AD.

While a further decrease of potassium ions would certainly result in increased methane yields, the separation factor was maintained at 70% to avoid high raw material costs incurred from the purchase of concentrated (99%) sulphuric acid. At the current market price of $300/ton (Alibaba, 2017), increasing the separation factor by 10% to 80% would increase the operating costs by 15% and also increase the capital costs of the ion-exchange equipment. Given the unproportioned increase in operation cost and potential increase in capital costs, the separation factor was maintained at 70%. However, it is worth noting that the ion-exchange model developed here is simplistic and serves as a high-level representation of the process. With detailed adsorption and crystallization modelling, in-depth sensitivity on the effects of separation efficiency can be conducted to make a more informed decision on the degree of vinasse pre-treatment.

5.1.3 Effect of the Ion Exchange Process on Project Feasibility

Sensitivity analyses conducted on the base case AD model (Section 4.4) showed that a decrease in inhibitor concentrations results in an increase in methane yields which has a positive influence on profitability due to higher revenues. This improvement in AD performance was further affirmed by the implementation of a pre-treatment system that removed inhibitory potassium ions to the increased the methane yields by 12%. This had a positive knock-on effect on the subsequent biogas utilization process where a 16% increase in electricity production was observed due to the higher methane yields. Economic gains from the implementation of ion exchange are very likely assuming the cost of operation does not exceed the benefit. To validate this assumption, it was important to evaluate the techno-economics of the pre-treated base case relative to the original (AD-CHP) route.

5.1.3.1 Capital Expenditure

The major additional equipment required for ion-exchange were a (1) vertical column, (2) regeneration column, (3) pumps and (4) a heating crystallization system to recover potassium sulfate crystals. Equipment costs for these units were calculated using the six tenths rule based on the feed flowrate into the ion exchange system. The initial cost was based on a manufacturer quote of $5 250 000 obtained from Davis et al. (2015) for an ion exchange system at a base plant throughput of 53 000 kg/hr. Given the throughput of the developed base case vinasse treatment plant (12 400 kg/hr), the capital cost of the ion-exchange system was scaled down accordingly using six tenths rule (Table 5.2)

Table 5.2: A breakdown of the capital investment costs to the nearest $1 000 (USD, 2016) for the pre-treated (IEX-AD-CHP) and untreated base case (AD-CHP) flowsheets

Capital Expenditure (USD, 2016)	**Base case**	**Pre-treated base case**
Purchase cost of equipment (PCE)	**AD – CHP**	**IEX – AD – CHP**
UASB reactor	1 055 000	1 055 000
Ion Exchange (columns, pumps, crystallization unit)	-	2 710 000
Jenbacher engine (CHP)	1 776 000	1 776 000
Total PCE	2 820 000	5 532 000
Installation, electrical, site, instrumentation factors	1.6	1.6
Physical Plant Cost (PPC)	4 513 000	8 850 000
Design, Engineering and Contingency factors	1.19	1.19
Location factor	1	1
Total	1.79	1.79
Fixed Capital Investment	**5 370 000**	**10 531 000**
Working Capital (15%)	805 500	1 580 000
Total Capital Investment	**$6 176 000**	**$12 112 000**

The reactor and CHP engine capacities were identical in both AD-CHP and IEX-AD-CHP routes which resulted in similar costs of these two equipment across the flowsheets (Table

5.2). Notably, the cost of ion exchange equipment, which included two packed columns, amberlite resin and the heating crystallizer, was significantly higher than the AD or CHP. This resulted in a 100% increase in the initial capital investment of the IEX-AD-CHP route relative to the base case (AD-CHP).

5.1.3.2 Operating Expenditure

Operating expenditures were, as before, divided into fixed and variable costs. Raw materials, utilities and transport expenses made up the variable costs whereas the fixed costs consisted of operation and maintenance costs as well as labour (Table 5.3). As with the base case investigation, the raw materials required for AD consisted of only the NaOH for pH control in the reactor. This was estimated to be 0.004 kg NaOH/kgCOD (Souza et al., 1992). To ensure maximum elution of potassium ions from the amberlite resin in the ion exchange column, an acid eluent to raw vinasse ratio of 1.5 was used. The volume of H_2SO_4 required was calculated from the abovementioned ratio.

Table 5.3: A breakdown of the operating costs to the nearest $1 000 for the pre-treated (IEX-AD-CHP) and untreated (AD-CHP) base case flowsheets

Operating Expenditure – Costs/year (USD, 2016)	**Base Case**	**Pre-treated Base Case**
Raw Materials	**AD – CHP**	**IEX – AD – CHP**
NaOH (dosing)	38 690	38 690
H_2SO_4 eluent	**-**	27 670
Utility costs (electricity)	80	(included in O&M)
Transport costs	15 000	14 500
Labour		
Labor Costs ($/yr)	$172 476	$185 315
Operation, Maintenance, Utility		
CHP system ($0.02/kWh)	68 400	76 000
AD system (1.5% of plant costs)	28 300	28 300
Ion exchange	-	272 000
Total Operating Costs	**324 000**	**643 000**
Indirect fertilizer revenue – Cost savings	92 600	73 200
Overall OC	**$231 000**	**$569 000**

With the addition of a pre-treatment system (IEX), a significant increase in the fixed and variable operating costs was noted as expected (Table 5.3). In terms of fixed costs, the sulfuric acid, which is critical in eluting adsorbed potassium ions from the resin in the packed column, is the major contributor to this increase. Increased labor costs are also observed due to an increase in number of processing areas. Operation and maintenance costs for the ion exchange process included resin replacement, vessel cleaning and electrical utility and were assumed to be 10% of the ion exchange equipment costs (Seider et al., 2003). This added a further 80% to the total operating costs. In addition, there is a 10% higher operation and

maintenance (O&M) cost for CHP in the flowsheet with pre-treatment (IEX-AD-CHP) owing to higher electricity production as compared to the base case.

For both configurations in Table 5.3, the liquid digestate was used for fertirrigation for the sugarcane fields which reduced the amount of synthetic fertilizer required. Due to lower potassium concentrations in the digestate from the IEX-AD-CHP process, the maximum fertirrigation area was reduced which resulted in a decline of the cost saving by 20% compared to the base case savings.

5.1.3.3 Cash Flow, Financial Analysis and Profitability Indicators

Despite increased costs, ion-exchange coupled with a crystallization process is advantageous as it results in the recovery of potassium sulfate. Economically, with electricity produced by the CHP, the potassium sulfate is considered an additional revenue stream to be sold at $300 per ton (Alibaba, 2017).

After compiling all information regarding the revenues and costs, a discounted cash flow analysis was developed to evaluate the effect of adding a pre-treatment process on the profitability of the base case. Base case (AD-CHP) indicators with amended results from the added pre-treatment process (IEX-AD-CHP) were then compared and analysed over a 20 year period (Figure 5.3 and Figure 5.4).

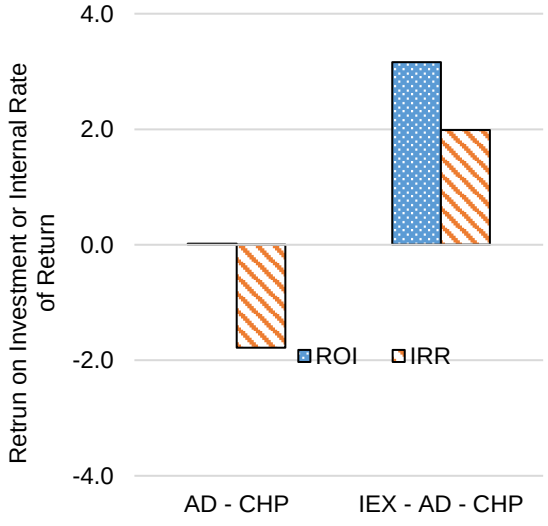

Figure 5.3: Effect of inclusion of a pre-treatment process on the profitability (USD 2016) of the pre-treated (IEX-AD-CHP) and untreated base case (AD-CHP) flowsheet over a 20 year project lifetime. Revenue generating and cost saving streams considered were electricity, potassium sulfate and liquid digestate

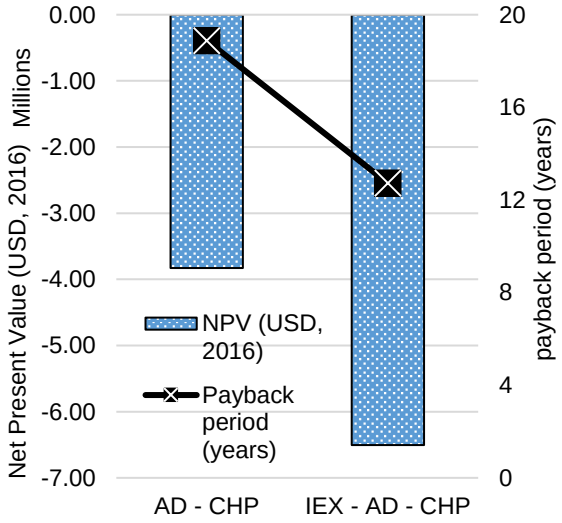

Figure 5.4: Effect of inclusion of a pre-treatment process on the profitability (USD 2016) of the pre-treated (IEX-AD-CHP) and untreated base case (AD-CHP) flowsheet over a 20 year project lifetime. Revenue generating and cost saving streams considered were electricity, potassium sulfate and liquid digestate

The base case (AD – CHP) exhibited a very low return on investment and a negative internal rate of return to result in an overall negative growth over the venture's lifetime. On the other hand, adding a pre-treatment step to the base case resulted in a significant increase in the ROI and IRR from 0.02% and -1.8% to 3.2% and 2% respectively (Figure 5.3). In addition, the

payback time and net present values for the venture was decreased by 32% and increased by 69% respectively.

The higher return on investment for the IEX-AD-CHP route shows that the additional capital expenditure incurred for pre-treatment is recovered by the increased revenue from electrical power and potassium sulfate sales (Figure 5.3). Similarly, the higher rate of return (0.02% to 3.2% in Figure 5.3) shows positive growth of the venture in terms of cash flow. However, the project returned a net loss as the internal rate of return remains below the weighted average cost of capital (15%). Further, the net present values for both configurations remain negative (Figure 5.4) which further confirms that the future earnings did not cover the anticipated costs of production.

The primary aim of the pre-treatment process was to decrease the concentration of inhibitory components to increase the efficiency of the AD process relative to methane yields. As expected, there was a 14% increase in the system performance coupled with a 32% decrease in payback time and further significant increases (>100%) in the ROI and IRR. These were however not enough to secure a net profit over its lifetime as the NPV remained negative.

Although ion exchange as a pre-treatment is unlikely to yield a net profit, its addition to the base case should be considered. This is because there exist alternative opportunities for value creation and revenue generation from the biogas and liquid digestate that may improve the projects financial standing. In addition, from an environmental perspective the reduction of potassium salt concentrations to below 5 g/L in the digested vinasse will reduce the risk of soil salinization with increased fertirrigation over the long term (Christofoletti et al., 2013). To potentially reduce the capital and operating costs of the pre-treatment process, the production of an aqueous stream rich in K^+ ions could be explored. Being a concentrated K^+ aqueous stream, it can be used as a fertilizer to result in further cost savings in addition to the savings accrued from fertirrigation using the vinasse digestate. However, several challenges exist with this route. Choosing to generate an aqueous stream will eliminate the crystallization step that facilitates the recovery of sulphuric acid to be recycled to the column (P. Zhang et al., 2012). In the absence of H_2SO_4 recovery and recycle, operating costs are likely to increase which may in turn negatively impact the profitability. To adequately investigate the viability of producing an aqueous stream with a high concentration of K^+, a rigorous ion exchange model based on adsorption kinetics as well as a crystallization model need to be developed, sized and costed to understand the techno-economics.

5.2 Selection and Implementation of Biogas Utilization Processes

The vinasse AD process in the base case flowsheet results in the production of biogas with a methane content of 65% and a calorific value of 22 kJ/L (Table 4.3). The biogas characteristics are comparable to results from both industrial scale biogas plants and published vinasse AD simulation results (Barrera et al., 2015; Fuess et al., 2017; Walsh et al., 1989). As such, it can be used as an energy source for electricity production.

The technical and economic feasibility of CHP as a biogas utilization process was investigated in Section 4.5 as part of the base case vinasse treatment project. Biogas was converted to electricity in a General Electric Jenbacher™ spark ignition engine operating at an electrical efficiency of 44% (General Electric, 2008). This is then sold to the electricity distributor through feedback into the national grid at a set tariff of $0.1/kWh. Although a significant amount of

electrical power was produced in the base case, the profitability remained low as evidenced by the 0% ROI and negative IRR. This was attributed to the high CHP engine costs and relatively low power output resulting from more than 50% of the energy lost as work in the form of heat and noise. While it is possible to recover heat from the exhaust gas through steam production, the above mentioned work (50% loss) lost in the form of heat and noise cannot be recovered. Following this, biogas upgrading was investigated as an alternative method of utilization.

Biogas upgrading involves removing CO_2 as well as other undesired components such as H_2S, NH_3 and water vapour to produce 95% - 97% pure biomethane which can be compressed and sold for domestic use or injected into a gas grid (Axelsson et al., 2012). The processes considered were (1) high pressure water scrubbing (HPWS), (2) amine scrubbing and (3) gas permeation through membranes (Bick et al., 2012). High pressure water scrubbing was preferred owing to its simplicity and sustainability. These characteristics are ascribed to moderate operating conditions below 10 bar and the exclusion of harsh chemicals to enhance CO_2 absorption within in these systems (Kapdi et al., 2005). It is also sustainable in this context as it uses water which can be recycled. The feasibility of biogas upgrading technologies is heavily dependent on the energy demands and unit cost of energy ($ per GJ). HPWS has a 5-10% lower unit cost compared to amine scrubbing and membrane separation (Leme and Seabra, 2017). This can be attributed to the high heat energy requirements for amine solvent regeneration, which is approximately 5 times greater than the energy needed for pumping and compression in HPWS (Axelsson et al., 2012). Although membrane processes are attractive in terms of size and simplicity, the running costs are high due to the frequency replacement as a result of membrane fouling or end of life.

The selection of a biogas utilization process should be dependent on cost, availability and sustainability of the technology. In addition, the internal energy requirements of the plant must be considered. To adequately compare utilization technologies, two process scenarios were developed and simulated. The first scenario consisted of a biogas plant fitted with a CHP system for electricity production based on the General Electric Jenbacher^{TM} spark ignition engine (base case: AD-CHP). Simulation of this scenario as well as the techno-economics are detailed in Section 4.5. In the second scenario, the CHP is substituted for a HPWS process (AD-Upgrade). Its simulation as well as mass balances are reported in this Section 5.2.1. Using results from the two scenarios, an economic and performance comparison was drawn to assist in decision making.

5.2.1 HPWS Simulation on Aspen Plus

HPWS takes advantage of the difference in solubility of the biogas components in the water. Carbon dioxide is 25 times more soluble than methane in water which makes this process suitable for its removal (Cozma et al., 2014). Figure 5.5 shows the developed simulation on Aspen Plus for the biogas upgrading technology used to replace the power generating plant (CHP) in preceding base case simulations.

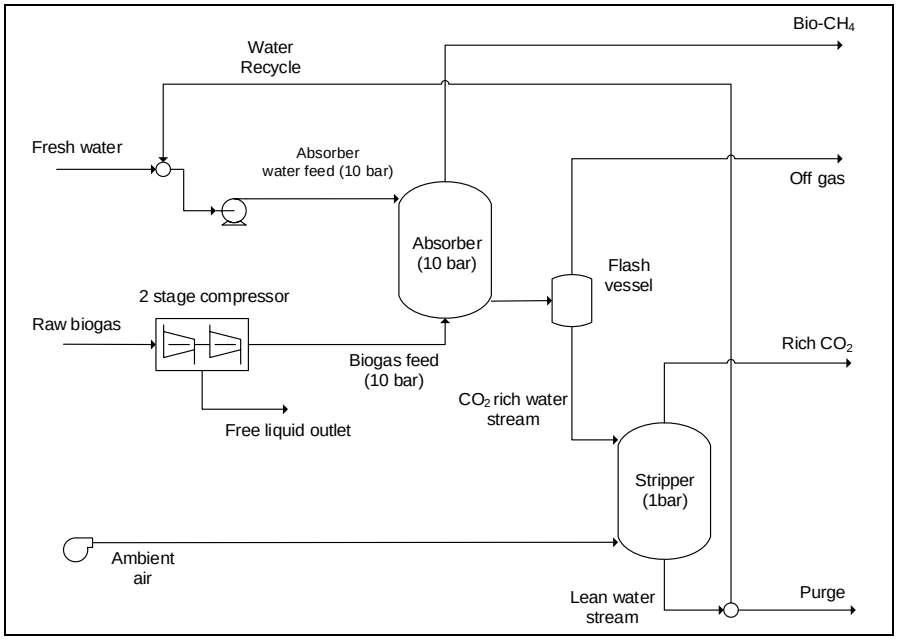

Figure 5.5: A schematic representation of the high pressure water scrubbing process for biogas upgrading as developed in Aspen Plus

Biogas from the AD plant was routed to the upgrading plant via the raw biogas stream as seen in Figure 5.5. It is then compressed to the absorber operating pressure. Moderate pressures between 6 to 10 bars are ideal for the absorption of CO_2. A sensitivity analysis performed on the absorber operating pressure (Figure 5.6) showed that increasing pressure from 1 to 6 bar resulted in a 35% increase in the methane mole fraction in the biomethane outlet stream ('Bio-CH_4').

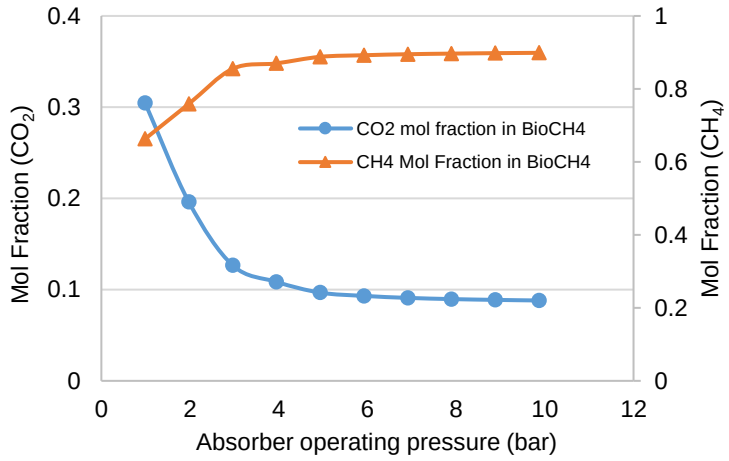

Figure 5.6: Sensitivity analysis on the absorber column operating pressure in the HPWS process on Aspen Plus

With further increases in pressure, the biomethane purity levelled out to ca. 90% (Figure 5.6). Following this result and recommendations from the literature (Cozma et al., 2014), the absorber operating pressure was set at 10 bar. After compression, the biogas was sent to the bottom of the absorber column that had 6 theoretical stages (Cozma et al., 2014, 2013a) and was packed with plastic pall rings. The water stream was fed at the first stage to promote a counter current flow with the biogas which allowed for the maximum mixing and mass transfer of CO_2 from the gas to liquid phase. To avoid downstream accumulation, an equilibrium flash

vessel was used to release excess methane from the CO_2 rich liquid stream at 2 bar. Although, the excess methane is sometimes recycled (Pöschl et al., 2010) a cost-benefit analysis (Table 5.4) showed that recycling increased the biomethane recovery by 5% but increased the costs by 18%.

Table 5.4: A summary of the cost-benefit analyses used for decision making when choosing to recycle methane in the HPWS process (USD, 2016)

	Recycled methane	No recycle	% change
Capital costs (absorber)	$ 17 940	$ 14 640	**18%**
Biomethane flowrate (m^3/yr)	133 200	126 600	**5%**

Recycling was therefore abandoned for repurposing the off gas as fuel for heating. The CO_2 rich water stream was routed to the stripping column where CO_2 and other gases were stripped from the water. To avoid a build-up of inert gases, 10% of the water was purged prior to recycling. A freshwater make-up stream was included to replace the purged amount. It was also used to control the purity of the biomethane (95%) stream through a design specification. Table 5.5 shows a mass and energy balance of the major streams in the upgrading plant.

Table 5.5: A summarized mass balance of the high pressure water scrubbing process simulation on Aspen Plus

	Raw Biogas (kg/hr)	Mixed Water Feed (kg/hr)	Biomethane (kg/hr)	Rich CO_2 liquid stream (kg/hr)
Methane	65.8	-	61.3	4.5
Carbon dioxide	85.4	-	0.8	84.7
Hydrogen	0.6	-	0.6	-
Water	20.5	25160	0.2	25184.0
Ammonia	0.3	1.9	-	2.2
Total stream	170	25162	63	25280
Discrepancy	0%			
m^3H_2O/m^3 Biogas	0.13			
Biomethane (mol%)	95%			
Calorific value (kJ/L)	38			
Electrical utility (kW)	41			

Simulation of the high pressure water scrubbing process proceeded seamlessly with minimal mass balance convergence errors. This is evidenced by the 0% difference between the mass into and out of the absorber column as seen in Table 5.5. Using the reconciled mass balance, performance indicators such as biomethane purity and calorific value were extracted. Biomethane at a purity of 95% and a calorific value of 38 kJ/L was recovered from the top stage of the absorber column. To achieve this, a water recirculation loop of approximately 0.13 m^3-H_2O/m^3 of raw biogas was required. This is comparable to industrial water requirements that range from 0.15 to 0.2 m^3-H_2O/m^3 of biogas (Axelsson et al., 2012; Pöschl et al., 2010).

Given the credible mass balance and the abovementioned performance indicators, the HPWS model was deemed fit for further simulation work, sizing and techno-economic analyses.

5.2.2 Effect of Alternative Biogas Utilization Processes on Process Performance

The aim of the biogas utilization processes was to increase the commercial and energy value of the biogas by conversion to biomethane (95%) or electricity through HPWS or CHP, respectively. To select the best process, performance data for the aforementioned scenarios was extracted from the resulting mass balances and compared. This included the calorific values as well as the total energy output for the electricity from CHP and biomethane from HPWS (Figure 5.7).

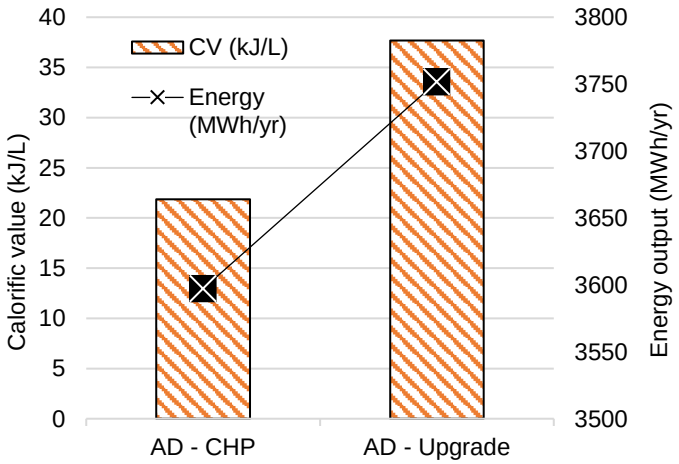

Figure 5.7: A comparison of the performance between CHP and HPWS processes as biogas utilization processes

As expected, biogas upgrading resulted in a significant increase in the calorific value of the raw biogas. This was attributed to the removal of CO_2 and other impurities such as NH_3, and H_2O that have negligible heating values. The biomethane had a calorific value of 38 kJ/L which was 72% higher than for raw biogas. In addition, the calorific value obtained was similar to values published for natural gas that range between 38 and 43 kJ/L (EcoMetrix Africa, 2013).

For comparative purposes, the total energy produced in either scenario was normalised to common units of measure (Figure 5.7). The electrical output obtained from the base case CHP simulation was converted to kWh per annum (410 kW in Table 4.3). In replacing the CHP with HPWS, the total energy output MJ per year was calculated as a product of the calorific value and standard gas volume flowrate. This was thereafter converted to kWh to allow for a normalized comparison between the energy outputs of the two scenarios. As seen in Figure 5.7, the annual energy output from the biogas upgrading was significantly higher than the CHP despite the 50% volume flow reduction from removal of CO_2 and other impurities. However, this volume reduction was offset by the 72% increase in the calorific value of the biomethane compared to biogas which led to a higher net energy output.

5.2.3 Effect of Alternative Biogas Utilization Processes on Feasibility

Although biomethane production seemed favourable from an energy perspective, it was necessary to evaluate the techno-economics of both scenarios so as to assess their profitability. The capital and operating costs associated with the two scenarios consisting of either CHP or HPWS as biogas utilization processes after AD were computed using the approaches as outlined in Section 4.5. In the first scenario, electricity generated from the CHP system was fed into the grid at the current REFIT for biogas as recommended by NERSA

(2011). Biomethane produced in the second scenario can be sold commercially as a substitute to natural gas at $19/GJ (EcoMetrix Africa, 2013). In both scenarios, the liquid digestate is transported to the cane fields to be used as fertilizer.

5.2.3.1 Capital Expenditure

The capital expenditure summary (Table 5.5) highlighted the costs of the major processing equipment. For the CHP plant, this included a General Electric Jenbacher™ 620 spark engine. The cost of this engine was obtained from an equipment manufacturer quote reported in Darrow et al. (2015). The HPWS (upgrading) process contained two packed columns, pumps and a compressor which were sized on Aspen Plus based on their capacity. These major pieces of equipment were costed using published heuristics and prices scaled up accordingly using the CEPCI from the year 2004 to 2016 (Balaban, 2000; Seider et al., 2003)

Table 5.6: A breakdown of the initial capital investment costs to the nearest $1 000 (USD, 2016) for the flowsheets comparing CHP and HPWS processes as additions to the base case AD process

Capital Expenditure (USD, 2016)	**Base Case**	**Improved base case**
Purchase cost of equipment (PCE)	**AD – CHP**	**AD – Biogas Upgrade (HPWS)**
UASB reactor	1 055 000	1 055 000
HPWS (Columns, compressors, pumps)		116 000
Jenbacher engine (CHP)	1 776 000	-
Total PCE	2 831 000	1 171 000
Installation, electrical, site, instrumentation factors	1.6	1.6
Physical Plant Cost (PPC)	4 513 000	1 871 000
Design, Engineering and Contingency factors	1.19	1.19
Location factor	1	1
Fixed Capital Investment	**5 370 500**	**2 226 500**
Working Capital (15%)	805 500	334 000
Total Capital Investment	**$6 176 000**	**$2 560 500**

Table 5.6 shows a summary of capital investments associated with the two scenarios. The capital costs of the CHP plant were 2.5 times higher than HPWS owing to the high equipment costs associated with Jenbacher gas engines. Jenbacher engines combine compression, fuel injection, combustion and heat recovery into a compact and highly specialized piece of equipment, hence their high price (Darrow et al., 2015).

5.2.3.2 Operating Expenditure

The operating expenditures featured the potential costs to be incurred in the day to day running of the plant. These were broken down into fixed and variable costs as previously described in Section 5.1.3.2. The overall operation and maintenance costs for the HPWS were assumed to be 10% of the equipment costs. Aside from electricity, HPWS also bore with it

water utility costs that arose from the fresh water stream needed to make up any lost water for CO_2 absorption. It was assumed that it would be sourced from the municipality at an industrial water tariff set by the national water distributor.

Table 5.7: A breakdown of the operating costs to the nearest $1 000 (USD, 2016) for the flowsheets comparing the AD-CHP and AD-HPWS processes

Operating Expenditure – Costs/year (USD, 2016)	**Base Case**	**Improved Base Case**
Raw Materials	**AD – CHP**	**AD – Upgrade**
NaOH (dosing)	38 690	38 690
Utility costs (electricity, water)	80	65 000
Transport costs (digested vinasse)	15 000	15 000
Labour		
Labor Costs ($/yr)	$173 000	$173 000
Operation, Maintenance, Utility		
CHP system ($0.02/kWh)	68 400	-
AD system (1.5% of plant costs)	28 300	28 300
HPWS system	-	12 000
Total Operating Costs	**323 000**	**331 000**
Indirect fertilizer revenue – Cost savings	92 600	92 600
Overall OC	**$231 000**	**$239 000**

Utility costs associated with the biogas upgrading route are significantly higher than the alternative (CHP) as seen in Table 5.7. This high utility cost arose from the fresh water make up stream that was approximately 63% of the utility costs. Further utility costs arose from the electrical energy required by the biogas feed compressor and recycle pump.

Most other running costs such as AD maintenance, raw materials and transport were similar as CHP and HPWS affected only downstream biogas processing. In both cases, the vinasse digestate was transported to the sugarcane fields and used for fertirrigation. This introduced transportation cost as well as a cost savings on the purchase of potassium based fertilizer. Overall, the operating costs (Table 5.7) for both processing routes were within 3% of each other despite the additional utility costs associated with HPWS.

5.2.3.3 Cash Flow, Financial Analysis and Profitability of HPWS and CHP

The capital costs and operating costs in Table 5.3 and Table 5.4 respectively, were used to develop a discounted cash flow analysis (Figure C 1 and Figure C 5) that took into account revenues from the sale of electricity and biomethane. Profitability indicators extracted from the discounted cash flow analyses were presented graphically in Figure 5.8 and Figure 5.9. It was expected that the high investment costs for CHP coupled with low electricity feed in tariffs would make this option unfeasible.

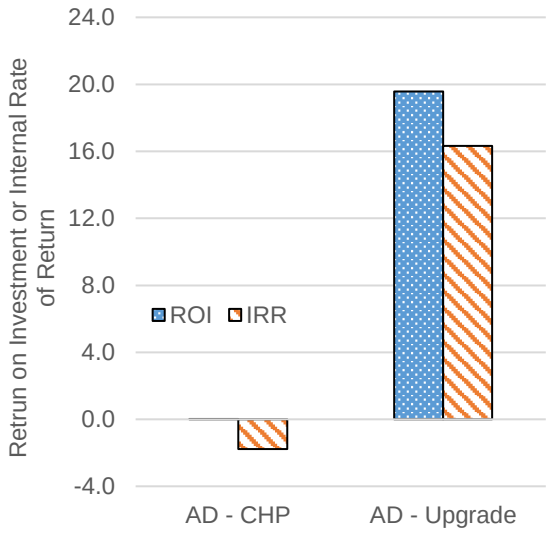

Figure 5.8: A comparison of the profitability between CHP and HPWS as biogas utilization processes in the vinasse treatment flowsheet over a 20-year project lifetime

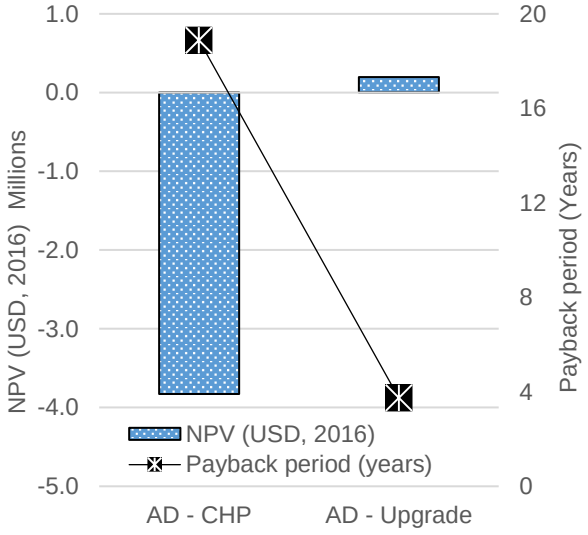

Figure 5.9: A comparison of the profitability indicators (NPV, PBP) between CHP and HPWS as biogas utilization processes in the vinasse treatment flowsheet over a 20-year project lifetime

As expected, the base case (AD-CHP) had a low profitability as evidenced by the 0% ROI and negative IRR (Figure 5.8). Replacing the CHP system with a biogas upgrading process resulted in a significant increase in the profitability owing to a 50% reduction in equipment costs. Despite operating costs (OC) incurred when using HPWS exceeding that of CHP, the 50% higher capital investment into the CHP outweigh its benefits (lower OC) to result in HPWS being more profitable over the long-term. In addition, biomethane had a higher energy content compared to biogas and brought in 59% more revenue compared to electricity. The payback time for the base case was also reduced by 80% to 3.7 years (Figure 5.9).

The growth of the two projects was evaluated by the internal rate of return and net present values after 20 years. From Figure 5.8, the base case (AD-CHP) exhibited low levels of growth as evidenced by the negative IRR and NPV of -$3 800 000. It is therefore unlikely to return a net profit over its lifetime. Production of biomethane (AD-Upgrade) on the other hand had a more positive outlook with an IRR of 16.3% that was higher than the average cost of capital (15%). The NPV for this case was $196 000, which indicated that the project was likely to payback the cost of capital and return a net profit.

Process improvements upstream such as vinasse pre-treatment have a positive effect on the revenues and consequently the profitability of both AD-CHP and AD-Upgrade routes. Pre-treatment of vinasse leads to more efficient AD processes with increased biogas quality and flowrates. This in turn translates to higher electricity generation or increased biomethane yields. The knock-on effects of these pre-treatments will be investigated further in Chapter 6. In this analysis, profitability of the CHP process is sensitive to the biogas production rate, as well as the renewable energy feed in tariff. Currently, a tenfold increase in the electricity production yields an IRR 15%. This indicates that feasibility of base case (AD-CHP) process could possibly be achieved at higher plant capacities as the IRR would approach the cost of capital (16%) However, capital and operational costs at larger capacities need to be computed to validate this prediction.

5.3 Selection and Implementation of Water Recovery Processes

The anaerobic digestion of vinasse results in the production of a nutrient rich liquid digestate that has several potential uses. Common applications include direct application to farm land, and dewatering to recover nutrient rich concentrates and water (Christofoletti et al., 2013). These concentrates can be used as animal feed supplements or applied to the land as fertilizer. Depending on the quality of the concentrates, nitrogen and phosphorous based nutrients can be extracted through further processing to be used as feedstock for bacterial and algal and bacterial cultivation. Dewatering processes such as multi-effect evaporation and reverse osmosis have often been practised in industry (Carvalho, 2011; Nataraj et al., 2006) and have varying characteristics which affect their economics and applicability in the context of vinasse treatment. To potentially improve revenue generating product quality from AD, it is worth investigating the feasibility of integrating dewatering operations into the process and to determine their applicability and prospective economic benefits.

5.3.1 RO Simulation on Aspen Plus

In incorporating the RO process, degassing of the digestate through a slight pressure drop in a horizontal flash vessel maintained at atmospheric pressure was performed. This allows for the release of dissolved biogas which is directed to a biogas storage area. A pre-filter (Figure 5.10) was then used to remove large suspended solids from the liquid digestate. The pre-filtrate was pumped at 20 bar and then routed to a nano-filtration system which decolorizes the digestate by removing colloidal compounds and heavy polymers responsible for the dark brown pigment (Nataraj et al., 2006). The pressure of the filtrate stream is increased to its osmotic pressure using a series of centrifugal pumps. Depending on the composition of this filtrate, the steady state osmotic pressure calculated by Aspen Plus varied between 50 and 55 bar. This is then routed to the RO modules which reduce the water content of the vinasse by 60% to form a concentrate that consists of minerals, salt ions and organic matter and water. Water and VFA are recovered in the permeate stream. Thereafter, an energy recovery device in the form of a turbine is used to simultaneously reduce the permeate pressure to 1 bar as well as recover its energy.

Reverse osmosis was modelled as a cross flow filtration process where the feed travels tangentially across the surface of the membrane filter. This facilitates constant washout of the filter cake by the feed and allows the process to run continuously. In this flowsheet, a simplified solution-diffusion model developed by Oh et al. (2009) was adapted to govern operation and predict performance of the reverse osmosis membrane. The following assumptions were adopted in the development of this RO model (Oh et al., 2009)

- Pressure drop across the spiral wound membrane module is 0.5 bar
- Osmotic pressure is proportional to the dissolved salt and solid concentrations. This facilitated easier calculation of the osmotic pressure by Aspen Plus (Aspen Technology, 2000)
- To maintain steady state operation, the mass transfer coefficient and solute transport coefficients are constant through the process. In addition, concentration polarization

and filter cake resistance were assumed to be negligible so as to reduce the model dynamism in terms of RO feed pressure.

For simplicity, solute transport through the membrane was assumed to be negligible. This was assumed to be the case due to the high rejection rates of salts and organic matter (>99%) reported for vinasse AD effluent systems (Nataraj et al., 2006; Shivajirao, 2012).

In modelling RO systems, three main streams are considered, namely the feed, permeate, and retentate. The permeate flow (Q_p) is governed by the volume flux of liquid passing through the membrane, number of membrane modules and the membrane surface area (Equation 5.1). In the case of vinasse in the base case flowsheet, the liquid volume that permeated included water and short chain VFAs.

$$Q_p = J * n_m * A_m \qquad \textit{Equation 5.2}$$

Where J, n_m and A_m in Equation 5.2 refer to the flux ($L.m^{-2}.hr^{-1}$), number of modules, and area (m^2) respectively. The volumetric flux (J) was calculated using the solvent transport formula (Equation 5.2) which is dependent on the solvent transport parameter (L_v) and a pressure difference (P_{feed} - P_{loss}) which acts as the driving force

$$J = L_v\left(P_{feed} - P_{loss}\right) \qquad \textit{Equation 5.3}$$

Given the proven effectiveness and energy efficiency of spiral wound membranes (Butt et al., 1997), they were preferred over the hollow fibre variety. The solvent transport parameter ($m.s^{-1}–Pa$) was calculated from the intrinsic solvent transport parameter ($L_{v,o}$), operating temperature and constants for solvent transport (α_1, α_2). These parameters are dependent on the membrane type. In this model, the spiral wound membrane constants used by Oh et al. (2009) were adopted (Table 5.8):

$$L_v = \frac{1}{\frac{1}{L_{v,o}e^{\frac{\alpha_1(T-293)}{293}-\alpha_2 P_f}}} \qquad \textit{Equation 5.4}$$

P_{loss} in Equation 5.5 refers the total pressure to be overcome by the high pressure pump before the RO system. It is calculated by a summing the feed osmotic pressure and pressure drop across the membrane filtration unit (0.5 bar) (Equation 5.5). Thereafter, it is used to calculate the driving force using Equation 5.3.

$$P_{loss} = \Delta\pi + P_{drop} \qquad \textit{Equation 5.5}$$

Where $\Delta\pi$ and P_{drop} refer to the feed osmotic pressure and total pressure drop.

The development of a RO process on Aspen Plus required a nano-filtration unit, high pressure pump and membrane module. RO membranes are mostly modelled using cross flow filters in most simulation platforms. However, Aspen Plus is limited in that regard as the cross flow filter solely models solid separations (Aspen Technology, 2000). To overcome this, a separation unit combined with a calculator block was used. The calculator block contained customized code and equations to efficiently simulate the RO process using the simplified solute-diffusion model (Equation 5.2, Equation 5.3, Equation 5.4 and Equation 5.5).

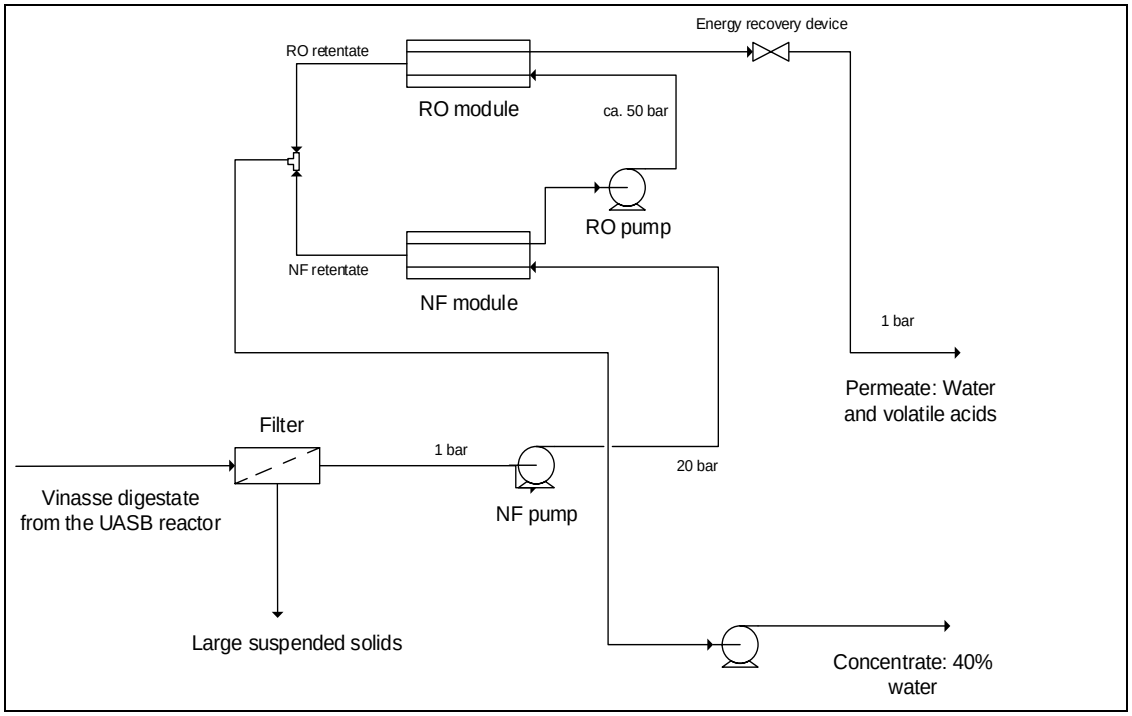

Figure 5.10: A schematic representation of the reverse osmosis system as developed on Aspen Plus

A calculator block was used to extract the relevant variables such as osmotic pressure and feed temperature from the input stream. Solute and solvent transport constants (Table 5.8 and Equation 5.4), dependent on the membrane type (spiral wound), were specified in the calculator block. In this model, the separation unit was used to define a permeate recovery. The osmotic pressure of the feed stream is first determined using the inbuilt Aspen Plus property sets. Thereafter, P_{Loss} and the solvent transport parameter are then calculated using Equation 5.5 and Equation 5.4. Equation 5.3 is used to compute the volumetric flux. Given the set separation efficiency and permeate flowrate, the volumetric flux (J) is used in Equation 5.1 to calculate the membrane area and number of RO modules required depending on the surface area per membrane.

Table 5.8: Operating conditions and constants specified for the RO system.

Condition	**Parameter**
Pressure drop (bar)	0.35
Permeate recovery (fraction)	0.7
Intrinsic solvent transport parameter (L_{vo})	$5.71*10^{-12}$
Area per membrane (m^2)	30
Solvent transport constant (bar^{-1})	α_1=8.6464, α_2=0.019

The intrinsic transport parameter was obtained from a RO unit set up in a seawater desalination system (Oh et al., 2009). Due to the scarcity of constants for vinasse RO modelling, the constants used by Oh et al. (2009) for seawater desalination were deemed feasible at this stage of process design.

5.3.2 MEE Implementation to the Base Case Flowsheet

As Aspen Plus lacks the complex organic compounds, salt ions and long chain polymers in digested vinasse that mostly report to the concentrate, a simplified black box approach to MEE simulation was taken. This way, uncertainty in the results was avoided. The Brazilian vinasse evaporation case study described in Carvalho and Luiz da Silva (2011) was adopted for implementation (Figure 5.11) into the base case flowsheet and scaled down to the base case plant capacity. Unlike the pre- and post-treatments (IEX and RO) highlighted in 5.1.1 and 5.3.1 that were simulated in Aspen Plus, material and energy flows in the MEE process were developed in MS Excel.

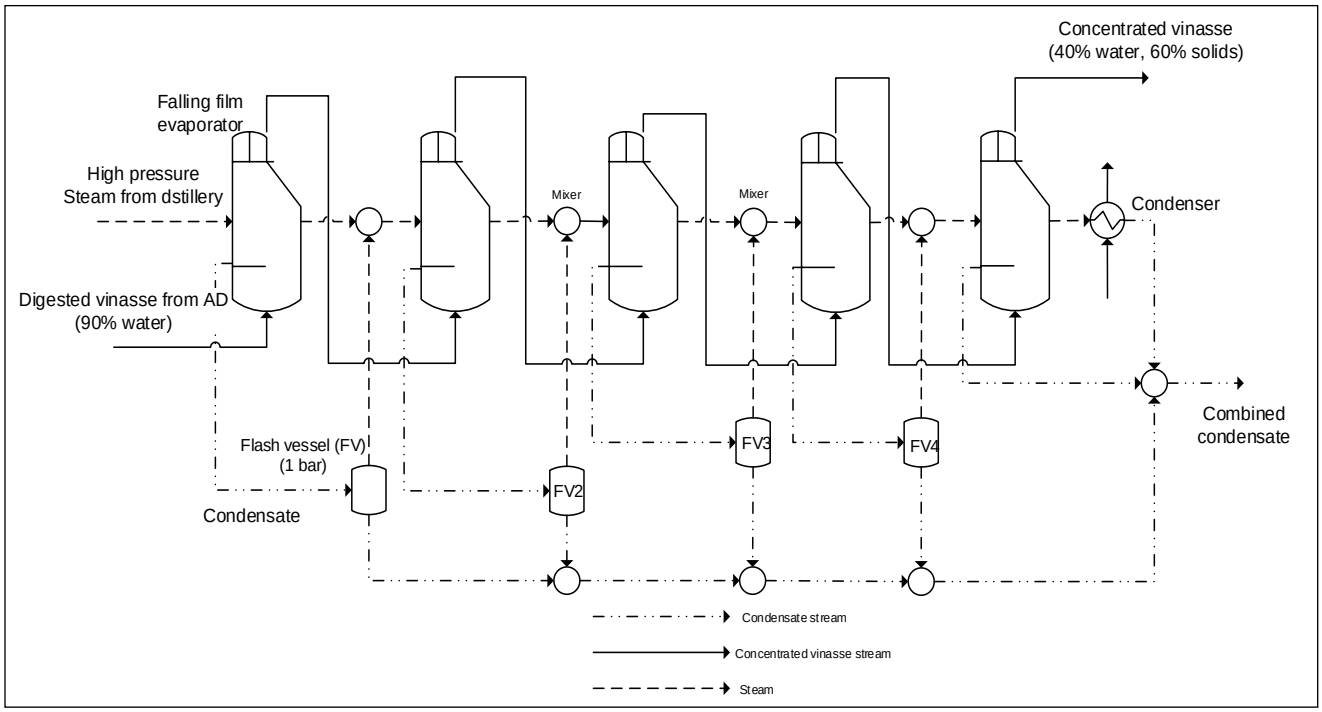

Figure 5.11: The MEE system adopted for the base case flowsheet from the case study by Carvalho and Luiz da Silva (2011)

The MEE process consists of 5 evaporators in series with intermediate condensers (Carvalho, 2011) (Figure 5.11). In analysing the evaporators, heat transfer coefficients used (Table 5.9) in cane juice evaporation processes were utilized as similar properties for vinasse have not been widely published. For cane juice evaporation, Rein (2007) found that the increasing viscosity and density of the concentrate led to a significant decline in the heat transfer coefficients. When using three effects, there was a 33% decline in heat transfer coefficient from the first effect relative to the third (2500 to 1700 $W.m^{-2}.K^{-1}$ in Table 5.9).

Table 5.9: A comparison of heat transfer coefficients between MEE systems with three and 5 evaporators in series

Evaporators	Heat transfer coefficients ($W.m^{-2}.K^{-1}$) (Design with 3 effects)	Heat transfer coefficients ($W.m^{-2}.K^{-1}$) (Design with 5 effects)
1st Effect	2500	2500
2nd Effect	2200	2500
3rd Effect	1700	2000
4th Effect	-	1500
5th Effect	-	700

However, the addition of two more effects reduced the abovementioned decline to 25% (2500 to 2000 $W.m^{-2}.K^{-1}$ in Table 5.9) (Rein, 2007). With higher heat transfer coefficients in the 5-effect system, the surface area was minimized thereby leading to reduced capital cost per evaporator. In accordance with the study by Rein (2007) and Carvalho and Luiz da Silva (2011), the 5 multi-effect evaporator sequence was chosen as it would reduce capital expenditure and guarantee higher heat transfer.

In the conceptual MEE black box model adopted from the case study by Carvalho and Luiz da Silva (2011), digested vinasse is routed to the first effect where it is concentrated by approximately 10% through the evaporation of water and volatile compounds using high pressure steam. To calculate the steam utility requirement for the first evaporator (Figure 5.11), a heating block was simulated separately on Aspen Plus to determine the flowrate of high pressure steam needed for a 10% reduction in the water content of the digested vinasse stream. Thereafter, vapour formed in the first effect is used as the energy source for the next effect where the digestate is further concentrated. The condensate is collected from each evaporator, mixed and thereafter flashed at atmospheric pressure to release any residual vapour. Concentrated vinasse from MEE commonly known as concentrated molasses solids is then drawn from the last effect and is assumed to have a water content of approximately 40% (Rein et al., 2011). This volume reduction to a moisture content of 40% reduces transport costs of the CMS to the sugarcane fields. Arguably, further reductions in moisture content would ultimately reduce volume. However, a reduction to 40% is recommended by Rein, (2007) to avoid elevated equipment costs of MEE with unproportioned savings in transport costs.

Although a simplified approach was taken to model MEE, adoption of the vinasse MEE case study (Carvalho, 2011) and as well as the heating block on Aspen Plus (Lewis et al., 2010) provided adequate information required for sizing and costing calculations.

5.3.3 Effect of Water Recovery Processes on Process Performance and Profitability

The RO model described in 5.3.1 and MEE case study were integrated into separate Aspen Plus simulations containing the base case process (AD-CHP) to form two routes, AD-CHP-RO and AD-CHP-MEE. The energy balance derived from the heating block on Aspen Plus was used to determine the energy required for steam generation in the first effect (Figure 5.12 and Table 5.10). By dividing the energy requirement for steam and the available energy from biogas combustion (Table 5.10), it was established that 10% of the biogas produced was required as fuel to generate the steam for the first evaporator stage. Taking into account boiler or combustion inefficiency, the fraction of biogas required may increase up to 15%.

Energy requirement/demand	
Energy (W) requirement for steam generation	201 200
Energy (W) released from biogas combustion	2 025 800
RO High Pressure Pump Power (W)	23 400

Table 5.10: A comparison of energy requirements or demand MEE and RO

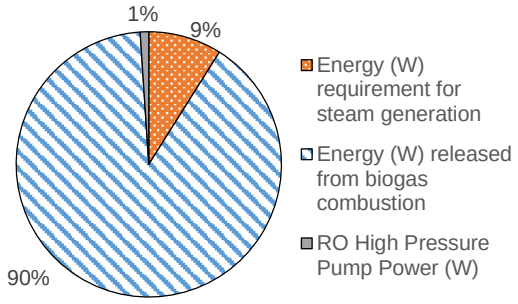

Figure 5.12: Comparative analysis of the energy requirements and demand of the MEE and RO process relative to the energy available from biogas combustion

When compared to the energy requirement for reverse osmosis (high pressure pump), MEE requires up to 9 times the energy utilized by the high pressure pump (Figure 5.12). Therefore, based on energy, RO consumed less energy compared to MEE which translates to lower operating costs.

5.3.3.1 Capital Expenditure

The equipment costs for the RO and MEE processes were calculated using manufacturer quotes (Davis et al., 2013) as well as published equipment costing heuristics (Balaban, 2000). These can be found in Table C 1 in Appendix C. For the reverse osmosis process, the major equipment included the high pressure pump and the spiral wound membrane modules for nano-filtration and reverse osmosis. The major equipment for MEE included 5 falling film evaporators and intermediate condensers. Table 5.5 shows a detailed breakdown of the equipment costs and fixed capital investments calculated using the Lang factor approach outlined by Amigun et al. (2009).

Table 5.11: A breakdown of the initial capital investments to the nearest $1 000 (USD, 2016) comparing the resulting flowsheets from addition of RO and MEE processes to the base case flowsheet.

Purchase cost of equipment (PCE)	**AD – CHP**	**AD – CHP – RO**	**AD – CHP – MEE**
UASB reactor	1 055 000	1 055 000	1 055 000
Jenbacher engine (CHP)	1 766 000	1 766 000	1 766 000
Reverse Osmosis		71 000	
Multi-Effect Evaporators			181 000
Total PCE	2 821 000	2 892 000	3 002 000
Installation, electrical, site, instrumentation factors	1.6	1.6	1.6
Physical Plant Cost (PPC)	4 514 000	4 627 000	4 803 000
Design, Engineering and Contingency factors	1.19	1.19	1.19
Location factor	1	1	1
Fixed Capital Investment	**5 371 000**	**5 507 000**	**5 716 000**
Working Capital (15%)	805 000	830 000	860 000
Total Capital Investment	**$6 176 000**	**$6 337 000**	**$6 576 000**

As seen in Table 5.11, the MEE equipment costs were 140% higher compared to RO. Given to the magnitude of the combined AD and CHP costs, additional downstream processing did not have a significant effect on the total capital investments. Despite the large difference in costs between RO and MEE, either technologies increased the total capital investment by 2% and 4% respectively.

5.3.3.2 Operating Expenditure

The operating expenditures were broken down into fixed and variable costs as described in Section 5.1.3.2. A standard approach of was followed in the calculation of overall O&M costs for RO and MEE. This assumed an O&M value of 10% of the equipment costs. Majority of the variable costs included electrical energy requirements for the high pressure RO pumps

Table 5.12: A breakdown of the operating costs to the nearest $1 000 (USD, 2016) for the flowsheets comparing the resulting flowsheets with addition of RO and MEE to the base case.

Operating Expenditure – Costs/year (USD, 2016)			
Raw Materials	**AD – CHP**	**AD – CHP – RO**	**AD – CHP – MEE**
NaOH (dosing)	38 690	38 690	38 690
Utility costs (electricity, water)	80	65 000	80
Transport costs (digested vinasse)	15 000	15 000	15 000
Labour			
Labor Costs ($/yr)	$173 000	$173 000	$173 000
Operation, Maintenance, Utility			
CHP system ($0.02/kWh)	68 400	68 400	68 400
AD system (1.5% of plant costs)	28 300	28 300	28 300
MEE			32 000
Reverse Osmosis		25 600	
Membrane replacement		40 000	
Total Operating Costs	**323 000**	**436 000**	**362 000**
Indirect fertilizer revenue – Cost savings	92 600	250 000	250 000
Overall OC	**$231 000**	**$186 000**	**$112 000**

The incorporation of either RO or MEE to the base case flowsheet resulted comparatively in a 34% and 12% increase of the total operating costs respectively. For the RO process, this was expected as the high pressure pumps increase the electrical utility usage. Due to fouling and general wear of the spiral would RO membranes, a lifetime of 5 years was assumed (Bick et al., 2012). This introduced a cost of membrane replacement that made up 9% of the total operating costs for the AD-CHP-RO process. The high pressure steam requirements for the MEE process was obtained from excess steam from upstream processes and the CHP heat recovery system and therefore not included in the cost analyses. This resulted in cost savings for the MEE process which kept the operating costs lower compared to the RO process. Labour and maintenance costs for the AD and CHP processes in each route remained similar as the water recovery processes only affected the digestate. Notably, there were significant

increases in the cost savings from fertilizer application with the addition of either water recovery processes. Due to increased potassium concentrations in the RO and MEE residues, application rates increased from 300 tons/ha as was for the liquid digestate (300 m^3/ha) to 3 tons/ha. The application area was therefore greater for the concentrates and consequently resulted in greater savings on synthetic fertilizer costs.

5.3.3.3 Cash Flow, Financial Analysis and Profitability of RO and MEE

The capital and operating costs were used in conjunction with the revenue and cost savings estimations from the sale of electricity and fit-for-purpose water to develop a discounted cash flow analysis of the two additional routes arising from the incorporation of water recovery processes. From this, the profitability indicators were extracted and used to gauge the feasibility of adding water recovery processes to the base case (AD-CHP) (Figure 5.13 and Figure 5.14). It was expected that RO and MEE would have a positive influence on the profitability of the base case scenario.

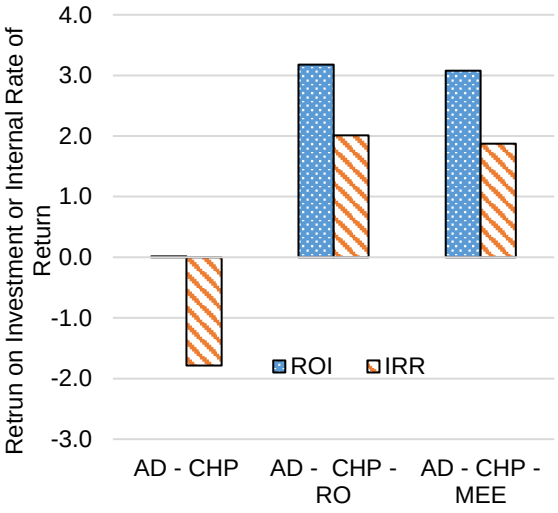

Figure 5.13: A comparison of the profitability (USD 2016) indicators (IRR and ROI) between RO and MEE as water recovery processes in the vinasse treatment flowsheet relative to the base case flowsheet (AD-CHP)

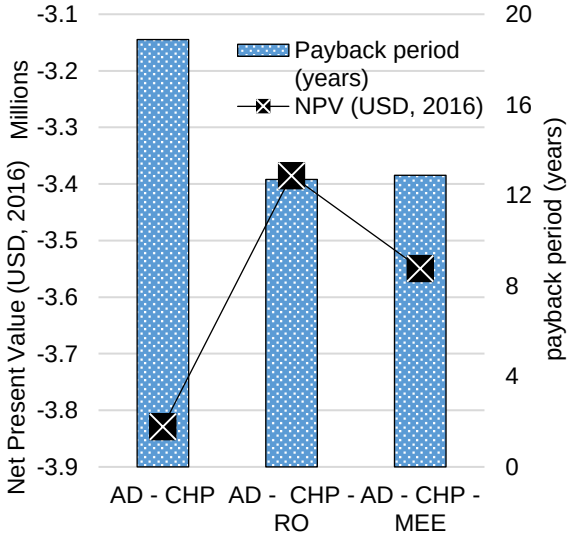

Figure 5.14: A comparison of the profitability indicators (PBP and NPV) (USD 2016) between RO and MEE as water recovery processes in the vinasse treatment flowsheet relative to the base case flowsheet (AD-CHP)

As seen in Figure 5.13, incorporation of water recovery processes increases the profitability of the base case as evidenced by the significantly higher ROI and IRR compared to the AD-CHP process. This was attributed to the 170% increase in cost savings arising from the use of concentrates as fertilizer as opposed to the liquid digested vinasse. The retentate from MEE and RO had significantly higher potassium concentrations and could be applied over larger areas of land.

Similar profitability in terms of ROI and IRR was observed for the AD-CHP-RO and AD-CHP-MEE processes. Although the RO process had 66% higher operating costs (Table 5.12) than MEE, the trend in capital costs (Table 5.11) for the aforementioned processes was reversed. Comparatively, a levelling out of capital and operating costs between the AD-CHP-RO and AD-CHP-MEE processes occurred thereby resulting in similar profitability as evidenced by the IRR and ROI obtained from the discounted cash flow analysis (Figure C 9 and Figure C 3). It

is noteworthy that the gradual increase in the energy requirement for pumping in RO was not modelled as concentration polarization and filter cake resistance were assumed to be negligible (see Section 5.3.1). In reality, concentration polarization and filter cake resistance are present and may impede the movement of liquid through the membrane thereby necessitating higher feed pressures over time to maintain a steady permeate flow. This would potentially to increased energy costs in the medium to long term for the RO process.

Looking at growth of the projects (AD-CHP-RO/MEE), the IRR predictions were lower than the weighted average cost of capital which shows that they are likely to result in a net loss over the 20 years. The negative NPVs for the projects (Figure 5.14) further accentuate this result.

It is important to consider the benefits of recovering water from the vinasse on the long term sustainability of the vinasse treatment process. Due to the presence of volatile acids in the water recovered, its domestic use without further treatment is constrained. In the two scenarios considered (AD-CHP-RO/-MEE), the recovered water is categorized as fit-for-purpose and was re-integrated upstream to meet municipal water requirements in the ethanol distillation process. Given that the water contains volatile compounds, it cannot be used for molasses dilution as it will cause a build up of VFA. However, an ideal utilization would be as a water make up stream for the cooling towers in the distillation process to replace water that is lost through evaporation. Alternatively, the water recovered may be recycled to the biogas upgrading process where it can be used to meet the fresh water requirement (22 000 m^3/yr) in the water scrubbing process. Considering the volume of water recovered from RO and MEE (68 700 m^3/yr) and a municipal water tariff of R5/kL, an overall cost savings is of $27 700 can be achieved on the purchase of water by the vinasse treatment plant and ethanol distillery upstream.

Given the scarcity of water in provinces such as the Western Cape in South Africa, recovered water from RO and MEE processes may be treated further to potable standards to supplement natural sources. Although not included in this work, physico-chemical treatment including coagulation, flocculation and absorption by activated carbon may be used to remove volatile compounds from the RO and MEE water (Ryan et al., 2009; Satyawali and Balakrishnan, 2008). Inclusion of the abovementioned processes will increase the cost of water recovery from vinasse that is currently R9.5/kL and R11/kL for AD-CHP-RO and AD-CHP-MEE processes respectively. As it stands, this is comparatively higher than the estimated cost (6 to 8 R/kL) of seawater desalination in South Africa reported by Swartz et al. (2006). Using the CEPCI, the equivalent costs reported by Swartz et al. (2006) in 2016 are R8/kL to R11/kL on average. The difference in costs is mostly due to the presence of an AD plant vinasse treatment routes that introduces running costs that are not present in the seawater desalination processes.

5.4 Conclusions on the Implementation of Pre- and Post-Treatments to the Base Case

The impact of the addition of either pre- or post-treatment processes was investigated relative to the profitability and system performance of each of these extensions to the base case AD flowsheet. Inclusion of these processes resulted in variations in energy utilization and output, methane yields. Using techno-economic analyses, the effect of the variations in performance arising from the extensions on feasibility were deduced. Figure 5.15 shows schematic detailing

the processes considered in this analysis as well as their merits and demerits in terms of profitability.

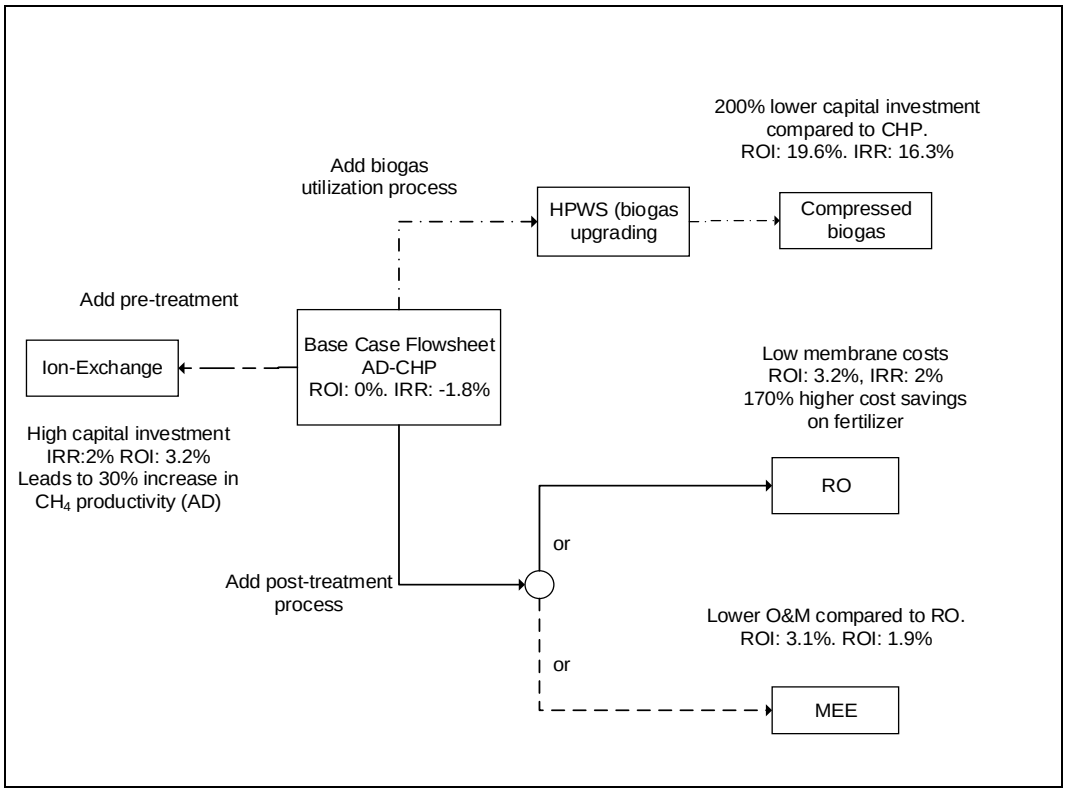

Figure 5.15: A summary of the sensitivity of the base case to addition of pre- and post-treatment unit operations in terms of performance and techno-economic feasibility.

Pre-treatment by ion-exchange resulted in a 30% increase in methane yield during AD owing to removal of inhibitory compounds. This addition brought about higher revenues from electricity sales and consequently increased the base case profitability by over 200% as evidenced by the increase in the ROI and IRR from 0% and -1.8% to 2% and 3.2, respectively (Figure 5.4). Notably, feedback of electricity to the grid may not be possible owing to government policy constraints on the minimum power generation capacity (EcoMetrix Africa, 2013; NERSA, 2011). Despite this, the revenues achieved from the sales may be considered as a cost savings on electricity purchase from the national distributor

Substituting CHP for HPWS in the base case flowsheet reduced the capital costs significantly. The calorific value of biomethane was improved by 72% compared to biogas directly from the AD reactor, which led to an increased total energy output and revenue from the AD-Upgrade process. Overall, switching from CHP to HPWS in the base case greatly increased profitability (ROI: 19.6%, IRR: 16.3% in Figure 5.8) most notably due to comparatively lower capital cost of upgrading equipment relative to the Jenbacher engine for CHP (ROI: 0%, IRR: -1.8% in Figure 5.8).

Addition of dewatering processes through RO or MEE increased the cost savings accrued from the use of concentrates as fertilizer for the sugarcane fields. This increased the profitability of the base case as seen by the indicators in Figure 5.13. The indicators for RO and MEE affiliated processes were still considerably lower than the weighted average cost of capital (15%) which suggests that the routes were unlikely to return any profits. Despite this, incorporation of dewatering processes should be considered to recover water that can be reused in upstream processes such as ethanol distillation. Alternatively, the recovered water

may be used in the HPWS process. These initiatives will reduce fresh municipal water use and thereby result in further cost savings of up to $67 700/yr.

The sensitivity analyses performed in this study indicate that by adding pre-treatment processes may have a knock-on effect on the choice of post-treatment and biogas utilization processes. An example of this is incorporating pre-treatment to realise increased methane yields from AD that may in turn increase the energy output from the downstream CHP or HPWS. The choice between these two processes would then be dependent on the capital and operating costs of both IEX-AD-CHP and IEX-AD-Upgrade routes. Similarly, in terms of profitability, having a pre-treatment process as well as a water-recovery process may not be optimal due to the high additional capital costs.

These interacting effects need to be investigated through the simultaneous addition of pre- and post-treatment combinations to the base case AD process. Subsequent comparison of the developed process options via a techno-economic evaluation can be used to establish the benefits of each process option. This will ultimately lead to development of a decision tool intended to aid the resolution of vinasse treatment options that curb the potentially negative environmental impacts of disposal strategies while extracting valuable products such as biogas, salts and water for commercial use to offset treatment costs and potentially increase profitability.

6. Development of a Decision-Making Tool for the Vinasse Treatment Project

The impact of including pre- and post-treatment strategies on the vinasse AD plant performance and profitability was investigated in Chapter 5. It was noted that from an economic perspective, the implementation of pre-treatments would influence the choice of biogas utilization and water recovery processes when developing vinasse treatment flowsheets. Given the high cost of equipment (Table 5.6), the choice between biogas utilization in the presence or absence of pre-treatment is likely to be dependent on whether the additional revenues from potassium sulfate and biomethane or electricity justify the additional costs. In addition, it is important to identify the desired product quality when choosing biogas utilization processes. When considering post-treatments, operating costs are more likely to influence the decisions owing to the disparity in operation costs between water recovery processes (Table 5.12).

Through development of a decision-making tool, this chapter studies the interacting influence of various process combinations of pre- and post-treatment operations on the overall system performance, product quality and the impact on profitability of the vinasse treatment project. This is presented as a flowchart showcasing potential vinasse treatment routes whilst graphically comparing their performance and economics. It is expected that this tool will provide a more holistic view of the vinasse treatment process and aid in the development of optimized and profitable processes at the conceptual design level.

6.1 Methodology and Development of the Decision-Making Tool

6.1.1 Definition of Vinasse Treatment Routes

The decision-making tool is aimed to provide detailed comparisons between vinasse treatment routes with varying combinations of pre- and post-treatment processes with AD as the primary treatment step. This tool allows the step-by-step development of vinasse treatment processes using decision points that provide the choice of adding pre- and post-treatment processes whilst highlighting the benefits in performance as well as marginal costs incurred. Each set of decisions taken leads to distinct vinasse processing routes with varying performance metered by the energy utilization, methane yield and economic feasibility. These decision options are presented graphically using flowchart techniques consisting of process units, relevant symbols and performance plots as a means of comparison.

The tool was developed to elucidate three decision levels involving the inclusion of pre-treatment, biogas utilization and post-treatment processes to form a total of 12 possible vinasse treatment routes. As seen in Figure 6.1, the first decision avails the option of adding a pre-treatment process to recover potassium ions by means of strong acid cation exchange system. From this, two processing routes arise. Route ‘A’ leads the vinasse directly into the AD reactor without any pre-treatment (path A-1 in Figure 6.1). Route ‘B’ directs the raw vinasse to the ion-exchange system and thereafter to the AD reactor (path B-1 in Figure 6.1). After the AD of the untreated (Route A) or treated (Route B) vinasse, decisions are presented regarding the biogas utilization and water recovery options available for either route.

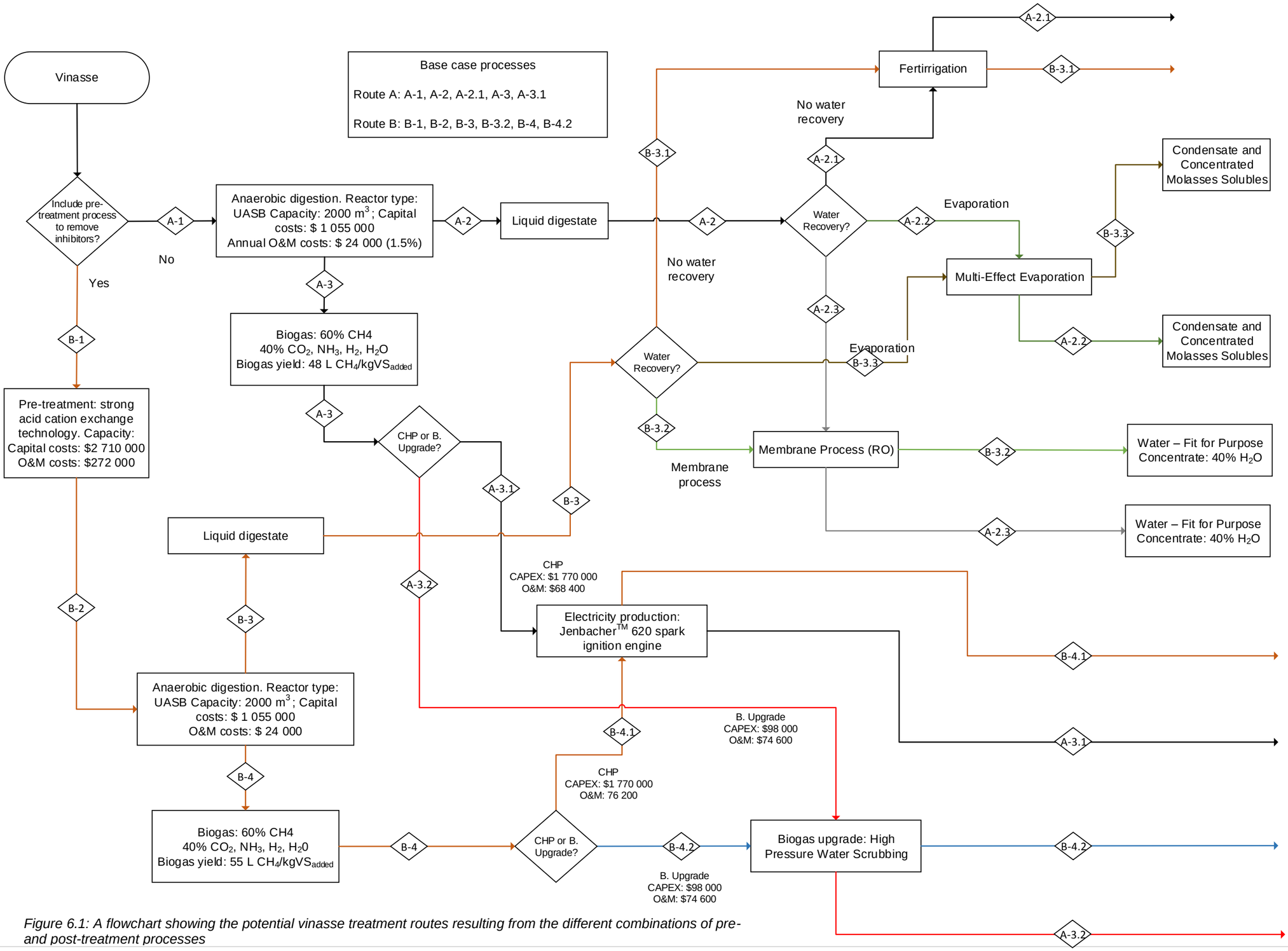

Figure 6.1: A flowchart showing the potential vinasse treatment routes resulting from the different combinations of pre- and post-treatment processes

These include combined heat and power (CHP) for electricity production or high-pressure water scrubbing (HPWS) for biomethane production from the biogas (path A-1, A-3, A-3.1 or A-3.2 and B-1, B-2, B-4, B-4.1 or B-4.2 in Figure 6.1). Two alternatives for water recovery emerge aside from using the water for the fertirrigation of sugarcane fields. These include reverse osmosis and multi-effect evaporation. The water recovered from both options are repurposed as either process water within the plant or purified further to potable standards. The concentrated vinasse digestate is reapplied to the sugarcane fields to result in cost savings in K based fertilizer purchase. However, this application to agricultural land is heavily dependent on nutrient concentrations in the soil.

To create a distinction between Route A and Route B, two identical AD reactors are included (Figure 6.1). The biogas and liquid digestate from the AD reactors are routed to the biogas utilization and water recovery decision points and thereafter to the respective process depending on the selection. Developing detailed comparisons between all 12 processes did not sufficiently uncouple the interacting effects of various process additions to the base case scenario (AD-CHP). As such, an elimination strategy similar to an experimental design was used to ensure meaningful comparative analyses.

The mass and energy balances for the processes shown in Table 6.1 were simulated using the developed, kinetic based, Aspen Plus AD model (Section 3.3). Techno-economic analyses were performed using the model results to evaluate profitability through discounted cash flow analyses.

Table 6.1: Vinasse treatment routes analysed in the decision-making tool. IEX – Ion Exchange, HPWS – High Pressure Water Scrubbing, RO – Reverse Osmosis and MEE – Multi-effect Evaporation

Study	Option	Pre-treatment	Treatment	Biogas Utilization	Digestate Treatment/Water Recovery
1	1	IEX	AD	CHP	Fertirrigation
	2	–	AD	CHP	Fertirrigation
	3	IEX	AD	HPWS	Fertirrigation
	4	–	AD	HPWS	Fertirrigation
2	5	IEX	AD	CHP	RO
	6	–	AD	CHP	RO
	7	IEX	AD	CHP	MEE
	8	–	AD	CHP	MEE
3	9	IEX	AD	HPWS	MEE
	10	–	AD	HPWS	MEE
	11	IEX	AD	HPWS	RO
	12	–	AD	HPWS	RO

Three main studies were conducted to explore the interacting effects of pre- and post-treatment additions. In the first study, the influence of four selected routes on the methane yield, energy output and overall profitability were investigated based on the combined effect of pre-treatment and biogas utilization process (CHP or HPWS) options (Study 1 in Table 6.1).

The second study focused on the effect of including ion-exchange on select water recovery processes (MEE or RO) (Study 2 in Table 6.1). Finally the effect of biogas utilization on the

choice between MEE and RO was investigated (Study 3 in Table 6.1). In each study, one aspect remained constant. For example, in all instances in Study 1, the liquid digestate was used for fertirrigation when investigating the effect of pre-treatment on biogas utilization processes in Study 1. Similarly, the biogas was sent to CHP in study 2 when analysing the effect of pre-treatment on water recovery processes. In study 3, the influence of pre-treatment was analysed when exclusively considering a biogas upgrading process. Given that Studies 2 and 3 in Table 6.1 both focused on water recovery processes, they were consolidated to form a more condensed outlook.

The presented studies (Table 6.1) deconstruct the decision matrix proposed in Figure 6.1 and provide detailed comparative analyses at the three decision points. The first avails the option of including a pre-treatment process before anaerobic digestion (A1 or B1 in Figure 6.1). This generates two processing routes which both have a selection between CHP and HPWS processes for biogas utilizations after the AD (A-3.1 or A-3.2 and B-4.1 or B-4.2 in Figure 6.1). These processing routes subsequently have a post-treatment option *via*. fertirrigation, reverse osmosis or multi-effect evaporation (A-2.1, A-2.2 or A-2.3, or B-3.1, B-3.2 or B-3.3 in Figure 6.1).

6.2 Study 1: The Influence of Pre-treatment on the Choice of Biogas Utilization Processes (CHP or HPWS)

The objective of a pre-treatment process in the vinasse treatment project was to increase the efficiency of the AD process through the reduction of potassium salt concentrations in the vinasse feed. Potassium salts are inhibitory and their recovery is expected to improve anaerobic digestion performance (Chen et al., 2008). Through sensitivity analyses presented in Section 4.4.1.3, a reduction of potassium salts increased the efficacy of the vinasse AD system as evidenced by higher methane yields. Further in Section 5.1.3, it was shown that inclusion of an ion exchange system increased profitability of the base case route (AD-CHP) (see Figure 5.3). However, the newly formed IEX-AD-CHP route was projected to incur a net loss over its lifetime. This showed that the additional capital investment and operational costs overshadowed the marginal revenue increase.

Consequently, in addition to incorporating ion exchange to the base case (AD-CHP), the first study in Table 6.1 seeks to explore the cost-benefits of ion-exchange to the AD-HPWS process. The added benefit between CHP and HPWS using the first four iterations listed in Table 6.1 is therefore also considered. In this study the biogas utilization process is varied while maintaining fertirrigation as the digestate disposal method.

6.2.1 Decisions between Biogas Utilization Processes: Combined Heat and Power and High Pressure Water Scrubbing

Biogas produced from anaerobic digestion is a valuable energy source with a calorific value, relative to the methane concentration, between 19 and 23 kJ/L (Seadi et al., 2008). This gas is either used internally as a fuel, converted to electricity or upgraded to biomethane (Walsh et al., 1989). Incorporating pre-treatment (IEX) to the base case process increased methane yields owing to a reduction in inhibitor concentrations. However, this was accompanied by a significant increase in capital expenditure which supressed profitability as evidenced by an IRR that was lower than the average cost of capital set at 15% (Figure 5.3). In a bid to explore the economic benefits of reduced capital costs, this section considers the replacement of CHP with biogas upgrading with HPWS to biomethane. In addition to its simplicity, equipment costs

for HPWS are 50% lower relative to CHP which is postulated to have a positive effect on profitability of the vinasse treatment routes.

In the base case process (Route A with path A-1, A-2, A-2.1, A-3, A-3.1 in Figure 6.2, AD-CHP), vinasse is routed to a 2000 m^3 UASB reactor where it is broken down to biogas with a calorific value of 22 kJ/L containing 53% methane with an equivalent yield of 48 L-CH_4/kgVS (Table 4.4). Approximately 410 kW of electricity can be produced from this biogas using a Jenbacher spark ignition engine with an operating efficiency of 44% (Darrow et al., 2015). In this study, the digested vinasse is sent to the sugar cane fields for fertirrigation without any further downstream treatment (Study 1 in Table 6.1).

As seen in Figure 6.2, a vinasse pre-treatment option before AD aimed at inhibitory potassium ion recovery using ion-exchange is shown (Route B in Figure 6.2). Similar to the base case scenario, it follows path B-1, B-2, B-2, B-3, B-3.1 and B-4, B-4.1 with the added pre-treatment step (IEX-AD-CHP). This deviation from the base case process results in a higher CH_4 yield of 55 L-CH_4/kgVS and electricity production of 457 kW (see Section 5.1.2).

The biogas streams from the AD reactors in both routes A and B were duplicated to give rise to the decision blocks (after A-3 and B-4 in Figure 6.2). An option to replace CHP with HPWS (Upgrade) is provided to introduce two more routes: A-1, A-2, A-2.1, A-3, A-3.2 (AD-HPWS) and B-1, B-2, B-3, B-3.1, B-4, B-4.2 (IEX-AD-HPWS). As described in Section 5.2.1, HPWS involves the counter current water scrubbing of CO_2 from biogas which results in the production of a 95% pure biomethane stream. The detailed description and modelling approach can be found in Section 5.2.1**.**

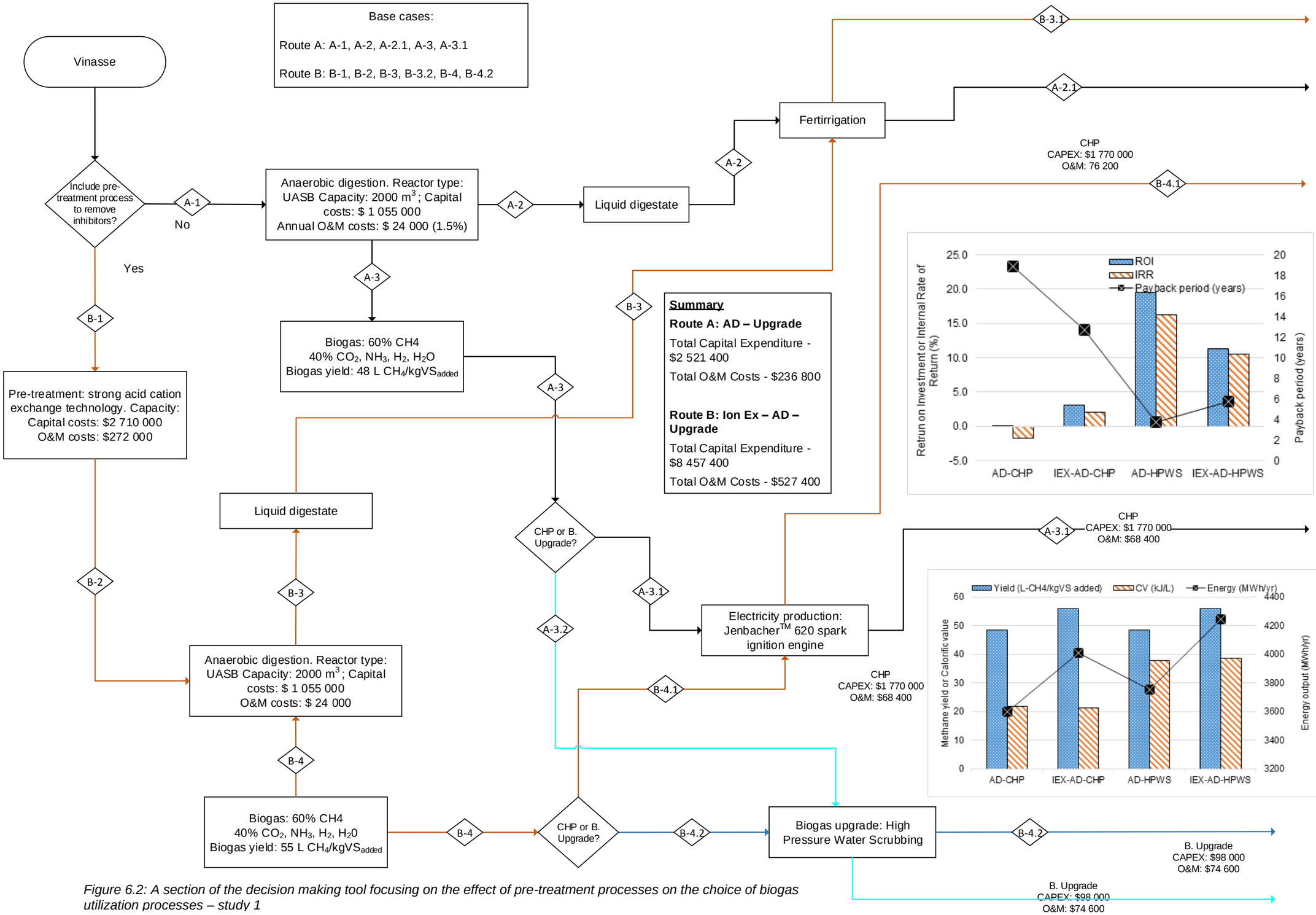

Figure 6.2: A section of the decision making tool focusing on the effect of pre-treatment processes on the choice of biogas utilization processes – study 1

6.2.1.1 Performance and Economic Comparisons between HPWS and CHP

As described in Section 5.2.2, energy data from CHP and HPWS was converted to an annual energy output measured in MWh/year. To normalize this performance comparison, the equivalent electricity production from biomethane was used as opposed to the raw biomethane energy. The equivalent electrical energy in biomethane was calculated by scaling the raw biomethane energy by 56% to mimic the electricity production efficiency of 44%. In addition to energy, the methane yields and calorific values of the biogas were also used to evaluate performance in these analyses (Figure 6.3).

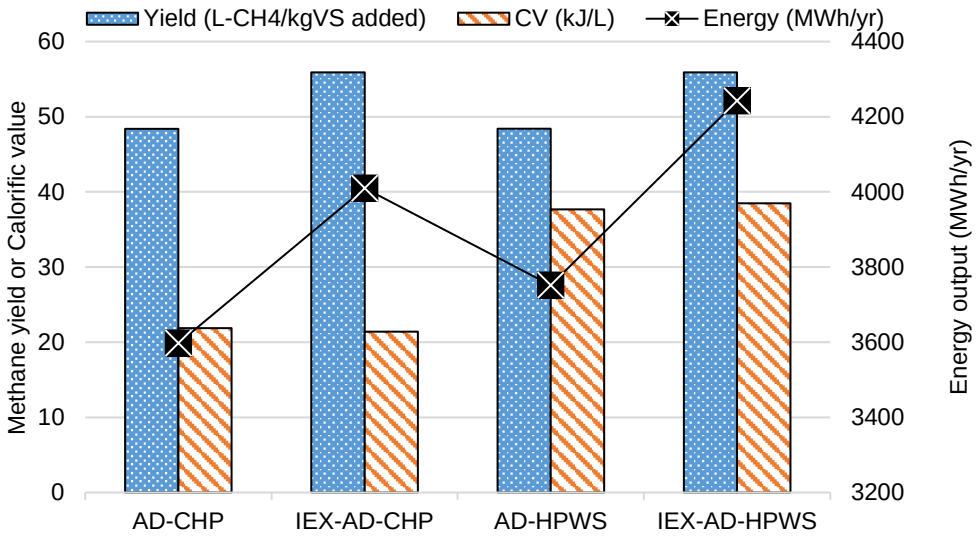

Figure 6.3: A performance comparison between CHP and HPWS affiliated processes in terms of energy output (equivalent electrical energy in MWh/yr), methane yields (L-CH_4/kgVS_{added}) and calorific values of the resulting gases (biogas and biomethane)

As seen in Figure 6.3, the methane yields remain constant as AD remains unaffected by CHP or HPWS in the routes that do not feature any pre-treatment (AD-CHP and AD-HPWS). Of these two routes (AD-CHP and AD-HPWS), biomethane from AD-HPWS exhibited a calorific value 72% higher than biogas from the AD-CHP process. This improvement is mostly due to the reduction in impurities and CO_2 concentration in the biogas upon upgrading. This, however, did not lead to a proportionate increase in the total energy stored in the biomethane compared to biogas. The relatively small increase in total energy output per annum (4%) was attributed to a reduction in volumetric flowrate, a consequence of the upgrading processes with the removal of CO_2 from the biogas stream. Similar trends were observed when analysing processes that featured pre-treatment (IEX-AD-CHP and IEX-AD-HPWS). In each case, the calorific value for biomethane from IEX-AD-HPWS was higher (78%) relative to the biogas from the IEX-AD-CHP process.

Due to the reduction in the potassium ion inhibitor (Figure 6.3), the inclusion of a pre-treatment process via ion-exchange resulted in 16% higher methane yields for both CHP and HPWS processes (see Section 5.1.2). For the CHP affiliated processes, pre-treatment did not increase the biogas calorific value as expected. The slight decrease in the CV by 2% from 21.8 kJ/L (AD-CHP) to 21.4 kJ/L (IEX-AD-CHP) was deemed negligible and therefore unchanging. Although the CV for the HPWS processes increased with the addition of an ion-exchange system, the change was similarly small as observed in the CHP affiliated processes. The small changes can be explained using the potassium inhibition kinetics. Looking at the

potassium ion inhibition mechanism presented in Section 5.1.2**,** a reduction in inhibitor concentration increases the methanogenic reaction rate thereby increasing the flowrate of all components in the biogas. Due to this, the methane concentration remains relatively unchanged. A similar trend is observed in Figure 6.3. Given the small magnitude (2 to 4%) of these changes in CV, the addition of a pre-treatment system was concluded to have no significant effect on the energy content of the biogas or biomethane.

From a performance perspective, the production of biomethane is more favourable compared to electricity. This is observed across all scenarios with the presence or absence of an ion-exchange system as pre-treatment option. However, the inclusion of a pre-treatment system to the AD-CHP or AD-HPWS processes did not have a significant impact on the energy content of the resulting gases (biogas or biomethane). On the other hand, in terms of energy output per annum, the pre-treated processes (IEX-AD-CHP/HPWS) performed best due to the higher methane quantities produced and improved conversion factors for organic carbon, owing to decreased inhibition. Having established the impact of pre-treatment, a techno-economic analysis was conducted to gauge economic feasibility considering the high initial capital costs associated with ion-exchange processes (Table 5.2).

Capital expenditures are computed using a modified Lang factor approach tailored to bioprocesses in Southern Africa (Amigun and von Blottnitz, 2009). It takes into account equipment costs, site preparation and working capital. Fixed and variable costs were calculated using published heuristics and estimations reported in the literature. The costs are summarized in Table C 1 in Appendix C. With the detailed techno-economic analysis approach reported in Section 3.5**,** profitability indicators for the AD-HPWS and IEX-AD-CHP/HPWS processes relative to the base case (AD-CHP) are summarized in Table C 2 and presented in Figure 6.4. In all four scenarios, digested vinasse is used for fertirrigation. The digestate is treated as a cost savings on potassium based fertilizer for the sugarcane fields. The electricity from the CHP process is sold to ESKOM at the recommended REFIT of $0.08/kWh, which is adjusted for inflation to $0.1/kWh (NERSA, 2011). On the other hand, biomethane is sold at $19/GJ which is equivalent to $0.07/kWh (EcoMetrix Africa, 2013).

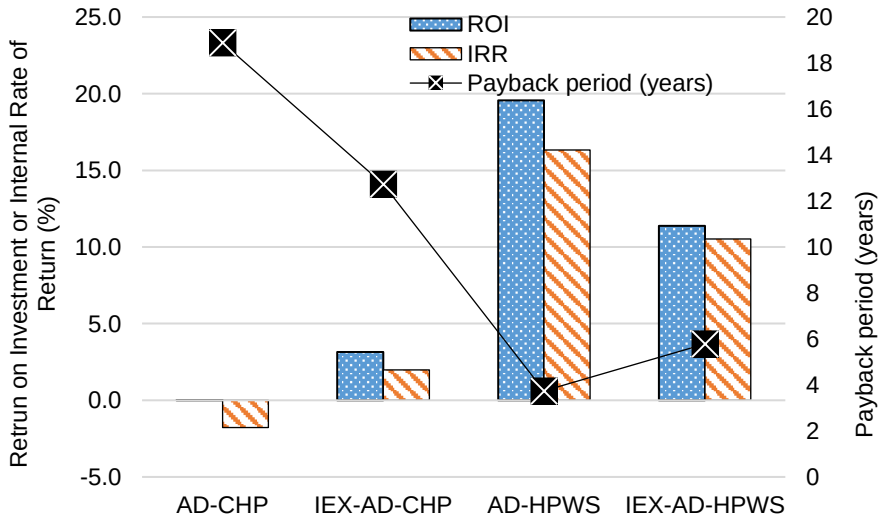

Figure 6.4: A comparison of profitability indicators (USD, 2016) between HPWS and CHP affiliated processes with the inclusion or absence of pre-treatment (IEX)

Discounted cash flow analyses were used to determine the profitability indicators (Figure 6.4). Overall, biogas upgrading (HPWS) exhibited higher profitability as evidenced by the improved ROI, IRR and decreased (78%) payback time of 4 years. This is mostly attributed to increased sales revenue from biomethane and reduced capital investments by 50% for the HPWS process compared to CHP options. Inclusion of a pre-treatment process increased the profitability of the CHP processes owing to higher methane yields and electricity production. While pre-treatment has been found to increase (16%) methane yields, the expected increase in profitability with its implementation to the AD-HPWS process is not observed. Instead, there is a decline which was attributed to the lower magnitude of marginal revenues (120%) obtained from biomethane and potassium sulfate sales in the IEX-AD-HPWS process compared to the additional capital investment (231%) required for an ion-exchange system see.

Electricity production from biogas exhibits negative growth (IRR < 0) and is likely to return a net loss over its 20-year life time (AD-CHP in Figure 6.4). These observations are in agreement with a recent study comparing biogas utilization processes (Lee, 2017). The study showed that CHP is not feasible due to low feed-in-tariffs set by the national energy regulator. Biomethane production exhibits better prospects for both untreated and pre-treated systems (AD-HPWS & IEX-AD-HPWS in Figure 6.4). This is due to higher energy output from biomethane as opposed to biogas (Lee, 2017). An IRR of 15.1% is noted for the AD-HPWS process, which matches the average cost of capital (15%). A NPV of $8000 is predicted after 20 years (Table C 2). The combination of these indicators demonstrates that the upgraded biogas from an AD process without pre-treatment will cover its cost of capital and is likely to turn a profit in the long run (AD-HPWS in Figure 6.4). While not profitable, the value of pre-treatment addition to the base case and AD-HPWS processes is significant in that it increases conversion in AD and subsequently methane recoveries which overall promotes better resource utilization.

6.2.2 Conclusions on Study 1

While investigating opportunities in either upgrading or electricity generation through CHP from biogas, upgrading to biomethane through HPWS (AD-HPWS) exhibited higher energy outputs and profitability relative to the base case (AD-CHP) (Figure 6.3 and Figure 6.4). Addition of a pre-treatment system to the AD-HPWS route negatively impacts profitability despite increased energy outputs. On the other hand, pre-treatment increases the performance and profitability of the base case scenario. If the objective is to produce biomethane, then a trade-off exists between performance and profitability when considering the addition of pre-treatment. Although ion-exchange is likely to improve AD efficiency, it does not guarantee higher profits when coupled with an upgrading system (HPWS) for biogas utilization. When aiming to produce electricity, pre-treatment is necessary to increase the biogas and methane yields although profits are likely to remain low in the long run. Given that the effluent was utilized for fertirrigation in all instances in study 1, the cost savings achieved in the AD-CHP and AD-HPWS processes were similar. As reported in Section 5.1.3.2, pre-treatment causes a decline in cost savings owing to decreased potassium concentrations in the effluent. This reduced the cost savings achieved in the IEX-AD-CHP/HPWS processes. Due to the small magnitude of cost savings relative to the revenues from biogas and biomethane (5 to 10 times the cost savings), the overall impact of fertirrigation on the economics and its influence on the choice between HPWS and CHP was not significant.

When selecting a biogas utilization process, it is important to consider the market demand for either electricity or biomethane. The renewable feed-in tariff for the sale of surplus electricity

by industry back into the grid was introduced to encourage electricity production from renewable sources such as wind, solar, landfill gas and biogas (NERSA, 2011). However, meeting regulatory and compliance standards has been a challenge for most small and medium scale biogas producers. The applied tariffs are significantly lower than the energy production costs which discourages potential investments in this field. In the context of vinasse treatment, electricity generated via CHP can be used internally and result in cost savings from reduced utility usage from the municipality. This is potentially a cost effective alternative to utilizing electricity generated from AD plants.

The market size for biomethane is projected to increase in South Africa with the introduction of dual fuel buses that run on both biodiesel and biomethane in metropolitan areas (Masebinu et al., 2014). Although this increases the potential for biomethane as a transportation fuel, some infrastructural constraints exist. These include the lack of refilling stations and adequate distribution networks (Masebinu et al., 2015). Nonetheless, the future for biomethane and its adoption as a vehicular fuel remains positive as plans are underway to retrofit public transport vehicles with conversion kits that will enable them to use compressed biomethane (EcoMetrix Africa, 2013).

6.3 Study 2 and 3: The Influence of Pre-treatment on the Choice of Water Recovery Process

Raw sugarcane vinasse has a high moisture content ranging between 85 and 90% brought about by the upstream dilution of molasses before fermentation (Christofoletti et al., 2013). Dilution of vinasse prior to its AD for the control of the OLR is also a common practice that contributes to the high water content (Shivajirao, 2012). The water is carried through AD and forms ca. 90% of the liquid digestate with the remainder comprising of unconverted organics, nutrients (N, P, K), minerals and VFA.

Several value creation strategies from the digestate have been implemented in industry. The presence of nutrients and organic matter make it suitable for the fertirrigation of sugarcane fields at an average application rate of 350 m^3 per hectare depending on the potassium concentration (Christofoletti et al., 2013). However, risks associated with this include soil salinization and release of GHG through breakdown of organics while in the soil. Alternatively, a dewatering process can be used to concentrate the effluent and thereafter be applied to sugarcane fields (3 tons/ha) as fertilizer or used as an animal feed supplement (Turner et al., 2002). The water recovered can then be re-used internally for dilution or as a cooling utility. In this Section, reverse osmosis and multi-effect evaporation are evaluated as alternatives to the free disposal of digested vinasse through fertirrigation as suggested in the base case (AD-CHP).

Addition of either systems (RO or MEE) improve process sustainability and result in cost savings in terms of potassium based fertilizer. However, the marginal costs need to be reviewed in the wider context of the vinasse treatment flowsheets. The initial investments required for RO have in the recent past reduced significantly although operating costs remain high due to electrical energy requirements for pumping to overcome osmotic pressures (Garud et al., 2011). On the other hand, multi-effect evaporation is well established in the sugarcane industry which may create a bias towards it (Christofoletti et al., 2013). Studies 2 and 3 seek to analyse the cost benefit of incorporating RO over MEE and vice versa when dealing with a pre-treated or untreated raw vinasse feed to the AD. In Study 2, CHP is used as the biogas

utilization process. Biogas upgrading through HPWS replaces CHP as the biogas utilization in study 3.

6.3.1 Study 2: Decisions between Water Recovery Processes – Reverse Osmosis and Multi-Effect Evaporation when Using CHP

The recovery of water from raw or digested vinasse is beneficial as it improves overall process sustainability and potentially results in cost savings on fresh water requirements for upstream processes. In Section 6.2, the liquid digestate is used for fertirrigation of sugarcane fields which introduces transport costs due to the sizeable effluent volumes following AD. In this section, alternative methods of digestate utilization (RO and MEE) are simulated. The techno-economics of these process routes are compared to determine the most feasible process in the presence or absence of a pre-treatment process prior to AD. Given the analyses reported in Section 6.2, this section seeks to extend the post-treatment analyses to consider the combined effect with select pre-treatment options (IEX-AD-CHP-RO/MEE) on system performance and economics.

The vinasse treatment routes following the addition of RO or MEE to the pre-treated and untreated base case presented in Figure 6.5 are similar to those described in Section 6.2.1 (Study 1 in Table 6.1) with added adjustments to the water recovery processes (Study 2 & 3 in Table 6.1). As seen in Figure 6.5, the vinasse, depending on inhibitor concentrations, can either be pre-treated using ion exchange or routed directly to the AD reactor. This results in two routes which further branch into four select water recovery alternatives (options 5 to 8 in Table 6.1).

Incorporating RO and MEE to the base case was expected to enhance process sustainability and increase net cost savings through the upstream reuse of RO water and downstream utilization of concentrates as fertilizer in the sugarcane fields. However, due to the difference in operating costs of the two processes (RO and MEE), a feasibility analysis is required to assess the economic viability of RO and MEE incorporation to the base case. Pre-treatment has shown to increase profitability of the base case (see Figure 5.4) and as such, it is necessary to investigate its influence on the economics in the presence of water recovery processes. Given the established effect of pre-treatments on base case profitability, the influence of either RO or MEE will be investigated by comparing the performance and profitability of the 4 routes (options 5 to 8 in Table 6.1) relative to the base case. As seen in Figure 6.5, the base case RO process option follows the route A-1, A-2, A-2.3, A-3, A-3.1 (AD-CHP-RO) while the pre-treated option follows B-1, B-2, B-3, B-3.1 and B-4, B-4.1 (IEX-AD-CHP-RO). The base case MEE process follows the route A-1, A-2, A-2.2, A-3, A-3.1 (AD-CHP-MEE) while the pre-treated option follows the B-1, B-2, B-2, B-3, B-3.2 and B-4, B-4.1 route (IEX-AD-CHP-MEE). Section 5.3 details the approach to RO and MEE simulations as well as the assumptions made. Through the analysis in study 2, CHP is maintained as the biogas utilization process.

6.3.1.1 Performance and Feasibility Comparisons between RO and MEE

Multi-effect evaporation and reverse osmosis were modelled on Aspen Plus and integrated into the existing base case simulations (Section 5.3.1 and 5.3.2). The resulting mass and energy balances were used to compile performance data as well as conduct equipment sizing procedures. In these analyses, energy consumption was used to evaluate the performance of the two technologies. Reverse osmosis was expected to have high electrical energy demands arising from the high pressure pump requirements.

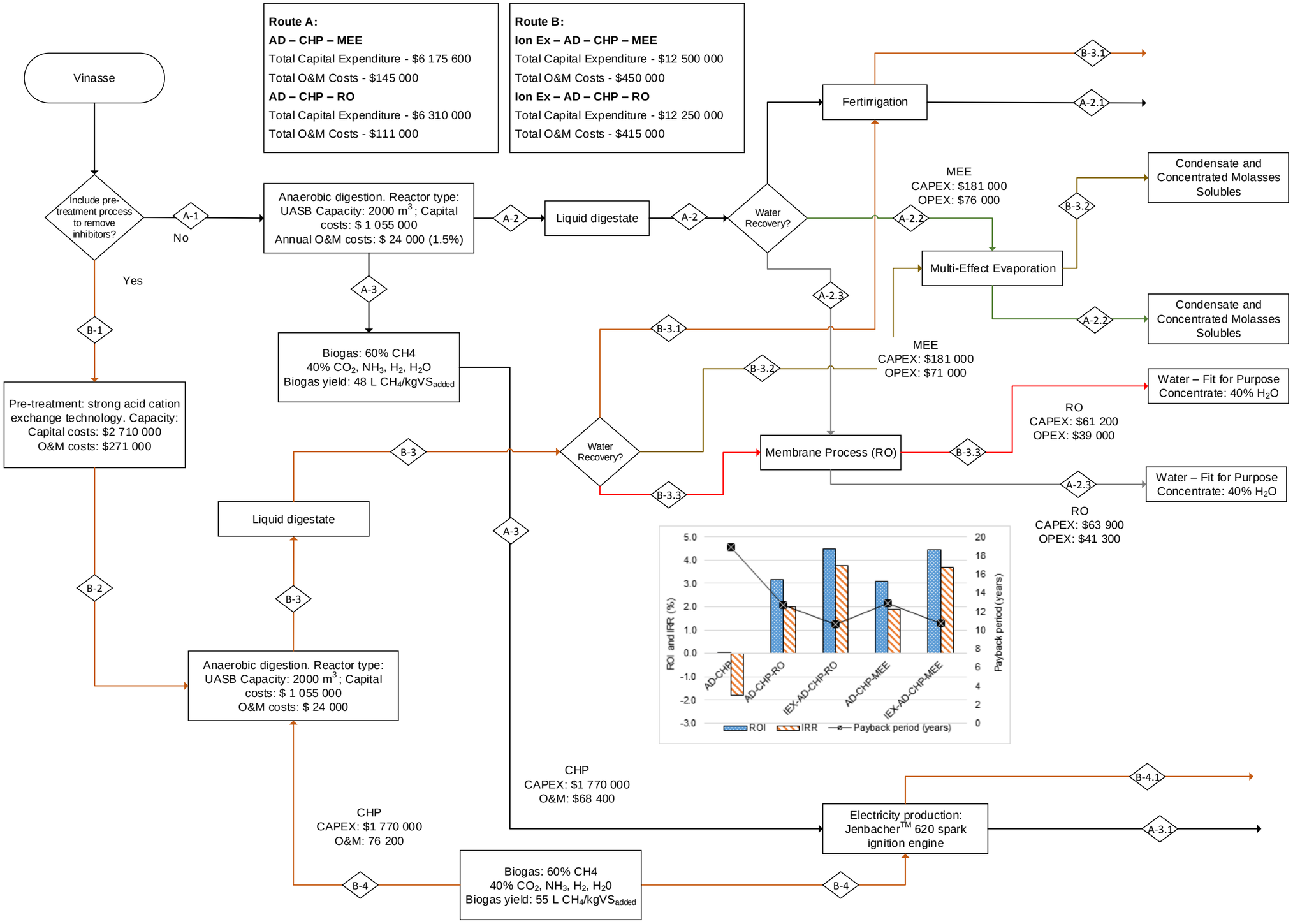

Figure 6.5: A section of the decision making tool focusing on the effect of pre-treatment processes on the choice of water recovery processes when using CHP

For MEE, the major energy requirement was the steam utility needed to heat or concentrate the digestate in the first evaporator. As reported in Section 5.3.3 , the AD-CHP-MEE energy balance (Table 5.10) shows that approximately 12% of the biogas produced is required as fuel to generate the steam for the first stage in MEE. This amounts to 4 times (on average) the energy requirement for the RO high pressure pump (Figure 5.12).

Following the performance comparison, a techno-economic feasibility was conducted using a discounted cash flow analysis to provide profitability indicators using the approach detailed in Section 3.5 (Figure 6.6). In all process options presented in Figure 6.5, the concentrated vinasse is used as fertilizer at an application rate of 3 tons/ha. This is factored in the process economics as a cost saving through the purchase of potassium based fertilizers. Revenue from electricity as well as the economics leading up to the discounted cash flow analyses evaluated in this study followed the same procedures outlined in study 1 (Section 6.2.1.1). Profitability indicators from the discounted cash flow analyses are summarized in Table C 2 presented in Figure 6.6.

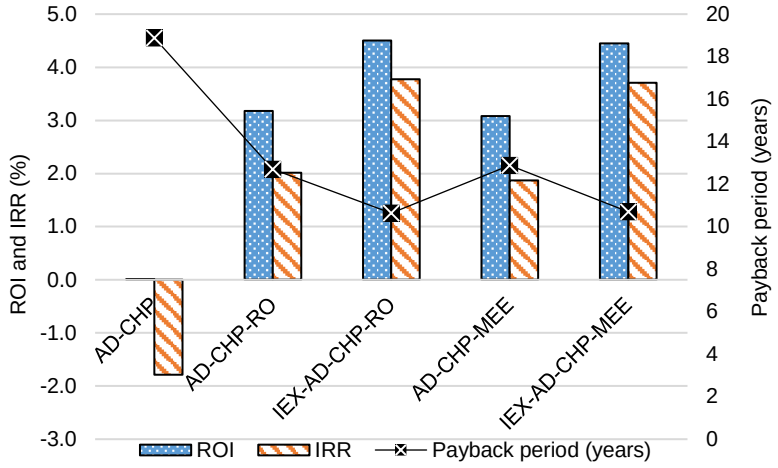

Figure 6.6: A comparison of profitability indicators (USD, 2016) between RO and MEE affiliated processes when considering the inclusion or absence of pre-treatment with CHP as the biogas utilization process.

Profitability is generally low for all the processes in Figure 6.6 as evidenced by the low ROI and IRR (<5%). Inclusion of a pre-treatment process (ion-exchange) with either selected downstream unit operation (RO or MEE) had an overall positive effect on the profitability. For the RO affiliated process (AD-CHP-RO), a 20-30% increase in the ROI and IRR is noted with the inclusion of an ion exchange process (IEX-AD-CHP-RO). Similarly, this is observed for MEE processes and is attributed to increased methane yields and energy output due to improved AD efficiency. Increased cost savings (170%) from application of the RO and MEE concentrates as fertilizer compared AD effluent (fertirrigation in AD-CHP) contributed greatly to the upward trend in profitability observed with the inclusion of water recovery processes. Further, upstream reintegration (see Section 5.3.3.3) of the condensate from MEE or permeate water increased cost savings by up to $27 000.

With improved profitability arising from the combined influence of cost savings and water reuse, the payback period for combined pre- and post-treatment routes decreased as expected. In line with the high energy requirements and the absence of improved performance potential with pre-treatment, the AD-CHP-MEE route had the longest payback (ca. 13 years).

All four routes have negative net present values after 20 years (see Table C 2) which suggests that they are unlikely to return net profits over the project life time.

6.3.2 Study 3: Decisions between Water Recovery Processes – Reverse Osmosis and Multi-Effect Evaporation when Using HPWS

Study 2 (Section 6.3.1) showed that the benefits of adding post-treatment (RO and (MEE) processes to the base case (AD-CHP) included improved process sustainability and increased cost savings from the use of concentrates as fertilizer. Compared to the base case, improved profitability was observed. However, this did not guarantee net profits in the long run as the IRR for all instances in study 2 were below the cost of capital (15%).

Electing to upgrade the biogas to biomethane when incorporating post-treatment processes has the potential to increase profitability given the 50% lower cost of HPWS equipment (Darrow et al., 2015) relative to CHP engines. Although post-treatments were not included in study 1 (Section 6.2.1.1), it was shown that switching to HPWS improved profitability of the base case. This study therefore seeks to explore the effect of adding water recovery processes on profitability of the un-treated or pre-treated process options when biogas upgrading (HPWS) is in use. In line with previous studies, pre-treatment was included to ascertain its effect on process profitability. A decision tree highlighting the four additional processes (options 8 to 12 in Table 6.1) as well as a summary of their capital and operating expenditures is developed (Figure 6.7).

6.3.2.1 Feasibility Comparisons between RO and MEE

Techno-economic analyses were conducted on the four additional routes using a similar approach described in Section 3.5 and the previous studies (Sections 6.2.1.1 and 6.3.1). Discounted cash flow analyses were thereafter used to calculate the profitability indicators over a 20-year project lifetime (Figure 6.8). As expected, substitution of the CHP system (Study 2, Figure 6.6) for HPWS with incorporation of RO or MEE greatly increases the profitability of the processes as seen in Figure 6.8. This is attributed to a 50% decrease in capital costs due to the low cost of HPWS equipment relative to CHP (Table 5.6).

For the untreated MEE affiliated route (AD-HPWS-MEE), addition of a pre-treatment process resulted in a decrease in profitability which was contrary to the trend observed in the previous study (see Section 6.3.1.1). Although ion-exchange increased the CH_4 yield and provided an additional revenue stream (K_2SO_4), the combined operating costs of the IEX-AD-HPWS-MEE are approximately 200% higher (Table C 1). These mainly consist of maintenance costs for ion exchange and MEE. Similarly, ion-exchange decreases the profitability of the RO affiliated processes owing to the higher combined operating costs of RO (utility and membrane maintenance) and ion-exchange (10% of CAPEX) (Table C 1**)**. However, RO equipment is 70% cheaper compared to MEE (Table 5.11) which boosted the overall profitability of both AD-HPWS-RO and IEX-AD-HPWS-RO routes over the AD-HPWS-MEE and IEX-AD-HPWS-MEE routes.

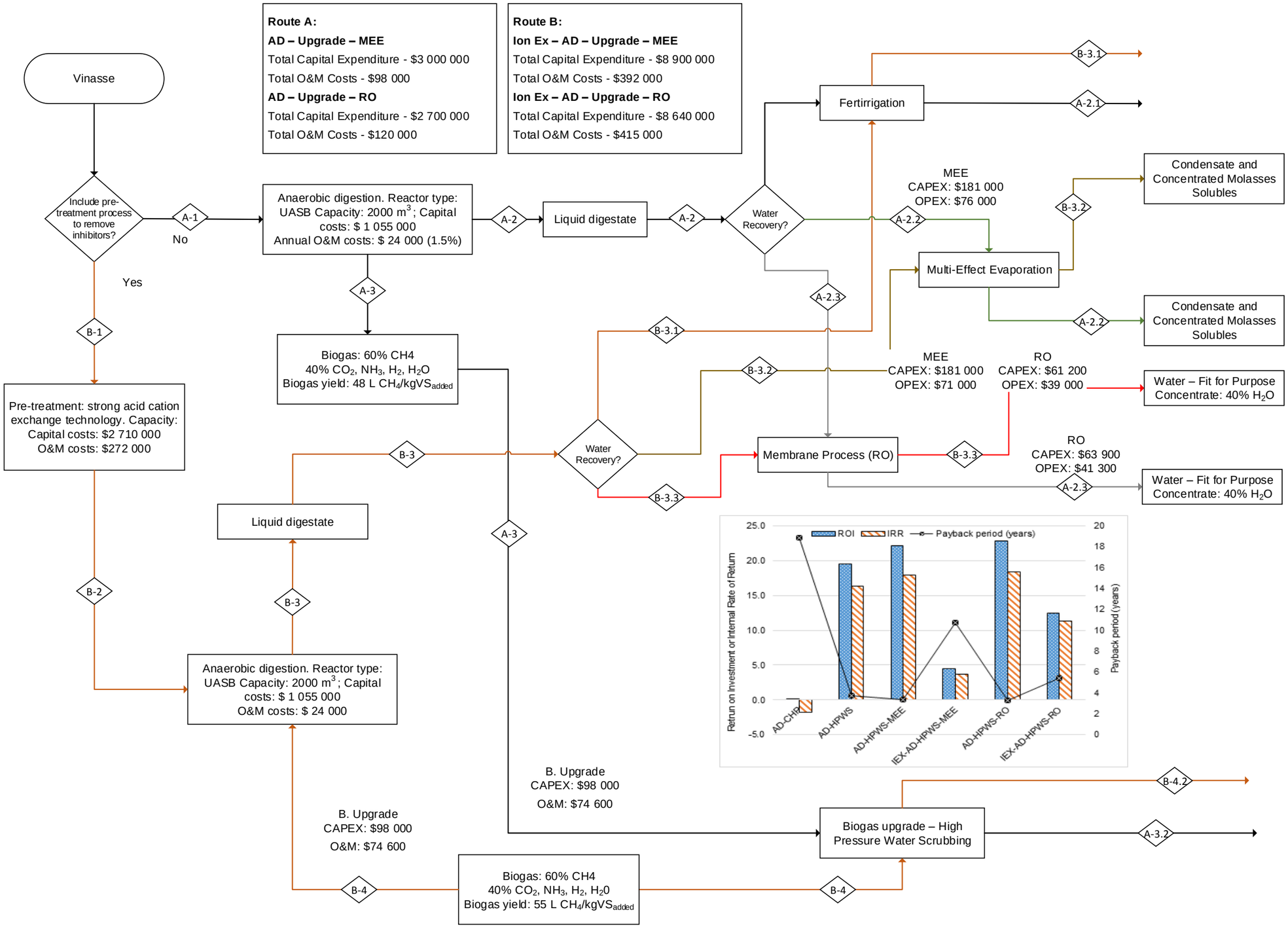

Figure 6.7: A section of the decision making tool focusing on the effect of pre-treatment processes on the choice of water recovery processes when using HPWS

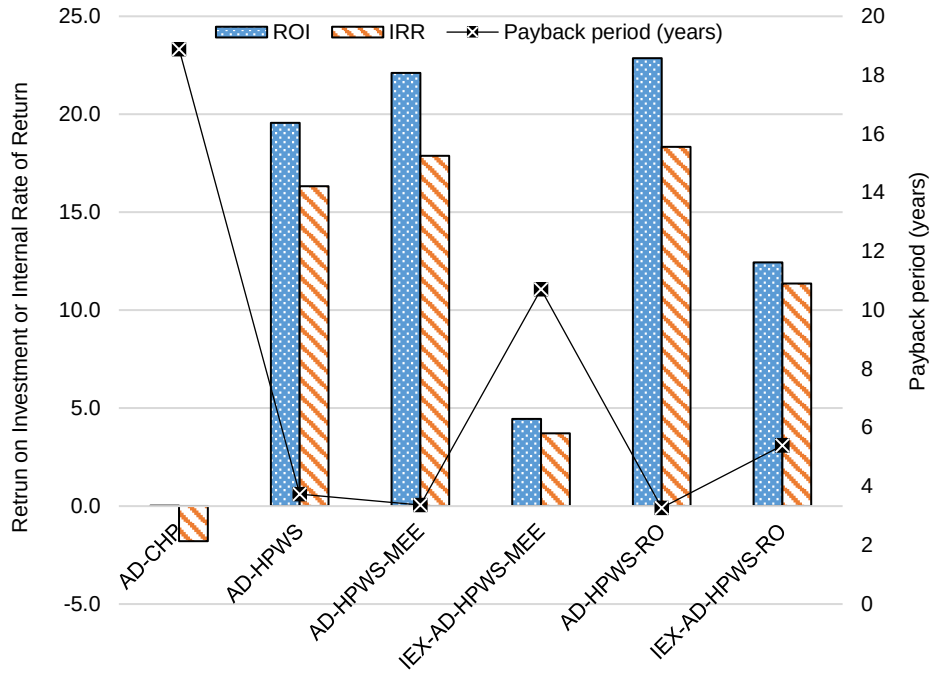

Figure 6.8: A comparison of profitability indicators (USD, 2016) between RO and MEE affiliated processes when considering the inclusion or absence of pre-treatment with HPWS as the biogas utilization process

Given that the extent of water recovery or quality is independent of the biogas utilization process, the water reuse initiatives and cost savings detailed in Section 5.3.3.3 and study 2 (section 6.3.1) were applied to the feasibility analysis in study 3 (Figure 6.8). An annual cost savings of $27 700 was achieved with upstream reintegration of 68 700 m^3/yr of RO permeate or MEE condensate water. This increased the ROI and IRR by approximately 2%. Alternatively, the water may be rerouted to the absorber in the HPWS process to affect a reduction in municipal water usage for the make up stream (CR figure) that is at 22 000 m^3/yr. A total cost savings of $8 000/yr is achieved and was incorporated in the techno-economics (Figure 6.8).

In terms of net profit, the AD-HPWS-RO process shows the best results. With an IRR of 18.3% (Figure 6.8), it is likely to return a net profit and match the average cost of capital. The AD-HPWS-MEE is the second best profitable alternative. A positive NPV (see Table C 2) as well as a high IRR of 17.9 % is predicted for this route.

6.3.3 Conclusions on Studies 2 and 3

The inclusion of reverse osmosis or multi-effect evaporation to the base case vinasse treatment process (AD-CHP) improves process sustainability and promotes value creation from the digestate through recovery of water. In addition, there is a significant increase in profitability with addition of either processes (RO or MEE) to the base case as more cost savings were accrued from the application of the resulting concentrates as fertilizer to replace potassium based synthetic fertilizer. At the recommended application rate of 3 tonnes/ha, the concentrates will improve crop yields (Christofoletti et al., 2013).

In the studies (2 and 3), it was observed that biogas utilization processes had no effect on the water quality or recovery as CHP and HPWS exclusively process the biogas. However, through investigating the substitution of CHP for HPWS in study 3, it was established that the

choice between the two biogas utilization processes significantly affected profitability in the presence of water recovery systems (RO or MEE). Due to the 50% reduction in capital costs achieved by using HPWS (Figure 6.8) instead of CHP (Figure 6.6), a significant increase in profitability was observed. Profitability indicators for the AD-HPWS-MEE/RO as well as IEX-AD-HPWS-MEE/RO (Figure 6.8) were over 100% higher compared to indicators for the CHP counterparts (Figure 6.6). This shows that the choice of biogas utilization is a decision criterion when developing vinasse treatment processes containing water recovery processes such as RO and MEE.

As described in Section 5.3, RO permeate and MEE condensate water contains volatile compounds that are not retained by the RO membranes or remain in the MEE concentrates. The VFAs essentially contaminate the water and further treatment is required for its domestic use. Water reuse initiatives within the ethanol distillery cooling towers and HPWS processes as make up water have been included in the techno-economics. When using CHP as the biogas utilization process, the recovered water from RO or MEE may be utilized as make up water in the cooling towers. Cost savings of up to $27 700/yr are realized. In the case of biogas upgrading, lower cost savings of up to $8 000 are accrued due to the lower water requirement relative to the upstream distillation. As the magnitude of the cost savings were comparatively lower than the operating costs, the knock-on effect on profitability of the flowsheets in Figure 6.5 and Figure 6.7 was not significant. This is evidenced by the 2% increase in profitability with incorporation of the cost savings initiatives. Despite this, water reuse was considered critical to the success of the project from a sustainability perspective due to the severity of the water shortage situation in South Africa.

6.4 Outcomes from the Decision-Making Tool

Through elucidation of the overall decision framework (Figure 6.1) using the studies in Table 6.1, outcomes in the form of decision criteria have been established. Pre-treatment processes were shown to remove potassium ion inhibitors thereby increasing performance and profitability of the flowsheets in Studies 1 and 2 (Sections 6.2.1 and 6.3.1). However, profitability decreased with implementation of pre-treatment in study 3 (Sections 6.3.2) due to increased combined operating costs of ion-exchange and water recovery.

The choice of biogas utilization processes is an important decision criterion in all the studies due to the difference in capital costs between CHP and HPWS. The comparisons between flowsheets that contained CHP and HPWS in all 3 studies (Figure 6.4, Figure 6.6 and Figure 6.8) confirmed that choosing to upgrade the biogas via HPWS to biomethane decreased capital costs and increased profitability.

The implementation of water recovery processes (Sections 6.3.1 and 6.3.2) yielded higher (170%) costs savings through the production of concentrates to be utilized as fertilizer as opposed to the AD effluent in the base case. This was due to increased K concentration in the AD effluent through the removal of water which allowed for its application as fertilizer to larger areas of agricultural land. It was noted that the water quality from RO and MEE was independent of the choice of pre-treatment and biogas utilization processes. Therefore, the cost savings accrued from upstream reuse of water are expected to remain similar with changing biogas utilizations or exclusion of pre-treatment.

7. Conclusions and Recommendations

Bioethanol production via fermentation processes results in the production of a voluminous liquid waste termed vinasse. It is typically generated at a rate of 12 to 15 litres per litre of ethanol. The production volume makes this wastewater difficult to handle as disposal into water bodies is restricted. Release into the municipal wastewater treatment system bears a cost which impacts profitability of the ethanol fermentation processes. Industrial processes have therefore been developed for vinasse treatment and potential recovery of valuable products such as biogas, water and salts. These include biological treatments for biogas production, physico-chemical processes for water and salt recovery, as well as biogas utilization systems for energy production.

This project therefore set out to develop integrated vinasse treatment flowsheets at a conceptual design level aimed at environmental protection and value creation through vinasse treatment and concomitant recovery of energy, salts and fit-for-purpose water. Having AD as the primary vinasse treatment process, it was hypothesized that incorporation of the raw vinasse pre-treatment processes and digested effluent post-treatment technologies will generate improved conversions, additional revenues, cost savings and have positive impact on the profitability of the flowsheets presented. This chapter therefore seeks to synthesise the important findings achieved during the execution of its main objectives which are as follows:

- Develop a simplified AD model on Aspen Plus through the adoption of existing AD frameworks in the literature and investigate its sensitivity to variations in the feed compositions and disturbances.
- Investigate the impact of the addition of pre- and post-treatments on the energy consumption, resource recovery and profitability. This will lead to the development of an economically preferred process route.
- Develop a tool that can assist and direct decision making when developing vinasse treatment processes.

7.1 Anaerobic Digestion Modelling and Base Case Process

The AD model was developed for the base case flowsheet using reactions, kinetic equations and parameters from the models by Angelidaki et al. (1993) and Batstone et al. (2002) (ADM1). It is a simplified model, with adequate complexity, that can predict AD results as well as the existing elaborate models. Important features of this model include: (1) substrate characterization into constituent carbohydrate, lipid and protein contents (2) 11 key reactions to represent the four AD steps (3) inhibition by ammonia, VFA and light metal cations. The characterization into the three constituents is a convention followed by previous AD modelling studies (Barrera et al., 2015; Batstone et al., 2002). This also aided in streamlining the simulation process. The model was benchmarked against existing simulations in the literature and reproduced experimental data for methane yields from published case studies detailing the AD of manure and municipal solid waste with an average error of 10%. As the model implements a simple and credible framework, it can be easily integrated into more complex flowsheets on Aspen Plus.

To ascertain its credibility and determine the relevant process thresholds, the developed AD model was subjected to compositional sensitivity analyses. Increasing inhibitory compound concentrations had a negative impact on the methane yield and biogas production in the AD

model. Declines in the methane yield by over 50% were observed with increasing K^+ ion concentrations in the raw vinasse feed. This indicated that performance improvements in the base case could be achieved through raw vinasse pre-treatment to remove inhibitory potassium ions to result in increased methane yields and higher electricity production from the CHP system. To determine the loading rate thresholds in the AD reactor, an OLR sensitivity was conducted. Increasing the organic loading rate increased the available substrate for uptake and consequently the methane yield up to a maximum of 86 L-CH_4/kgVS_{added} at an OLR of 7 kgCOD/m^3.day. Due to a build up of inhibitory compounds, there was decline in performance as evidenced by the subsequent decline in methane yields at loading rates above 8 kgCOD/m^3.day.

Given the close agreement of the model results and literature data as well as the observed trends in sensitivity that were similar to literature findings, the developed AD model was deemed fit for further simulation of base case process. The base case consisted of a vinasse AD reactor and CHP system (Jenbacher gas engine) for electricity production from the biogas. To better simulate industrial processes, a reactor size of 2000 m^3 and OLR of 25 kgCOD/m^3.day were selected. At this capacity, a methane yield of 48.5 L-CH_4/kgVS and electrical production capacity of 410 kW were achieved. Techno-economic analyses conducted using published costing heuristics, OOM estimations and reported manufacturer quotes showed that the base case was not profitable as evidenced by the 0% ROI and negative NPV. Although not profitable, treatment of the raw vinasse effluent using the base case process should be considered as it leads the reduction of wastewater strength while enhancing environmental protection. Moreover, choosing to release this stream as an industrial effluent to the municipality bears a cost of $80 700/yr.

7.2 Pre-, Post-Treatment and Biogas Utilization Process Additions to the Base Case

Given the low carbon conversion to methane and the profitability of the base case, addition of pre- and post-treatment processes was explored to extend base case functionality, increase resource recovery and enhance profitability. For pre-treatment, a strong acid cation exchange system was chosen as it was less energy intensive, and more selective towards potassium ions compared to direct ozonation (using O_3), electrodialysis and reverse osmosis. Implementation of the ion exchange system to the flowsheet resulted in 30% higher in methane yields during AD owing to the removal (70%) of inhibitory K^+ compounds which brought about higher revenues from electricity sales and improved effluent quality. This positively influenced profitability of the IEX-AD-CHP route as evidenced by the ROI and IRR that were comparatively 200% higher than base case (AD-CHP) profitability indicators.

While the CHP in the base case enhanced energy generation, the capital costs of the chosen Jenbacher spark engine were high. Biogas upgrading, an equally effective technology, through high pressure water scrubbing was therefore explored as a cost-effective substitute to produce biomethane. Compared to the base case, the AD-HPWS system increased energy output (MWh/yr) due to increased energy content in biomethane relative to biogas. As equipment costs for HPWS were 50% cheaper compared to CHP, profitability of the AD-HPWS route was also significantly higher (>200%) relative to the base case.

To improve process sustainability and increase cost savings through water reuse, addition of RO and MEE were investigated for the recovery of water from the liquid digestate. Through

upstream re-integration of RO permeates or MEE condensate water, annual cost savings of up to $27 700 were achieved. Despite the cost savings and an improved process in terms of water efficiency, profitability remained low with incorporation of RO or MEE processes to the base case. This was evidenced by the profitability indicators such as the IRR that remained lower than the average cost of capital (15%). However, it was concluded that the water recovery systems should be considered as process sustainability is key in securing the future success of the vinasse treatment project considering the increasing abundance of water-scarce regions and associated the looming water shortages in provinces such as the Eastern Cape and Western Cape in South Africa.

The individual incorporation of pre-treatments, post-treatments and biogas utilizations had varying degrees of economic benefit to the base case. It was necessary to investigate the addition of combined pre- and post-treatment variations so as to uncouple existing interacting effects. Through this, different processing routes were analysed on the basis of performance and economics which ultimately led to the formulation of a visual decision making tool intended to assist in the development of vinasse treatment processes in a South African context.

7.3 Decision-Making Tool

The decision-making tool sought to provide in-depth comparisons between 12 vinasse treatment routes resulting from various combinations of pre- and post-treatment options. To aid in this analysis, a visual framework with decision points was developed to facilitate the step by step development of distinct vinasse treatment routes whilst highlighting the benefits and demerits of each process addition (pre- or post-treatment). Through this, important decision criteria were identified to aid in the future development of vinasse treatment routes.

Given the positive impact on performance and economics of incorporating pre-treatment (IEX) to the base case (AD-CHP) and other variations for water re-use (AD-CHP-RO/MEE), it was concluded that the presence of potassium ions was a key decision criterion in the development of vinasse treatment routes. However, this is dependent on the K^+ concentration in the vinasse feed given the inhibition threshold of 11.6 g/L. Although pre-treatment increased conversion of organic carbon and its removal from the liquid stream, methane yields and electricity production, profitability was low and net profits unlikely as the IRR remained below the average cost of capital (15%) for the IEX-AD-CHP, IEX-AD-CHP-RO and IEX-AD-CHP-MEE routes over a 20 year project lifetime. This was due to the high cost of CHP equipment which was compounded by the operating costs of the additional processes over the project lifetime. As biogas upgrading equipment (HPWS) was cheaper, electing to substitute CHP for HPWS not only increased energy output but also increased profitability as evidenced by the higher ROI and IRR of the AD-HPWS, AD-HPWS-RO/MEE compared to the counterparts with CHP. The choice of biogas utilization was therefore concluded to be a decision criterion, particularly affecting profitability of the developed vinasse treatment routes.

Adding water recovery processes (RO and MEE) to the base case and its variations was observed to contribute significantly to the cost savings in terms of potassium fertilizer purchase. Relative to the base case AD effluent, utilization of RO or MEE concentrates secured 170% higher cost savings as the resulting concentrates with increased K content could be applied over larger areas of agricultural land. Due to the presence of volatile acids, the RO permeate water and MEE condensates were deemed fit for upstream re-use as cooling water in the ethanol distillation process. Considering the industrial municipal water tariff (R5/kL), re-integration of the water in all RO and MEE affiliated processes resulted in a cost

savings of $27 700. From a cost perspective, capital costs of the MEE process were higher than RO with the opposite applying for the operating costs. From this analysis, it was concluded that the recovery of concentrates from vinasse was a key decision criterion when looking to increase profitability and that water recovery from vinasse is necessary to enhance process sustainability. However, given that bio-methanated vinasse often has a high suspended solids content, elaborate models for MEE and RO featuring both solute and solvent mass transfer kinetics are required to reduce the uncertainty in the water recoveries and reported cost savings estimates. In this research, availability of high pressure steam (for MEE) from the upstream sugar refining process was assumed. In scenarios where fresh high pressure steam is required, validation of the steam costs ($/ton) against industry trends is key as this may affect feasibility of MEE processes due to high steam costs.

7.4 Recommendations

7.4.1 Vinasse Treatment Routes

Based on the profitability analyses in the decision-making tool, it is recommended that the vinasse treatment process include an anaerobic digester coupled with a high-pressure water scrubbing system for biomethane production and reverse osmosis process for water recovery. In addition to the increased energy output from biomethane production, cost savings on fertilizer purchase and RO permeate water re-use will be achieved to increase both process profitability and sustainability. As pre-treatment is missing in the recommended route (AD-CHP-RO), inhibition by K^+ ions may lead to the low conversion of organics in AD. There is therefore a need to develop cost effective pre-treatment processes that reduce the potassium loading in vinasse. One technique could be through dilution to ensure low potassium as well as COD concentrations.

This route (AD-Upgrade-RO) is projected to have a 22.9% rate of return and a net present value of $540 000 after a 20-year project lifetime. Moreover, there is a growing market in SA for biomethane as a vehicular fuel which potentially secures business continuity as the project will fill a crucial gap in the market through provision of a renewable energy source.

7.4.2 Further Research

Opportunities for further research based on this body of work exist especially in the anaerobic digestion modelling and techno-economic evaluation areas. While the AD model reproduced experimental data relatively well, it is necessary to extend its functionality to aspects such as pH prediction and dynamic modelling of AD systems on laboratory and pilot scales. Developing ionic speciation routines on Aspen Plus by adding weak acid-base chemistry to the reaction blocks will provide hydrogen ion concentrations that can be utilized by FORTRAN routines for pH calculations. This will facilitate investigations of the interplay between free ammonia, NH_4^+ and VFA concentrations in AD and their role as inhibitors to methanogenic activity.

In addition, as kinetics are originally derived for mesophiles, there is a need to refine kinetic parameters based on thermophiles through experimentation and subsequent validation. Further work on inhibitors present in vinasse is required to give insight into adequate pre-treatment processes their removal which will potentially increase conversion of organic material to methane. Given the presence of H_2S in biogas streams, there is a need to include reactions and associated kinetics of action by SRBs. However, this may not lead to significant changes in CAPEX/OPEX estimates as the HPWS method considered in this research

ensures removal of both H_2S and CO_2. A review of vinasse based AD plants in Southern Africa is required. This will promote the use of industry based assumptions concerning organic loading rates that are reported to be significantly lower (1-3 kgCOD/m^3.day) compared to reported values in high rate anaerobic systems in South America and India (25 kgCOD/m^3.day).

Concerning the approach to techno-economic analysis, it is recommended that manufacturer quotes from suppliers within South Africa be used more often as opposed to costing heuristics in the literature. This is expected to increase the accuracy of the capital and operating cost estimations.

8. References

Ahmed, O., Sulieman, A.M.E., Elhardallou, S.B., 2013. Physicochemical , Chemical and Microbiological Characteristics of Vinasse , A By-product from Ethanol Industry 3, 80–83. https://doi.org/10.5923/j.ajb.20130303.03

Albanez, R., Chiaranda, B.C., Ferreira, R.G., Frana, A.L.P., Honrio, C.D., Rodrigues, J.A.D., Ratusznei, S.M., Zaiat, M., 2016. Anaerobic Biological Treatment of Vinasse for Environmental Compliance and Methane Production. Appl. Biochem. Biotechnol. 178, 21–43. https://doi.org/10.1007/s12010-015-1856-z

Alibaba, 2017. Potassium Sulphate Pricing [WWW Document]. URL https://www.alibaba.com/showroom/potassium-sulfate.html (accessed 7.25.17).

Amigun, B., Blottnitz, H. Von, 2007. Investigation of scale economies for African biogas installations. Energy Convers. Manag. 48, 3090–3094. https://doi.org/10.1016/j.enconman.2007.05.009

Amigun, B., von Blottnitz, H., 2009. Capital cost prediction for biogas installations in Africa: Lang factor approach. Environ. Prog. Sustain. Energy 28, 134–142. https://doi.org/10.1002/ep.10341

Amigun, B., Von Blottnitz, H., 2010. Capacity-cost and location-cost analyses for biogas plants in Africa. Resour. Conserv. Recycl. 55, 63–73. https://doi.org/10.1016/j.resconrec.2010.07.004

Ang, W.L., Nordin, D., Mohammad, A.W., Benamor, A., Hilal, N., 2017. Effect of membrane performance including fouling on cost optimization in brackish water desalination process. Chem. Eng. Res. Des. 117, 401–413. https://doi.org/10.1016/j.cherd.2016.10.041

Angelidaki, I., Ellegaard, L., Ahring, B.K., 1999. A comprehensive model of anaerobic bioconversion of complex substrates to biogas. Biotechnol. Bioeng. 63, 363–372.

Angelidaki, I., Ellegaard, L., Ahring, B.K., 1993. A mathematical model for dynamic simulation of anaerobic digestion of complex substrates: Focusing on ammonia inhibition. Biotechnol. Bioeng. 42, 159–166. https://doi.org/10.1002/bit.260420203

Aquino, S., Pires, E.C., 2016. Assessment of ozone as a pretreatment to improve anaerobic digestion of vinasse. Brazilian J. Chem. Eng. 33, 279–285. https://doi.org/10.1590/0104-6632.20160332s20140141

Aspen Technology, I., 2000. Aspen Plus ® User Guide. Aspen Technol. Inc. 936.

Axelsson, L., Franzén, M., Ostwald, M., Berndes, G., Lakshmi, G., Ravindranath, N.H., 2012. Perspective: Jatropha cultivation in southern India: Assessing farmers' experiences. Biofuels, Bioprod. Biorefining 6, 246–256. https://doi.org/10.1002/bbb

Balaban, A.T., 2000. Process Design Principles: Synthesis and Analysis. J. Chem. Inf. Comput. Sci. 40, 882–883.

Barrera, E.L., Spanjers, H., Solon, K., Amerlinck, Y., Nopens, I., Dewulf, J., 2015. Modeling the anaerobic digestion of cane-molasses vinasse: Extension of the Anaerobic Digestion Model No. 1 (ADM1) with sulfate reduction for a very high strength and sulfate rich wastewater. Water Res. 71, 42–54. https://doi.org/10.1016/j.watres.2014.12.026

Barros, V.G. de, Duda, R.M., Oliveira, R.A. de, 2016. Biomethane production from vinasse in upflow anaerobic sludge blanket reactors inoculated with granular sludge. Brazilian J. Microbiol. 47, 628–639. https://doi.org/10.1016/j.bjm.2016.04.021

Batstone, D.J., Keller, J., Angelidaki, I., Kalyuzhnyi, S. V, Pavlostathis, S.G., Rozzi, A., Sanders, W.T.M., Siegrist, H., Vavilin, V.A., 2002. The IWA anaerobic digestion model

no 1 (ADM1). Water Sci. Technol. 45, 65–73.

Bick, A., Gillerman, L., Manor, Y., Oron, G., 2012. Economic assessment of an integrated membrane system for secondary effluent polishing for unrestricted reuse. Water (Switzerland) 4, 219–236. https://doi.org/10.3390/w4010219

Bischof-Niemz, T., Fourie, R., 2016. Cost of new power generators in South Africa Comparative analysis based on recent IPP announcements. pp. 1–9.

Budiyono, I.N., Widiasa, I.N., Johari, S., Sunarso, 2011. Study on Slaughterhouse Wastes Potency and Characteristic for Biogas Production. Internat. J. Waste Resourcs 1, 4–7.

Butt, F.H., Rahman, F., Baduruthamal, U., 1997. Hollow fine fiber vs. spiral-wound reverse osmosis desalination membranes part 2: Membrane autopsy. Desalination 109, 83–94. https://doi.org/10.1016/S0011-9164(97)00054-4

Carvalho, T.C. De, 2011. Reduction of vinasse volume by the evaporation process. Brazilian Congr. Mech. Eng.

Cengel, Y.A., Boles, M.A., 2002. Thermodyamics an engineering approach. Energy 1, 51. https://doi.org/10.1017/CBO9781107415324.004

Chandra, R., Bharagava, R.N., Rai, V., 2008. Melanoidins as major colourant in sugarcane molasses based distillery effluent and its degradation. Bioresour. Technol. 99, 4648–4660. https://doi.org/10.1016/j.biortech.2007.09.057

Chaudhari, L.B., Murthy, Z.V.P., 2009. Treatment of Distillery Spent Wash By Combined Uf and Ro Processes. Ground Water 11, 235–240.

Chen, Y., Cheng, J.J., Creamer, K.S., 2008. Inhibition of anaerobic digestion process: A review. Bioresour. Technol. 99, 4044–4064. https://doi.org/10.1016/j.biortech.2007.01.057

Chen, Y.R., Hashimoto, A.G., 1980. Substrate utilization kinetic model for biological treatment process. Biotechnol. Bioeng. 22, 2081–2095.

Christofoletti, C.A., Escher, J.P., Correia, J.E., Marinho, J.F.U., Fontanetti, C.S., 2013. Sugarcane vinasse: Environmental implications of its use. Waste Manag. 33, 2752–2761. https://doi.org/10.1016/j.wasman.2013.09.005

Contois, D.E., 1959. Kinetics of bacterial growth: relationship between population density and specific growth rate of continuous cultures. Microbiology 21, 40–50.

Cozma, P., Ghinea, C., Mămăligă, I., Wukovits, W., Friedl, A., Gavrilescu, M., 2013a. Environmental Impact Assessment of High Pressure Water Scrubbing Biogas Upgrading Technology. CLEAN – Soil, Air, Water 41, 917–927. https://doi.org/10.1002/clen.201200303

Cozma, P., Wukovits, W., Mamaliga, I., Friedl, A., Gavrilescu, M., 2014. Modeling and simulation of high pressure water scrubbing technology applied for biogas upgrading. Clean Technol. Environ. Policy 17, 373–391. https://doi.org/10.1007/s10098-014-0787-7

Cozma, P., Wukovits, W., Mămăligă, I., Friedl, A., Gavrilescu, M., 2013b. Analysis and modelling of the solubility of biogas components in water for physical absorption processes. Environ. Eng. Manag. J. 12, 147–162.

DAFF, 2015. South African Fertilizers Market Analysis Report.

Darrow, K., Tidball, R., Wang, J., Hampson, A., 2015. Catalog of CHP Technologies 1, 131.

Dave, S.K., Rotliwala, Y.C., Shah, J.A., 2012. Distillery Spent wash treatment with the use of Nanofiltration followed by Reverse osmosis process 12, 975–6744.

Davis, R., Tao, L., Tan, E.C.D., Biddy, M.J., Beckham, G.T., Scarlata, C., Jacobson, J.,

Cafferty, K., Ross, J., Lukas, J., Knorr, D., Schoen, P., 2013. Process Design and Economics for the Conversion of Lignocellulosic Biomass to Hydrocarbons: Dilute-Acid and Enzymatic Deconstruction of Biomass to Sugars and Biological Conversion of Sugars to Hydrocarbons. https://doi.org/10.2172/1107470

Decloux, M., Bories, A., Lewandowski, R., Fargues, C., Mersad, A., Lameloise, M.L., Bonnet, F., Dherbecourt, B., Osuna, L.N., 2002. Interest of electrodialysis to reduce potassium level in vinasses. Preliminary experiments. Desalination 146, 393–398. https://doi.org/10.1016/S0011-9164(02)00520-9

Djalma Nunes Ferraz Junior, A., Koyama, M.H., de Araujo Junior, M.M., Zaiat, M., 2016. Thermophilic anaerobic digestion of raw sugarcane vinasse. Renew. Energy 89, 245–252. https://doi.org/10.1016/j.renene.2015.11.064

Djalma Nunes Ferraz Júnior, A., Koyama, M.H., de Araújo Júnior, M.M., Zaiat, M., 2016. Thermophilic anaerobic digestion of raw sugarcane vinasse. Renew. Energy 89, 245–252. https://doi.org/10.1016/j.renene.2015.11.064

Donoso-Bravo, A., Mailier, J., Martin, C., Rodríguez, J., Aceves-Lara, C.A., Wouwer, A. Vande, 2011. Model selection, identification and validation in anaerobic digestion: A review. Water Res. 45, 5347–5364. https://doi.org/10.1016/j.watres.2011.08.059

dos Reis, C.M., Carosia, M.F., Sakamoto, I.K., Amâncio Varesche, M.B., Silva, E.L., 2015. Evaluation of hydrogen and methane production from sugarcane vinasse in an anaerobic fluidized bed reactor. Int. J. Hydrogen Energy 40, 8498–8509. https://doi.org/10.1016/j.ijhydene.2015.04.136

EcoMetrix Africa, 2013. Facilitation of Large Scale Uptake of Alternative Transport Fuels in South Africa - The case of Biogas.

Eliyan, C., 2007. Anaerobic Digestion of Municipal Solid Waste in Thermophilic Continuous Operation. Asian Institute of Technology.

EPASA, 2013. Ethanol Producers Association of South Africa [WWW Document]. URL http://www.epasa.org.za/about-us.html (accessed 12.2.17).

España-Gamboa, E., Mijangos-Cortes, J., Barahona-Perez, L., Dominguez-Maldonado, J., Hernández-Zarate, G., Alzate-Gaviria, L., 2011. Vinasses: characterization and treatments. Waste Manag. Res. 29, 1235–1250. https://doi.org/10.1177/0734242X10387313

España-Gamboa, E., Mijangos-Cortés, J.O., Hernández-Zárate, G., Maldonado, J.A.D., Alzate-Gaviria, L.M., 2012. Methane production by treating vinasses from hydrous ethanol using a modified UASB reactor. Biotechnol. Biofuels 5, 82–87. https://doi.org/10.1186/1754-6834-5-82

Ethekwini Water and Sanitation, 2018. ETHEKWINI WATER AND SANITATION. TARIFF : Sewerage Disposal User Charge (2017/ 2018).

Forgács, G., Pourbafrani, M., Niklasson, C., Taherzadeh, M.J., Hováth, I.S., 2012. Methane production from citrus wastes: process development and cost estimation. J. Chem. Technol. Biotechnol. 87, 250–255. https://doi.org/10.1002/jctb.2707

Francisca Kalavathi, D., Uma, L., Subramanian, G., 2001. Degradation and metabolization of the pigment - Melanoidin in distillery effluent by the marine cyanobacterium Oscillatoria boryana BDU 92181. Enzyme Microb. Technol. 29, 246–251. https://doi.org/10.1016/S0141-0229(01)00383-0

Francois, J., Abdelouahed, L., Mauviel, G., Patisson, F., Mirgaux, O., Rogaume, C., Rogaume, Y., Feidt, M., Dufour, A., Haye, D., Blanc, M., Universite, N., 2013. Detailed process modeling of a wood gasification combined heat and power plant. Biomass and Bioenergy 51, 68–82. https://doi.org/10.1016/j.biombioe.2013.01.004

Fuess, L.T., de Araujo Junior, M.M., Garcia, M.L., Zaiat, M., 2017. Designing full-scale biodigestion plants for the treatment of vinasse in sugarcane biorefineries: How phase separation and alkalinization impact biogas and electricity production costs? Chem. Eng. Res. Des. 119, 209–220. https://doi.org/10.1016/j.cherd.2017.01.023

Fuess, L.T., Zaiat, M., 2017. Economics of anaerobic digestion for processing sugarcane vinasse: Applying sensitivity analysis to increase process profitability in diversified biogas applications. Process Saf. Environ. Prot. 1–11. https://doi.org/10.1016/j.psep.2017.08.007

Fujita, M., Scharer, J.M., Moo-Young, M., 1980. Effect of corn stover addition on the anaerobic digestion of swine manure. Agric. Wastes 2, 177–184. https://doi.org/10.1016/0141-4607(80)90014-1

Garud, R.M., Kore, S. V, Kore, V.S., Kulkarni, G.S., 2011. A Short Review on Process and Applications of Reverse Osmosis. Univers. J. Environ. Res. Technol. 1, 233–238. https://doi.org/10.1016/j.desal.2010.09.001

General Electric, 2008. Jenbacher Engines 2002, 8–9.

Georgiadis, M.C., 2012. CAPE Software Tools for Modelling and Simulation. Encycl. Life Support Syst. III.

Griggs, D., Stafford-Smith, M., Gaffney, O., Rockström, J., Öhman, M.C., Shyamsundar, P., Steffen, W., Glaser, G., Kanie, N., Noble, I., 2013. Policy: Sustainable development goals for people and planet. Nature 495, 305–307.

Guerreiro, L.F., Rodrigues, C.S.D., Duda, R.M., de Oliveira, R.A., Boaventura, R.A.R., Madeira, L.M., 2016. Treatment of sugarcane vinasse by combination of coagulation/flocculation and Fenton's oxidation. J. Environ. Manage. 181, 237–248. https://doi.org/10.1016/j.jenvman.2016.06.027

Hamza, R.A., Iorhemen, O.T., Tay, J.H., 2016. Advances in biological systems for the treatment of high-strength wastewater. J. Water Process Eng. 10, 128–142. https://doi.org/10.1016/j.jwpe.2016.02.008

Hierholtzer, A., Akunna, J.C., 2014. Modelling start-up performance of anaerobic digestion of saline-rich macro-algae. Water Sci. Technol. 69, 2059–2065. https://doi.org/10.2166/wst.2014.100

Hill, D.T., 1982. A Comprehensive Dynamic Model for Animal Waste Methanogenesis. Trans. ASAE 25, 1374. https://doi.org/https://doi.org/10.13031/2013.33730

Ikumi, D.S., 2011. The Development of a Three Phase Plant-Wide Mathematical Model for Sewage Treatment. University of Cape Town.

Ikumi, D.S., Brouckaert, C.J., Ekama, G.A., 2011. A 3 phase anaerobic digestion model, in: Proceedings of the 8th IWA International Symposium on Systems Analysis and Integrated Assessment in Water Management (Watermatex2011), 20–22 June.

Illovo Sugar, 2013. Integrated Report - 2013.

INTELLIGEN, I., 2005. SuperPro Designer® user guide 1–516.

Jain, N., Minocha, A.K., Verma, C.L., 2002. Degradation of predigested distillery effluent by isolated bacterial strains. Indian J. Exp. Biol. 40, 101–105.

Janke, L., Leite, A., Nikolausz, M., Schmidt, T., Liebetrau, J., Nelles, M., Stinner, W., 2015. Biogas Production from Sugarcane Waste: Assessment on Kinetic Challenges for Process Designing. Int. J. Mol. Sci. 16, 20685–703. https://doi.org/10.3390/ijms160920685

Kapdi, S.S., Vijay, V.K., Rajesh, S.K., Prasad, R., 2005. Biogas scrubbing, compression and

storage: Perspective and prospectus in Indian context. Renew. Energy 30, 1195–1202. https://doi.org/10.1016/j.renene.2004.09.012

Kasikamphaiboon, P., Chungsiriporn, J., Bunyakan, C., Wiyaratn, W., 2013. Simultaneous removal of CO2 and H2S using MEA solution in a packed column absorber for biogas upgrading. Songklanakarin J. Sci. Technol. 35, 683–691. https://doi.org/10.1016/j.energy.2010.04.014

Kim, D.H., 2011. A review of desalting process techniques and economic analysis of the recovery of salts from retentates. Desalination 270, 1–8. https://doi.org/10.1016/j.desal.2010.12.041

Koch, K., Lübken, M., Gehring, T., Wichern, M., Horn, H., 2010. Biogas from grass silage - Measurements and modeling with ADM1. Bioresour. Technol. 101, 8158–8165. https://doi.org/10.1016/j.biortech.2010.06.009

Kugelman, I.J., Mccarty, P.L., 1965. Cation toxicity and stimulation in anaerobic waste treatment. Water Pollut. Control Fed. 37, 97–116. https://doi.org/10.2307/25035219

Lameloise, M.-L., Gavach, M., Bouix, M., Fargues, C., 2015. Combining reverse osmosis and ion-exchange allows beet distillery condensates to be recycled as fermentable dilution water. Desalination 363, 75–81. https://doi.org/10.1016/j.desal.2014.09.036

Lauwers, J., Appels, L., Thompson, I.P., Degrève, J., Van Impe, J.F., Dewil, R., 2013. Mathematical modelling of anaerobic digestion of biomass and waste: Power and limitations. Prog. Energy Combust. Sci. 39, 383–402. https://doi.org/10.1016/j.pecs.2013.03.003

Lee, D.H., 2017. Evaluation the financial feasibility of biogas upgrading to biomethane, heat, CHP and AwR. Int. J. Hydrogen Energy 42, 27718–27731. https://doi.org/10.1016/j.ijhydene.2017.07.030

Leme, R.M., Seabra, J.E.A., 2017. Technical-economic assessment of different biogas upgrading routes from vinasse anaerobic digestion in the Brazilian bioethanol industry. Energy 119, 754–766. https://doi.org/10.1016/j.energy.2016.11.029

Lewis, A.E., Khodabocus, F., Dhokun, V., Khalife, M., 2010. Thermodynamic simulation and evaluation of sugar refinery evaporators using a steady state modelling approach. Appl. Therm. Eng. 30, 2180–2186. https://doi.org/10.1016/j.applthermaleng.2010.05.031

Lier, J.B. Van, Mahmoud, N., Zeeman, G., 2008. Anaerobic Wastewater Treatment, Biological Wastewater Treatment : Principles, Modelling and Design. https://doi.org/10.1021/es00154a002

Liu, Z., Stromberg, D., Liu, X., Liao, W., Liu, Y., 2015. A new multiple-stage electrocoagulation process on anaerobic digestion effluent to simultaneously reclaim water and clean up biogas. J. Hazard. Mater. 285, 483–490. https://doi.org/10.1016/j.jhazmat.2014.10.009

Lokshina, L.Y., Vavilin, V.A., Kettunen, R.H., Rintala, J.A., Holliger, C., Nozhevnikova, A.N., 2001. Evaluation of kinetic coefficients using integrated Monod and Haldane models for low-temperature acetoclastic methanogenesis. Water Res. 35, 2913–2922.

Loutatidou, S., Arafat, H.A., 2015. Techno-economic analysis of MED and RO desalination powered by low-enthalpy geothermal energy. Desalination 365, 277–292. https://doi.org/10.1016/j.desal.2015.03.010

Magnusson, H., 2011. Process Simulation in Aspen Plus of an Integrated Ethanol and CHP plant. Univ. UMEA. Universitet UMEA.

Malakahmad, A., Basri, N.E.A., Zain, S.M., 2012. Design and Process Simulation of a Small Scale Waste-To-Energy Bioreactor. J. Appl. Sci. 12, 2586–2591. https://doi.org/10.3923/jas.2012.2586.2591

Masebinu, S.O., Aboyade, A.O., Muzenda, E., 2015. Economic analysis of biogas upgrading and utilization as vehicular fuel in South Africa. Lect. Notes Eng. Comput. Sci. 2220.

Masebinu, S.O., Aboyade, A.O., Muzenda, E., 2014. Operational Study and Simulation of a Biogas Upgrading Plant. Proc. World Congr. Eng. II, 0–6. https://doi.org/10.13140/2.1.3518.7201

Meireles, M.A.A., 2008. Extracting bioactive compounds for food products: theory and applications. CRC press.

Mignard, D., 2014. Correlating the chemical engineering plant cost index with macro-economic indicators. Chem. Eng. Res. Des. 92, 285–294. https://doi.org/10.1016/j.cherd.2013.07.022

Mohammed, M., Egyir, I.S., Donkor, A.K., Amoah, P., Nyarko, S., Boateng, K.K., Ziwu, C., 2016. Feasibility study for biogas integration into waste treatment plants in Ghana. Egypt. J. Pet. 26, 695–703. https://doi.org/10.1016/j.ejpe.2016.10.004

Mohana, S., Acharya, B.K., Madamwar, D., 2008. Distillery spent wash: Treatment technologies and potential applications. Bioresour. Technol. 99, 4621–4626. https://doi.org/10.1016/j.biortech.2007.06.060

Monod, J., 1949. The Growth of Bacterial Cultures. Annu. Rev. Microbiol. 3, 371–394. https://doi.org/10.1146/annurev.mi.03.100149.002103

Moraes, B.S., Junqueira, T.L., Pavanello, L.G., Cavalett, O., Mantelatto, P.E., Bonomi, A., Zaiat, M., 2014. Anaerobic digestion of vinasse from sugarcane biorefineries in Brazil from energy, environmental, and economic perspectives: Profit or expense? Appl. Energy 113, 825–835. https://doi.org/10.1016/j.apenergy.2013.07.018

Moraes, B.S., Zaiat, M., Bonomi, A., 2015. Anaerobic digestion of vinasse from sugarcane ethanol production in Brazil: Challenges and perspectives. Renew. Sustain. Energy Rev. 44, 888–903. https://doi.org/10.1016/j.rser.2015.01.023

Nataraj, S.K., Hosamani, K.M., Aminabhavi, T.M., 2006. Distillery wastewater treatment by the membrane-based nanofiltration and reverse osmosis processes. Water Res. 40, 2349–2356. https://doi.org/10.1016/j.watres.2006.04.022

NERSA, 2011. NERSA Consultation Paper Review of Renewable Energy Feed - In Tariffs.

Nguyen, H.H., 2014. Modelling of food waste digestion using ADM1 integrated with Aspen Plus. University of Southampton.

Oh, H.J., Hwang, T.M., Lee, S., 2009. A simplified simulation model of RO systems for seawater desalination. Desalination 238, 128–139. https://doi.org/10.1016/j.desal.2008.01.043

Pant, D., Adholeya, A., 2007a. Identification, ligninolytic enzyme activity and decolorization potential of two fungi isolated from a distillery effluent contaminated site. Water. Air. Soil Pollut. 183, 165–176. https://doi.org/10.1007/s11270-007-9366-4

Pant, D., Adholeya, A., 2007b. Biological approaches for treatment of distillery wastewater: A review. Bioresour. Technol. 98, 2321–2334. https://doi.org/10.1016/j.biortech.2006.09.027

Payscale SA, 2017. Salary Data & Career Research Center (South Africa) [WWW Document]. URL http://tinyurl.com/lfjjz3x

Peris, R.S., 2011. Biogas Process Simulation using Aspen Plus. Dep. Chem. Eng. Biotechnol. Environ. Technol. Syddansk Univ. Syddanks University.

Pöschl, M., Ward, S., Owende, P., 2010. Evaluation of energy efficiency of various biogas production and utilization pathways. Appl. Energy 87, 3305–3321.

https://doi.org/10.1016/j.apenergy.2010.05.011

Rajendran, K., Kankanala, H.R., Lundin, M., Taherzadeh, M.J., 2014. A novel process simulation model (PSM) for anaerobic digestion using Aspen Plus. Bioresour. Technol. 168, 7–13. https://doi.org/10.1016/j.biortech.2014.01.051

Ramsay, I.R., Pullammanappallil, P.C., 2001. Protein degradation during anaerobic wastewater treatment: Derivation of stoichiometry. Biodegradation 12, 247–257. https://doi.org/10.1023/A:1013116728817

Rein, P., 2007. Cane Sugar Engineering.

Rein, P., Turner, P., Mathias, K., 2011. Good Management Practices For The Sugar Cane Industry. Johannesburg.

Rodrigues Reis, C.E., Hu, B., 2017. Vinasse from Sugarcane Ethanol Production: Better Treatment or Better Utilization? Front. Energy Res. 5, 7. https://doi.org/10.3389/fenrg.2017.00007

Roels, J.A., 1980. Application of macroscopic principles to microbial metabolism. Biotechnol. Bioeng. 22, 2457–2514. https://doi.org/10.1002/bit.260221202

Romli, M., Keller, J., Lee, P.L., Greenfield, P.F., 1995. Model prediction and verification of a two-stage high-rate anaerobic wastewater treatment system subjected to shock loads. Process Saf. Environ. Prot. 73, 151–154.

Ryan, D., Gadd, A., Kavanagh, J., Barton, G.W., 2009. Integrated biorefinery wastewater design. Chem. Eng. Res. Des. 87, 1261–1268. https://doi.org/10.1016/j.cherd.2009.04.016

Ryckebosch, E., Drouillon, M., Vervaeren, H., 2011. Techniques for transformation of biogas to biomethane. Biomass and Bioenergy 35, 1633–1645. https://doi.org/10.1016/j.biombioe.2011.02.033

Saha, N.K., Balakrishnan, M., Batra, V.S., 2005. Improving industrial water use: Case study for an Indian distillery. Resour. Conserv. Recycl. 43, 163–174. https://doi.org/10.1016/j.resconrec.2004.04.016

Satyawali, Y., Balakrishnan, M., 2008. Wastewater treatment in molasses-based alcohol distilleries for COD and color removal: A review. J. Environ. Manage. 86, 481–497. https://doi.org/10.1016/j.jenvman.2006.12.024

Scull, I., Savón, L., Gutiérrez, O., Valiño, E., Orta, I., Mora, P.O., Orta, H., Ramos, Y., Molineda, A., Coto, G., Noda, A., 2012. Physic-chemical composition of concentrated vinasse for their assessment in animal diets. Cuba. J. Agric. Sci. 46, 385–389.

Seadi, T.A., Rutz, D., Prassl, H., Köttner, M., Finsterwalder, T., Volk, S., Janssen, R., 2008. Biogas Handbook, Igarss 2014. https://doi.org/10.1533/9780857097415.1.85

Seider, W.D., Seader, J.D., Lewin, D.R., 2003. Product and Process Design Principles - Synthesis, Analysis, and Evaluation.

Sevella, B., Bertalan, G., 2000. Development of a MATLAB based bioprocess simulation tool. Bioprocess Eng. 23, 621–626. https://doi.org/10.1007/s004490000211

Shanklin, T., Roper, K., Yegneswaran, P.K., Marten, M.R., 2001. Selection of bioprocess simulation software for industrial applications. Biotechnol. Bioeng. 72, 483–489. https://doi.org/10.1002/1097-0290(20010220)72:4<483::AID-BIT1010>3.0.CO;2-3

Shayegan, J., Pazouki, M., Afshari, A., 2005. Continuous decolorization of anaerobically digested distillery wastewater. Process Biochem. 40, 1323–1329. https://doi.org/10.1016/j.procbio.2004.06.009

Shivajirao, P.A., 2012. Treatment of Distillery Waterwater using Membrane Technologies 1,

275–283.

Siles, J.A., García-García, I., Martín, A., Martín, M.A., 2011. Integrated ozonation and biomethanization treatments of vinasse derived from ethanol manufacturing. J. Hazard. Mater. 188, 247–253. https://doi.org/10.1016/j.jhazmat.2011.01.096

Sinnott, R.K., 2005. Coulson & Richardson's Chemical Engineering Design, 4th ed, ELSEVIER - Coulson & Richardson's Chemical Engineering series. Elsevier. https://doi.org/10.1016/S1385-8497(00)00184-4

Souza, M.E., Fuzaro, G., Polegato, A.R., 1992. Thermophilic anaerobic digestion of vinasse in pilot plant UASB reactor. Water Sci. Technol. 25, 213–222.

Strachan, L., Pass, J., 2012. CLEAN DEVELOPMENT MECHANISM (CDM) ENERGY FROM WASTE : AN OVERVIEW OF AFRICA'S FIRST LANDFILL GAS TO ENERGY CDM PROJECTS.

Sung, S., Liu, T., 2003. Ammonia inhibition on thermophilic anaerobic digestion. Chemosphere 53, 43–52. https://doi.org/10.1016/S0045-6535(03)00434-X

Swartz, C.D., Du Plessis, J.A., Burger, A.J., Offringa, G., 2006. A desalination guide for South African municipal engineers. Water SA 32, 641–647. https://doi.org/10.4314/wsa.v32i5.47845

Symons, G.E., Buswell, A.M., 1933. The methane fermentation of carbohydrates. J. Am. Chem. Soc. 55, 2028–2036. https://doi.org/10.1021/ja01332a039

Tewari, P.K., Batra, V.S., Balakrishnan, M., 2007. Water management initiatives in sugarcane molasses based distilleries in India. Resour. Conserv. Recycl. 52, 351–367. https://doi.org/10.1016/j.resconrec.2007.05.003

Tongaat Hulett, 2015. Integrated Annual Report 2015.

Turner, P.E., Meyer, J.H., King, A.C., 2002. Field Evaluation of Concentrated Molasses Stillage As a Nutrient Source for Sugarcane in Swaziland. Proc S African Technolofy Assoc. 76, 61–70.

Turton, R., Bailie, R.C., Whiting, W.B., Shaeiwitz, J.A., 2008. Analysis, synthesis and design of chemical processes. Pearson Education.

Uellendahl, H., Ahring, B.K., 2010. Anaerobic digestion as final step of a cellulosic ethanol biorefinery: Biogas production from fermentation effluent in a UASB reactor - Pilot-scale results. Biotechnol. Bioeng. 107, 59–64. https://doi.org/10.1002/bit.22777

Walsh, J.L., Ross, C.C., Smith, M.S., Harper, S.R., 1989. Utilization of biogas. Biomass 20, 277–290.

Wheeler, P., Holm-Nielsen, J.B., Jaatinen, T., Wellinger, A., Lindberg, A., Pettigrew, A., 1999a. Biogas Upgrading and Utilisation 3–20.

Wheeler, P., Holm-Nielsen, J.B., Jaatinen, T., Wellinger, A., Lindberg, A., Pettigrew, A., 1999b. Biogas Upgrading and Utilisation 3–20.

Wilkie, A.C., Riedesel, K.J., Owens, J.M., 2000. Stillage characterization and anaerobic treatment of ethanol stillage from conventional and cellulosic feedstocks. Biomass and Bioenergy 19, 63–102. https://doi.org/10.1016/S0961-9534(00)00017-9

Woinaroschy, A., 2009a. Simulation and Optimization of Citric Acid Production with SuperPro Designer using a Client-Server Interface. Rev. Chim 1–5.

Woinaroschy, A., 2009b. Simulation and Optimization of Citric Acid Production with SuperPro Designer using a Client-Server Interface. Rev. Chim 1–5.

Wooley, R.J., Putsche, V., 1996. Development of an ASPEN PLUS Physical Property

Database for Biofuels Components. Victoria 1–38. https://doi.org/10.2172/257362

Yeo, K., 2010. Cost Analysis of Membrane Bioreactors to Reverse Osmosis Filters.

Yu, L., Wensel, P., Ma, J., Chen, S., 2013. Mathematical Modeling in Anaerobic Digestion (AD). J. Bioremediation Biodegrad. S4, 12. https://doi.org/10.4172/2155-6199.S4-003

Zhang, P., Zhao, Z.G., Yu, S.J., Guan, Y.G., Li, D., He, X., 2012. Using strong acid-cation exchange resin to reduce potassium level in molasses vinasses. Desalination 286, 210–216. https://doi.org/10.1016/j.desal.2011.11.024

Zhang, Y., Ghyselbrecht, K., Vanherpe, R., Meesschaert, B., Pinoy, L., Van der Bruggen, B., 2012. RO concentrate minimization by electrodialysis: Techno-economic analysis and environmental concerns. J. Environ. Manage. 107, 28–36. https://doi.org/10.1016/j.jenvman.2012.04.020

Appendices

A. Equipment sizing curves

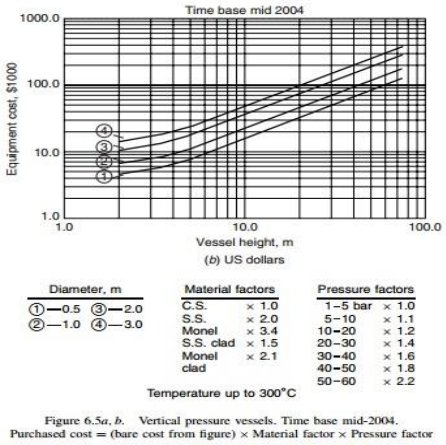

Figure 6.5*a*, *b*. Vertical pressure vessels. Time base mid-2004.
Purchased cost = (bare cost from figure) × Material factor × Pressure factor

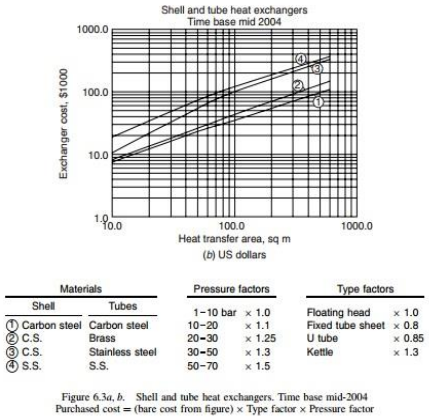

Figure 6.3*a*, *b*. Shell and tube heat exchangers. Time base mid-2004
Purchased cost = (bare cost from figure) × Type factor × Pressure factor

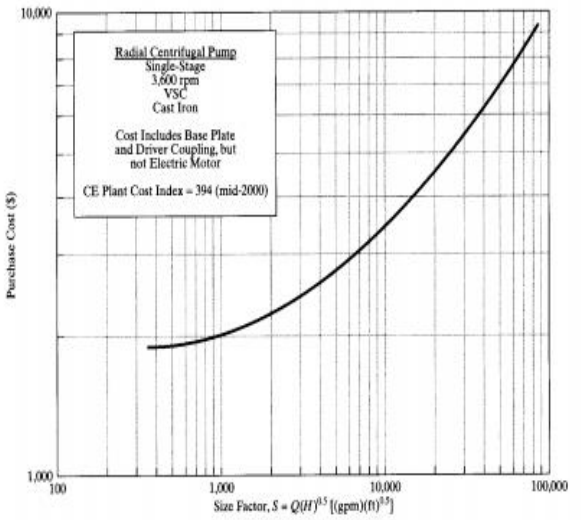

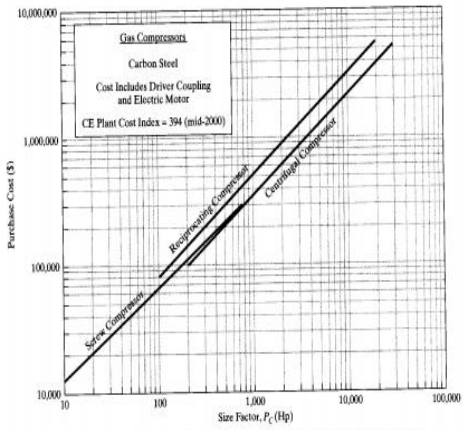

Figure 16.9 Base f.o.b. purchase costs for centrifugal, reciprocating, and screw compressors.

Figure A 1: Equipment cost curves for vertical vessels, shell and tube heat exchangers, centrifugal pumps and compressors (Seider et al., 2003; Sinnott, 2005)

Table A 1: Equations, heuristics and standards used in equipment cost calculations

Equipment type	**Size factor**	**Range of X**	**Cost Equation**	**Reference**
Falling Film evaporator	Heat transfer area	150 – 4000 ft^2	$C = 10000.A^{(0.55)}$	(Seider et al., 2003)
Ion Exchange system	Throughput (kg/hr)	-	C ($, 2014) = $5 250 000* $(S1/53\ 204)^{(0.9)}$	(Davis et al., 2013)
UASB reactor	Volume (m^3)	-	C ($, 2016) = $615 160*$(S1/1820)^{0.6}$	(Fuess et al., 2017)
RO system			Membrane cost: $1000. Module cost: $1200 (USD, 2012)	(Ang et al., 2017; Bick et al., 2012)

B. Fortran code implemented in the Calculator Blocks of the AD simulation

Glucose acidogenesis

```
T=T+273.15
T0=55+273.15
PH = 6
IF ( PH .LT. 5.5) THEN
S =  (( PH - 5.5 ) / (5.5 - 4. ) )
IF (S .LT. 0.) THEN
 S= -S
ENDIF
R = ((-3.)*(S**2.))
Q =(2.7182818284**(R))
ELSE
Q = 1
ENDIF
Z = 30*EXP(-(-35616.457/8.314)*(1/T-1/T0))
L = ( 1. / ( 3600. * 24. ) ) * Z
P = 0.27 + 0.025 * ( T - T0 )
N = 1. / ( P + (GLUFLOW / VOLFLOW ) )
M = 1. / ( 0.05 + ( TNH3FLOW / VOLFLOW ) )
O = 5 / (5. + ( LCFAF/ VOLFLOW))
K = L *N * M *Q*O
KNTC=K
```

Amino acids acidogenesis

```
A = 0.0000001
AA = GLU
BB = LYS;  CC = ASP

IF (AA .EQ. 0.) THEN
AA = AA +A
ENDIF
DD = AA + BB + CC

PH = 6
IF ( PH .LT. 5.5 ) THEN
S = ((PH - 5.5) / ( 5.5 - 4 ))
ENDIF
IF (S .LT.0) THEN
S = -S
ENDIF
R =((-3.)*(S**2.))
Q= ( 2.7182818284**(R))

N =1. / (0.2112 + (DD/ VOLFLOW))
T = T + 273.15
TO = 55 + 273.15
Z =50 * EXP (-(-14143.72619 / 8.314) * (1/T -
1/TO))
L = ( 1. / (3600. * 24. )) * Z
K =  L*N*Q

KGLUTC = K
KLYS TC= K
KASPTC = K
```

Glycerol acidogenesis

```
L = ( 1. / ( 3600. * 24. ) )*6
N = ( 1. / ( 1. + .01 / ( GLYCE / VOLF) ) )
M = ( 1. / ( 1. + .05 / ( NH3F / VOLF) ) )

PH = 6
IF ( PH .LT. 5.5) THEN
S =  (( PH - 5.5 ) / (5.5 - 4. ) )
IF (S .LT. 0.) THEN
S= -S
ENDIF
R = ((-3.)*(S**2.))
Q =(2.7182818284**(R))
ELSE
Q = 1
ENDIF

KNTC = L * N * M * Q
```

GTO degradation

```
T=T+273.15
T0=55+273.15
Z = 6 *EXP(-(-21472.7308/8.314)*(1/T-1/T0))
L = ( 1. / ( 3600. * 24. ) ) * Z
O = ( LCFA / VOLF ) / 5.
N = 1. / ( 0.1379 + (LCFA/VLF))
M = 1. / ( 0.05 + ( TNH3FLW / VLF))

PH = 6
IF ( PH .LT. 5.5) THEN
V =  (( PH - 5.5 ) / (5.5 - 4. ) )
IF (S .LT. 0.) THEN
V= -V
ENDIF
R = ((-3.)*(V**2.))
Q =(2.7182818284**(R))
ELSE
Q = 1
ENDIF
K = L * N * M * Q
KNTC=K
```

Acetogenesis - Butyric acid

```
A = .00000001
IF (ACF .EQ. 0.) THEN
ACF = ACF + A
ENDIF
IF (VOLF .EQ. 0.) THEN
VOLF = VOLF + A
ENDIF
IF (NH3F .EQ. 0.) THEN
NH3F = NH3F + A
ENDIF
IF (BUTF .EQ. 0.) THEN
BUTF = BUTF+A
ENDIF
T=T+273.15
T0=55+273.15
PH = 6
IF ( PH .LT. 5.5) THEN
V =  (( PH - 5.5 ) / (5.5 - 4. ) )
IF (V .LT. 0.) THEN
V= -V
ENDIF
R = ((-3.)*(V**2.))
Q =(2.7182818284**(R))
ELSE
Q = 1
ENDIF
Z = 20 *EXP(-(-17043.8653/8.314)*(1/T-
1/T0))
L = (1. / ( 3600. * 24. ) ) * Z
U = .11 + .01*(T-T0)
N = 1. / (U + ( BUTF / VOLF ) )
M = 1. / ( 0.05 + ( NH3F / VOLF ) )
O = 0.72 / ( 0.72 + ( ACF / VOLF))
XX = 5 / (5 + (LCFAF/ VOLF))
K = L * N * M * O* Q * XX
KNTC=K
```

Propionic degradation

```
T=T+273.15
T0=55+273.15
PH = 6
IF ( PH .LT. 5.5) THEN
V =  (( PH - 5.5 ) / (5.5 - 4. ) )
IF (V .LT. 0.) THEN
V= -V
ENDIF
R = ((-3.)*(V**2.))
Q =(2.7182818284**(R))
ELSE
Q = 1
ENDIF
Z = 15 *EXP(-(-18108.108/8.314)*(1/T-1/T0))
L = (1. / ( 3600. * 24. ) ) * Z
U = 0.06607
N = 1. / ( U + ( PROPF / VOLF ) )
M = 1. / (0.05 + ( TNH3FLOW / VOLF ) )
O = 0.96 / (0.96 + ( ACF / VOLF))
IL = 5 / (5 + ( LCFAF/ VOLF))
K = L * N * M * O* Q* IL
KNTC=K
```

Valeric acid degradation

```
T=T+273.15
T0=55+273.15
PH = 6
IF ( PH .LT. 5.5) THEN
V =  (( PH - 5.5 ) / (5.5 - 4. ) )
IF (V .LT. 0.) THEN
V= -V
ENDIF
R = ((-3.)*(V**2.))
Q =(2.7182818284**(R))
ELSE
Q = 1
ENDIF
Z = 30 *EXP(-(-17043.8653/8.314)*(1/T-1/T0))
L = (1. / ( 3600. * 24. ) ) * Z
U = .175 + .01*(T-T0)
N = 1. / (U + ( VALF / VLF ) )
M = 1. / ( 0.05 + ( NH3F / VLF ) )
O = 0.4 / ( 0.4 + ( ACF / VLF))
XX = 5 / (5 + (LCFAF/ VOLF))
K = L * N * M * Q
KNTC=K
```

Methanogenesis (Acetic acid degradation)

```
A = .00000001
IF (NH3F .EQ. 0.) THEN
 NH3F = NH3F + A
ENDIF
IF (VOLF .EQ. 0.) THEN
 VOLF = VOLF + A
ENDIF
IF (ACF .EQ. 0.) THEN
 ACF= ACF + A
ENDIF
IK= 0.5
T=T+273.15
T0=55+273.15
PH = 6
R = (1.+2.*10.**(.5*(6.-7.)))/(1.+10.**(PH-
7.)+10.**(6.-PH))
Z = 9.4 *EXP(-(-29136.6801/8.314)*(1/T-1/T0))
L = (1. / ( 3600. * 24. ) ) * Z
V = .14026 +  .0075*(T-T0)
N =  1. /( V +( ACF/ VOLF ) )
M =  1. / ( 0.05 + ( NH3F / VOLF ) )
W = .26 + .00046*(T-T0)
O =  W / ( W + ( NH3F / VOLF ) )
IX = 5 / (5 + ( LCFAF/ VOLF))
IK = 5.86/(5.86 + ( K2FR*RHO))
K = L * N * M * O * IK
KINETIC=K
X=(1. / ( 3600. * 24. ) ) * 43
U= 0.00005 + 0.00000215* (T - TO)
S = 1
Q = (1.+2.*10.**(.5*(5.-6.)))/(1.+10.**(PH-
6.)+10.**(5.-PH))
K2 = X * S * Q
KINETIC2=K2
```

Jenbacher Engine – ICEngine – Aspen Custom Modeller

```
// <parameter name> as <parameter type> (<default>, description:"<description>");
// <variable name>  as <variable type> (default, <spec>, description:"<description>");
// <submodel name>  as <model type> (<submodel variable> = <variable name>,...);
// <structure name> as external <structure type>("<default instance>");
// <port name>      as <Input or Output> <port type>;
// <equation_name> : <expression1> = <expression2>;
// Call (<output argument list>) = <procedure name>(<input argument list>);
Feed as input HeatPort;
//out as output MoleFractionPort;
//f as input MoleFractionPort;
//g = f.F;
//out.F = f.F;
Electricity as output WorkPort;
Heat as output HeatPort;
efficiency as fraction (description:"efficiency", value:0.8, spec:Fixed);
Electricity.W = efficiency*Feed.Q*1000000/3600;
Heat.Q = Feed.Q*(1-efficiency);
Electricity.Speed = 0;

End
```

C. Summary of Capital and Operating Costs and Discounted Cash Flow Analyses

Table C 1: A breakdown of capital and operating costs for the vinasse treatment routes (USD, 2016)

Process Routes	**IEX - AD - CHP - RO**	**IEX-AD-Upgrade**	**AD - Upgrade - RO**	**IEX - AD - Upgrade - RO**	**IEX - AD - CHP - MEE**	**IEX - AD - UP - MEE**	**AD - UP - MEE**	**IEX - AD - CHP - MEE**
Capital Expenditures (USD, 2016)								
Purchase cost of equipment (PCE)	$5 598 638	$3 880 228	$1,240,123	$3,950,117	$5 712 023	$4 060 854	$1 349 861	$5 712 023
Lang Factor - installation, electrical,structures, piping	1.6	1.6	1.6	1.6	1.6	1.6	1.6	1.6
Physical Plant Cost	8 957 820	6208365	1984196.	6320187.2	9139237	6497367	2159778	9139237
Lang Factor - Design, Engineering and Contingency	1.19	1.19	1.19	1.19	1.19	1.19	1.19	1.19
Location factor	1	1	1	1	1	1	1	1
Fixed Capital Investment USD, 2016	10 659 806	7387954	2361194	7 521 022	10875693	7731867	2570136	10875693
Working Capital (15%)	1 598 971	1108193	354179	1 128 153	1631353	1159780	385520	1631353
Total Capital Investment	$12 258 777	$8 496 148	$2 715 373	$8 649 176	$12 507 047	$8 891 647	$2 955 656	$12 507 047

OPEX	IEX - AD - CHP - RO	IEX-AD-Upgrade	AD - Upgrade - RO	IEX - AD - Upgrade - RO	IEX - AD - CHP - MEE	IEX - AD - UP - MEE	AD - UP - MEE	IEX - AD - CHP - MEE
Variable costs								
Innoculum								
NaOH (dosing)	**38690**	38690	38690	38690	38690	38690	38690	38690
H2SO4 eluent	**$27 670**			$27 670	$27 670	$27 670		$27 670
Membrane replacement	**$40 000**		$40 000	$40 000				
Labor Costs ($/yr)	**$185 31**	$172 476	$185 315	$185 315	$185 315	$185 315	$185 315	$185 315
Utility costs	**$14 353**	$31 953	$47 213	$46 307	$38 848	$38 848	$43 165	$38 848
Transport costs for vinasse		15546						
Fixed costs								
CHP (O&M)	76186				76186			76186
AD O&M (1.5% of plant costs)	$28 304	$28 304	$28 304	$28 304	$28 304	$28 304	$28 304	$28 304
RO (O&M)	$24 711		$25 652	$24 711	$32 332.14	$32 332.14	$32 332.14	$32 332.14
IEX (O&M)	$271 099	$271 099		$271 099	$271 099	$271 099		$271 099
Biogas Upgrade (OOM)		11504	11504	11504		20593	20593	
Total OC	**$706 330**	$569 575	$376 680	$673 602	$698 447	$642 854	$348 401	$698 447
Indirect fertilizer revenue	250913	73224	250913	250913	250913	250913	250913	250913
Overall OC	**$455 417**	$496 351	$125 766	$422 689	$447 533	$391 940	$97 487	$447 533

Table C 2: A summary of profitability indicators (USD, 2016) evaluated for the 12 vinasse treatment options for a 20-year project lifetime. Net Present Value presented in millions (USD)

	AD-CHP	**AD-CHP-RO**	**IEX-AD-CHP**	**IEX-AD-CHP-RO**	**AD-HPWS**	**IEX-AD-HPWS**	**AD-CHP-MEE**	**IEX-AD-CHP-MEE**	**AD-HPWS-MEE**	**IEX-AD-HPWS-MEE**	**AD-HPWS-RO**	**IEX-AD-HPWS-RO**
ROI (%)	0.0	3.2	3.2	4.5	19.6	11.4	3.1	4.5	22.1	4.5	22.9	12.4
IRR (%)	-1.8	2.0	2.0	3.8	16.3	10.5	1.9	3.7	17.9	3.7	18.3	11.4
PBP (%)	18.9	12.7	12.7	10.6	3.7	5.7	12.8	10.7	3.4	10.7	3.28	5.4
NPV	-3.82	-3.3	-6.5	-5.9	0.19	-1.9	-3.5	-6.1	0.5	-6.1	0.54	-1.6

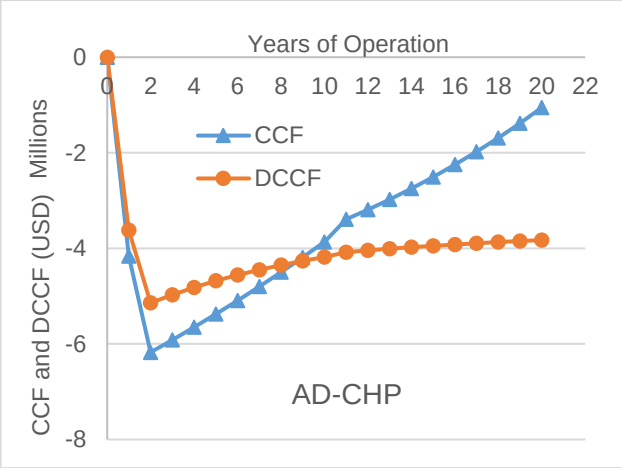

Figure C 1: Discounted cash flow analysis of the AD-CHP process (20 year project lifetime. USD, 2016)

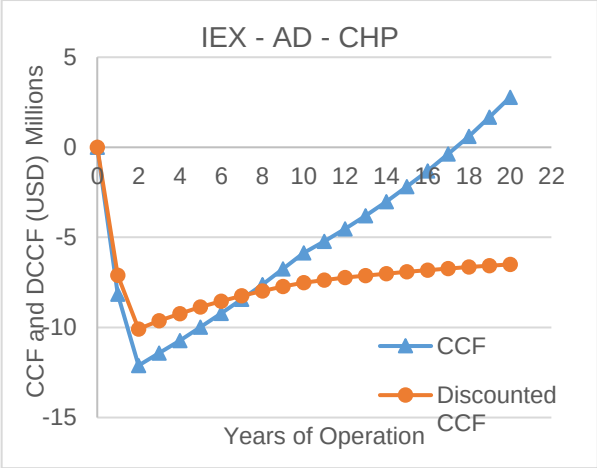

Figure C 2: Discounted cash flow analysis of the IEX-AD-CHP process (20 year project lifetime. USD, 2016)

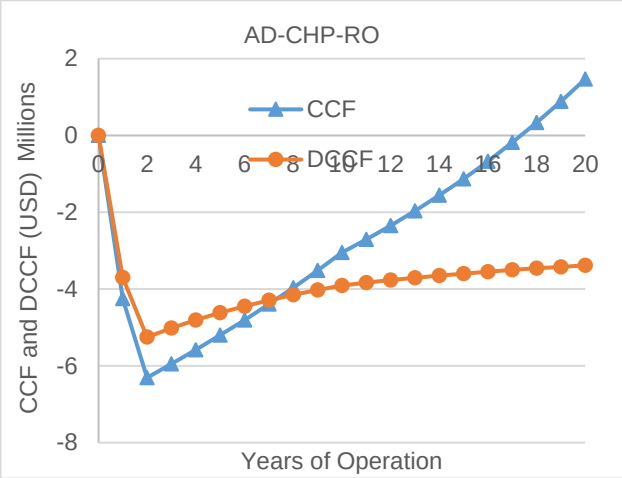

Figure C 3: Discounted cash flow analysis of the AD-CHP-RO process (20 year project lifetime. USD, 2016)

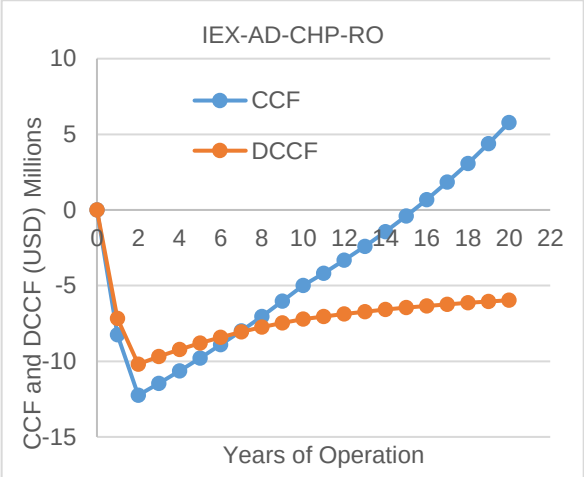

Figure C 4: Discounted cash flow analysis of the IEX-AD-CHP-RO process (20 year project lifetime. USD, 2016)

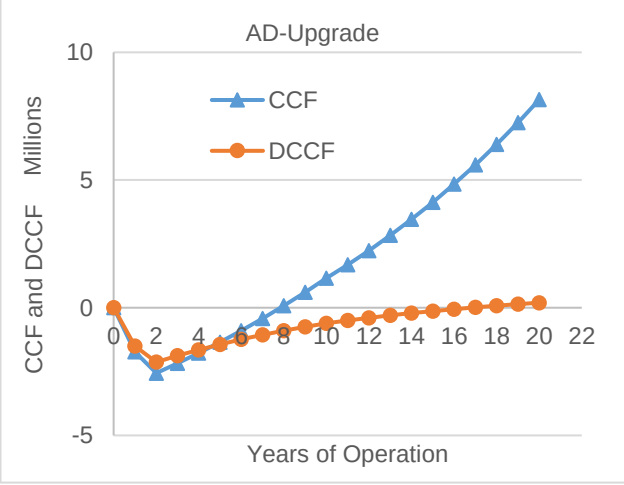

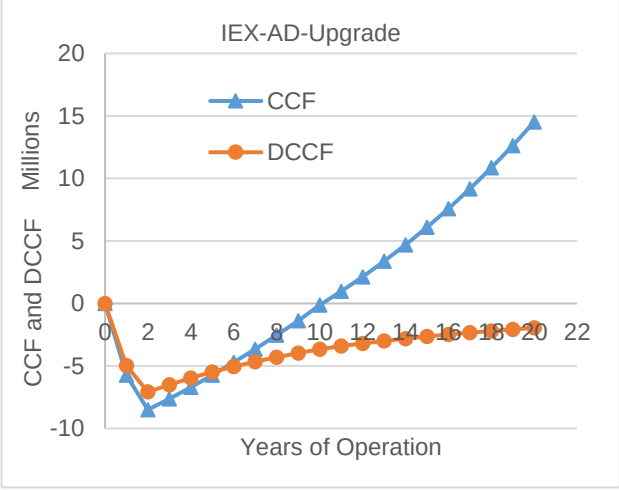

Figure C 5: Discounted cash flow analysis of the AD-Upgrade/HPWS process (20 year project lifetime. USD, 2016)

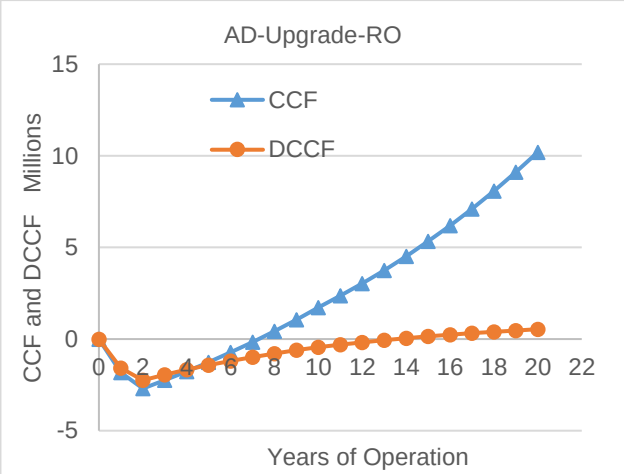

Figure C 6: Discounted cash flow analysis of the IEX-AD-Upgrade process (20 year project lifetime. USD, 2016)

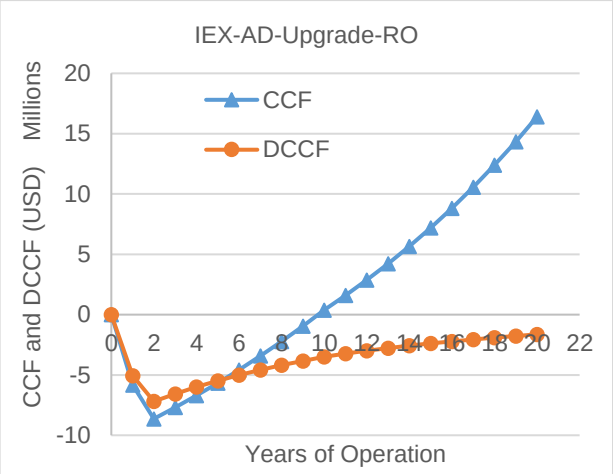

Figure C 7: Discounted cash flow analysis of the AD-Upgrade-RO process (20 year project lifetime. USD, 2016)

Figure C 8: Discounted cash flow analysis of the IEX-AD-Upgrade-RO process (20 year project lifetime. USD, 2016)

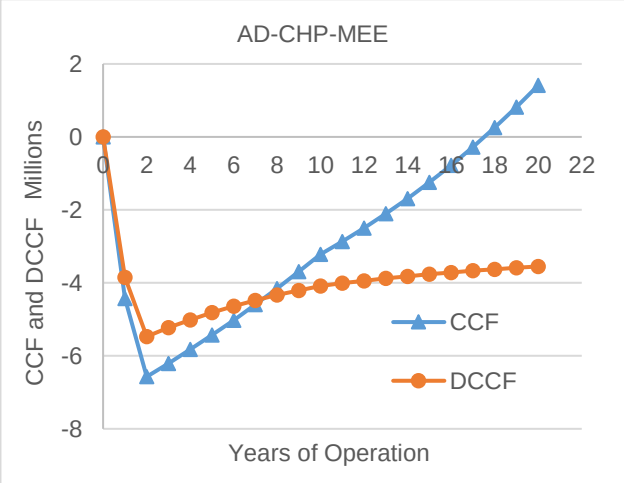

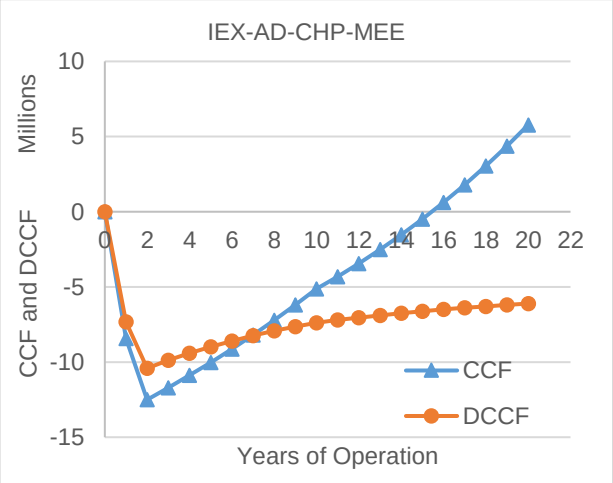

Figure C 9: Discounted cash flow analysis of the AD-CHP-MEE process (20 year project lifetime. USD, 2016)

Figure C 10: Discounted cash flow analysis of the IEX-AD-CHP-MEE process (20 year project lifetime. USD, 2016)

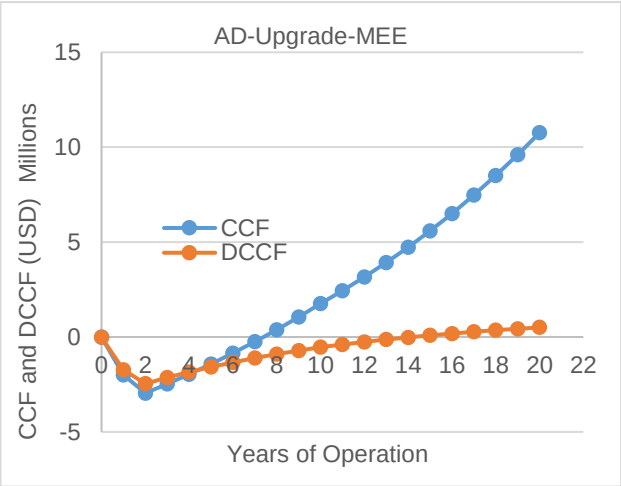

Figure C 11: Discounted cash flow analysis of the AD-Upgrade-MEE process (20 year project lifetime. USD, 2016)

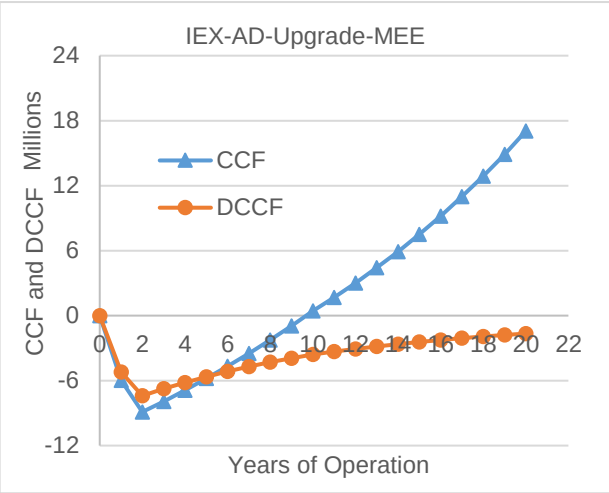

Figure C 12: Discounted cash flow analysis of the IEX-AD-Upgrade-MEE process (20 year project lifetime. USD, 2016)